
New Vaccines for Infectious Diseases:
Immunological targeting of the quorum sensing
system of *Pseudomonas aeruginosa*

Aditi Pathak, MPharm (Hons)

Thesis submitted to the University of Nottingham for
the degree of Doctor of Philosophy

July 2012

ABSTRACT

Pseudomonas aeruginosa is an opportunistic pathogen of animals and humans causing medical complications in burns, wounds, and cystic fibrosis. *P. aeruginosa* is efficient at adapting its virulence phenotype depending on the site of infection. Emerging multi-drug resistant strains and a limited number of effective anti-pseudomonal antibiotics renders *P. aeruginosa* infections increasingly difficult to treat.

To address this need, this thesis considers targeting bacterial quorum sensing, which regulates the production of virulence factors, as an alternative prophylactic strategy. The *P. aeruginosa* quorum sensing system is comprised of three interlinked but independent systems, Las, Rhl and Pqs, which produce and utilise quorum sensing system molecules, 3OC₁₂-HSL, C₄-HSL and PQS respectively. Immunological targeting of the quorum sensing system molecule 3OC₁₂-HSL, through active immunisation (vaccines), inhibits the Las system, resulting in a longer life expectancy in mice infected with *P. aeruginosa* *in vivo*.

However, *P. aeruginosa* has the capacity to develop resistance, through compensatory mechanisms, towards quorum sensing inhibition that targets the Las system only. This emphasises the need to target all three quorum sensing systems, Las, Rhl, and the Pqs, in order to inhibit quorum sensing. The present study focuses particularly on the development of a multi-component anti-quorum sensing system vaccine that would target the three main quorum sensing system molecules, effectively compromising the quorum sensing system and minimising compensatory mechanisms.

This involved the synthesis of haptens based on the quorum sensing system molecules, which were used to haptenise the immunogenic carrier keyhole limpet haemocyanin. Syntheses of the haptens, **AP1** (derivative of 3OC₈-HSL) and **AP2** (derivative of PQS), were conducted using adapted published methods. The resulting conjugates, **AP1**-keyhole limpet haemocyanin and **AP2**-keyhole limpet haemocyanin were immunogenic in mice and rabbits. The specific anti-hapten polyclonal antibodies that were generated demonstrated cross-reactivity with the natural quorum sensing system molecules of *P. aeruginosa* that translated in significant and specific anti-quorum sensing system molecule activity in bioluminescence reporter assays. Anti-**AP1** polyclonal antibodies were able to reduce biofilm formation at high concentrations, however, significant reduction of biofilm formation was seen when the anti-hapten antibodies were used in combination.

In this study, it has been demonstrated that the inhibition of the quorum sensing system should include the three systems, Las, Rhl and PQS, and that this can be done by a multi-component anti-quorum sensing system vaccine. These data suggest that a multi-component anti-quorum sensing system vaccine takes us a step forward to a viable prophylaxis against *P. aeruginosa* for susceptible patients.

ACKNOWLEDGEMENTS

I would like to thank my supervisors, Professor Peter Fischer and Professor David Pritchard for their continuous support, advice, and time. I offer my sincerest gratitude to them both for giving me this opportunity, and for making it possible for me to complete this thesis.

There have been a number a people, past and present, who have helped me during these four years and I would like to thank them for all their help. In particular, Dr Alan Brown, Dr Gary Telford, and Dr Daniel Blount for always answering my ‘quick questions’, even though the questions were never quick. I owe a great deal to Dr Alan Brown for his training, advice, valued insights (and for going running with me) and for explaining (very patiently) all the jokes and references to popular culture. I would like to thank Dr Shailesh Mistry and Dr Gopal Jadhav for their help and advice, I have learnt some valuable chemistry skills to which I attribute to their willingness to help. Sincere thanks to Dr Steve Diggle, Professor Paul Williams, and Professor Miguel Cámara for being generous with their time, advice and resources. Thank you to Lee, Graeme, and Colleen for superb technical assistance and for coping admirably with my occasional mishaps with glassware and equipment. I would also like to thank BBSRC and the University of Nottingham for funding.

I thank all the members, past and present, of my research groups, all of whom were always supportive, and also the entire C-floor, CBS for letting me shamelessly borrow everything, Dan, Will, Austin, Sarah, Andrea, Shaun and Christophe – Thank you! I have been very lucky to have worked with some amazing people, who reside on C-floor, CBS and D-floor Boots Building, I am very fortunate to count them as my friends – they have made these four years most enjoyable. I would like to thank Ellie, Indi, Stef, Adnan, and Nargis for their friendship, optimism, good humour, and valuable infortainment, and for always providing a torch (and lots of batteries) when there was no light at the end of *that* tunnel.

I would like to thank my brother, Sachin Pathak, who always made sure I got to work in the snow, ice, and rain. He has been extremely supportive and I could not have wished for a better brother (this is the only time I shall admit that). I would like to take this opportunity to thank my parents, my late father, Ashok Kumar Pathak, who passed away before he could see that I was able to complete his wish and to my mother, Surekha Rani Pathak, to whom I wish to dedicate this thesis. This thesis is a testament to my mother’s energy and hard work; she made sure that I always had the time, ambition, and energy to focus on work. I will be eternally grateful for her love, support, and encouragement and for making it possible and easy to pursue my ambitions.

ABBREVIATIONS	10
1 INTRODUCTION.....	16
1.1 COLONISATION, INFECTION AND DISEASE.....	16
1.1.1 BURNS AND WOUNDS.....	18
1.1.2 ULCERATIVE KERATITIS	18
1.1.3 CYSTIC FIBROSIS	18
1.1.4 URINARY TRACT INFECTIONS	19
1.1.4.1 INNATE IMMUNE EFFECTORS.....	19
1.2 THERAPY AND ANTIBIOTIC RESISTANCE.....	19
1.2.1 <i>P. AERUGINOSA</i> AND MECHANISMS OF RESISTANCE	20
1.2.1.1 BIOFILMS	20
1.2.1.2 THE PROBLEM OF RESISTANCE.....	24
1.3 ALTERNATIVE THERAPEUTICS.....	24
1.3.1 VACCINES AND ANTIBODIES.....	24
1.3.1.1 IMMUNE SYSTEM AND ANTIGENS.....	25
1.3.1.2 ANTIBODIES.....	26
1.3.1.3 VACCINE INDUCED IMMUNITY	27
1.4 ANTI-PSEUDOMONAL VACCINES AND THERAPEUTIC ANTIBODIES	29
1.4.1 SUMMARY	34
1.5 REGULATORY SYSTEM FOR VIRULENCE FACTOR PRODUCTION - POTENTIAL TARGET	35
1.5.1 QUORUM SENSING	35
1.5.2 QSSM OF <i>P. AERUGINOSA</i>	37
1.5.2.1 QSSM OF OTHER GRAM-NEGATIVE BACTERIA	37
1.5.3 THE QUORUM SENSING SYSTEM (QSS) OF <i>P. AERUGINOSA</i>	39
1.5.3.1 INTERNAL QSS REGULATION.....	39
1.5.3.2 GLOBAL REGULATION OF QSS	39
1.5.3.3 ENVIRONMENTAL REGULATION OF QSS	39
1.5.4 QSS AND VIRULENCE	44
1.5.4.1 QSSM AS VIRULENCE FACTORS	45
1.5.5 QS AND BIOFILMS.....	46
1.5.6 QS AND DISEASE.....	47
1.6 THE QSS – ALTERNATIVE THERAPEUTIC TARGET	48
1.6.1 QSS INHIBITION.....	48
1.6.2 QUORUM SENSING SYSTEM INHIBITORS (QSSi)	49
1.6.2.1 NATURAL INHIBITORS	49

1.6.2.2	CHEMICAL INHIBITORS	49
1.6.2.3	IMMUNOLOGICAL INHIBITORS.....	50
1.6.2.3.1	ANTI-AHL VACCINES AND ANTIBODIES	50
1.6.3	SUMMARY	51
1.7	IMMUNOGENICITY OF ANTI-AHL VACCINE ANTIGENS	52
1.7.1	HAPTEN DESIGN	53
1.7.1.1	HAPTEN STRUCTURE	53
1.7.1.2	LINKER.....	54
1.7.2	THE ‘MANY’ QSS OF <i>P. AERUGINOSA</i>	54
1.7.2.1	DISADVANTAGES OF ANTI-AHL VACCINES	55
2	MULTI-COMPONENT ANTI-QSS VACCINE – COMPLETE QSS INHIBITION	56
2.1	AIMS AND OBJECTIVES.....	57
3	RESULT 1 – HAPTEN SYNTHESIS.....	60
3.1	HAPTEN DESIGN.....	60
3.1.1	AHL HAPTEN, AP1.....	60
3.1.2	PQS HAPTEN, AP2	60
3.2	SYNTHESIS OF AP1 , 7-((S)-2-OXOPYRROLIDIN-3-YLCARBAMOYL)-6- OXOHEPTANOIC ACID, 37	63
3.2.1	AMIDATION METHOD A	63
3.2.2	AMIDATION METHOD B	65
3.2.2.1	SYNTHESIS OF NATURAL QSSM.....	65
3.2.3	DISCUSSION.....	65
3.2.3.1	ACYLATION OF MELDRUM’S ACID	66
3.2.3.2	β -KETO DICARBOXYLATES	66
3.2.3.3	PROTECTING GROUP STRATEGY	67
3.2.3.4	FORMATION OF β -KETO AMIDE 36	68
3.2.4	SUMMARY	69
3.3	SYNTHESIS OF AP2 , 7-(1,4-DIHYDRO-3-HYDROXY-4-OXOQUINOLIN-2- YL)HEPTANOIC ACID 47	70
3.3.1	METHOD A	70
3.3.2	METHOD B	71
3.3.3	METHOD C	71
3.3.4	DISCUSSION.....	72
3.3.4.1	α -HALO-KETONES	72
3.3.4.1.1	METHOD A	72
3.3.4.2	CYCLISATION.....	73
3.3.4.2.1	METHOD A AND B	73

3.3.4.3	METHOD C	73
3.3.5	SUMMARY	74
3.4	SYNTHESIS OF OTHER MOLECULES OF INTEREST	75
3.4.1	PQS	75
3.4.2	HHQ	75
3.4.3	HMAQS OF <i>BURKHOLDERIA</i> SPP.	76
4	MATERIALS AND METHODS.....	78
5	RESULT 2 – HAPTENISATION AND CHARACTERISATION	84
5.1	HAPTEN-CARRIER CONJUGATE.....	84
5.1.1	HAPTEN AND CARRIER CONJUGATION	84
5.1.2	EPITOPE DENSITY	85
5.1.3	CHARACTERISATION METHODS.....	85
5.2	RESULTS – HAPTEN-CARRIER CONJUGATE CHARACTERISATION	86
5.2.1	CONJUGATION.....	86
5.2.2	MALDI-TOF MS.....	86
5.2.3	2D-SDS PAGE.....	87
5.3	RESULTS - ANTIBODY CHARACTERISATION	89
5.3.1	MOUSE IMMUNISATION	89
5.3.1.1	SPECIFICITY	92
5.3.2	RABBIT IMMUNISATION	94
5.3.2.1	SPECIFICITY	94
5.3.2.1.1	AHL.....	94
5.3.2.1.2	PQS.....	96
5.4	DISCUSSION	97
5.4.1	HAPTEN-CARRIER CONJUGATES AND CHARACTERISATION	97
5.4.2	CHARACTERISATION OF ANTI-HAPTEN ANTIBODIES	97
5.4.3	FUTURE WORK	97
6	RESULT 3 – CROSS-REACTIVITY.....	98
6.1	CROSS-REACTIVITY OF ANTI-HAPTEN ANTIBODIES	98
6.1.1	OPTIMISATION	100
6.1.2	QSSM AND SOLVENT EFFECT	100
6.2	RESULTS.....	100
6.2.1	CROSS-REACTIVITY PROFILE OF MOUSE ANTI-AP1 ANTIBODIES.....	100
6.2.2	CROSS-REACTIVITY PROFILE OF ANTI-AP2 ANTIBODIES	102
6.3	DISCUSSION	102

6.3.1	CROSS-REACTIVITY	102
6.3.1.1	LIMITATIONS OF THIS TECHNIQUE	103
6.3.2	FUTURE WORK	103
7	RESULT 4 - ANTI-QSSM ACTIVITY	105
7.1.1	BIOLUMINESCENCE.....	105
7.1.1.1	BIOLUMINESCENCE REPORTER.....	105
7.1.2	RESULTS.....	105
7.1.2.1	3OC ₁₂ -HSL AND RABBIT ANTI- AP1 pIgG	107
7.1.2.2	C ₄ -HSL AND RABBIT ANTI- AP1 pIgG.....	111
7.1.2.3	PQS AND RABBIT ANTI- AP2 pIgG	115
7.2	DISCUSSION	122
7.2.1	ANTI-QSSM ACTIVITY.....	122
7.2.2	FUTURE WORK	123
8	RESULT 5 - ANTI-QSS ACTIVITY	125
8.1.1	DETERMINATION OF ANTI-QSS ACTIVITY OF ANTI-HAPTEN pIgG	125
8.1.2	RESULTS.....	126
8.2	DISCUSSION	128
8.2.1	FUTURE WORK	128
9	SUMMARY OF RESULTS	130
10	FUTURE DIRECTIONS AND CONCLUSION	131
10.1	FUTURE DIRECTIONS	131
10.1.1	HAPTEN DESIGN	131
10.1.1.1	CHAIN LENGTH	131
10.1.1.2	ORIENTATION	131
10.1.2	SYNTHETIC STRATEGY FOR AP3 AND AP4	132
10.1.2.1	(2S,4S)-4-ACYLAMINO-5-OXOPYRROLIDINE-2-CARBOXYLIC ACIDS, AP3 ..	132
10.1.2.2	2-HEPTYL-1,4-DIHYDRO-3-HYDROXY-4-OXOQUINOLINE-7-CARBOXYLIC ACID, AP4	133
10.1.3	OTHER BACTERIAL TARGETS.....	134
10.1.4	GRAM-POSITIVE AND GRAM-NEGATIVE ANTI-QSS VACCINE	134
10.2	CONCLUSION	136
11	EXPERIMENTAL PROCEDURES	137
12	APPENDIX 1	148
12.1.1	CROSS-REACTIVITY OF ANTI-AP1 ANTIBODIES	148
12.1.2	CROSS-REACTIVITY OF ANTI-AP2 ANTIBODIES	153

13 REFERENCES	157
Figure 1-1: Innate and adaptive immune responses.	25
Figure 1-2: The adaptive immune response.	28
Figure 1-3: Immune system response to secondary exposure to antigen.	29
Figure 1-4: Depiction of QS in <i>P. aeruginosa</i>	36
Figure 1-5: The QSSM of <i>P. aeruginosa</i>	37
Figure 1-6: The quorum sensing system (QSS) of <i>P. aeruginosa</i>	42
Figure 1-7: QSS inhibition.	48
Figure 1-8: Squaric monoester monoamide, 5	51
Figure 1-9: Published haptens based on natural AHLs.	53
Figure 2-1: Immunological targeting of the QSS with the multi-component QSS vaccine.	58
Figure 3-1: 7-((S)-2-oxopyrrolidin-3-ylcarbonyl)-6-oxoheptanoic acid, AP1	60
Figure 3-2: 7-(1,4-dihydro-3-hydroxy-4-oxoquinolin-2-yl)heptanoic acid, AP2	61
Figure 3-3: Aims and objectives.	62
Figure 3-4: Enolate form of acylated Meldrum's acid.	69
Figure 5-1: MALDI-TOF MS spectra.	87
Figure 5-2: 2D-SDS PAGE analysis of hapten-BSA conjugates (pH 3-10, 10%).	88
Figure 5-3: Depiction of an indirect ELISA.	89
Figure 5-4: The anti-hapten antibody response by CD1-1 and Balb/c-4 mice to each immunisation measured by indirect ELISA.	90
Figure 5-5: Titres of the sera derived from the terminal bleed using indirect ELISA.	91
Figure 5-6: Schematic of indirect ELISA for antibody specificity.	93
Figure 5-7: Indirect specificity ELISA of pooled serum from CD1 and Balb/c mice.	94
Figure 5-8: Anti- AP1 -KLH specificity ELISA.	95
Figure 5-9: Specificity ELISA for rabbit anti- AP1 -pIgG.	95
Figure 5-10: Indirect ELISA specificity of rabbit serum against AP2 -KLH conjugates.	96
Figure 6-1: Competitive indirect ELISA used to study the cross-reactivity of anti-hapten pAb.	99
Figure 7-1: <i>E. coli</i> S17.1 reporter strain with the pSB1075 plasmid.	107
Figure 7-2: The bioluminescence response of <i>E. coli</i> S17.1 reporter strain pSB1075.	108
Figure 7-3: <i>E. coli</i> S17.1 reporter strain contains the pSB536 plasmid.	111
Figure 7-4: The bioluminescence response of <i>E. coli</i> S17.1 reporter strain pSB536.	112
Figure 7-5: <i>P. aeruginosa</i> PAO1 $\Delta pqsA$ CTX- <i>luxCDABE::pqsA</i> reporter.	115
Figure 7-6: The bioluminescence response of <i>P. aeruginosa</i> PAO1 $\Delta pqsA$ CTX- <i>luxCDABE::pqsA</i> reporter strain.	116
Figure 7-7: The bioluminescence response of <i>P. aeruginosa</i> PAO1 $\Delta pqsA$ CTX- <i>luxCDABE::pqsA</i> reporter strain.	119
Figure 7-8: The bioluminescence response of <i>P. aeruginosa</i> PAO1 $\Delta pqsA$ CTX- <i>luxCDABE::pqsA</i> reporter strain.	120

Figure 7-9: PQS bioavailability and anti- AP2 pIgG	123
Figure 8-1: Static biofilm formation with and without rabbit anti-hapten pIgG.	127
Figure 10-1: Proposed haptens for the investigation of carrier attachment, (a) AP3 , and (b) AP4	132
Figure 12-1: 3OC ₆ -HSL and anti- AP1 serum.....	148
Figure 12-2: 3OC ₈ -HSL and anti- AP1 serum.....	149
Figure 12-3: 3OC ₁₂ -HSL and anti- AP1 serum.	149
Figure 12-4: C ₄ -HSL and anti- AP1 serum.....	150
Figure 12-5: C ₆ -HSL and anti- AP1 serum.....	150
Figure 12-6: C ₈ -HSL and anti- AP1 serum.....	151
Figure 12-7: PQS and anti- AP2 sera.....	153
Figure 12-8: HHQ and anti- AP2 sera.....	154
Figure 12-9: 3-Methyl-quinolin-4(1 <i>H</i>)-one and anti- AP2 sera.	155
 Scheme 3-1: Amidation method A	64
Scheme 3-2: Amidation method B	65
Scheme 3-3: Proposed mechanism for decarboxylation of oxosuccinic acid, 38	67
Scheme 3-4: Proposed nucleophilic addition-elimination.	68
Scheme 3-5: Proposed reaction mechanism between α -oxo-ketene 39 and nucleophilic species.	69
Scheme 3-6: Formation of AP2 , 47 , via method A.....	70
Scheme 3-7: Formation of AP2 , 47 , via method B.....	71
Scheme 3-8: Formation of AP2 , 47 , via method C.....	72
Scheme 3-9: Mechanistic view of intramolecular condensation to form 2-substituted-3-hydroxy-4(1 <i>H</i>)-quinolones.....	73
Scheme 3-10: Formation of PQS 4 via method A and B.....	75
Scheme 3-11: Alternate synthesis of HHQ 3	75
Scheme 3-12: Synthesis of 2-heptyl-3-methyl-quinolin-4(1 <i>H</i>)-one, 77	77
Scheme 10-1: Synthesis of (2 <i>S</i> ,4 <i>S</i>)-4-acylamino-5-oxopyrrolidine-2-carboxylic acids (243).133	
Scheme 10-2: Synthesis of 2-heptyl-1,4-dihydro-3-hydroxy-4-oxoquinoline-7-carboxylic acid, AP4 , 90	134
 Table 1-1: Diseases caused by <i>P. aeruginosa</i>	16
Table 1-2: Virulence factors produced and used by <i>P. aeruginosa</i>	17
Table 1-3: Resistance mechanisms of <i>P. aeruginosa</i>	23
Table 1-4: Examples of vaccines and antibodies developed against <i>P. aeruginosa</i>	33
Table 1-5: Examples of Gram-negative bacteria that have been reported to use AHL and HAQ derivatives.	38
Table 1-6: QSS-controlled virulence factors.	44
Table 5-1: Mean titres obtained from the terminal bleed for each mouse per conjugate.....	91

Table 6-1: Concentration at which significant ($p = < 0.05$) inhibition of the anti- AP1 pAb binding to AP1 -BSA occurred (μM).....	101
Table 6-2: Concentration at which significant ($p = < 0.05$) inhibition of the binding of anti- AP2 pAb to AP2 -BSA occurred (μM).	102

ABBREVIATIONS

Δ	Heat
Δ	Knockout/gene mutation
$^{\circ}\text{C}$	Degrees centigrade
(g)	Gaseous
Ab	Antibody
ADCC	Antibody-dependent cell cytotoxicity
Ag	Antigen
AHL	Acylated homoserine lactone(s)
AI	Auto-inducer
AIDs	Acquired immune deficiency syndrome
ANOVA	Analysis of variance
AP	(S)-3-amino-pyrrolidin-2-one
APC	Antigen presenting cell
aq.	Aqueous
ASB-14	Amidosulfobetaine
$\text{BF}_3 \cdot \text{Et}_2\text{O}$	Boron trifluoride diethyl etherate
BMSU	Biomedical Services Unit
Bn	Benzyl
BnOH	Benzyl alcohol
Boc_2O	Di-tert-butyl dicarbonate
br. s	Broad singlet
Br_2	Bromine
BSA	Bovine serum albumin
BuOH	Butanol
C	Carbon
$\text{C}_5\text{H}_5\text{N}$	Pyridine
cat.	Catalytic
CAUTI	Catheter associated urinary tract infections
CBT	Checkerboard titrations
Cbz	Benzyloxycarbonyl
CDCl_3	Deuterated chloroform
CF	Cystic fibrosis
CFTR	Cystic fibrosis transmembrane conductance regulator
CO_2	Carbon dioxide
conc.	Concentrated
COX-2	Cyclo-oxygenase-2

CSA	Camphorsulfonic acid
CuI	Copper iodide
Da	Daltons
DC	Dendritic cells
DCC	<i>N,N'</i> -dicyclohexylcarbodiimide
dd	Doublet of doublets
dH ₂ O	Deionised water
DIC	<i>N,N'</i> -diisopropylcarbodiimide
DIPEA	<i>N,N</i> -diisopropylethylamine
DIU	Diisopropylurea
DMAP	4-(Dimethylamino)pyridine
DMF	Dimethyl formamide
DMSO	Dimethyl sulfoxide
DMSO-d ₆	Deuterated dimethyl sulfoxide
DNP	Dinitrophenyl
DTT	Dithiothreitol
ECDC	European Centre for Disease Prevention and Control
EDC	1-Ethyl-3-(3-dimethylaminopropyl)carbodiimide
ELISA	Enzyme linked immunosorbent assay
ESBL	Extended spectrum β -lactamase
Et ₂ O	Diethyl ether
Et ₃ N	Triethylamine
Et ₃ N.3HF	Triethylamine trihydrofluoride
EtBr	Ethyl bromide
EtOAc	Ethyl acetate
EtOH	Ethanol
Exo	Exoenzyme
FCA	Freund's complete adjuvant
FMNH ₂	Flavin mononucleotide (reduced)
FT-IR	Fourier-transform infrared spectroscopy
g	Grams
GacS/GacA	Global antibiotics and cyanide
GFP	Green fluorescent protein
H	Proton
h	Hour(s)
H ₂	Hydrogen
H ₂ O	Water
H ₂ O ₂	Hydrogen peroxide
HAQ	2-alkyl-4(1 <i>H</i>)-quinolone
HATU	<i>N,N,N',N'</i> -Tetramethyl-O-(7-azabenzotriazol-1-yl)uronium

	hexafluorophosphate
HCl	Hydrochloric acid
HCO ₂ H	Formic acid
HHQ	2-Heptyl-4(1 <i>H</i>)-quinolone
HMAQ	2-Alkyl-3-methyl-4(1 <i>H</i>)-quinolone
HMWPS	High molecular weight polysaccharides
HOBt	Hydroxybenzotriazole
HR-ESI-MS	High resolution-electrospray ionisation-mass spectrometry
Hz	Hertz
IC ₅₀	Half maximal inhibitory concentration
IEF	Isoelectric focussing
IFA	Incomplete Freund's adjuvant
IFN- α	Interferon-alpha
Ig	Immunoglobulin
IL	Interleukin
IPG	Immobilised pH gradient
IR	Infra red spectroscopy
K ₂ CO ₃	Potassium carbonate
KBr	Potassium bromide
KDa	Kilodaltons
KH ₂ PO ₄	Potassium phosphate
KLH	Keyhole limpet haemocyanin
LB	Lysogeny broth
LES	Liverpool epidemic strain (cystic fibrosis <i>P. aeruginosa</i>)
LiCl	Lithium chloride
LPS	Lipopolysaccharide(s)
m	Multiplet
M	Molar (moles per litre)
<i>m/z</i>	Mass to charge ratio
Mab	Monoclonal antibody
MALDI-TOF	Matrix assisted laser desorption ionisation-time of flight spectrometry
<i>m</i> -CPBA	<i>meta</i> -Chloroperoxybenzoic acid
MDR	Multi-drug resistant
Me	Methyl
Me ₂ CuLi	Dimethylcopper lithium
MeCN	Acetonitrile
MeLi	Methyl lithium
MeOH	Methanol
mg	Milligram(s)
Mg	Magnesium

MgSO ₄	Magnesium sulfate
MHC	Major histocompatibility complex
MHz	Megahertz
Min	Minute(s)
mL	Millilitre(s)
mM	Millimolar
mmol	Millimole(s)
MoA	Mode of action
mol	Mole(s)
Mp	Melting point
M_r	Relative molecular mass
MRSA	Methicillin-resistant <i>Staphylococcus aureus</i>
MS	Mass spectrometry
MW	Microwave irradiation
MWCO	Molecular weight cut-off
N ₂	Nitrogen
Na ₂ HPO ₄ ·7H ₂ O	Dibasic sodium phosphate heptahydrate
NaCl	Sodium chloride
NaHCO ₃	Sodium hydrogen carbonate
NaOH	Sodium hydroxide
NH ₄ Cl	Ammonium chloride
NH ₄ HCO ₃	Ammonium formate
NHS	<i>N</i> -hydroxysuccinimide
NK	Natural killer cells
nM	Nanomolar
NMP	<i>N</i> -methyl-2-pyrrolidone
NMR	Nuclear magnetic resonance spectroscopy
NO	Nitric oxide
NuH	Nucleophile
O ₂	Oxygen
OD	Optical density
Opr	Outer membrane protein
OVA	Ovalbumin
pAb	Polyclonal antibodies
PAMP	Pathogen associated molecular pattern
PBS	Phosphate buffer saline
PBST	Phosphate buffer saline-tween
PBST-M	Phosphate buffer saline-tween-milk powder
Pd-C	Palladium on carbon
PE	Petroleum ether

PGE ₂	Prostaglandin E ₂
Ph ₂ O	Diphenyl ether
pI	Isoelectric point
pIgG	Polyclonal immunoglobulin G
pM	Picomolar
PMN	Polymorphonuclear cell(s)
pmol	Picomole(s)
PPA	Polyphosphoric acid
PPK	Polyphosphate kinase
PQS	<i>Pseudomonas</i> quinolone signal; 2-Heptyl-3-hydroxy-4(1 <i>H</i>)-quinolone
PRR	Pattern recognition receptor
PS	Polysaccharide(s)
<i>p</i> TsOH	<i>para</i> -Toluenesulfonic acid
QS	Quorum sensing
QscR	Quorum sensing control regulator
QSS	Quorum sensing system
QSSi	Quorum sensing system inhibitor(s)
QSSM	Quorum sensing system molecule(s)
RBF	Round bottom flask
R _f	Retention factor
rpm	Rates per minute
Rsm	Regulator of secondary metabolites
rt	Room temperature
s	Singlet
s/c	Sub-cutaneous
SAM	(<i>S</i>)-adenosylmethionine
scAb	Single chain antibody
SD	Standard deviation
SDS	Sodium dodecyl sodium
SDS-PAGE	Sodium dodecyl sodium-polyacrylamide gel electrophoresis
SO ₂ Cl ₂	Sulfuryl chloride
spp.	Species
t	Triplet
<i>t</i> -BuOH	Tertiary butanol
<i>t</i> -BuOK	Potassium tertiary butoxide
T _C	Cytotoxic T-lymphocytes
td	Triplet of doublets
TFA	Trifluoroacetic acid
T _H	T-helper lymphocytes
THF	Tetrahydrofuran

TIPSOTf	Triisopropylsilyl trifluoromethane sulfonate
TLC	Thin layer chromatography
TLR	Toll-like receptor
TMB	3,3', 5,5'-Tetramethylbenzidine
TMSCl	Trimethylsilyl chloride
TNBS	2,4,6-Trinitrobenzenesulfonic acid
TNF- α	Tumour necrosis factor-alpha
US-FDA	United States - Food and drug administration
UTI	Urinary tract infection
VfR	Virulence factor regulator
VqsM	Virulence and quorum sensing modulator
VqsR	Virulence and quorum sensing regulator
w	Watt
WT	Wild-type

1 INTRODUCTION

1.1 COLONISATION, INFECTION AND DISEASE

Pseudomonas aeruginosa, a Gram-negative bacterium, can survive in many different environments, such as soil, marshes or water, including harsh conditions such as high temperatures (42 °C) or in low O₂ (1). *P. aeruginosa* is an opportunistic pathogen of animals and humans; it is considered to be one of the major causes of nosocomial infections, presumably as the pathogen can survive on dry surfaces for up to 16 months (2) and can colonise on sinks, floors, toilet surfaces and dialysis machines and the other ‘in-dwelling’ appliances (3). If allowed, *P. aeruginosa* can infect any site of the immunocompromised host to cause various clinical conditions (Table 1-1), such as pneumonia, urinary tract infections, and complications in clinical burns, wounds, and cystic fibrosis (CF) (4).

Respiratory tract infections

Bacteraemia and septicaemia

Otitis externa

Skin conditions: ecthyma gangrenosum, pyoderma, folliculitis, acne vulgaris

Eyes: ulcerative keratitis, endophthalmitis, neonatal ophthalmia

Rare conditions: meningitis; endocarditis; peri-rectal infections and specific forms of osteomyelitis

Table 1-1: Diseases caused by *P. aeruginosa*.

Adapted from (4).

The pathogenicity of *P. aeruginosa*, once it has adhered and colonised, is due to the diverse virulence factors that contribute to disease aetiology. Table 1-2 lists some of the virulence factors produced and used by *P. aeruginosa*, however, the virulence phenotype of *P. aeruginosa* is subject to change depending on the site of infection, the primary disease condition and progression.

Virulence factor	Action
Colonisation	
Flagella	Involved in motility, adherence, and invasiveness.
Pili	Adhesin and involved in transfer of type III secretions.
Exopolysaccharides,	Alginates are involved in adherence and pathogen persistence (biofilms, antibiotic and immune system effector resistance).
Lipopolysaccharide (LPS)	Endotoxin and an inflammatory agent, also involved in adherence and biofilms.
Invasion	
Alkaline protease	Degrades immune system components such as complement factors.
Elastase	Las B and Las A. Degrade elastin; disrupt membranes; impair monocyte chemotaxis and degrade complement proteins. Las B also destroys collagen, IgA and IgG and impairs wound repair.
Lipase A and C	Unknown role - possibly involved in degradation.
Phospholipase C	Haemolytic and disrupts lung surfactant.
Protease	Degrades complement factors, plasmin, IgG, and fibrinogen.
Pyocyanin	Inhibits lymphocyte proliferation; causes apoptosis of neutrophils; impairs mucocilliary motility by stimulating production of H ₂ O ₂ by polymorphonuclear (PMN) cells.
Siderophores	Pyoverdine and pyochelin are iron scavengers. Pyoverdine regulates secretion of exotoxin A and proteases.
Pathogenesis	
Exotoxin A	Unknown role - possibly causes apoptosis of eukaryotic cells.
Biofilm	Confers protection against biocides and immune system effectors as impenetrable to antibodies (Ab), antibiotics, and biocides.
Hydrogen cyanide	Unclear role – toxic agent.
Rhamnolipids	Dissolve phospholipids; cause apoptosis of leukocytes; impair mucocilliary motility and are solubilising agents.
Type III secretion system	Exoenzyme (Exo) S, T and Y, and exotoxin U. Exoenzyme S inhibits phagocytic motility; induces death of macrophages and PMNs and disrupts tight junctions of epithelial cells. Exotoxin U is cytotoxic to eukaryotic cells.

Table 1-2: Virulence factors produced and used by *P. aeruginosa*.

Adapted from (5-7).

1.1.1 BURNS AND WOUNDS

Skin and mucosa are part of the non-specific innate immune system, providing physical barriers against invading pathogens (8). However, wounds or burns disrupt the barrier and weaken the immune system, allowing opportunistic pathogens such as *P. aeruginosa* to take advantage. The hospital environment tends to cultivate the multi-drug resistant (MDR) *P. aeruginosa* strains, increasing the risk of complications caused by MDR pathogens. In burns, it is believed that alginate, pili, flagella, lipopolysaccharide (LPS), exotoxins of the type III system, elastase, siderophores and biofilms, which can be formed within 8 hours of infection (*in vitro*) (9), are key virulence factors produced by *P. aeruginosa* (7).

1.1.2 ULCERATIVE KERATITIS

Tears and blinking are further examples of non-specific innate defence mechanisms; tears contain lysozymes, amylase, and immunoglobulin (Ig) A, which can form antibody (Ab) and antigen (Ag) complexes stimulating the effectors of the innate immune response such as phagocytes (macrophages and PMNs). Pathogen associated molecular patterns (PAMPs) allow the immune system to recognise pathogenic antigens through the stimulation of appropriate pattern recognition receptors (PRRs) such as the toll-like receptors (TLR) (8, 10). *P. aeruginosa* protects itself from phagocytosis by releasing the adherent glycocalyx whilst the immunogenic LPS and flagella, typical PAMPs, bind to TLR-4 and TLR-5 respectively (6, 11), stimulate PMN activation and chemotaxis, exacerbating tissue damage in ulcerative keratitis (7).

1.1.3 CYSTIC FIBROSIS

Cystic fibrosis is a recessive genetic disorder; a mutation in the cystic fibrosis transmembrane conductance regulator (CFTR) causing impaired chloride ion transport. Development and function of certain organs (pancreas, intestines and the immune system) are affected and the condition is associated with a low life expectancy. Complications are usually caused by infections, acute or chronic, which promote tissue damage by continuous stimulation of the immune system effectors. *P. aeruginosa* is a leading pathogen in CF, often colonising young CF patients, and remaining throughout adulthood.

The CF lung is an extreme environment with nutrient and oxygen gradients. Oxygen gradients develop due to mucus plugs and increased consumption of epithelial cells, unique to CF (12). *P. aeruginosa* adapts and presents many phenotypes in this environment; it was found that the bacterial genome from one isolate from a single patient had acquired 68 mutations over 90 months (13). In acute *P. aeruginosa* infections, proteases, flagella, LPS with O-side chains (smooth LPS), elastase, and pyocyanin, contribute to the pathology in the lung (7, 11).

Chronic *P. aeruginosa* infections exist in biofilms, overproduce alginate, have no flagella, and produce rough LPS (no O-side chains) with decreased production of elastase, pyocyanin, and pyoverdine, typical of the mucoid phenotype. However, *P. aeruginosa* can revert to the non-mucoid state in the absence of selective pressure imposed by antibiotic therapy. Small colony variants, selected after prolonged antibiotic treatment, produce glucose- (*pel*) or mannose-rich (*psl*) polysaccharides and are hyper-piliated, which contribute to the persistent characteristic of this phenotype (13). Epidemic *P. aeruginosa* strains such as the Liverpool epidemic strain (LES) over-produce pyocyanin (14).

1.1.4 URINARY TRACT INFECTIONS

P. aeruginosa causes 35% of catheter-associated urinary tract infections (CAUTIs) (15). The genotype and phenotype of 30 CAUTI *P. aeruginosa* isolates were studied, a mixture of phenotypes were discovered; isolates from the CAUTI displayed biofilm formation, low motility, and were haemolysin and exoenzyme (Exo) S positive, in contrast, other isolates had decreased elastase, pyocyanin, and alginate production. It was noted that a specific phenotype, different from the isolates of the CF lung, was needed for *P. aeruginosa* to survive in catheters and urinary tracts (15).

1.1.4.1 INNATE IMMUNE EFFECTORS

The immune system is the natural defence against invading pathogens. The non-specific innate system will immediately respond upon stimulation of PRRs, initiating innate effector responses such as (a) phagocytosis by macrophages and PMN such as neutrophils, and dendritic cells (DC) (b) cell death (i) by natural killer (NK) cells that target infected or malignant cells or (ii) by the complement system via the membrane attack complex formed from complement proteins. The inflammatory response induced by various chemokines recruits the effectors to the site of infection. Continuous stimulation of the effectors by PAMPs and virulence factors result in tissue damage that can be irreversible (8, 10).

1.2 THERAPY AND ANTIBIOTIC RESISTANCE

Antibiotics are the traditional treatment for bacterial infections that the immune system is unable to contain and eradicate. The bactericidal mode of action (MoA) is different for each class of antibiotics; for example, β -lactams (penicillin and amoxicillin), and cephalosporins (cefalexin or cefradine) inhibit bacterial cell wall synthesis. Aminoglycosides (gentamicin, tobramycin) target bacterial ribosomes and inhibit protein synthesis, whilst fluoroquinolones (ciprofloxacin) prevent DNA repair and replication (16).

The anti-pseudomonal drugs include aminoglycosides, β -lactams (imipenam but not penicillins), 3rd and 4th generation cephalosporins, and fluoroquinolones. In addition, colistin, a

drug that has a poor side-effect profile, is now used against MDR *P. aeruginosa* strains. Prudent prescribing methods and early but aggressive antibiotic treatment have improved treatment outcomes of certain diseases such as CF. Strict hygiene protocols, separation of infected and susceptible but non-infected patients have also reduced transmission (17).

The consequence of the bactericidal MoA is survival of the fittest through selective pressure. Bacteria that are tolerant to an antibiotic are selected and establish in the absence of competition for environmental resources such as nutrients. An alternative class of antibiotic can circumvent specific antibiotic resistance. However, bacteria have developed some effective defence mechanisms leading to MDR species such as methicillin-resistant *Staphylococcus aureus* (MRSA), *Acinetobacter baumannii*, or *Escherichia coli*. *P. aeruginosa* has been promoted to ‘super bug’ status, as MDR strains have made eradication of these opportunistic pathogens difficult (18).

1.2.1 *P. AERUGINOSA* AND MECHANISMS OF RESISTANCE

Table 1-3 (p 23) summarises the mechanisms of resistance used by *P. aeruginosa* against antibiotics, which can be intrinsic, adaptive, or acquired. *P. aeruginosa* is innately resistant to many antibiotics; the intrinsic almost impermeable cell wall, outer membrane protein (Opr) channels (restrict substrate entry by size and hydrophobicity), and multi-drug efflux pumps additively give the bacteria a basal level of resistance to certain antibiotics. Higher therapeutic doses and extended treatment programmes will eventually result in complete resistance through continued exposure (18-24).

1.2.1.1 BIOFILMS

Once the pathogen has colonised as planktonic bacteria, the cells convert to the sessile state and form biofilms. These are hydrated structured matrices of exopolysaccharides and proteins, with a characteristic ‘slimy’ layer and can form on most surfaces from catheters to eukaryotic and prokaryotic cells. Biofilms are the real cause of persistent chronic infections; essentially impenetrable, the bacterial inhabitants are protected from biocides, thus physical removal of the biofilm through surgery is usually the only remaining treatment option (25, 26).

Biofilms often have heterogeneous bacterial populations owing to intra-species (genotype, phenotype and growth) and inter-species diversity; *P. aeruginosa* can comfortably exist as the dominant pathogen or in synergy with other pathogens such as Gram-positive *S. aureus* or Gram-negative *Burkholderia cenocepacia* respectively.

Biofilms have distinct microenvironments due to the heterogeneous bacterial population. Peripheral cells are metabolically active and consume most of the available oxygen, often causing oxygen gradients within the biofilm; deeper layers of the biofilm are usually hypoxic,

and bacteria are less metabolically active. Metabolic, actively growing bacterial cells, at the periphery of biofilms may be susceptible to antibiotics, provided the drug can penetrate the biofilm slime layer. Susceptibility to antibiotics varies with the phenotype and the progression of the infection (25, 27, 28).

P. aeruginosa acquires antibiotic resistance through inter- and intra-transfer of resistance genes. Biofilms are ideal environments for genetic transfer, during biofilm formation alone, numerous mutations occur, which can also result in antibiotic target modifications. The origin of fluoroquinolone-resistant strains has been linked to aquatic bacteria (22), whilst extended spectrum β -lactamase (ESBL) strains resistant to cephalosporins and carboxypenicillins (20) were the result of genetic transfer between *P. aeruginosa* and *Enterobacteriaceae* spp. (24).

Mechanism	Antibiotic	Notes
Intrinsic		
Low permeable membrane - OprF, OprB, OprD - Constitutive expression of efflux pumps Constitutive antibiotic degrading enzymes	Trimethoprim; ampicillin; amoxicillin; 1 st and 2 nd generation cephalosporin.	Constitutive enzymes include basal levels of β -lactamase.
Adaptive		
AmpC depression	Penicillins.	Increase of β -lactamase above basal levels.
Loss of OprD	Carbapenam.	
Up regulation of: - Multi-efflux pumps - MexA-MexB-OprM - MexE-MexF-OprN - MexX-MexY-OprM	β -Lactams; cephalosporins; aztreonam. β -Lactams including imipenam; fluoroquinolones Cefoperazone; meropenam; aminoglycosides; fluoroquinolones.	Ciprofloxacin is affected by the increased expression of the MexA-MexB-OprM.
Gyr/parE/parC	Fluoroquinolones.	Expression of gyrase and topoisomerase IV respectively are affected. This leads to the reduced binding affinity of fluoroquinolones.

Membrane changes	Polymyxin; aminoglycosides.	Mutations causing phenotypical changes to LPS results in colistin resistance.
Acquired		
β-Lactamases		
- ESBLs	Carboxypenicillins; cephalosporins; aztreonam.	Strains isolated in France; Greece; Poland; Turkey; Korea; China; Belgium, and South Asia.
- Metallo-β-lactamases	Carbapenam.	Isolated in Japan/Asia; South America; Greece and Italy.
Aminoglycoside-modifying enzymes	Gentamicin; tobramycin.	

Table 1-3: Resistance mechanisms of *P. aeruginosa*.

Adapted from (4, 18-24, 27).

1.2.1.2 THE PROBLEM OF RESISTANCE

In 2009, the European Centre for Disease Prevention and Control (ECDC) reported that *P. aeruginosa* resistance was stable in Europe. However, it was also reported that 23% (n = 8,376) of tested isolates were resistant to three or more of the five classes of antibiotics (fluoroquinolones, cefatazidine, aminoglycosides, carbapenams, piperacilin:tazobactam) (29). This is a concern, especially as the problem of MDR is not counter-balanced by new classes of anti-pseudomonal antibiotics.

The pharmaceutical industry is focussing on the improvement of antibiotic delivery to the respiratory tract, specifically in CF, examples include amikacin (inhaled or liposomal delivery) aztreonam with lysine (Cayston® US-FDA approved) and inhaled ciprofloxacin (30). New antibiotic drugs are being added to the existing classes of antibiotics (31), however, this does not equate to better anti-pseudomonal activity. Doripenam, a relatively new antibiotic, has only marginal increased anti-pseudomonal activity (18). Research and development of new classes of antibiotics is no longer a priority.

Antibiotic resistance is the consequence of the MoA, therefore introducing new antibiotic drugs even with improved delivery may not solve the issue of resistance but simply slow the rate at which the bacteria develop resistance. The development of novel therapies that can enhance the natural or chemical eradication of bacteria without selective pressure may be the way forward.

1.3 ALTERNATIVE THERAPEUTICS

1.3.1 VACCINES AND ANTIBODIES

Vaccines are biological preparations that introduce the modified antigen to the naïve immune system in order to establish immune memory. An antigen is an umbrella term describing agents that are immunogenic, in other words, are able to stimulate an immune system response. This can include the whole pathogen or components of the pathogen, such as virulence factors - LPS is an example. Vaccines effectively provide the immune system with the capacity to recognise, contain, and eradicate the pathogen before the bacterium has the opportunity to colonise. Long-lived immunity against the pathogen is possible using a suitable native antigen, on the proviso that the pathogen does not significantly modify the native antigen so that it is no longer recognised by the primed immune system.

Specific antibodies generated against the antigen can be given to the host through passive immunisation. This therapy confers immediate and specific protection against the antigen provided the antibodies enhance innate effector responses or neutralise the antigen. However, the specific protection is dependent on the half-life of the exogenous antibody and does not provide long-term immunity. Antibodies can be polyclonal (pAbs), a mixture of antibodies

with diverse avidity to the various epitopes of the antigen, or monoclonal antibodies (Mabs), with specific affinity for an epitope of the antigen.

1.3.1.1 IMMUNE SYSTEM AND ANTIGENS

The immune system is divided into the innate immune system that provides immediate but non-specific defence against antigens, and the adaptive immune system, which on appropriate stimulation, will initiate a slower but specific response that acts to enhance the non-specific innate immune effectors and has memory. The dendritic cells, which are professional antigen presenting cells (APC), link the innate immune system to the adaptive immune system (Figure 1-1) (8, 32, 33).

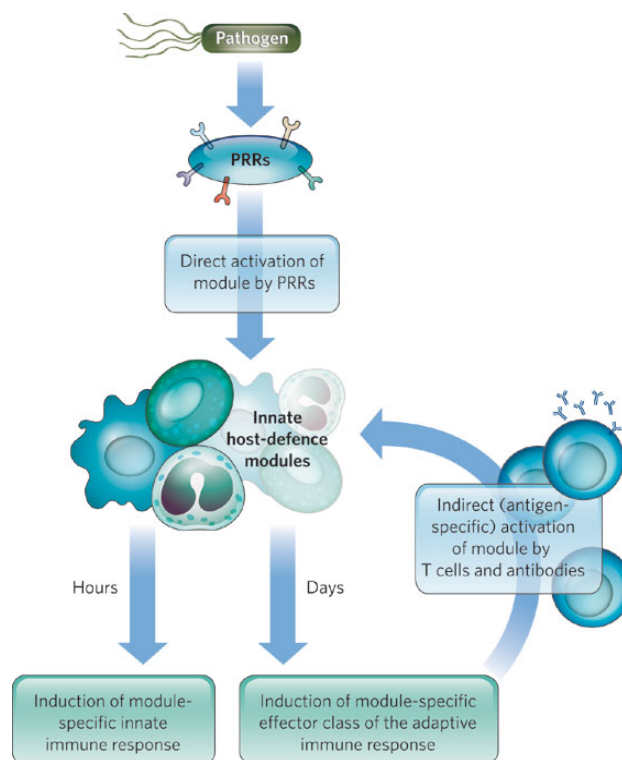


Figure 1-1: Innate and adaptive immune responses.

Image was taken with permission from 'Recognition of microorganisms and activation of the immune response' by Ruslan Medzhitov, (2007). Nature 449 (7164):819-826 (33). The diagram illustrates how the innate and adaptive systems are interconnected. Innate immune responses are activated by PAMPs, which activate innate immune effectors (referred to in this diagram and subsequent article (33) as modules) such as phagocytes, PMNs, NK cells, and complement system proteins. These are enhanced by the adaptive immune system effectors, controlled by T- and B-lymphocytes.

The specific adaptive immune system has two responses, the cellular response, which is carried out by cytotoxic (T_C -, $CD8^+$) lymphocytes and the humoral response, which is the production of antibodies by B-lymphocytes. The peptide antigen is internalised by resident dendritic cells

- the mechanism of internalisation depends on whether the antigen is exogenous or endogenous in relation to the host cell. This dictates the method of processing and presentation, as well as the adaptive response (8, 32, 33). The next section refers only to exogenous antigens.

Dendritic cells process the exogenous antigens into short peptides revealing numerous epitopes. These are combined with major histocompatibility complex-II peptides (MHC) and are presented to naïve $CD4^+$ T-lymphocytes termed T-helper (T_H) lymphocytes in co-ordination with specific T-lymphocyte receptors and co-stimulatory signals. Depending on the cytokines released by the dendritic cells, the uncommitted T_H -lymphocytes will differentiate to T_H1 -, or T_H2 -lymphocytes, (naïve T_H -lymphocytes can also differentiate to T_H17 -lymphocytes, which are involved in protection against fungi and extracellular bacteria), each with different functions. T_H1 -lymphocytes release specific interleukins (IL) and cytokines that (a) activate the $CD8^+$ T_C -lymphocytes, initiating the cytotoxic cellular response causing cell death; (b) enhance phagocytosis by macrophages, which are also APCs; and (c) stimulate B-lymphocyte production of antibodies, specifically immunoglobulin (Ig) G_2 . These enhance innate immune effector responses against intracellular pathogens. T_H2 -lymphocytes, via cytokines and ILs, activate B-lymphocyte production of IgE, and innate effector cells including mast cells, basophils and eosinophils, to mediate protection against parasites (8, 32, 33).

B-lymphocytes are professional APCs, and will present the processed antigen as a MHC-II complex to naïve T_H -lymphocytes, or become activated in a T_H -lymphocyte dependent manner. Activation is supported by specific co-stimulatory signals and the cytokines released by the T_H -lymphocytes, which determines the class of Ig produced. Cytokines are important for B-lymphocyte differentiation to antibody-producing plasma with isotype switching and affinity maturation, and memory cells. This is absent in independent T_H -lymphocyte activation of B-lymphocytes, by antigens such as LPS that bind to the TLR-4 expressed by B-lymphocytes (8, 32, 33).

1.3.1.2 ANTIBODIES

An immunoglobulin (Ig) is a Y-shaped protein, with two identical heavy chains and two identical light chains held together by disulfide bridges. Ig have an antigen binding domain, termed the Fab region, and the effector domain, F_C , which binds to complement proteins and receptors of effector cells (8). Depending on the isotype, antibodies enhance the innate effector responses by (a) stimulation of phagocytosis through opsonisation of antigen; (b) activation of the membrane attack complex by stimulating the classic complement pathway; (c) stimulation of NK cells via the antibody-dependent cell cytotoxicity response (ADCC) or (d) neutralisation of the antigen.

Human Ig is divided into five isotypes depending on the heavy chain, IgG, IgM, IgA, IgE, and IgD. IgG is divided into four subclasses that vary in biological effect, collectively IgG is

involved in opsonisation and activation of the complement system. IgG is expressed in secondary immune response after isotype switching from IgM. IgM is the first Ig produced in primary immune response and is a strong activator of the complement system. IgA prevents bacterial colonisation, IgE is involved in hypersensitivity responses and IgD are membrane receptors although their biological effector role is unknown (8, 32).

1.3.1.3 VACCINE INDUCED IMMUNITY

Upon appropriate stimulation, T_H-, T_C-, and/or B-lymphocytes will differentiate into effector and memory lymphocytes. These memory lymphocytes can circulate or remain in the lymph node, but are easier to activate and depending on the half-life, are present in greater numbers than the naïve uncommitted counter-parts. A vaccine antigen is processed as described above and induces the primary response.

Figure 1-2 (34) depicts the processes involved in the primary response, whilst Figure 1-3 (p 29) illustrates the difference between the primary and secondary response. Primary response is muted in regards to the speed of response, which can take days to weeks (Figure 1-1, p 25), and protective IgG concentration. IgM is produced in a relatively higher concentration in the primary response and the isotype switch to IgG is slow resulting in relatively low titres of the protective IgG. In contrast, due to the easily activated memory lymphocytes, when the immune system encounters the antigen in the native form or on re-exposure through secondary infection, the protective specific response of the adaptive immune system is strong, quick and persists for longer periods. The protective immunity depends on the half-lives of the memory lymphocytes, but can be maintained with boosters.

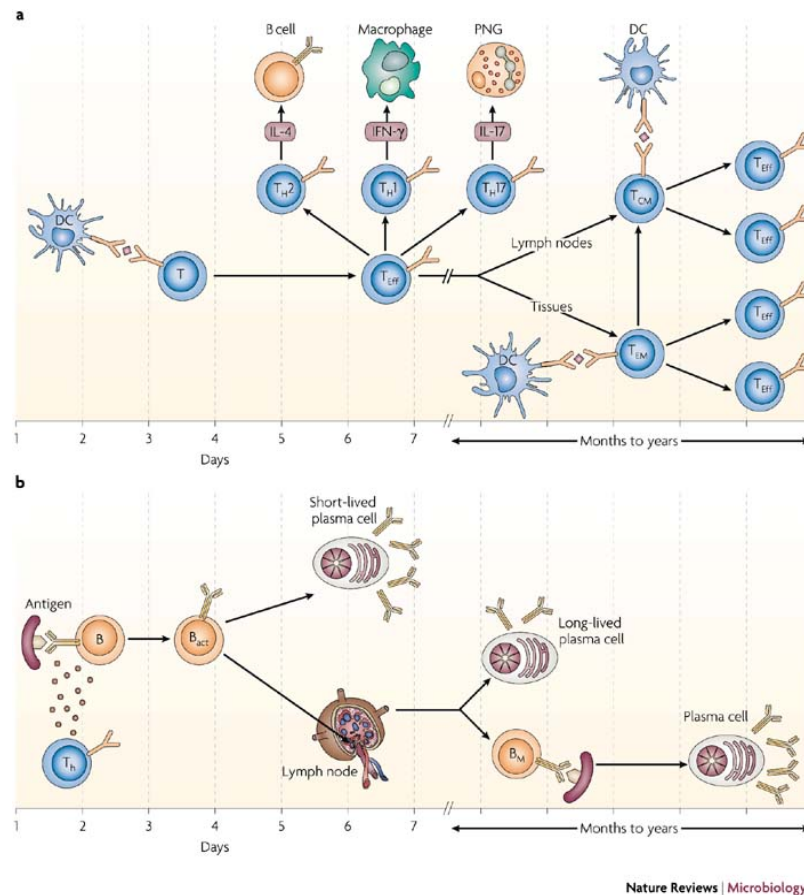


Figure 1-2: The adaptive immune response.

Image taken with permission from ‘The contribution of immunology to the rational design of novel antibacterial vaccines.’, by Stefan Kaufmann, (2007). Nature Reviews Microbiology 5 (7):491-504 (34).

(a) The effector T-lymphocytes (T_{EFF}) refers, in this context, to activated T-lymphocytes. T_{CM} refers to central memory T-lymphocytes that reside in the lymph nodes while the T_{EM} refer to migrating memory T-lymphocytes. (b) B_{act} refers to activated B-lymphocytes, which differentiate according to cytokine environment. DC (dendritic cell); IFN, (interferon), which is a cytokine; IL (interleukin); PNG, (polymorphonuclear granulocyte), in this context, refers to PMNs. The image depicts the immune system processes and the differentiation to memory cells. Memory cells can have half-lives of months to years. The secondary response upon re-exposure to the antigen is quicker and stronger as the memory cells are in greater numbers and are easily activated.

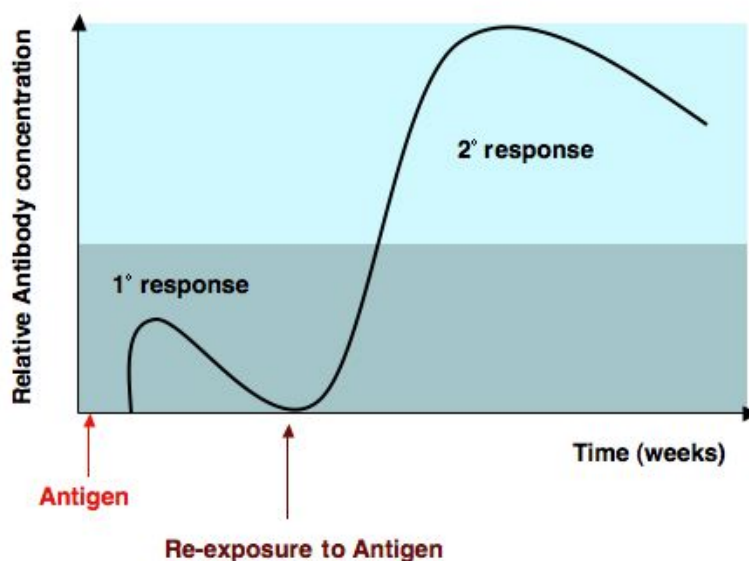


Figure 1-3: Immune system response to secondary exposure to antigen.

Adapted from (8, 32). The primary response to the antigen is slow and muted in terms of protective antibody concentration and the half-life of the response. IgM (not indicated) is the abundant antibody and IgG (indicated, black solid line) is produced subsequent to isotype switching in lower concentrations. However, upon re-exposure to the antigen, the immune response is rapid, with a high concentration of protective IgG. This response can persist for longer periods in comparison to the primary response. IgM (not indicated) is produced in low amounts as isotype switching occurs more rapidly.

1.4 ANTI-PSEUDOMONAL VACCINES AND THERAPEUTIC ANTIBODIES

The potential of anti-pseudomonal vaccines, as a prophylaxis for susceptible patients pre-empting *P. aeruginosa* infections, or therapeutic antibodies, is viable. Susceptible patients refer to persons with a compromised immune system resulting from conditions such as CF, acquired immune deficiency syndrome (AIDs), diabetes mellitus, or treatment such as chemotherapy or immune suppression (7). Bacterial vaccines have successfully been used to eradicate smallpox and for efficient immunisation programs against diphtheria, tetanus and pertussis to name a few (8). However, despite the considerable research into anti-pseudomonal vaccines, there is still no successful anti-pseudomonal vaccine on the market (35, 36).

Live or attenuated vaccines introduce the antigen, which can be the inactivated whole cell, to the immune system. The antigen retains the native epitopes, and growth capacity, thus the immune system is exposed to the antigen for longer periods without the bacteria causing disease, although, there is a risk that the bacteria can revert to the native virulent form (8). In regards to *P. aeruginosa*, attenuated vaccines increased survival in animal models, however as discovered with the heptavalent LPS vaccine, Pseudogen[®], the immunogenicity of the lipid moiety of LPS proved too toxic, resulting in a poor safety profile; this vaccine has not been developed further (35). Various experimental vaccines and therapeutic antibodies have been

designed against certain virulence factors of *P. aeruginosa*. Table 1-4 (p 33) lists some of the vaccines and antibodies against *P. aeruginosa* that have been investigated (35, 36).

Conjugate vaccines refer to antigens that are conjugated to an immunogenic carrier in order to stimulate the T- and B-lymphocytes dependent responses. For efficient vaccine programmes, the T- and B-lymphocytes need to be activated. Aerugen[®], an O-polysaccharide octavalent conjugate vaccine, showed promising results in phase II trials but failed to show any benefit in phase III trials (36). Based on these results, the development and use of anti-pseudomonal vaccines in CF, were not recommended (37).

Unfortunately, *P. aeruginosa* can tailor the virulence factor phenotype to suit the site of infection and disease state. Therefore, vaccines based on single virulence factors such as alginate or exotoxin A may not be appropriate for all pathologies, as the virulence phenotype differs according to site of infection (as described in 1.1.1 - 1.1.4, p 16-19). Some of the investigated vaccines (Table 1-4, p 33) are strain specific, which is due to the targeted virulence factors. *P. aeruginosa* infections are heterogeneous in regards to isolates, thus the vaccine must confer protection against *P. aeruginosa* rather than specific isolates; for example, in the case of conjugate vaccine, outer membrane protein (Opr) F-OprI-flagellin A and B was protective against non-mucoid strains but less protective against mucoid strains, which did not express flagella. Mucoid strains are common in chronic *P. aeruginosa* CF infections.

Vaccines based on the conserved OprF show potential strain cross-reactivity. OprF, an outer membrane porin, allows non-specific diffusion of small molecules (below 1519 Da) such as polysaccharides (38). OprF is involved in modulating virulence of *P. aeruginosa*; Fito-Boncompagni observed reduced toxicity of an *oprF* mutant (*P. aeruginosa* H636), which the authors attributed to poor eukaryotic cell adhesion and considerably decreased production of virulence factors pyocyanin, exotoxin A and lectin PA-1L, and delayed elastase production (38). DNA vaccines are plasmids that contain the genetic information for the antigen. On immunisation (intra-muscular) the DNA is incorporated into the host muscle cell and dendritic cells and the antigen is expressed, inducing a cell and humoral immune response resulting in immune memory (8). OprF-OprI DNA vaccines are protective however the method of immunisation, either by gene gun or by intramuscular electroporation (imePT), impacts on the efficacy of the vaccine (39).

Passive immunisation has also been investigated, antibodies against exotoxin A, flagella and OprF increased the incidents of survival in infected mice (35, 36); a human IgM Mab against *P. aeruginosa* serotype O11 has shown clinical benefit with 100% survival of patients with hospital-acquired pneumonia (40). Passive immunisation as adjunct treatment with antibiotics such as piperacillin provided strain specific protection (41).

Vaccine	Results
Live/attenuated/purified vaccines	
Exotoxoid A	93.8% (n = 48) pre-immunised mice survived after inoculation with <i>P. aeruginosa</i> .
OprF-OprI ((Al(OH) ₃) (systemic) or OprF-OprI with attenuated <i>Salmonella typhi</i> (oral) or OprF-OprI (nasal)	Mucosal vaccines (oral and nasal) with systemic immunisations, produced long lasting Ig (6 months) when nasal and systemic vaccination was used in COPD. Healthy volunteers – nasal and oral vaccination resulted in OprF-OprI specific IgA at bronchial surface. Nasal vaccination induced serum Ab response. Well tolerated and
Met-Ala-(His)6OprF190-342-OprI21-83	resulted in increase in IgG and IgA in burn patients.
Peptide immunogen of receptor binding domain of type IV pilus	pAb produced against peptide immunogen (carrying key amino acids from two strains PAK and PAO) were cross-reactive for two strains of <i>P. aeruginosa</i> .
Attenuated <i>P. aeruginosa</i> PAO1ΔaroA	Protective against certain O2/O5 serogroups but not all LPS-serogroups.
Alginate	Poorly opsonic Ab. Not considered protective.
Elastase-alkaline phosphatase-exotoxin A toxoids	Used in combination increases survival in immunocompromised gut sepsis mouse model.
OprI	Protective as an oral vaccine. No Abs produced in mice.
Flagella or Flagellin type A and B	Anti-serum against flagella was opsonic, 83.3% mice survived against infection with PAK strain of <i>P. aeruginosa</i> , whilst anti-serum against flagellin was not significantly opsonic.
DNA vaccines	
OprF-OprI	Protective.
OprF	No further development.
Mutated/modified gene of exotoxin A	No further development.

Conjugate vaccines

OprF-OprI-Flagellin A and B	Protective (mouse model) against non-mucoid strains (<i>P. aeruginosa</i> PAO1, PAK and 1286) less protective against mucoid strains.
PcrV	Type III system effector translocation protein. 50% mice survived to day 10 vs. 20% mice (placebo). Survival was increased to 60% with anti-toxin.
High molecular weight polysaccharides (HMWPS)	<i>N</i> -acetyl-fucosamine and glucose PS components . Protective Abs produced with possible weak serotype cross-reactivity.
Pseudogen [®] Heptavalent vaccine prepared from 7 LPS O-polysaccharide serotypes	Poor safety profile. No clinical benefit in CF patients. Exacerbated certain disease conditions.
Aerugen [®] Octavalent vaccine based on 8 O-polysaccharide serotypes conjugated to exotoxin A	Failed to show any protection in randomised trial (phase III).
Non-integral outer membrane proteins	Enhanced clearance of <i>P. aeruginosa</i> from lungs.
AdC70-OprF	Prolonged survival in mice (7-12 days) vs. placebo (0-3 days).
Pilin-exotoxin A	
Pilin-tetanus	
Alginate-PS	Poor immunogen; antagonistic immune response.
D-Alginate-exotoxin A	Opsonic antibody response to 2 strains of <i>P. aeruginosa</i> . Abandoned.
Mucoid exopolysaccharide (MEP) -alginate-KLH	Pre-clinical trials. Protective specific IgG, which showed cross-reactivity to 6 CF clinical mucoid isolates.
Alginate-tetanoid	Protective against alginate producing strain.

Polymannuronic acid-Flagellin	Anti-sera (intra-nasal) enhanced pulmonary clearance by reducing the colony forming units of mucoid strains by 71.5 -85.5% after 4 hours. Protective in acute pneumonia model infected with non-mucoid strains.
Passive immunisation	
Mab F429	Human IgG ₁ monoclonal antibody against alginate. Therapeutic protection in ulcerative keratitis against mucoid producing strains. Prophylactic protection due to reduced internalisation of specific mucoid strains.
Fab 1A8	Engineered human Fab specific for PcrV. Protective in PA13 pneumonia/sepsis mouse model. Comparable to MA166, the murine Mab against PcrV.
KB001: Pegylated Fab' against PcrV from humanising murine MAb 166	Protective against strains expressing PcrV.
Anti-PS human IgG2 against 9 O-specific side chains (different serotypes)	Serotype specific. Protective in an immunocompromised sepsis mouse model.
Gamimmune-N [®] and Gammagard [®] S/D	Dose-dependent survival (10 days) of a burn model infected with of M2 (73%), MSR17072 (47%), and IFO3455 strain (82%). (% of surviving mice).
Ps-IVIg	Pooled human plasma, which has elevated titres against <i>P. aeruginosa</i> . Showed transient clinical improvement.
Antibiotic and passive immunisation	
Piperacillin and human anti-LPS IgG and pooled plasma Ig preparation	Strain specific in murine thigh infection.
Ceftazidime and murine MAb Ld3-2F2 to LPS	Used for MDR and non-MDR strains in burn models.

Table 1-4: Examples of vaccines and antibodies developed against *P. aeruginosa*.

Adapted from (35, 36, 41-61).

1.4.1 SUMMARY

P. aeruginosa is an opportunistic bacterium with innate resistance to many available antibiotics. The pathogen causes clinical complications in burns, wounds, and CF. Therapeutic options are now limited to isolation of infected patients and aggressive antibiotic therapy. The pathogen is difficult to treat due to the effective resistance mechanisms, consequently, the selection of anti-pseudomonal antibiotics is slowly shrinking due to emerging MDR strains.

P. aeruginosa efficiently adapts to the site of infection and it seems that the pathogen cleverly selects the virulence factors appropriate for the environment, thus presenting diverse phenotypes with varying susceptibility to antibiotics. Immunological targeting of virulence factors through active or passive immunisation, acts to neutralise the damaging effects of virulence factors, and effectively attenuates the pathogenicity. Extensive research has been conducted into anti-pseudomonal vaccines and therapeutic antibodies, but none have remained on the market.

The disadvantage of the anti-pseudomonal vaccines and therapeutic antibodies listed in Table 1-4 (p 33) is the conferred protection is specific for the strain and this may limit the viability of active and passive immunisation in all *P. aeruginosa* disease pathologies. In other words, immunisation may only be suitable in conditions infected with the specific strains, it may not be protective against the diverse phenotypes presented by each strain. Targeting conserved antigens such as OprF-OprI appears to be the better option, further study will indicate if cross-strain conferred protection is possible.

It should be noted that for the production of toxic virulence factors (Table 1-2, p 17), *P. aeruginosa* has to colonise and establish. Flagella and pilin help this process, and targeting such virulence factors increases survival of strain-specific infected models (Table 1-4, p 33). A secondary response, which is relatively quicker than the primary response, still requires day(s) to produce protective antibodies, *P. aeruginosa* can colonise, establish and form biofilms (and no longer express flagella at this point) within hours. A similar situation is applicable to all the virulence factors (Table 1-2, p 17). However, active immunisations against bacterial infections have been successful; the prospect of long-lived immunity against *P. aeruginosa* emphasises the benefits of active immunisation. An alternative target is needed, so the host has sufficient time to generate protective antibodies, which are still useful before the pathogen has released virulence factors, resulting in unmanageable pathogenicity.

1.5 REGULATORY SYSTEM FOR VIRULENCE FACTOR PRODUCTION - POTENTIAL TARGET

1.5.1 QUORUM SENSING

Quorum sensing (QS) is a system used by Gram-positive and Gram-negative bacteria for intra- and inter-species communication, a method to sense the immediate environment. Several systems have been characterised, such as those from *Vibrio fischeri*, *P. aeruginosa*, and *S. aureus*. Essentially, bacteria release small quorum sensing system molecules (QSSM) into the immediate environment (Figure 1-4, p 36), as bacteria proliferate the concentration of the QSSMs increase until a particular concentration is reached. This indicates that the bacteria have reached the quorum, with this 'information' bacteria can act as a co-ordinated entity, participating in social behaviours (62), which benefit the pathogen; such as colonisation of the site of infection without alerting the host's immune system. The pathogen's virulence factors are immunogenic, therefore if only released when the pathogen has established and the number of bacterial cells is higher, the immune system once stimulated is unable to contain and eradicate the pathogen effectively, which may have otherwise been possible during colonisation. Thus, the quorum sensing system (QSS), a highly adaptable system, regulates the production of virulence factors in accordance with various factors such as nutrition, pH, and growth phase.

P. aeruginosa uses QS for inter-species communication. As briefly mentioned, *P. aeruginosa* is a co-infecter in many conditions, in particular CF. *Burkholderia cenocepacia* complex encompasses approximately 15 species and is common in older CF patients (63). Equally as difficult to treat as *P. aeruginosa*, the bacterium can communicate quite effectively with *P. aeruginosa* as it also produces derivatives of *P. aeruginosa* QSSMs (Table 1-5, p 38).

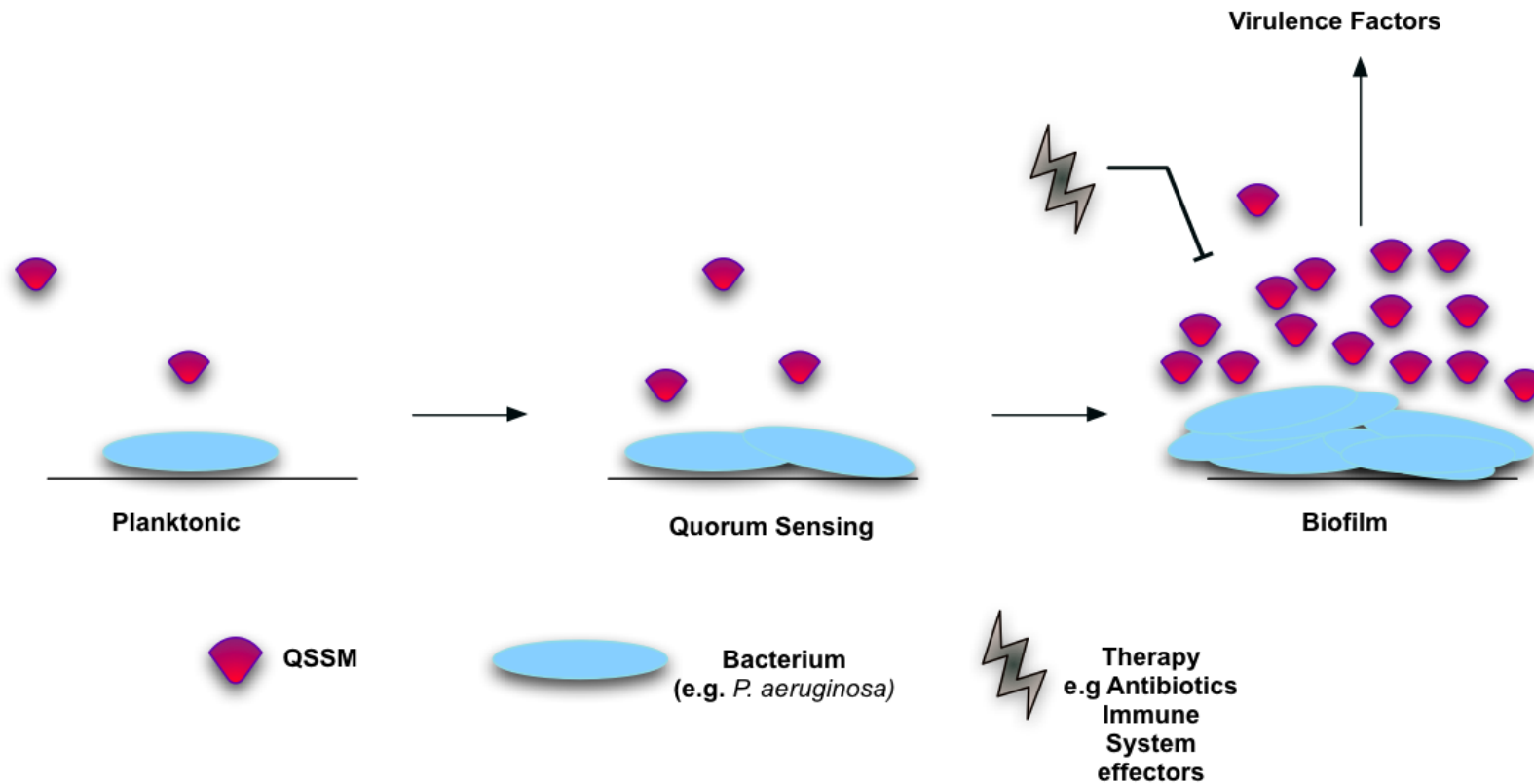


Figure 1-4: Depiction of QS in *P. aeruginosa*.

QS contributes to the pathogen's covert colonisation of the host. As the bacterium grows, QSSM are released into the environment. The optimum concentration of QSSM indicates the quorum has been reached. Bacteria act as a single entity and initiate co-ordinated QS-controlled responses, such as the maturation of biofilm and other damaging virulence factors. At this stage, the immune effectors are ineffective.

1.5.2 QSSM OF *P. AERUGINOSA*

QSSMs are termed auto-inducers (AI) as the molecule, as part of the transcriptional regulator protein complex, controls its own synthesis. In Gram-positive bacteria, the signal molecules are post-translationally modified proteins; *S. aureus*, for example, utilises cyclic oligopeptides. Other AI have been reported; AI-2, a furanosyl diester, is thought to be a common QSSM; certain Gram-positive bacteria such as *S. aureus* and Gram-negative bacteria such as *Salmonella typhi* produce AI-2. *P. aeruginosa* does not produce AI-2 but does respond to the QSSM. Enterohemorrhagic *E. coli* produce AI-3, which may be structurally similar to noradrenaline/adrenaline and is involved in inter-kingdom communication. *P. aeruginosa*, on the other hand, produces acylated homoserine lactones (AHL) QSSMs (Figure 1-5), *N*-3-oxododecanoyl-L-homoserine lactone **1**, and *N*-butanoyl-L-homoserine lactone **2** (64, 65).

P. aeruginosa produces approximately 55 2-alkyl-4(1*H*)-quinolones (HAQs), which have antimicrobial activity (66, 67). Two HAQs (Figure 1-5, **3** and **4**) are involved in QS, 2-heptyl-4(1*H*)-quinolone (**3**, HHQ) and 2-heptyl-3-hydroxy-4(1*H*)-quinolone (**4**, PQS; *Pseudomonas* quinolone signal). PQS is specific to *P. aeruginosa*, however, *Burkholderia* spp. use HHQ as a QSSM in inter-species communication (68) and produce a variety of 2-alkyl-3-methyl-4(1*H*)-quinolones (HMAQs) that may be used in QS (69, 70).

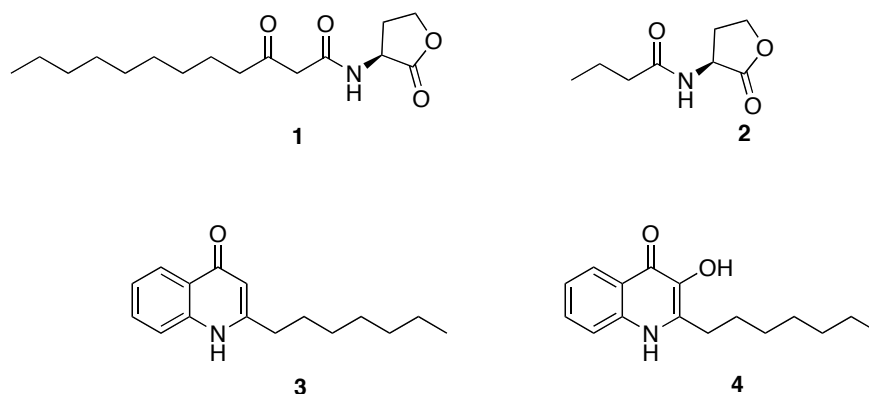


Figure 1-5: The QSSM of *P. aeruginosa*.

N-3-oxododecanoyl-L-homoserine lactone, (OdDHL, PAI-1, 3OC₁₂-HSL), **1**; *N*-butanoyl-L-homoserine lactone, (BHL, PAI-2, C₄-HSL), **2**; 2-heptyl-4(1*H*)-quinolone, (HHQ), **3**; and 2-heptyl-3-hydroxy-4(1*H*)-quinolone, (PQS, *Pseudomonas* quinolone signal), **4**.

1.5.2.1 QSSM OF OTHER GRAM-NEGATIVE BACTERIA

Table 1-5 lists the Gram-negative bacteria that have been reported to produce QSSM and have homologue QSSs, which contribute to the regulation of the pathogen's pathogenicity. Gram-negative bacteria produce AHLs that differ in acyl chain length and saturation, and by the substitution on the third carbon of the acyl chains. HAQs and HMAQs have been reported in only a few Gram-negative bacteria such as *B. cenocepacia* and *B. pseudomallei*.

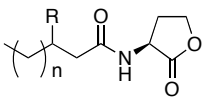
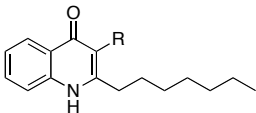
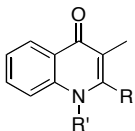
Bacteria	 $R = O, OH$ $n = 0 - 9$, saturated/unsaturated	 HHQ: $R = H$ PQS: $R = OH$	Significance
<i>Acinetobacter baumannii</i>	3OHC ₁₂ -HSL		MDR strains; nosocomial infections; wounds; burns; pneumonia.
<i>Aeromonas hydrophila</i>	C ₄ -HSL		Gastroenteritis and cellulitis in humans.
<i>Burkholderia cenocepacia</i> complex	C ₆ -HSL; C ₈ -HSL	HHQ; HMAQS:	Cystic fibrosis.
<i>Burkholderia pseudomallei</i>	C ₈ -HSL; C ₁₀ -HSL; 3OHC ₈ -HSL; 3OHC ₁₀ -HSL; 3OHC ₁₄ -HSL	 $R = CH_2(CH_2)_n, R' = H, n = 3 - 9$ $R = CH_2(CH_2)_n, R' = O, n = 3 - 9$ $R = CH:CH(CH_2)_n, R' = H, n = 3 - 9$ $R = CH:CH(CH_2)_n, R' = O, n = 3 - 9$	Biological warfare agent.
<i>Burkholderia mallei</i>	C ₈ -HSL; C ₁₀ -HSL		Glanders; biological warfare agent.
<i>Pseudomonas aeruginosa</i>	C ₄ -HSL; 3OC ₁₂ -HSL; 3OC ₈ -HSL; 3OC ₁₀ -HSL	HHQ; PQS	Nosocomial infections; cystic fibrosis; wounds; burns.
<i>Serratia marcescens</i> SS-1	C ₆ -HSL; 3OC ₆ -HSL		Nosocomial infections; wounds; urinary and gastro infections as well as catheter associated infections.
<i>Yersinia enterocolitica</i>	C ₆ -HSL; 3OC ₆ -HSL; 3OC ₁₀ -HSL; 3OC ₁₂ -HSL; 3OC ₁₄ -HSL		Yersiniosis.
<i>Yersinia pestis</i>	C ₆ -HSL; C ₈ -HSL; 3OC ₆ -HSL; 3OC ₈ -HSL		Plague; biological warfare agent.
<i>Yersinia pseudotuberculosis</i>	C ₆ -HSL; 3OC ₆ -HSL; C ₈ -HSL		Pathogen of animal and human.

Table 1-5: Examples of Gram-negative bacteria that have been reported to use AHL and HAQ derivatives.

Adapted from (71-73).

1.5.3 THE QUORUM SENSING SYSTEM (QSS) OF *P. AERUGINOSA*

The QSS of *P. aeruginosa* has three interlinked divisions, the Las, Rhl, and Pqs system. Each division is controlled by a specific QSSM.

1.5.3.1 INTERNAL QSS REGULATION

The protein components of the Las system are expressed by the transcriptional regulator gene, *lasR* and the synthase gene, *lasI*, which expresses LasI, responsible for the synthesis of the QSSM, 3OC₁₂-HSL **1** (Figure 1-5, p 37), which complexes with the LasR protein to control its synthesis by stimulating *lasI*, creating a positive feedback loop. LasR-3OC₁₂-HSL activates the expression of several virulence factors, as well as positively activating *rhlR*, *pqsH*, and *pqsR* of the Pqs QSS (Figure 1-6, p 42).

The transcriptional regulator *rhlR*, and the synthase *rhlI* express the protein components of the Rhl system. RhlI synthesises the AHL QSSM, C₄-HSL **2** (Figure 1-5, p 37), which complexes with RhlR to positively control its synthesis and activate or repress the production of virulence factors. This complex negatively regulates the Pqs system, although one report suggests that the complex has positive control over this system (74).

The Pqs system consists of the *pqsABCDE* and *phnAB* operons, which are stimulated under different conditions, but activate the biosynthesis of HHQ **3**. HHQ is the precursor to many of the HAQs produced by *P. aeruginosa*, but is converted by PqsH to PQS **4**. HHQ is also considered to have QSSM activity in *P. aeruginosa* and *Burkholderia* spp., which is one of the co-infectors in CF (63). PQS is specific to *P. aeruginosa* and complexes with PqsR to regulate specific virulence factors, which are also under the control of the Las and Rhl systems (Table 1-6, p 44) (71-73, 75).

1.5.3.2 GLOBAL REGULATION OF QSS

The global regulators of the QSS have been presented in Figure 1-4 (p 36). The QSS has two orphan transcriptional regulators, quorum sensing control regulator (QscR) and virulence and quorum sensing regulator (VqsR), which respond to AHLs of the *P. aeruginosa* QSS. QscR can repress or activate the Las/Rhl system under specific conditions to prevent early induction of QSS-controlled gene products, whilst VqsR positively controls the Las/Rhl system.

1.5.3.3 ENVIRONMENTAL REGULATION OF QSS

The environment controls the QSS and global regulators, contributing to the adaptability of *P. aeruginosa*; many QSS-controlled genes will only be activated in specific growth phases or in specific environments. Under conditions of iron deficiency, instigated by the host as a defence

mechanism (for example, the iron-binding lactoferrin) many QSS processes are up regulated. Low phosphate can lead to Las-independent activation and up-regulation of the Pqs system via the PhoB regulator (76-79).

This page has been left intentionally blank

Figure 1-6: The quorum sensing system (QSS) of *P. aeruginosa*.

This diagram illustrates the quorum sensing system of *P. aeruginosa* and the complex global regulatory system of QS. The dashed line (---) has been used to illustrate a figurative upper level separating the QSS and the global regulatory system. The global regulatory system regulates the quorum sensing system; the global regulatory system and the QS is dependent on the environment, native or of the host, at the site of infection ([]). QscR and VqsR are transcriptional regulators, whilst the virulence and quorum sensing modulator (VqsM) positively modulates the Las and Rhl system. RelA is important in essential amino acid deficiency whilst DksA is a co-factor of the substrate of the RelA protein. AlgR2 represses expression of RhlI and PPK1 (polyphosphate kinase) regulates the synthesis of AHLs. The virulence factor regulator (VfR) controls LasR and RhlR systems and corresponding virulence factors. PtxR negatively regulates Pqs and Rhl but positively regulates the Las system. Global antibiotics and cyanide (GacA/GacS) is a two-component regulatory system and positively regulates the QSS through RNA regulatory proteins (regulator of secondary metabolites, RsmAYZ). Hfq is also involved in this system and has positive regulatory effects on QscR and *pqsH*; RpoS and RpoN are stationary-phase sigma factors involved in stationary phase regulation of QSS. MvaT is important in biofilm and represses synthesis of HSL in low cell densities, PmpR negatively regulates Pqs and Rhl, and PpyR negatively regulates PQS synthesis. HHQ complexed with PqsR positively controls its synthesis and may have QSSM activity (represented by ?). PqsE may also regulate the virulence factors, pyocyanin and rhamnolipid independent of the PQS-PqsR complex, but still requires activation by this complex. Adapted from (72, 75-80).

1.5.4 QSS AND VIRULENCE

It is estimated that QSS controls up to 11% of the *P. aeruginosa* genome (81, 82), which consists of genes that control the expression of virulence factors. Table 1-6 lists the virulence factors and the controlling QSS. This is not an exhaustive list, especially as it has been shown that there may be genes, which have elements of QSS control but only under certain conditions (81, 82).

Las	Rhl	PQS
Alkaline protease	Alkaline protease	
Biofilm	Biofilm	Biofilm
Rhl		Rhl
Elastase	Elastase	Elastase
Lipase	Lipase	
	Pyocyanin	Pyocyanin
Hydrogen Cyanide	Hydrogen Cyanide	
Motility (Swimming, Swarming and Twitching)	Motility (Swarming and Twitching)	
	Siderophores	Siderophores
PQS	PQS	HAQ
	Lectins	Lectins
	Type III secretion system*	Type III secretion system*
	Rhamnolipids	Rhamnolipids
Exotoxin A		
Alginate		
Neuraminidase		
	Xcp secretion	
	Chitinase	
		RsmZ

Table 1-6: QSS-controlled virulence factors.

(* repressed). Adapted from (5, 7, 83, 84).

1.5.4.1 QSSM AS VIRULENCE FACTORS

Immune modulatory activity of the QSSMs, 3OC₁₂-HSL and PQS, have been reported with suggestions that the QSSMs appear to influence the adaptive behaviour of *P. aeruginosa*, thus are considered as virulence factors *per se*. 3OC₁₂-HSL induces apoptosis in dendritic cells and CD4⁺ T_H-lymphocytes (85); Jurkat T-lymphocytes (86); murine fibroblasts (87); mast cells (88); murine derived bone-marrow macrophages and neutrophils (89) at 6-100 μ M *in vitro*. PQS was cytotoxic to murine monocyte/macrophage J774A.1 at approximately 4 μ M *in vitro* (90). Although these data demonstrate apoptotic effects, it seems to be cell-line and study specific, as there are conflicting reports that suggest that 3OC₁₂-HSL and PQS do not induce apoptosis (91, 92).

3OC₁₂-HSL, PQS and HHQ reduced cytokine TNF- α production (90-93); indeed 1 μ M [PQS] was sufficient to inhibit the production of TNF- α and IL-6 *in vitro* (90). This is possibly physiological relevant as concentrations of up to 2 μ M [PQS] have been detected in CF sputum and bronchoalveolar lavage (94). IL-12 and IL-2 were negatively affected by 3OC₁₂-HSL and PQS. These chemokines promote the T_H1-lymphocyte-dependent immune responses specific for intracellular bacteria. 3OC₁₂-HSL increased the release of IL-4 and IL-10 (85) and IgG₁ (93, 95), indicators of the T_H2-lymphocyte-dependent response. 3OC₁₂-HSL interferes with dendritic cell maturation preventing the APC functionality as well inhibiting the differentiation of naïve T-lymphocytes, whilst both PQS and 3OC₁₂-HSL inhibit activated T-lymphocyte proliferation (92). These data suggest that 3OC₁₂-HSL and PQS induce a T_H2-lymphocyte-dependent immune response, albeit with different mechanisms (92). This response is protective against parasites and clearly beneficial for *P. aeruginosa* as presumably the typically induced T_H1-lymphocyte-dependent immune effector responses are inhibited. In addition, 3OC₁₂-HSL (96) and the metabolite, C₁₂-tetramic acid (97) have anti-microbial activity against *S. aureus*. PQS is involved in the regulation of HAQs, which have anti-microbial activity (67).

In contrast, 3OC₁₂-HSL promotes a T_H1 response. 3OC₁₂-HSL stimulated the release of COX-2 and PGE₂, pro-inflammatory cytokines, as well as IL-1 α and IL-6. These cytokines are involved in activation of macrophage release of pro-inflammatory mediators and antibody production respectively. Indeed, 1 μ M [3OC₁₂-HSL], which may also be within the physiological concentrations (up to 600 μ M [3OC₁₂-HSL] has been detected in biofilms *in vitro*), was sufficient to induce significant inflammation and tissue damage *in vivo* (98-100). The QSSM is a strong PMN chemotactant (101) and induces the release of chemotactant IL-8, at high concentrations (50 μ M) as well as demonstrating antagonistic activity towards peroxisome proliferators activated receptor (PPAR)- γ that inhibit pro-inflammatory processes (102). This appears to be detrimental to *P. aeruginosa*, as the QSSM promotes the bacteria specific immune effector response. However, *P. aeruginosa* has specific virulence factors (Table 1-2, p 17), which destroy immune cells, for example rhamnolipids, which causes apoptosis of PMNs. Ritchie *et al.* (103) surmised that the conflicting immune modulatory

responses of 3OC₁₂-HSL was because the QSSM emphasises the pre-disposition of the immune system, which can be either T_{H1} or T_{H2} biased, thus contributing to *P. aeruginosa* adaptation to the host's environment (103). Collectively, the data suggests that 3OC₁₂-HSL and PQS contribute to the protection of *P. aeruginosa* from host defences (83) whilst ensuring that the pathogen is the dominant species in infection. C₄-HSL does not appear to have immune modulatory activity.

PQS acts as an iron trap due to its iron-chelation properties; 60% of PQS is associated with the bacterial cell membrane allowing siderophores, such as pyoverdine, which are under the control of the Pqs system, to transport iron trapped by PQS into the cells. This mechanism prevents *P. aeruginosa* from wasting resources, such as siderophores, while still benefiting from iron acquisition (104). PQS has been termed a 'cellular trainer' by regulating endogenous stress, bacteria that have survived this 'stress' are protected from reactive oxidative species released by phagocytes, by the anti-oxidant effect of PQS (105). In fact, excess PQS caused *P. aeruginosa* cell autolysis (106), which may be an example of the endogenous stress.

1.5.5 QS AND BIOFILMS

QS has an important role in the differentiation and maturation of the mushroom-shaped biofilms. A *lasI* mutant produced a thin and uniform biofilm that was susceptible to sodium dodecyl sodium (SDS) treatment, however in the presence of exogenous 3OC₁₂-HSL, the same mutant strain was able to form biofilms similar to that of the wild-type (WT) strain that were unaffected by the detergent, showing that LasR-3OC₁₂-HSL was involved in biofilm development (107). In addition, biofilms of the *pqsA* mutant strain were thin and flat (108), suggesting that PQS has a role in biofilm development.

Certain biofilm components are under the specific control of QS. Exopolysaccharide matrices of biofilms can be alginate- (*alg*), glucose- (*pel*) or mannose-rich (*psl*); the *pel* gene is thought to be under the control of the Las system (109). Extracellular DNA (eDNA) is a cohesive factor in early biofilm formation, but is also important in mature biofilms, which were susceptible to DNAase treatment (110). There is a basal level of eDNA that is released in a QS-independent manner. However, during late log phase high concentrations of eDNA is released, which is thought to be under QS-control; Allesen-Holm and colleagues (110) observed that *ΔlasI ΔrhII* (unable to produce 3OC₁₂-HSL and C₄-HSL respectively) mutant and *ΔpqsA* (reduced production of HAQs) mutant strains produced low levels of eDNA compared to WT strains (110). It has been speculated that PQS is involved in cell lysis (106) causing the release of eDNA (111). Rhamnolipids, which are regulated by PQS and C₄-HSL, are involved in the maintenance of open channels that allow transport of nutrients, oxygen, and waste products within the biofilm as well as structure, microcolony formation and detachment (109, 112). It has been suggested that rhamnolipids deactivate neutrophils (113), protecting the

biofilm from the innate immune response.

P. aeruginosa can convert to anaerobic metabolism utilising nitrogen-based metabolites through denitrification (114). This is useful as the biofilm in chronic CF infections has an oxygen gradient. The Rhl system is thought to regulate growth during anaerobic metabolism in order to protect bacteria from metabolic nitric oxide (NO) suicide (108, 114).

1.5.6 QS AND DISEASE

Guina *et al.* (115) investigated five clinical isolates (CF259, CF1488, CF1641, CF471 and CF1153) from CF patients aged 24-36 months and noted that these isolates produced relatively more PQS than isolates from urinary tract infections. The authors concluded that in young CF patients, *P. aeruginosa* might induce QSS, specifically the Pqs system, as a response to certain nutrient deficiencies, such as limited magnesium (115). It has been reported that the ratio of C₄-HSL to 3OC₁₂-HSL is higher in the CF sputum and lung tissue than in other *P. aeruginosa* infections (5, 116). CF *P. aeruginosa* isolates eventually lost QSS activity (years) however C₄-HSL production persisted into late infection (years), correlating with rhamnolipids levels (117).

It has been found that the pathogenicity of a double QSS mutant, *P. aeruginosa* PAO1-JP2 (*ΔlasI ΔrhlI*, mutant cannot synthesise 3OC₁₂-HSL and C₄-HSL) was significantly compromised in a burn mouse model. The strain could not achieve efficient local and systemic spread when compared to a WT strain. This could not be attributed to loss of the expression of a particular virulence factor; therefore, it was concluded that this reduced virulence was due to the collective loss of QSS-controlled virulence factors (118).

As described (1.1.4, p 19), LPS and flagella contribute to the continuous stimulation of innate immune responses, in ulcerative keratitis, which leads to eventual blindness. *P. aeruginosa* has been documented to produce C₄-HSL, 3OC₁₂-HSL and C₆-HSL resulting in expression of virulence factors such as elastase, alkaline protease and protease IV, including exoS and exoU, which are negatively regulated by QS in certain conditions. Conversely, a QSS mutant was unable to induce murine ocular damage (119). Pyelonephritis, caused by the QSS mutant PAOI-JP3 (*ΔlasI ΔrhlR*, mutant cannot synthesise 3OC₁₂-HSL or express the RhlR protein, required to form the complex with C₄-HSL) was cleared within three days compared to an infection caused by the WT strain that persisted for twelve days (120). It appears that strains that have compromised QSS have reduced lethality (83) and cause milder pathologies. This was noted in a rat lung model infected with *P. aeruginosa* PAO1-JP2, which had mild lung pathology compared to the WT infection, attributed to less virulence factor production. Additionally, an early but stronger and quicker immune response was induced leading to the rapid clearance of the QSS mutant bacteria (121).

1.6 THE QSS – ALTERNATIVE THERAPEUTIC TARGET

The above mentioned published reports show that compromised QSSs did not affect the growth but severely limited the pathogenicity of *P. aeruginosa* in most disease states due to the multiple loss of virulence factors. This resulted in mild pathologies and most importantly, the pathogen was rapidly cleared from the host.

Inhibition of QSS has attenuated multiple virulence factors irrespective of the pathogen virulence phenotype and reflected the avirulence of mutant QSS *P. aeruginosa* strains. Growth was not affected, therefore, the selective pressure, the accompaniment to antibiotic treatment, is absent, thus minimising resistance. QSS inhibition was proposed as a novel therapeutic approach against *P. aeruginosa*.

1.6.1 QSS INHIBITION

Inhibition of QSS will prevent the intra- and inter-species communication; *P. aeruginosa* will be unaware of the quorum or the environment and cannot co-ordinate unified QSS-controlled responses (Figure 1-7). The immune system will be able to manage the pathogen more effectively, with or without the adjunct antibiotic therapy.

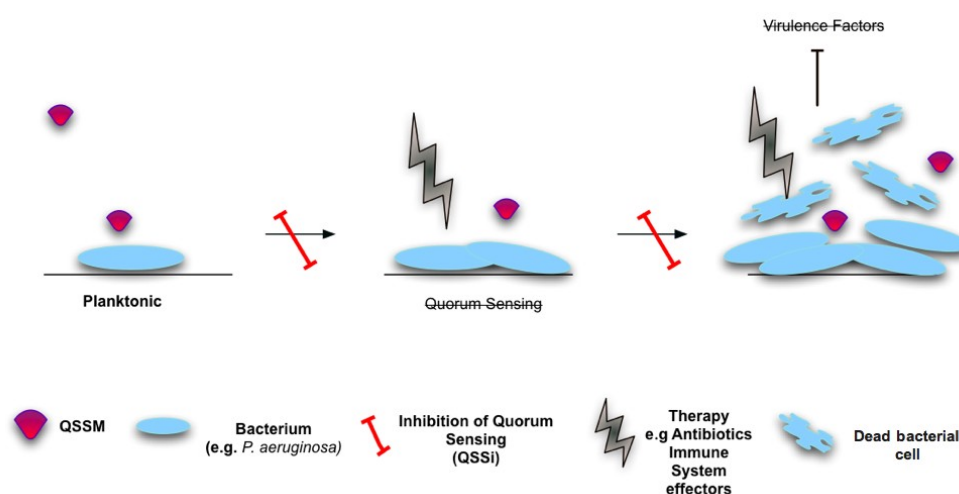


Figure 1-7: QSS inhibition.

Quorum sensing system inhibitors (QSSI) that affect (a) production of QSS proteins and/or (b) production of the QSSMs and/or (c) activity of the QSSMs. If given as prophylactics or adjuncts in antimicrobial therapy, QSSI may prevent the production of virulence factors and reduce the pathogenicity of *P. aeruginosa*. Therapy, inherent (immune system) or chemotherapy (antibiotics) is more efficacious, resulting in a mild to non-existent pathology and rapid clearance of the pathogen.

1.6.2 QUORUM SENSING SYSTEM INHIBITORS (QSSI)

1.6.2.1 NATURAL INHIBITORS

AHLs are degraded by lactonases that target the lactone ring (122), acylases that hydrolyse the amide bond (123) and AHL oxidase or reductase, which target the acyl chain. Prokaryotes release such enzymes as part of a defence or regulatory mechanism. Certain eukaryotic cells such as specific epithelial cells and mammalian serum contain enzymes such as paraoxanase (124), which degrade AHLs (125). *Arthrobacter nitroguajacolicus* dioxygenase HOD can degrade PQS but can be competitively inhibited by HHQ (126). *Delisea pulchra* produces halogenated furanones, which have anti-QSS activity in *Vibrio fischeri* and *V. harveyi* (127) but have no activity in *P. aeruginosa*. However, the synthetic furanone-C30 increases *P. aeruginosa* biofilm susceptibility to SDS and tobramycin resulting in rapid clearance of *P. aeruginosa* in a murine infection model (128). Clove oil (129), furocoumarins in grapefruit juice (130), honey (131), garlic (132), patulin, and penicillic acid (133) have demonstrated anti-QSS activity.

1.6.2.2 CHEMICAL INHIBITORS

S-adenosylmethionine (SAM) and anthranilic acid are biochemical precursors of AHLs and PQS respectively. Derivatives of SAM and anthranilic acid reduced *in vitro* production of AHLs and HAQs respectively. The substrate specificity of purified RhII, which synthesises C₄-HSL, was tested using derivatives of SAM resulting in the inhibition of RhII activity (134). Halogenated anthranilic acid derivatives increased the survival of thermal injured mouse model by 35-50%, although protection was transient (135), whilst methyl anthranilate reduced the expression of elastase *in vitro* (135-137). However, there is an alternate biosynthetic route to HAQs, which utilises amino acid tryptophan (138), therefore may overcome any inhibition of biosynthesis of these QSSMs.

There has been considerable work in producing libraries of AHL derivatives with agonist or antagonist activity (139-141). Geske *et al.* (139) noted that QSS antagonist was able to reduce biofilm formation by 75% in a dose-dependent manner using *in vitro* green fluorescent protein (GFP) reporter *P. aeruginosa* strain. Ishida *et al.* (142) focussed on *N*-acyl cyclopentylamides, these inhibitors reduced β -galactosidase activity in response to expression of *rhIA* and *lasB*, in a dose-dependent (0-250 μ M) manner. These genes encode for rhamnolipids and elastase respectively, suggesting that synthesis of these virulence factors were reduced, this anti-QSS activity was comparable to halogenated furanones (143). Liu *et al.* (144) observed that halogenated furanones were able to inhibit the formation of the QscR-3OC₁₂-HSL complex. The QscR is part of the global regulatory system (Figure 1-6, p 42) and inhibition at this level may lead to disruption of the QSS.

Using GFP reporter strains (WT and an isogenic *lasR* mutant *P. aeruginosa* *rhIA::gfp* (ASV)

and *P. aeruginosa* *pqsA::gfp* (ASV)), salicylic acid, nifuroxazide, and chlorzoxazone reduced fluorescence in response to *rhlA* and *pqsA* expression *in vitro*, demonstrating anti-QSS activity, which was partially directed at the Rhl and Pqs system (the synthesis of rhamnolipids and PqsA, needed for PQS synthesis, are under Rhl and PQS control respectively). Salicylic acid was able to prevent the *in vitro* production of rhamnolipids at 200 µg/mL (145).

Sub-inhibitory concentrations of macrolide antibiotics have been used as QSSi. Azithromycin (2 µg/mL) reduced the β -galactosidase activity in response to the expression of *lasI* by 80% and by 50% in response to *rhlI* expression (146). Furthermore, other anti-pseudomonal antibiotics such as ciprofloxacin (fluoroquinolone), and the ceftazidime (cephalosporin) as well as azithromycin were able to reduce QSS-controlled virulence factors - rhamnolipids, elastase and protease (147). However, prolonged exposure of azithromycin was needed (146), and long-term treatment with azithromycin has resulted in *S. aureus* resistance against the antibiotic (147). As bacteria, particularly *P. aeruginosa*, are adept at acquiring resistance, promoted by continued exposure to the antibiotic, the use of antibiotics at sub-inhibitory concentrations as QSSi should not be recommended.

1.6.2.3 IMMUNOLOGICAL INHIBITORS

1.6.2.3.1 ANTI-AHL VACCINES AND ANTIBODIES

Kende *et al.* (148) produced an anti-QSS conjugate vaccine based on 3OC₁₂-HSL. Immunisation of Balb/c mice with the conjugate resulted in polyclonal immune sera that reduced the release of β -galactosidase by 70%, in response to the expression of *lasI* in a β -galactosidase reporter assay. The corresponding 618.4 Mab was able to reduce the release by 80% in the same assay (148).

Charlton *et al.* (149, 150) produced a single chain antibody (scAb) using phage technology and the probe, dDHL-COOH (C₁₂-HSL-COOH). The scAbs, G3G2 and G3B12, were able to reduce *P. aeruginosa* mediated nematode killing by over 90% in a 60-80 hour incubation period, the inventors applied the same technology to develop an anti-AI-2 antibody. The scAbs were efficient in reducing biofilm formation in a concentration dependent manner, 70 nM was sufficient to cause an 80% reduction, and in addition the inventors observed that tetracycline and scAb had an additive inhibitory effect on biofilm formation (149, 150).

Charlton *et al.* (151) hypothesised that the bacterial load could be reduced using anti-AHL Abs without direct bactericidal activity, thus avoiding the imposition of selective pressure. The inventors assumed as excess PQS would cause cell lysis, this will automatically lead to a reduction in bacterial cell density, but as an additional measure, *P. aeruginosa* will slow down growth as a counter-defence mechanism, in order to prevent further cell death by autolysis. This excess PQS could be achieved by either addition of exogenous PQS or by the disruption of the AHL:PQS balance. Charlton *et al.* (151) noted a decrease in bacterial load after 24

hours post-infection in the presence of scAbs, G3G2 or G3B12, and in combination with gentamicin. It is understood that the inventors were working on the assumption that neutralisation of the AHLs with the specific antibodies, would result in the physical disruption of the AHL:PQS balance rather than effects at the molecular level. Although, data has shown that excess PQS caused autolysis the mechanism is unknown and it was concluded that PQS has an undefined role in the mechanism (106). The importance of the AHL:PQS ratio has not been discussed in the literature presented in this study. Therefore, the inventors' interpretation that the reduced bacterial load was due to excess PQS or that the bacteria sensed an 'excess' of PQS as the result of the neutralisation of the AHLs by the scAbs, needs further clarification.

Miyairi *et al.* (152) produced an anti-QSS vaccine with specificity for 3OC₁₂-HSL. Immunised mice (36%) were able to survive a *P. aeruginosa* infection for four days compared to no survivors in the non-immunised mice. TNF- α levels were reduced, as was the concentration (pmol) of 3OC₁₂-HSL, in serum and lung homogenates. The immune serum inhibited 3OC₁₂-HSL induced apoptosis in macrophages *in vitro* (152).

Kaufmann *et al.* (153), using the Mab RS2-G19, were able to show a decrease in fluorescence in response to 3OC₁₂-HSL, in a GFP assay using WT and QS mutant reporter strains; the Mab was able to inhibit 3OC₁₂-HSL mediated apoptosis of bone marrow derived macrophage (154). De Lamo Marin *et al.* (155) generated the catalytic monoclonal antibody, XYD-11G2, against squaric monoester **5** (Figure 1-8) which hydrolysed the lactone ring of 3OC₁₂-HSL with 'moderate catalytic activity', the Mab demonstrated anti-QSS activity by reducing pyocyanin levels (155). Preliminary data on the synthesis of a probe that mimics the transition state of AHL lactone hydrolysis so other catalytic antibodies in phage libraries can be identified has also been published (156).

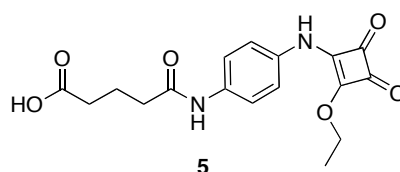


Figure 1-8: Squaric monoester monoamide, **5**.

Taken from (155).

1.6.3 SUMMARY

The development and use of anti-pseudomonal vaccines in CF has not been recommended (37). This was based on results from the phase III trials with Aerugen[®], however reports have shown that attenuation of multiple virulence factors leads to reduced pathogenicity of *P. aeruginosa* allowing the immune system to contain and eradicate the pathogen with or without adjuvant antibiotic therapy.

Significant attenuated virulence is characteristic of QSS mutants. QSS is the communication system used by *P. aeruginosa* to assess the immediate environment and population. The quorate *P. aeruginosa* are able to co-ordinate and stimulate QSS-regulated production of virulence factors, which includes the QSSM 3OC₁₂-HSL and PQS, at the opportune moment most beneficial to the pathogen.

QSSi have been developed which disrupt the QSS, effectively mirroring the avirulence of QS mutants. No effect was seen on growth therefore the risk of resistance appears to be low. Importantly, anti-AHL vaccines and antibodies have been developed that conferred protection against *P. aeruginosa* infection *in vivo*.

1.7 IMMUNOGENICITY OF ANTI-AHL VACCINE ANTIGENS

Anti-AHL vaccines and Mabs have successfully reduced the virulence of *P. aeruginosa* and enhanced natural eradication, even though QSSM and other such small molecules (M_r of 1500 Da and below) (157), are not recognised by the immune system as antigens. They lack the immunogenicity needed to stimulate innate and adaptive immune responses.

Immunogenicity of AHL has been improved through haptenisation, which is the conjugation of a non-immunogenic antigen to a carrier to produce an immunogen. The anti-AHL antibodies described in 1.6.2.3.1 (p 50) were produced against an AHL hapten (Figure 1-9, p 53). Haptens are antigens that have been chemically or biologically modified for subsequent conjugation to an immunogenic carrier. Carrier molecules are usually large macromolecules such as tetanoid (55), exotoxoid A, bovine serum albumin (BSA) or keyhole limpet haemocyanin (KLH) (158).

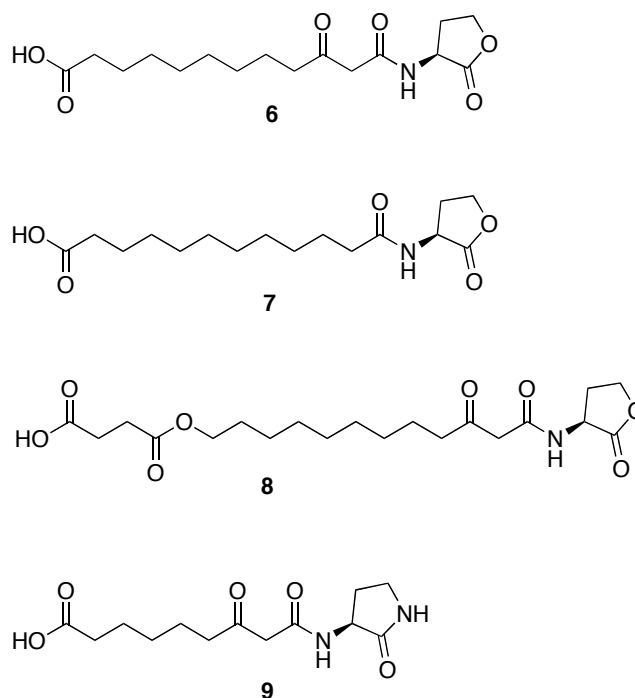


Figure 1-9: Published haptens based on natural AHLs.

These have been successfully conjugated to carrier proteins and have been used to generate antibodies to the relevant AHL, **6**, PAI-1 (148); **7**, Hap-2 (149, 150); **8**, 3OC₁₂HSL-COOH (152); **9**, RS2 (153).

1.7.1 HAPTEN DESIGN

1.7.1.1 HAPTEN STRUCTURE

Landsteiner established the fundamental principles for efficient haptenisation (159); the hapten must replicate or share the conserved structural components (the key epitopes) with the chosen antigen. Antibodies can cross-react with haptens that have subtle differences in structure; however, Landsteiner determined that the significant changes in chemical composition, stereoisomerism or positions of functional groups prevent antibody recognition (160). For example, Landsteiner used various azoproteins as antigens to generate antibodies, he noted that antibodies generated against a ‘carboxylic acid antigen’ would recognise ‘sulfonic acid antigens’ however, this was not applicable to sera generated against sulfonic acid antigens, which displayed specificity towards sulfonic acid antigens only. Landsteiner observed that sera generated against L-, D- and *meso*-tartaric acid showed specificity and only weakly reacted with the other stereoisomers (159). The L-configuration of the homoserine lactone chiral centre was maintained for all the published haptens (Figure 1-9).

Haptens **6-9** (Figure 1-9) have been designed so the molecules closely resemble the natural AHLs, including the conserved lactone ring. However, the lactone ring of AHLs hydrolyses at increasing pH and temperature, the rate of hydrolysis largely depends on the chain length (161). Conversely, Kaufmann and colleagues documented half-lives of 13.1 - 18.1 hours in phosphate buffer saline (PBS), pH 7.4, for specific AHL derivatives, which were independent

of increasing chain length or the oxidation state of C3 of the acyl chain (153). Following this observation, Kaufmann *et al.* (153) substituted the lactone ring for a lactam ring (Figure 1-9, **9**, p 53), which was stable during haptensisation and immunisation. The antibodies generated against **9** (Figure 1-9, p 53) recognised the cognate 3OC₁₂-HSL in competitive indirect ELISA (K_d : 150 nm to 5 μ M) (153).

1.7.1.2 LINKER

Haptens have an appropriate functional group to form covalent bonds with the carrier protein. The AHL haptens (Figure 1-9, **6-9**, p 53) have a carboxylic acid moiety at the terminus of the acyl chain for conjugation to the carriers via amide bonds. The carrier proteins have numerous amino acid residues available for conjugation such as ϵ -lysine residues, which bind to carboxylic acid groups.

The antigen needs to be sufficiently immunogenic to stimulate both the T- and B-lymphocyte directed responses and to establish immune memory (8, 158). The AHL haptens are degradable, which is essential for processing within the APC prior to presentation to T-lymphocytes. Landsteiner observed that antibodies were generated to the important epitopes if the hapten was completely accessible to the immune system (159). A distance of 3-6 carbons between the epitope(s) and the carrier protein is considered optimal and can be achieved by a linker system (162). In regards to the published AHL haptens (Figure 1-9, **6-9**, p 53) the acyl chain, a conserved structural component of AHLs, doubles as the linker making any antibodies generated specific to the linker useful.

1.7.2 THE ‘MANY’ QSS OF *P. AERUGINOSA*

It is accepted that the QSS is an interlinked system (Figure 1-6, p 42), however, specific reports allude to the independent activation of certain divisions of the QSS. Under certain growth conditions, PQS production and Rhl activation can occur without LasR activation (74, 163). For example, in an iron-limited medium the expression of *rhlR* and *rhlI* increased and in a CF-supplemented media (M9 minimal media with glucose supplemented with 2.5 and 5% CF sputum extract), a concentration-dependent increase in QSS-regulated gene expression was noted (164). PQS was seen to induce *rhlA*, the rhamnolipid gene, in the presence of RhlR and PqsE but without the AHL QSSM (165). PqsE has been shown to control rhamnolipid and pyocyanin production independently from PqsR-PQS through the Rhl system (Figure 1-6, p 42) (80).

The QSS hierarchy, where Las is the pinnacle, may only be one variation of the QSS, typical in laboratory culture conditions, but is subject to change depending on environmental factors (164). Inhibition of QSS has largely focused on the AHL controlled branches of the QSS, in particular, the Las system. Inhibition of one QSSM, does not inhibit QS but merely allows the

bacteria to adapt and compensate by using an alternative QSSM or up-regulate the active divisions of QSS, which could be translated as QSSi resistance (166). For example, *V. fischeri*, which uses 3OC₆-HSL, was able to utilize exogenous C₈-HSL and C₄-HSL (*in vitro*) after only a small number of mutations (167). Clinical isolates of *P. aeruginosa* can produce 3OC₁₀-HSL and 3OC₈-HSL, 3OC₆-HSL and C₆-HSL (168) and can respond to AHLs produced by other Gram-negative species. Inhibition of each division of the QSS may prevent these potential compensatory mechanisms.

1.7.2.1 DISADVANTAGES OF ANTI-AHL VACCINES

The benefits of immune memory indeed favours the development of vaccines, and AHL hapten-carrier conjugates have been successful vaccine candidates, however, the resultant antibodies lack significant reactivity towards the shorter AHLs in particular, C₄-HSL, which regulates the Rhl system (Figure 1-6, p 42). Kende *et al.* (148) generated polyclonal immune sera and 618.4 Mab against hapten **6** (Figure 1-9, p 53), which recognised the cognate 3OC₁₂-HSL but no information was given in regards to avidity towards the other natural AHLs (148).

Miyairi *et al.* (152) conjugated hapten **8** (Figure 1-9, p 53) to ovalbumin (OVA), which resulted in decreased 3OC₁₂-HSL levels *in vivo*, yet was associated with an increase in pyocyanin production (152). This may be a compensatory mechanism adopted by *P. aeruginosa*, up-regulating the Pqs and Rhl systems, in response to the presumed Las system inhibition, although in contrast, the pyocyanin levels were lowered in response to anti-AHL antibodies in other studies (153, 155).

The Mab RS-1G29 (generated against **9**, Figure 1-9, p 53) cross-reacted with 3OC₁₂-HSL but showed a 1000-fold lower affinity for C₄-HSL (153) due to loss of Ab-Ag interactions (169). Charlton *et al.* (149) were able to produce a scAb against **7**, (Figure 1-9, p 53), which cross-reacted with C₁₄-HSL (IC₅₀: 21 μ M), but had an IC₅₀ of mM with 3OC₆-HSL and C₄-HSL in competitive indirect ELISA studies. There are no published reports detailing the haptenisation with derivatives of PQS for the generation of anti-PQS antibodies.

2 MULTI-COMPONENT ANTI-QSS VACCINE – COMPLETE QSS INHIBITION

Attenuated pathogenicity of *P. aeruginosa* is due to multiple loss of virulence factors, the result of a compromised QSS. Infections with such strains cause mild pathologies and are easily cleared by the immune system. QSSi have been developed and have effectively disrupted the QSS.

Inhibition of the QSS however, has focussed on inhibiting the Las system as it is regarded as the top of the supposed QSS hierarchy. However, the QSS is highly adaptable and the hierarchical QSS may only be typical in the laboratory environment. The pathogen may be able to compensate for the inhibition of one division of the QSS, by the up-regulation of the Rhl and/or Pqs system, which remain active.

Complete inhibition of the QSS is possible if all three divisions of the QSS, Las, Rhl and Pqs systems, are inhibited minimising compensatory mechanisms. There are only a few examples of potential inhibitors of the Pqs and Rhl system. Immunological targeting of the AHL has been studied, and effective anti-AHL vaccine and therapeutic antibodies have been developed. One such vaccine, produced by Miyairi *et al.* (152) has shown that protective immunity was achieved. For complete QSS inhibition, a prophylactic multi-component QSS vaccine, which targets the QSSM will provide long-lived immunity due to immune memory. The QSSM are the target antigens, therefore upon recognition, the immune system will be able to initiate the secondary immune response, the concentration of QSSM will always be low thus *P. aeruginosa* cannot sense the quorum or the environment, preventing release of virulence factors and efficient adaptation. The immune system will be able to contain and eradicate with or without adjunct antibiotic therapy.

Figure 2-1 (p 58) illustrates the envisaged effects of the multi-component anti-QSS vaccine and therapeutic antibodies. By targeting the QSSM, prophylactic anti-QSS vaccines and therapeutic anti-QSS antibodies are not dependent on the virulence phenotype, strain, or disease pathology as QSS is a conserved system. The passive immunisation with the anticipated therapeutic anti-QSS antibodies would offer immediate therapy, however the anti-QSS vaccine will be appropriate as a prophylaxis given to those hosts most susceptible to *P. aeruginosa* infections, in other words, hosts with a compromised immune system resulting from disease or treatment. For example, as *P. aeruginosa* colonises young CF patients, the vaccine would be given at the time when cystic fibrosis was diagnosed and so forth. It is anticipated that a multi-component QSS vaccine would be suitable for MDR strains. Most importantly, as with QSSi, growth is not affected, therefore resistance through selective pressure is minimal.

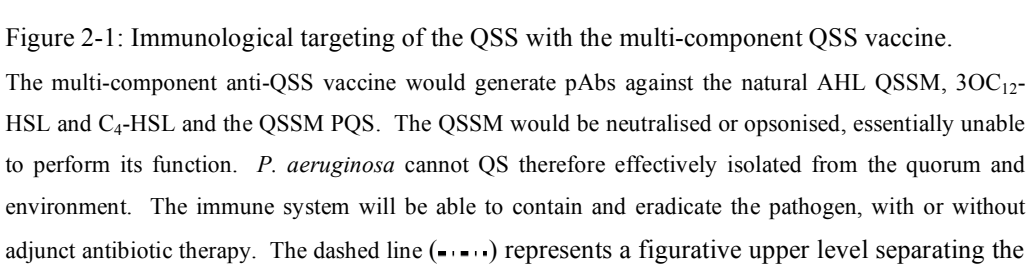
2.1 AIMS AND OBJECTIVES

The aim of this study is to develop a multi-component anti-QSS vaccine, consisting of a hapten-carrier conjugate that stimulates antibodies that cross-react with both the natural AHLs, 3OC₁₂-HSL and C₄-HSL, and a hapten-carrier conjugate that targets PQS.

This may be achieved by the synthesis of an AHL hapten and a PQS hapten, which are stable for conjugation to the carrier and immunisation. The AHL hapten-carrier and PQS hapten-carrier conjugate formed upon haptensisation of the protein carriers will be used to immunise mice, and if proven successful, rabbits. The haptens will be conjugated to KLH using *N*-hydroxysuccinimide (NHS) in an active ester method, and used for immunisations.

The generated polyclonal antibodies (pAbs) will be tested for cross-reactivity with the natural QSSMs of *P. aeruginosa*. A competitive indirect ELISA will be appropriate for this characterisation. For this purpose, hapten-BSA conjugates will be useful as the coating antigen (Figure 5-3, p 89). The two carriers are phylogenetically dissimilar; therefore, no significant cross-reactivity is anticipated between generated anti-hapten-KLH pAbs and BSA.

Characterisation of the anti-QSSM activity, specifically against 3OC₁₂-HSL, C₄-HSL and PQS, of the generated pAbs will serve as an indication for potential *in vivo* QSS inhibition. The viability of the AHL hapten-carrier and PQS hapten-carrier conjugate, as anti-QSS vaccine candidates will be demonstrated *in vitro* and *in vivo* anti-QSS assays, designed to test for the inhibition of virulence factor production which require the complete QSS, such as biofilms.



QSS and the global regulatory system; the global regulatory system and therefore the QS is dependent on the environment, native or of the host, at the site of infection ([]) and the use of (?) indicates that HHQ may also act as a QSSM.

3 RESULT 1 – HAPTEN SYNTHESIS

3.1 HAPTEN DESIGN

3.1.1 AHL HAPTEN, AP1

The chosen AHL hapten, **AP1**, (Figure 3-1), was based on 3OC₈-HSL, a natural QSSM produced by *P. aeruginosa* to accommodate the optimum 3-6-carbon distance between key epitopes and the carrier. The lactone ring and the external amide moiety are conserved structural components of the AHLs (Figure 1-5, **1** and **2**, p 37). For stability during haptenisation and immunisation, the lactone ring was substituted with a lactam ring as described by Kaufmann and colleagues (153), therefore the lactam ring and external amide moiety of **AP1** were considered as the key epitopes. It was anticipated that any antibodies generated against these epitopes will react with the long and short chain 3-oxo and unsubstituted AHLs; particularly resulting in significant cross-reactivity with C₄-HSL, not reported with the published haptens, (**6-9**, Figure 1-9, p 53) with the implication of Rhl system inhibition as well as the Las system (Figure 2-1, p 25). Additional anticipated epitopes have been highlighted in Figure 3-1, the acyl chain is the linker as with the published haptens (Figure 1-9, p 53).

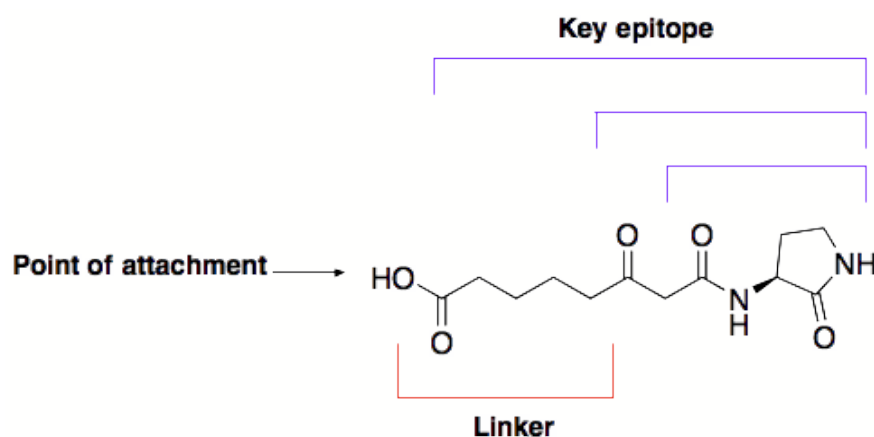


Figure 3-1: 7-((*S*)-2-oxopyrrolidin-3-ylcarbamoyl)-6-oxoheptanoic acid, **AP1**.

3.1.2 PQS HAPTEN, AP2

The PQS hapten, **AP2** (Figure 3-2, p 61), had a carboxylic acid moiety at the terminus of the acyl chain for attachment to the carrier. It was believed that this would make the molecule more soluble. PQS is extremely hydrophobic and sparingly soluble in aqueous solutions. Improvement in aqueous solubility will ensure efficient conjugation to the carrier. The key epitope was thought to be the quinolone structure as this is the conserved component of the HAQs.

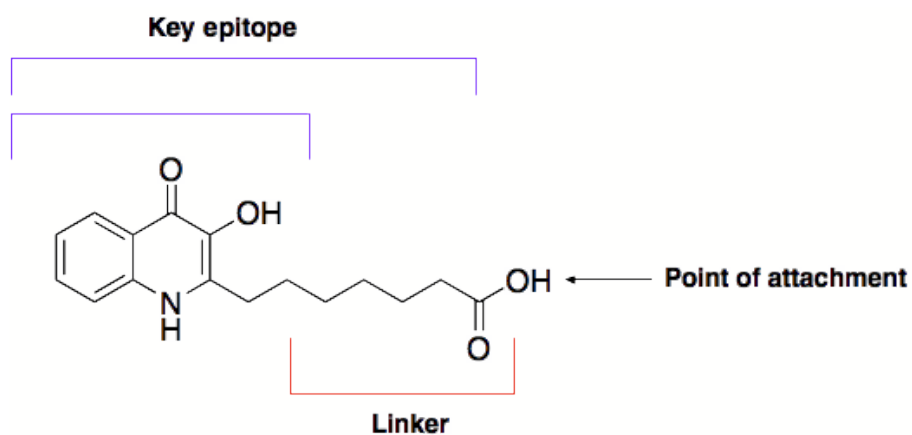


Figure 3-2: 7-(1,4-dihydro-3-hydroxy-4-oxoquinolin-2-yl)heptanoic acid, **AP2**.

The objective was to produce **AP1** and **AP2** in sufficient quantities for haptenisation. There are established synthetic strategies (170-173) used to produce QSSMs and derivatives. Indeed, Kaufmann *et al.* (153) have synthesised hapten **9** (Figure 1-9, p 53) in good yields and Purcell (173) has reported the synthesis of ethyl 2-(1,4-dihydro-3-hydroxy-4-oxoquinolin-2-yl)acetate, which is a derivative of **AP2** with a yield of 31% by cyclisation of an aminobenzoate intermediate, 2-oxopropyl 2-aminobenzoate.

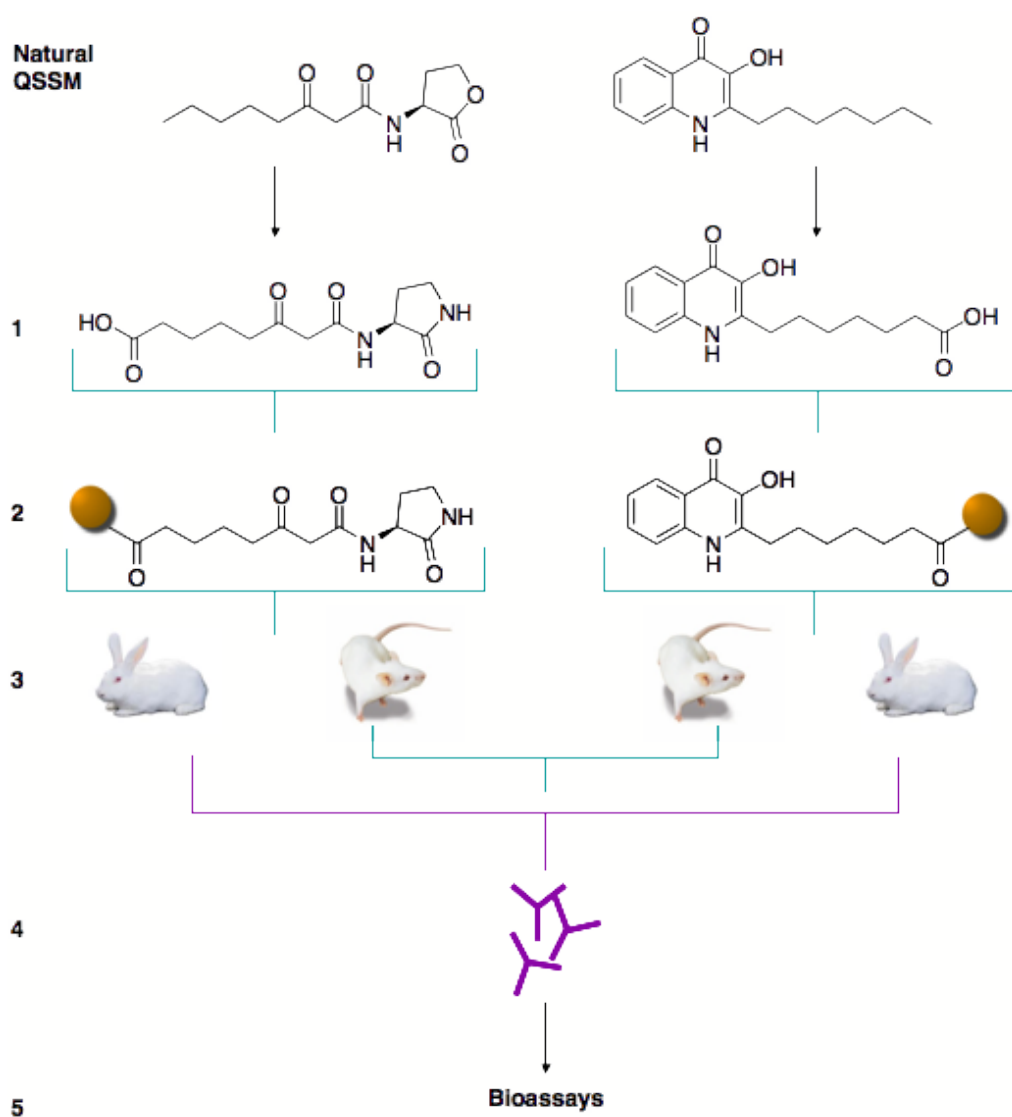


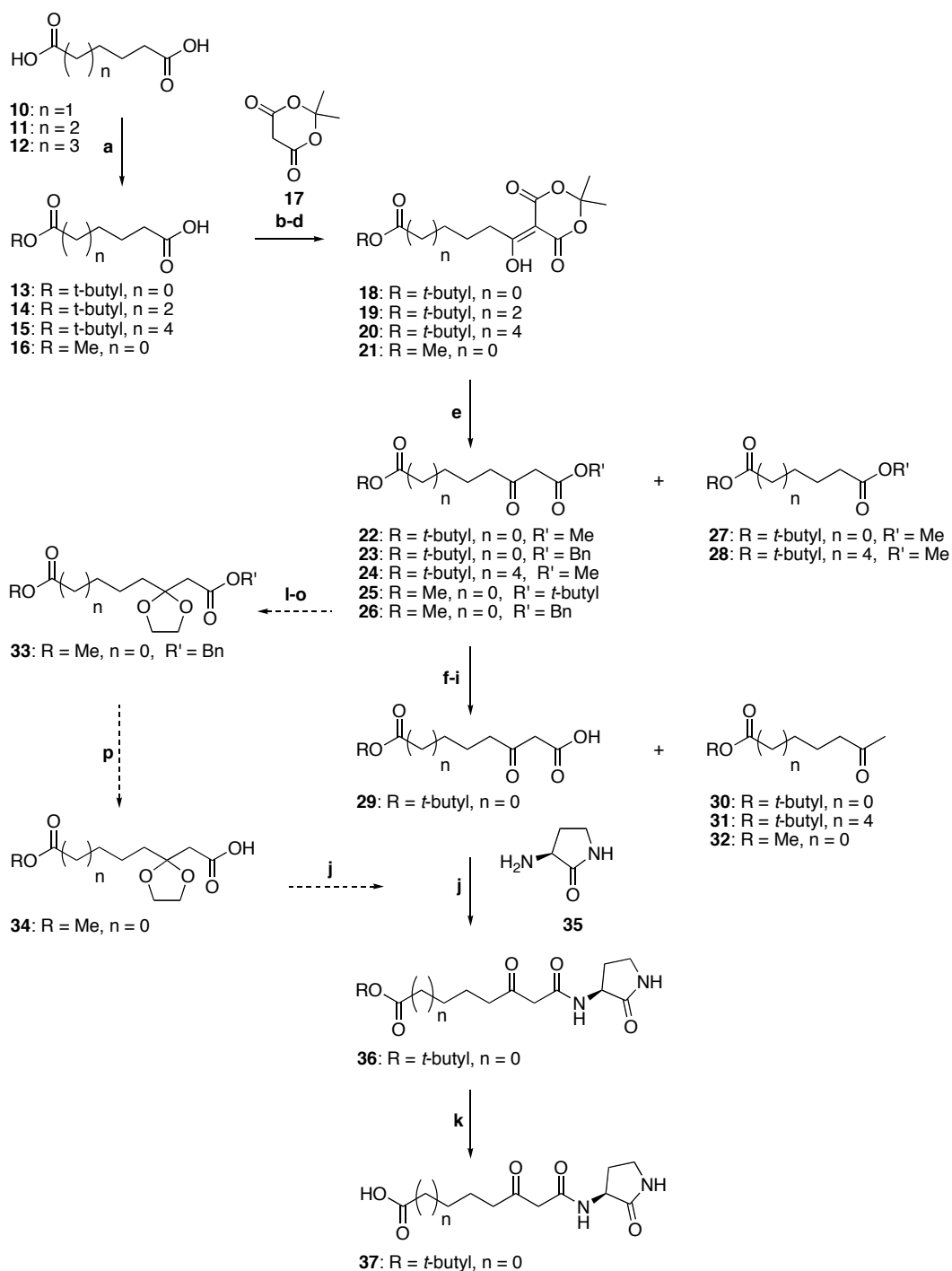
Figure 3-3: Aims and objectives.

(1) Synthesis of **AP1** and **AP2**; (2) Haptenisation of immunogenic carrier, KLH, with **AP1** and **AP2**; (3) Immunisation of mice and rabbit; (4) Characterisation of generated antibodies to hapten-carrier conjugate; (5) Test for anti-QSSM and anti-QSS activity.

3.2 SYNTHESIS OF **AP1**, 7-((*S*)-2-oxopyrrolidin-3-ylcarbamoyl)-6-oxoheptanoic acid, **37**

3.2.1 AMIDATION METHOD A

The β -keto dicarboxylate **22** (Scheme 3-1), formed by refluxing acylated Meldrum's acid **18** in anhydrous methanol (174), underwent selective base-mediated hydrolysis to generate **29**. Acid **29** was coupled to (*S*)-3-amino-pyrrolidin-2-one (AP) (175) **35** using DIC to afford amide **36** in 10% yield. Acid-mediated deprotection of the *t*-butyl ester afforded **37** in near-quantitative yields.



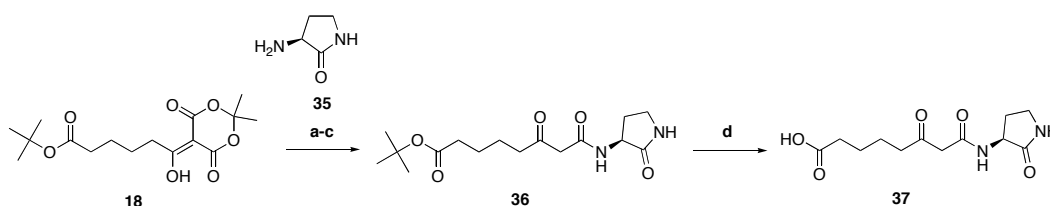
Reagents and conditions: (a) DIC, DMAP, CH_2Cl_2 , *tert*-BuOH, 0 °C to rt, (26-70%); (b) DIC, DMAP, CH_2Cl_2 , (**18-21**, crude >100%); (c) i) $(\text{COCl})_2$, cat. DMF, CH_2Cl_2 , rt; ii) $\text{C}_5\text{H}_5\text{N}$, **17**, CH_2Cl_2 , (**21**, 45%); (d) EDC, DMAP, CH_2Cl_2 , 0 °C to rt, (**18**, 97%); (e) ROH, reflux, (13-86%); (f) $R' = \text{Me}$, 1 M NaOH, H_2O ; (g) $R' = \text{Bn}$, 10% Pd-C, MeOH, H_2 , rt; (h) $R' = \text{Bn}$, 10% Pd-C, THF, 0 °C, (96%); (i) $R' = t\text{-butyl}$, TFA/ CH_2Cl_2 (1:1), rt; (j) DIC, DMAP, CH_2Cl_2 , 0 °C to rt, (10%); (k) TFA/ CH_2Cl_2 (1:1), (98%); (l) **26**, $(\text{CH}_2\text{OH})_2$, cat. CSA, $\text{CH}(\text{OEt})_3$; (m) **26**, toluene, $(\text{CH}_2\text{OH})_2$, rt to reflux; (n) **26**, $\text{BF}_3 \cdot \text{Et}_2\text{O}$, MeOH, rt; (o) **26**, $\text{BF}_3 \cdot \text{Et}_2\text{O}$, $(\text{CH}_2\text{OH})_2$, CH_2Cl_2 , rt; (p) 10% Pd-C, H_2 THF, 0 °C.

Scheme 3-1: Amidation method A

3.2.2 AMIDATION METHOD B

Using the protocol reported by Chhabra *et al.* (171) the acid adduct **18** (Scheme 3-2) was stirred with the free amine **35** for two hours at room temperature (rt) and then refluxed for a further three hours. The reaction resulted in trace amounts of amide **36**. Stirring the reaction overnight did not improve the yield but omitting Et₃N benefited the reaction. Amide **36** was detected by ¹H NMR however could not be isolated in appreciable quantity. The method was modified by adopting the protocol reported by Xu *et al.* (176), in pilot studies, adduct **18** was heated in MeCN with amine **35** with and without the addition of catalytic TFA. There was a concern that the inclusion of TFA would lead to the acidolysis of the *t*-butyl ester, however, the ester remained intact. Notably, in the presence of 0.3 molar equivalent TFA, β -keto acid **29** was detected as well as amide **36**.

On a larger scale (without TFA), the reaction was heated at 40 °C overnight then the temperature increased to 60 °C until completion, though no improvement in yield was observed. Conversely, a complex mixture was produced which was difficult to purify, nonetheless amide **36** was obtained in 20% yield. Deprotection of amide **36** proceeded smoothly with TFA/CH₂Cl₂ (1:1), giving acid **37** in near-quantitative yields (method A, step k).



Reagents and conditions: (a) MeCN, Et₃N, rt to reflux; (b) MeCN, rt to reflux; (c) MeCN, 40-60 °C, (20%); (d) TFA/CH₂Cl₂ (1:1), (20%).

Scheme 3-2: Amidation method B

3.2.2.1 SYNTHESIS OF NATURAL QSSM

Both method A and the method presented by Chhabra *et al.* (171) were used to synthesise the natural 3-oxo substituted QSSMs of *P. aeruginosa* (1.7.2, p 54) and 3OC₈-AP for use in competitive indirect ELISA (6.1, p 98). In this study, the synthesis was unsuccessful, often producing the equivalent unsubstituted QSSM as a by-product.

3.2.3 DISCUSSION

Synthesis of 7-((*S*)-2-oxopyrrolidin-3-ylcarbonyl)-6-oxoheptanoic acid **37** began with the *mono*-protection of adipic acid **10** (Scheme 3-1) via Steglich esterification (177, 178). *tert*-

Butyl esters are robust protecting groups for carboxylic acids, and stable to the conditions used in the synthesis. Acid mediated deprotection using trifluoroacetic acid (TFA) affords the free acid in good yields (179). Use of diisopropylcarbodiimide (DIC), with catalytic 4-(dimethylamino)pyridine (DMAP), proved an effective alternative to the typical reagents, dicylohexylcarbodiimide (DCC) and DMAP, whereas a combination of 1-ethyl-3-(3-dimethylaminopropyl)carbodiimide (EDC) and catalytic DMAP was not (180). The *mono*-protection of dicarboxylic acids **10-12** was controlled by using one equivalent of DIC in excess *tert*-butanol. The *mono*-protected dicarboxylic acids **13-16** were easily isolated by short path vacuum distillation, using Kugelrohr apparatus. Traces of the side product diisopropylurea (DIU) were removed by silica gel column chromatography. This method gave a reasonable yield for **13**, (70%) but much lower yields for **14** and **15** (26-37%).

3.2.3.1 ACYLATION OF MELDRUM'S ACID

Initially **13-16** were coupled with Meldrum's acid **17**, using DIC/DMAP to obtain the adducts **18-21** as crude products (Scheme 3-1, p 64). Purification by crystallisation was reported for derivatives of **18** (170), however, crystallisation attempts proved unsuccessful as did purification by silica gel column chromatography, which resulted in poor yields. It was anticipated that DIU would not interfere in subsequent reactions and therefore the crude products were used without further purification.

In an attempt to optimise the yield for this step, the acid chloride of **13** (formed by treatment with oxalyl chloride under Vilsmeier conditions) (181), was reacted with Meldrum's acid **17** in the presence of pyridine (174). Although this was suitable for small-scale reactions, use of EDC and stoichiometric amounts of DMAP or hydroxybenzotriazole (HOBt) proved to be more effective for large-scale reactions, as the by-products were water-soluble. The crude product was sufficiently pure after an acidic aqueous workup to proceed to the next step.

3.2.3.2 β -KETO DICARBOXYLATES

β -Keto dicarboxylates **22-26** were synthesised using the method of Oikawa *et al.* (174). Briefly, acylated Meldrum's acid adducts **18-21** (Scheme 3-1, p 64) were refluxed in anhydrous alcohol and purified by Kugelrohr distillation. The authors reported good yields for the conversion of Meldrum's acid adducts to the corresponding β -keto carboxylates but in this study, the results were variable, with yields of 12-86%. Surprisingly, in some cases, diesters **27-28** were obtained. This is unusual as the expected side-product would be ketones **30-32** resulting from thermal decarboxylation. The mechanism remains unknown but it was noted that extending reaction times to beyond completion (TLC) resulted in increased formation of diesters **27-28**. Wierenga and Skulnick (182) documented an alternative method for the formation β -keto carboxylates, and produced a variety of compounds using a directed C-acylation of *mono*-ethyl malonate lithium enolates by acid chlorides. Kaufmann *et al.* (153)

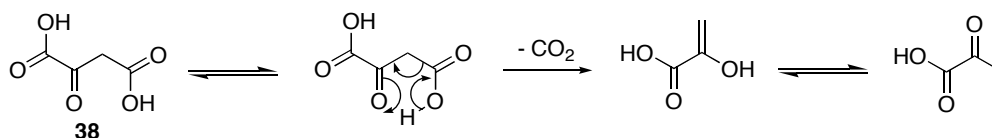
used a variation of this method for the formation of 1-benzyl-9-trimethylsilyl ether-3-oxononandioate, a derivative of **22**, in good yields. This route was not investigated in the present study, but may offer improved yields of β -keto dicarboxylates **22-26** (Scheme 3-1, p 64) for any future reaction optimisation.

3.2.3.3 PROTECTING GROUP STRATEGY

Orthogonal protecting strategies were necessary to obtain the β -keto dicarboxylic acid monoester **29**. Base-mediated hydrolysis of methyl esters is an established deprotection strategy (179), however methyl esters **22** and **24** (Scheme 3-1) were surprisingly resistant to saponification. The β -keto-dicarboxylate **22** was subjected to variety of saponification methods (183, 184) but these usually resulted in decarboxylation to give **30**. Acidolysis of ester **25** with TFA also led to the decarboxylation product **30**. A similar reaction has been reported where decarboxylation was the desired outcome (185). Attempts at protecting the ketone function of **26** as a cyclic ketal **32** (186-188), in order to avoid decarboxylation during selective deprotection and consequent amidation (Scheme 3-1) were unsuccessful. Hydrogenolysis of **23** in MeOH using catalytic Pd-C produced a mixture of acid **29** and ketone **30**. However, by changing the solvent to THF, and cooling to 0 °C, **29** was obtained in excellent yields (96%) (153).

Selective deprotection of the β -keto dicarboxylate esters has highlighted the instability of the resulting β -keto acid products. β -Keto carboxylic acids are known to decarboxylate under thermal conditions (189), β -keto dicarboxylic acids, however, can decarboxylate spontaneously in aqueous conditions, particularly at pH 4 at ambient temperatures (190). Studies have shown that decarboxylation in aqueous conditions can be catalysed by the presence of metal cations such as Mg^{2+} (191) or in ethanol with salts such as LiCl (192).

It is believed that simple β -keto dicarboxylic acids such as oxosuccinic acid **38** (Scheme 3-3), decarboxylate through a six-membered transition state (193) as the keto-tautomer, and more rapidly as a mono anion (190), presumably, as the anion is stabilised by the second carboxylic acid group. This is not limited to simple β -keto dicarboxylic acids but has been reported in other β -keto dicarboxylic acids (193).



Scheme 3-3: Proposed mechanism for decarboxylation of oxosuccinic acid, **38**.

As an alternative strategy, selective deprotection could be restricted to neutral methods. As noted, acid or base catalysed ester hydrolysis led to partial or complete decarboxylation but

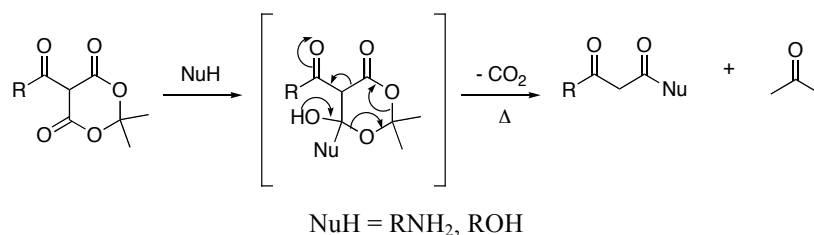
hydrogenolysis of benzyl esters afforded acid **29** with trace amounts of ketone **30** (Scheme 3-1, p 60).

3.2.3.4 FORMATION OF β -KETO AMIDE **36**

It appeared that in the present study, neither DIC nor EDC were efficient reagents for amide bond formation in regards to yield. Kaufmann *et al.* (153) reported a 50% yield using EDC, however, in the coupling of acid **29** to amine **35** (Scheme 3-1), using EDC and hydroxybenzotriazole (HOBt) (as described by the authors), no appreciable improvement was noted. Other peptide coupling agents were investigated such as *N,N,N',N'*-tetramethyl-O-(7-azabenzotriazol-1-yl)uronium hexafluorophosphate (HATU) (194) but this reaction was unsuccessful. The acyl chloride of **29**, obtained under Vilsmeier conditions (181), failed to react with the amine **35** although this method has been successful in generating the unsubstituted derivatives of **37** as well as the natural QSSM, C₄-HSL.

The data presented by Bruice *et al.* (195) may be relevant, as it suggested that as well as primary and secondary amines (196, 197), tertiary amines can catalyse the decarboxylation of β -keto dicarboxylic acids through imine and iminium intermediates. Indeed, only **30** (Scheme 3-1) was isolated after use of the peptide-coupling reagent, HATU and the tertiary base, *N,N*-diisopropylethylamine, (DIPEA). Such reagents are part of a diverse range of new and more effective peptide coupling reagents, however, tertiary bases are usually needed in the activation step. Currently the amidation step (Scheme 3-1) is the yield-limiting step and further optimisation is necessary. Peptide coupling reagents that require tertiary bases will have to be excluded, however, the possible effects of the secondary amine **35** should be investigated before any other approaches are considered.

The substitution and concomitant decarboxylation of acylated Meldrum's acid **18** (Scheme 3-4) is believed to begin with the nucleophilic addition by the free amine **35** at room temperature, which drives the elimination of acetone and CO₂ that is promoted by heat. The inclusion of Et₃N in method B (Scheme 3-2) hinders the reaction as it has been suggested that **18** is forced to remain as the unreactive enolate (Figure 3-4) (176).



Scheme 3-4: Proposed nucleophilic addition-elimination.

Adapted from Oikawa *et al.* (174).

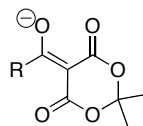
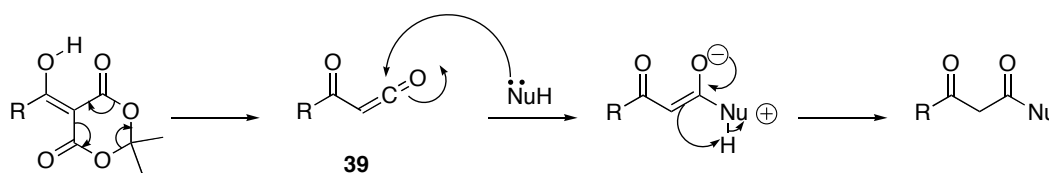


Figure 3-4: Enolate form of acylated Meldrum's acid.

In contrast, Xu *et al.* (176) suggested that the acylated Meldrum's acids decarboxylate to form an α -oxo-ketene **39** (Scheme 3-5) that reacts with nucleophilic species, specifically, RNH_2 . Furthermore, catalytic TFA promotes this decarboxylation at lower temperatures. However, in a published report (198) the method presented by Xu *et al.* (176) was used to produce natural AHLs, however yields of <30% with poor enantiometric purity were reported, it was also noted that the acidic conditions caused the formation of the unsubstituted QSSM as a side-reaction. This was suppressed by substituting TFA with Et_3N , however, this does not correlate with the idea that the unreactive enolate species (Figure 3-4) is formed in basic conditions, in this study, the unsubstituted QSSM by-products resulted in the presence of Et_3N (171).



$\text{NuH} = \text{RNH}_2$

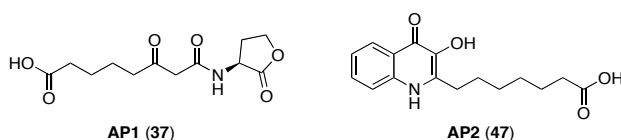
Scheme 3-5: Proposed reaction mechanism between α -oxo-ketene **39** and nucleophilic species.

Adapted from Xu *et al.* (176).

3.2.4 SUMMARY

AP1[^] (**37**) was produced in sufficient quantities to continue with haptenisation. Method A (Scheme 3-1, p 64) produced in a cumulative yield of 10% over seven steps; method B (Scheme 3-2, p 65) produced **37** in a cumulative yield of 4% over two steps. Method A is the preferred method, further optimization is required including the protection of the β -keto function of **22-26**, essential for protection against decarboxylation through subsequent deprotection and amidation.

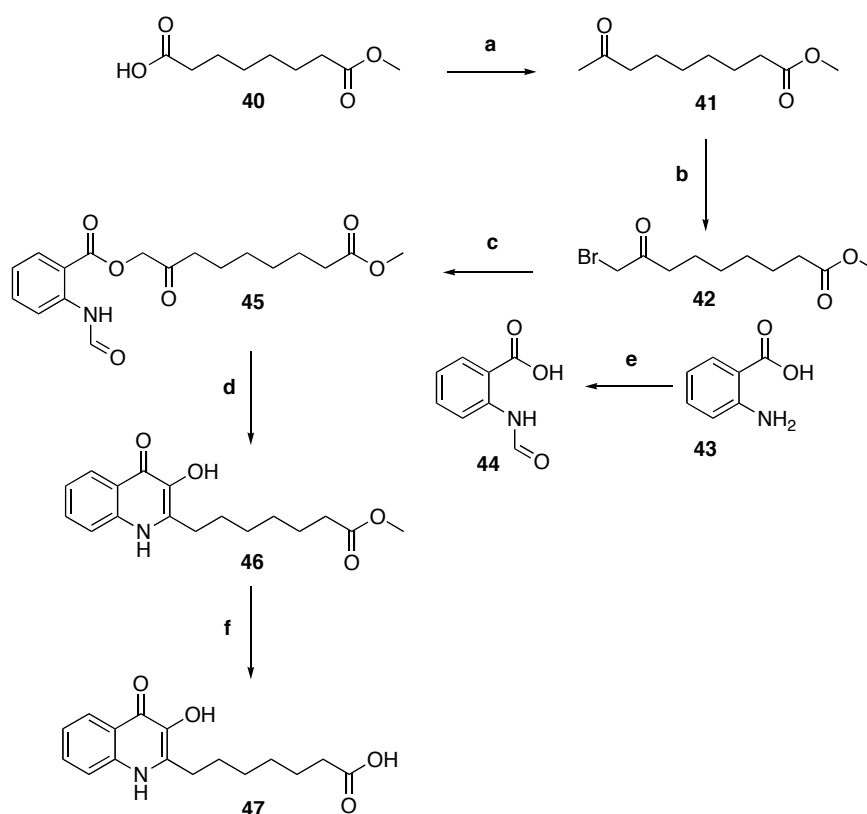
^



3.3 SYNTHESIS OF **AP2**, 7-(1,4-DIHYDRO-3-HYDROXY-4-OXOQUINOLIN-2-YL)HEPTANOIC ACID **47**

3.3.1 METHOD A

A method adapted from Hradil *et al.* (199) was used to synthesise 7-(1,4-dihydro-3-hydroxy-4-oxoquinolin-2-yl)heptanoic acid **47** (**AP2**) (Scheme 3-6). Commercially available *mono* methyl suberate **40** was converted to the corresponding acyl chloride under Vilsmeier conditions (181), which was transformed to the ketone **41** with Gilman's reagent, Me_2CuLi (200) via a nucleophilic substitution of the acyl chloride (201). Subsequent bromination of the terminal α -carbon was possible using bromine under acidic conditions (202) to furnish bromoketone **42**, which was used to alkylate *N*-formyl anthranilic acid **44** (203). The β -keto diester **45** was cyclised in excess ammonium formate (NH_4HCO_2) and formic acid (HCO_2H) (199) using microwave irradiation to form a mixture of ester **46** and acid **47**. Final acid-mediated deprotection and subsequent crystallisation afforded acid **47** in a cumulative yield of 33% over six steps (Scheme 3-6).

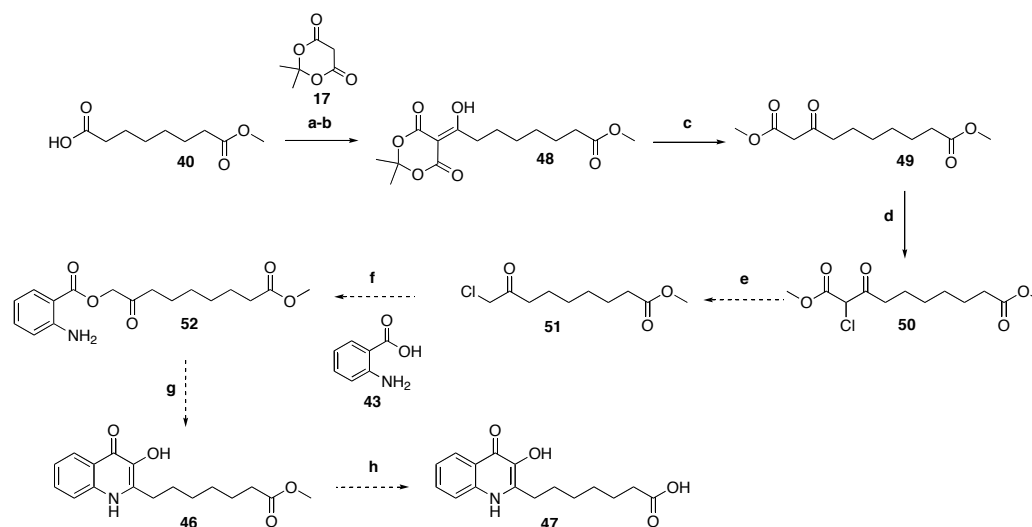


Reagents and conditions: (a) i) $(\text{COCl})_2$, CH_2Cl_2 , cat. DMF ii) MeLi , CuI , Et_2O , -78°C , (75%); (b) Br_2 , MeOH , -10°C to rt, aq. H_2SO_4 (crude yields $> 100\%$); (c) Et_3N , $(\text{CH}_3)_2\text{CO}$ (crude yields $> 100\%$); (d) NH_4HCO_2 , HCO_2H , MW, 120°C (**46/47**, 60%); (e) 98% HCO_2H , reflux; 98% HCO_2H , rt (52%); (f) THF, conc. HCl , rt, (73%).

Scheme 3-6: Formation of **AP2**, **47**, via method A.

3.3.2 METHOD B

Using the protocol reported by Purcell (173), the acylated Meldrum's acid derivative **48** (Scheme 3-7) was refluxed in MeOH to form the β -keto diester **49** in good yield (73%). This was treated with sulfuryl chloride to form the chlorinated β -keto diester **50**, which in pilot studies was transformed to the chloroketone **51** after refluxing in aqueous H₂SO₄. However, when the same reaction was repeated, hydrolysis of the methyl ester resulted. Reprotection by esterification with *t*-butanol and EDC or acid-catalysed esterification with MeOH was unsuccessful, preventing synthesis of **47** by this method.

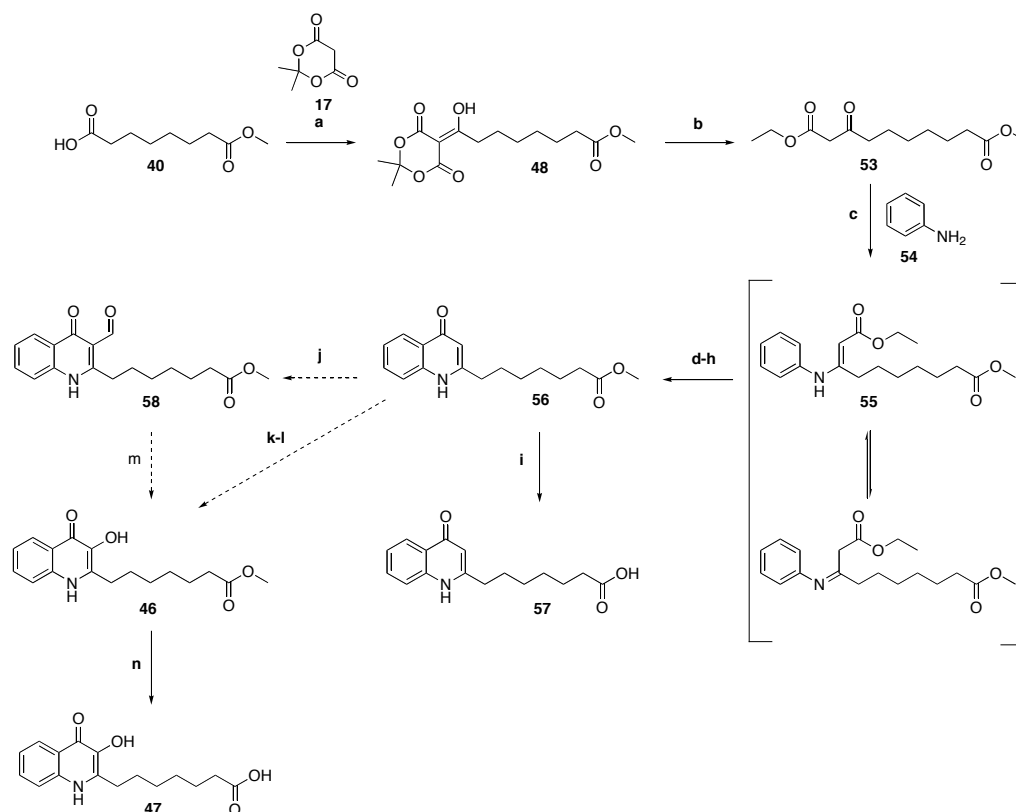


Reagents and conditions: (a) DIC, DMAP, CH₂Cl₂, 0 °C to rt (crude >100%); (b) EDC, DMAP, CH₂Cl₂, 0 °C to rt, (qualitative); (c) MeOH, reflux (73%); (d) SO₂Cl₂, 0 °C to rt; (e) aq. H₂SO₄, reflux; (f) i) K₂CO₃, **43**, DMF, 90 °C to rt; ii) **51**, rt to 50 °C; (g) NMP, reflux; (h) THF, conc. HCl.

Scheme 3-7: Formation of **AP2**, **47**, via method B.

3.3.3 METHOD C

Method C is based on the adaptation by Pesci *et al.* (66) of a Conrad Limpach reaction (204). The β -keto diester **53** (Scheme 3-8, p 72) was condensed with aniline **54** under Dean-Stark conditions to form the Schiff base **55**, an enamine-imine intermediate. Isolation of **55** was not possible, as attempted purification resulted in rapid degradation. Consequently, **55** was generated *in situ*, and cyclised without isolation, to afford ester **56**. Base-mediated hydrolysis of ester **56** afforded the HHQ derivative, 7-(1,4-dihydro-4-oxoquinolin-2-yl)heptanoic acid **57**. Formylation of **56** by the Duff method (66), to give the desired product **58** was not possible, as was the conversion of **56** to ester **46** via Elbs oxidation (205) and Rubottom reaction (206), thus preventing the synthesis of acid **47** by this route.



Reagents and conditions: (a) DIC, DMAP, CH_2Cl_2 , 0 °C to rt, (crude >100%); (b) EtOH, reflux (63%); (c) **54**, toluene, cat. *p*-TsOH, reflux; (d) Ph_2O , 250 °C (22%); (e) Eaton's reagent, 90 °C; NMP, reflux; (f) Ph_2O , MW, 250 °C; (g) NMP, MW, 250 °C (11%); (h) Eaton's reagent, MW, 90 °C; (i) 1 M NaOH, $(\text{CH}_3)_2\text{CO}:\text{H}_2\text{O}$ (70%); (j) i) $(\text{CH}_2)_6\text{N}_4$, TFA, reflux ii) aq. MeOH, reflux iii) 3M HCl, reflux; (k) i) 1.6 M NaOH, $\text{K}_2\text{S}_2\text{O}_8$, rt, ii) HCl, reflux to rt; (l) i) DIPEA, THF, *n*-BuLi, -15 °C to 0 °C to -15 °C to rt, **56**, TMSCl, N_2 ii) THF, *m*-CPBA, -78 °C to rt; iii) CH_2Cl_2 , $\text{Et}_3\text{N} \cdot 3\text{HF}$, rt; (m) H_2O_2 , aq. EtOH, rt; (n) THF, conc. HCl.

Scheme 3-8: Formation of **AP2**, **47**, via method C.

3.3.4 DISCUSSION

3.3.4.1 α -HALO-KETONES

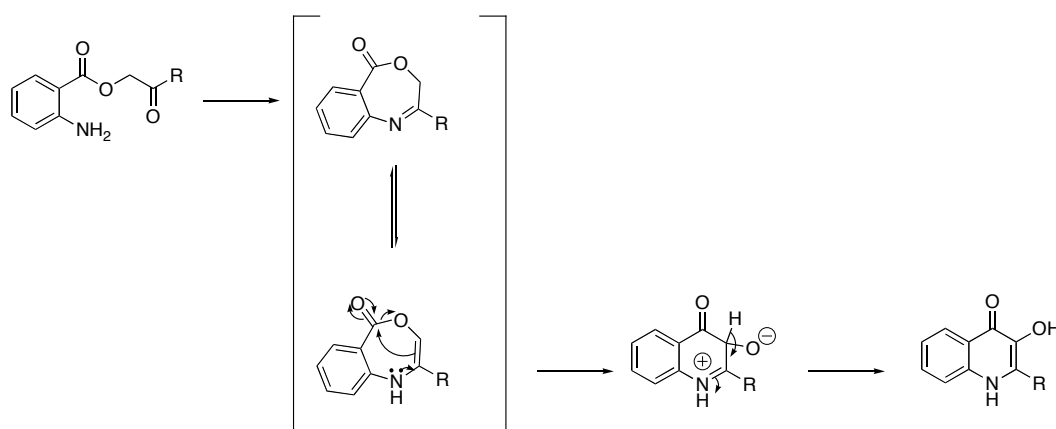
3.3.4.1.1 METHOD A

Formation of the methyl ketone **41** (Scheme 3-6, p 70) was facile, taking advantage of the Gilman's reagent reactivity towards acyl halides. Gilman's reagents tend not to react with esters, amides and ketones thus further transformation of the ketone is avoided. In contrast, Grignard reagents will further react with the ketone formed initially (189). Gilman reagents are prepared *in situ*, one equivalent of CuI and two equivalents of RLi (for example, R = Me) forming one equivalent of Gilman's reagent, R_2CuLi . Exact stoichiometry needs to be observed, as excess CuI resulted in the formation of MeCuLi , which is a coloured inert compound, whereas excess MeLi led to several competing side-reactions. Subsequent bromination was successful without affecting the protected methyl ester.

3.3.4.2 CYCLISATION

3.3.4.2.1 METHOD A AND B

The aniline **43** (Scheme 3-6, p 70) is a relatively poor nucleophile due to the delocalisation of the lone pair of electrons of nitrogen into the aromatic ring, with a further mesomeric deactivation from the *ortho*-acid group, which may be alleviated somewhat by alkylation. However, the high temperatures (250 °C) in method B (Scheme 3-7, p 71) are still necessary to disrupt the mesomeric effect of the aromatic ring and allow the amine, the poor nucleophile, to participate in the intramolecular condensation resulting in the 4-(1*H*)-quinolone (173, 207, 208). The intermediate **52** (Scheme 3-7), upon cyclisation would form the unstable 7-membered ring which rearranges to the preferred 6-membered ring with further proton rearrangement to form 2-substituted-3-hydroxy-4(1*H*)quinolone (Scheme 3-9) (173).



Scheme 3-9: Mechanistic view of intramolecular condensation to form 2-substituted-3-hydroxy-4(1*H*)-quinolones.

Adapted from (173, 207, 208).

Formylating anthranilic acid **43** to form *N*-formyl anthranilic acid **44** may reduce the delocalisation of the lone pair of electrons into the aromatic ring. Presumably, less energy therefore lower temperatures would be needed to promote the intramolecular condensation. However, the *N*-formamide is a poor nucleophile as the formyl group exerts mesomeric effect. Yet, in this study, method A (Scheme 3-6, p 70) was successful. In the original method (199), the authors refluxed the reaction mixture in a microwave reactor, using sealed vessels. Mindful of the volatile by-products, ammonia and carbon dioxide, it was known that the reaction would generate pressure; this was solved by employing a batch method but on a large scale this may be impractical.

3.3.4.3 METHOD C

Copious amounts of petroleum ether (60-80 °C) were required to precipitate **56** (Scheme 3-8, p 72) from diphenyl ether (Ph₂O) followed by additional column chromatography to remove residual Ph₂O. Although the use of a high-vacuum centrifuge instrument (Genevac) was

effective in removing most of the Ph₂O, this took considerable time (18 hours) and further purification was always needed to remove remaining traces of Ph₂O.

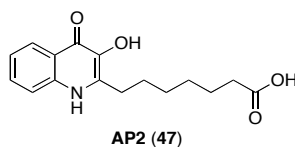
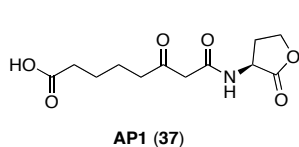
Use of Eaton's reagent (209), a methansulfonic-phosphorus oxide mixture (210), under microwave irradiation, was useful for cyclisation of **55**, though it was not possible to isolate pure **56**. Use of NMP aided cyclisation and was easier to remove than Ph₂O, but the yield was comparatively lower (11%). Other methods were tried such as acetic anhydride and H₂SO₄ (211) and polyphosphoric acid (PPA) (212), but were unsuccessful.

3.3.5 SUMMARY

The synthesis of PQS has advanced since the strategy proposed by Pesci *et al.* (66). Hodgkinson *et al.* (208) have used microwave irradiation and high through-put methods to advance Purcell's method (173). Although the mechanism remains unknown, method A is another approach to produce the 3-hydroxy HAQs and, **AP2**[^] was produced in a cumulative 33% yield over six steps, which provided sufficient quantity to continue with protein conjugation.

In this study, method C (Scheme 3-8, p 72) was not useful for the syntheses of PQS and derivatives, due to the failed formylation attempts of the C3 position of the quinolone. However, acid **57** is a potential hapten. The cyclisation is the yield-limiting step and attention should be given to the optimisation of method C in future work and development of the alternate approach (Scheme 3-11, p 75).

^

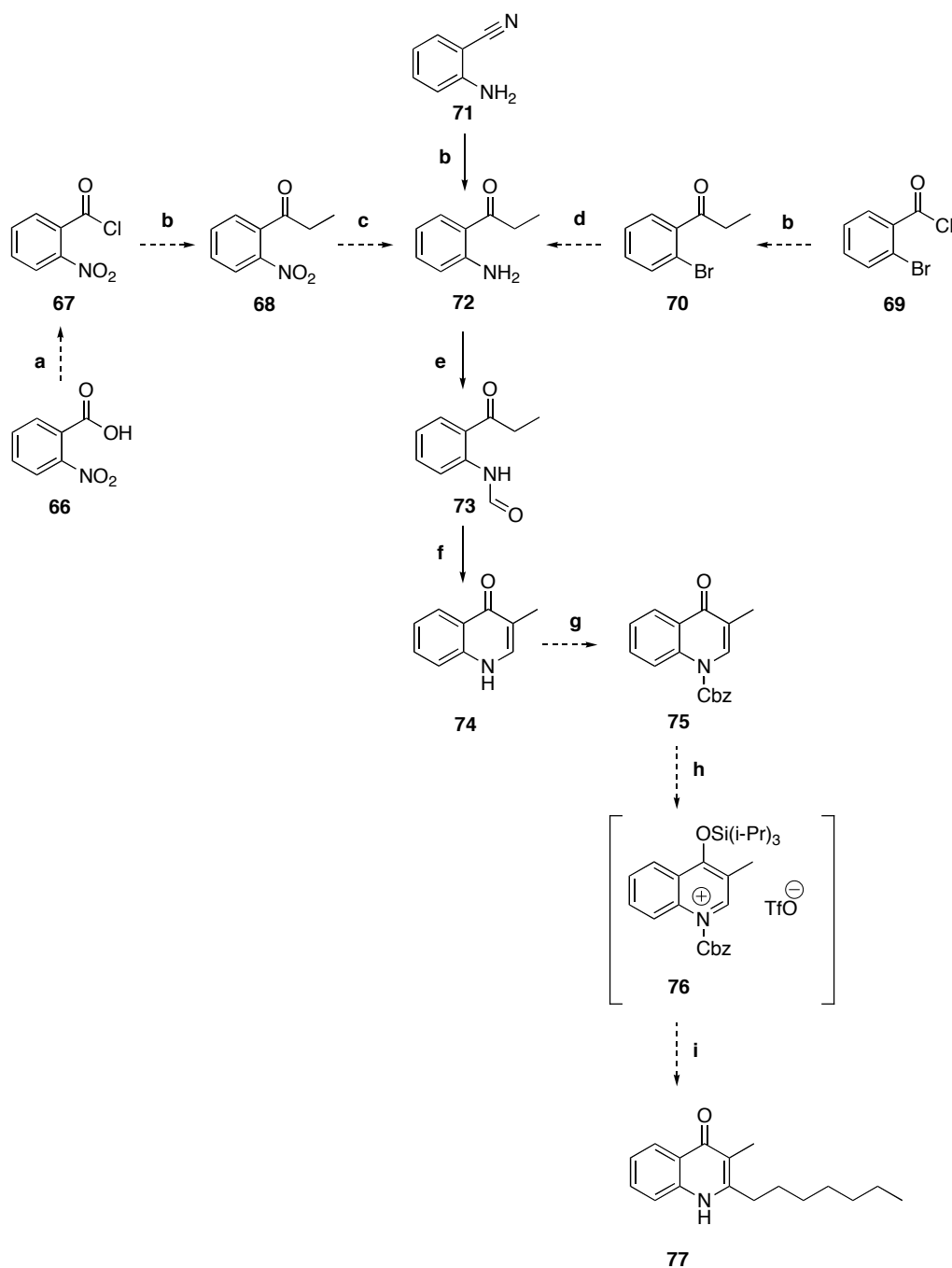


the C2 position of the quinolone by Grignard reagents (216). The development of this strategy is of interest as it can be a robust method to produce the HHQ derivatives, which are potential haptens.

3.4.3 HMAQs OF *BURKHOLDERIA* SPP.

Using the Conrad-Limpach reaction, Moon *et al.* (217) have produced the saturated HMAQs in high yields. However, it is probable, as the cyclisation method is similar to that tried in method C (Scheme 3-8, p 72), that it may be difficult to replicate the authors' results (217). A retro-synthesis of HMAQs shows that unsaturated and saturated acyl chains can be introduced at the C2 position of the quinolone by a Grignard reaction (216). Huang *et al.* (214) have reported the synthesis of quinolin-4(1*H*)-one through Camp's quinoline synthesis, which is appropriate for the production of the synthon **74** (Scheme 3-12, p 77). A Grignard reaction is also useful to afford **68** and **70** from acyl chlorides **67** and **69** respectively. However, in this pilot study, **69** could not be converted to the ketone **70** and the reaction with **67** resulted in a complex mixture as the nitro group is also sensitive to Grignard reagents.

The Grignard reagent, EtMgBr, was produced *in situ* and used in a 3:1 ratio to the substrate 2-aminobenzonitrile **71** (Scheme 3-12) to compensate for the reaction of the amine moiety with the Grignard reagent (216). The reagent, through a nucleophilic addition, forms an organometallic imine intermediate. The ketone **72** was obtained from the acidic hydrolysis of the intermediate in disappointing yields (14%). Subsequent *N*-formylation (218) and cyclisation in basic conditions using microwave irradiation afforded 3-methyl-quinolin-4(1*H*)-one **74**. Protection with benzyloxycarbonyl group (Cbz) (219) was restricted by limited solubility in THF. The pilot studies indicate that this procedure requires further investigation. Adjustments to the current strategy may be necessary, in particular, an alternative method for the formation of 1-(2-aminophenyl)propan-1-one **73**, which was obtained in unexpectedly low yields. It is anticipated that this will still be a robust method but further development is needed. There were some minor contaminants present in **74** that could not be removed, for the purpose of this study, **74** was used in competitive indirect ELISA studies (6.2, p 100).



Reagents and conditions: (a) $(\text{COCl})_2$, cat. DMF, CH_2Cl_2 , rt; (b) i) EtBr, Mg, Et_2O , -78°C ; ii) **71**, (14%); (c) Catalytic reduction; (d) 5% CuI, K_3PO_4 , $\text{HO}(\text{CH}_2)_2\text{OH}$, isopropanol, 80°C ; (202) (e) HCO_2H , 50°C (37%); (f) NaOH, 1,4-dioxane, MW, 120°C , (36%); (g) i) NaH, THF, $50-60^\circ\text{C}$ ii) $\text{C}_6\text{H}_5\text{CH}_2\text{O}_2\text{CCl}$, $50-60^\circ\text{C}$; (h) i) **75**, TIPSOTf, rt ii) $\text{CH}_3(\text{CH}_2)_5\text{CH}_2\text{Br}$, Mg, Et_2O , -78°C iii) CH_2Cl_2 , 2,6-lutidine; (i) 10% Pd-C, MeOH, rt.

Scheme 3-12: Synthesis of 2-heptyl-3-methyl-quinolin-4(1H)-one, **77**.

4 MATERIALS AND METHODS

GENERAL

MALDI-TOF spectra were recorded using a Ultraflex III MALDI-TOF instrument using samples (100 μ g) prepared in pure H₂O with sinapinic acid ((in TFA:H₂O:MeOH, 0.1:50:50%) 200 μ g/mL). Matrix was spotted to the loading plate and dried, the matrix:sample solution was then spotted on the loading plate. The absorbance (recorded as optical density (OD)) was read at the specified wavelength using the MRX plate-reader. Bioluminescence was recorded in arbitrary units using a Parkard Bell Top-Count reader, (temperature 37 °C). Reagents, unless specified, were obtained from Sigma Aldrich and Alfa Aesar. All buffers and reagents were prepared using laboratory standard operating procedures or used as received by the manufacturers. LB broth and regents used for M9 minimal media were autoclaved before use. M9 minimal media (5 mL M9 minimal media: 1 mL M9 salts (48 mM Na₂HPO₄·7H₂O, 22 mM KH₂PO₄, 19 mM NH₄Cl, and 8.6 mM NaCl), 0.5 μ L CaCl₂, 10 μ L MgSO₄ and 3.88 mL dH₂O) was aseptically prepared. AHL QSSMs were kindly donated by A Truman, Pr Paul Williams, University of Nottingham. Reporter strains, *P. aeruginosa* PAO1 Δ pqsA CTX-luxCDABE::pqsA, *E. coli* S17.1 pSB1075, *E. coli* S17.1 pSB536 and WT Nottingham *P. aeruginosa* PAOI were kindly donated by Dr Diggle, University of Nottingham. *P. aeruginosa* PACY1 (PAO1-lausanne PKm-lux) was kindly donated by Pr Miguel Càmara, University of Nottingham. All procedures were planned and executed in a Category 2 laboratory in accordance with local regulations including standard operating procedures and risk and safety assessments.

GENERAL PROCEDURE FOR THE SYNTHESIS OF NHS ESTERS

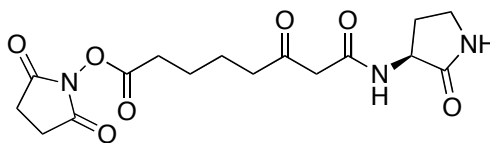
N-hydroxysuccinimide (NHS) (10.1 mg, 0.09 mmol) was added to an ice-cold stirred solution of the hapten (21 mg, 0.08 mmol) and EDC (18.4 mg, 0.10 mmol, Fluorochem Ltd) in anhydrous 1,4-dioxane (0.73 mL). Anhydrous DMF was added drop-wise until the solution was clear. The reaction was stirred at room temperature (rt) under an atmosphere of N₂ for 16 h until the reaction was complete (TLC, EtOAc). The solvent was rotary evaporated and the crude mixture was dissolved in EtOAc and washed with dH₂O followed by brine. The solution was dried over MgSO₄. The solvent was removed by rotary evaporation and triturated with EtOAc and hexane. The precipitate was carefully collected and transferred to a pre-weighed oven dried vial and kept under N₂ until further use. (NHS esters can be stored for long periods under N₂ in a dessicator, but it was noted that the best results were obtained with immediate use. NHS esters are sensitive to moisture, therefore, the compound was minimally handled).

HYDROXYSUCCINIMIDE-7-((S)-2-OXOPYRROLIDIN-3-YLCARBAMOYL)-6-OXOHEPTANOATE

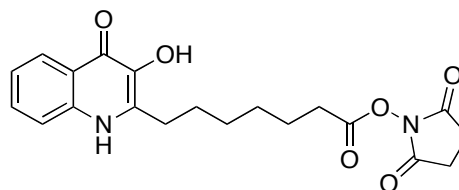
7-((S)-2-oxopyrrolidin-3-ylcarbamoyl)-6-

oxoheptanoic acid (**37**) was used in the above procedure to afford the title compound as an off-white solid (21 mg, 74%). HR-ESI-MS-

ESI: m/z 368.1529 [M + H], 391.0886 [M + H + Na]⁺, 328.0858, C₁₆H₂₁N₃O₇ requires 367.1380 and [C₁₆H₂₂N₃O₇Na]⁺ requires 390.1277.

**HYDROXYSUCCINIMIDE-7-(1,4-DIHYDRO-3-HYDROXY-4-OXOQUINOLIN-2-YL)HEPTANOATE**

N-hydroxysuccinimide (NHS) (13.5 mg, 0.12 mmol) was added to an ice-cold stirred solution of the 7-(1,4-dihydro-3-hydroxy-4-oxoquinolin-2-yl)heptanoic acid (**47**, 30 mg, 0.1 mmol) and EDC (24 mg, 0.13 mmol) in anhydrous 1,4-



dioxane (0.73 mL) was used to prepare the final NHS ester. The contaminant (methyl-7-(1,4-dihydro-3-hydroxy-4-oxoquinolin-2-yl)heptanoate, (**46**) could not be removed during the purification of **47**, but was removed after conjugation and subsequent ultracentrifugation. The subsequent procedure was followed as described as above to afford the title compound as a beige solid (crude >100%). ¹H NMR was conducted, the distinct multiplet (¹H NMR (CDCl₃): δ 2.74 (m, 4H, (CH₂)₂)) indicated that the *N*-hydroxysuccinimide ester had formed. The sample degraded during MS analysis.

GENERAL PROCEDURE FOR PROTEIN HAPTENISATION*BSA/KLH*

NHS ester (4.18 mg, 0.0114 mmol) was dissolved in DMSO (81 μL) and added drop-wise to carrier KLH (11.4 mg, (100 000 g is equivalent to 1 mole)) or BSA (10.3 mg) in filtered phosphate buffer solution (1.32 mL, 50 mM, pH 7.4). The reaction solution was agitated at 200 rpm at 4 °C for 24 h. The solution was purified using Vivaspın ultrafiltration cartridges with 10 000 MWCO with filtered phosphate buffer solution (50 mM, pH 7.2) to afford the hapten-carrier conjugate as a concentrated solution. Protein estimation using Bio-rad[®] Bradford assay was conducted. BSA was used as standard known concentrations (0-1000 μg/mL) were titrated against the sample as a neat, 1:10, 1:20 and 1:100 (v/v) dilutions (n = 3). Briefly, 5 μL of standard or sample was transferred to a 96-well polystyrene flat-bottomed microtitre plate to which 250 μL of Bio-rad[®] Bradford reagent (1:4, reagent:dH₂O) was added. This was left for 5 min and the absorbance was recorded at 590 nm. The samples were interpolated from the standard curve.

The sample was prepared for MALDI-TOF analysis by exchanging the buffer with pure H₂O

using Vivaspin ultrafiltration cartridges with 10 000 MWCO (100 μ L capacity).

2D-SDS PAGE

The protein sample (30 μ g) was dissolved in 125 μ L rehydration buffer (7 M urea, 2 M thiourea, 1% (w/v) ASB-14, 40 mM Tris, 0.001% bromophenol blue, 0.2% ampholytes, 0.5% DTT). The solution was transferred to the rehydration tray and the IPG strip (Bio-rad, pH 3-10, 7 cm) was placed gel facing onto the sample. Once covered with mineral oil, the tray was covered with the lid and rehydrated under active conditions and focused using the Protean IEF cell (Bio-rad®). Upon completion, the mineral oil was carefully removed from the IPG strip using dH₂O. The IPG strip was transferred gel facing upwards to the equilibrium buffer tray and incubated at rt in Equilibrium buffer I (Bio-rad®) for 10 min. After washing with dH₂O, the strip was incubated in Equilibrium buffer II (Bio-rad®) for a further 10 min. The buffer was removed by washing the strip with dH₂O and adjusted to the appropriate size by cutting the edges of the strip. This was transferred to the pre-set stacking gel (4% polyacrylamide)/resolving SDS-gel (10% polyacrylamide)), secured in place with 5% agarose. After the electrophoresis (20 mV) was complete, the gel was stained with Coomassie blue in destain buffer (MeOH/glacial acetic acid/H₂O, 25:0.1:75%) and incubated at rt for 16 h. The excess stain was removed using destain buffer.

IMMUNISATION PROTOCOL

Mouse

Three CD1 female mice and three Balb/c female mice were immunised (s/c) with 100 μ g of hapten-KLH conjugate in Freund's complete adjuvant (FCA) in two divided doses. Three booster injections in incomplete Freund's adjuvant (IFA) were given at 2-week intervals. Test bleeds were taken seven days after each immunisation. The mice were euthanised seven days after the 3rd booster and terminal bleed was taken. Immunisations were carried out by BMSU, Queens Medical Centre, Nottingham using standard procedures; test bleeds were collected on-site within 1 h. The serum was separated from each bleed by centrifugation and characterised separately; the terminal bleed was then pooled for further tests.

Rabbit

One New-Zealand white female rabbit was immunised with 200 μ g hapten-KLH conjugate in FCA. Five boosters in IFA were given at 2-week intervals, and test bleeds were taken seven days post immunisation. The rabbit was euthanised on the 77th day and the terminal bleed was collected. Harlan Laboratories, UK, conducted the immunisations using standard procedures. The serum was used as received.

STANDARD INDIRECT ELISA PROCEDURE

A 96-well polystyrene flat-bottomed microtitre plate was coated with 100 μ L hapten-BSA conjugate in PBS, (20 mM, pH 7.2) at pre-determined concentrations (checkerboard titrations, CBT) and incubated overnight at 4 °C. This was washed three times with PBST (pH 7.2, 0.05% Tween) and tapped dry. Each well was blocked with 300 μ L 5% PBST-M (PBS, 0.05% Tween and 5% milk powder) for 1 h at rt. The microtitre plate was washed four times and dried as described above, 50 μ L of the test sample in specific concentrations were added to the appropriate wells. This was incubated at rt for 2 h and washed four times as above. After drying as described above, 50 μ L of HRP conjugated secondary antibody (R&D System) was added to the appropriate wells and incubated for 2 h at rt. The microtitre plate was washed four times and 50 μ L of the substrate solution (3,3',5,5'-tetra-methylbenzidine dihydrochloride tablet (1 mg)) in 10 ml of 0.05 M phosphate-citrate buffer, pH 5.0 and 2 μ L of 30% hydrogen peroxide) was added and incubated whilst protected from light, at rt for 10 min. The reaction was stopped by the addition of 2.5 M H₂SO₄ (25 μ L) and the OD was recorded at 450 nm. Anti-BSA:HRP secondary antibody (AbD Serotec) was used to confirm success of antigen coating.

Checkerboard titrations (CBT)

The above protocol was followed, however, the hapten-BSA conjugates were prepared in 1 in 2 serial dilutions (v/v) from 30 μ g/mL. The anti-hapten serum was prepared as 1 in 10 serial dilutions in PBST.

Specificity

BSA, KLH, PBS, and hapten-BSA were used to coat the appropriate wells of a 96-well polystyrene microtitre plate at the pre-determined concentration of hapten-BSA. The indirect ELISA protocol was followed as described.

Competitive indirect ELISA

The QSSM (3OC₁₂-HSL, 3OC₈-HSL, 3OC₆-HSL, C₈-HSL, C₆-HSL, C₄-HSL, PQS, HHQ and HSL, and tetramic acid, AP, anthranilic acid and 3-methyl-quinolin-4(1H)-one) were prepared in 100 μ L stock solutions with a concentration of 5% DMSO. These were diluted to the test concentrations, 1000 μ M, 100 μ M, 10 μ M, 1 μ M, 0.1 μ M and 0 μ M with 100 μ L of stock anti-hapten serum in PBST so the final working concentrations were: 2.5% DMSO and 1 in 2 dilution of stock anti-hapten antibody. Subsequent procedure was followed as described above. The controls were 2.5% DMSO-PBST and mouse or rabbit anti-serum in PBST.

AFFINITY CHROMATOGRAPHY USING PROTEIN G-SEPHAROSE

The protein G-Sepharose and PD10 columns were flushed with sodium phosphate buffer (20 mM, pH 7.2). The rabbit serum was added to PD10 column and eluted with sodium phosphate buffer in 1 mL fractions. The absorbance for each fraction was read at 280 nm, and fractions

with OD of over 0.40 were collected and combined, this was added to the protein G-Sepharose column via a 20 ml syringe and eluted with sodium phosphate buffer in 1 mL fractions. This was continued until the OD was 0.05 and below (280 nm). The pooled fractions were collected and tested negative for pIgG using the standard indirect ELISA protocol.

The column was eluted with 0.1 M glycine HCl (pH 2.3) in 1 mL fractions into eppendorfs with 20 μ L 1 M Tris buffer (pH 9). The fractions were collected until the OD was < 0.40 (280 nm). These fractions were collected and dialysed (membrane, MWCO 10 000) against PBS (20 mM, pH 7.2) for two days at 4 °C with one buffer change per day. The dialysed sera were tested for: protein content using the Bio-rad® Bradford assay; and pIgG using the standard indirect ELISA protocol. The pIgG were stored in fractions at -20 °C until use.

BSA ADSORPTION USING NITROCELLULOSE MEMBRANE

This procedure was only used for small-scale adsorption. Two strips of nitrocellulose membrane were added to filtered BSA solution (20 % w/v in PBS) and rotary mixed for 24 h at 4 °C. One strip was used as a control and tested for BSA adsorption using a modified Western blot procedure. The second strip was added to 0.5 mL anti-hapten pIgG in PBS, and the volume was increased to 1 mL with PBS, Tween was added so the final solution was 0.05% PBST. This was gently rotary mixed at 4 °C for 24 h. The solution was removed and concentrated using Vivaspın ultrafiltration cartridges with 10 000 MWCO and tested for BSA specific pIgG using the specificity ELISA procedure.

The control strip was blocked with 5% PBST-M for 1 h at rt. This was washed with PBS three times and incubated with 1 in 500 (v/v) diluted solution of anti-BSA:HRP secondary antibody for 2 h. This was washed three times with PBS and once with dH₂O. The substrate (50 mg 4-chloro-1-naphthol in EtOH:PBS, 10:40 mL and 30 μ L 30% H₂O₂) was added to the strip, incubated until visual colour detection and the reaction was stopped by replacing the solution with water.

BIOLUMINESCENCE

Reporter strains

5ml of sterile LB broth containing 128 μ L of 5 mg/mL tetracycline in 70% EtOH was inoculated with *P. aeruginosa* PAO1 Δ pqsA CTX-luxCDABE::pqsA; 5 mL of sterile LB broth and 20 μ L of 5 mg/mL tetracycline was inoculated with *E. coli* S17.1 pSB1075; 5 mL of sterile LB broth and 12.5 μ L of 20 mg/mL ampicillin was inoculated with *E. coli* S17.1 pSB536; 5 mL of sterile LB broth was inoculated with *P. aeruginosa* PACY1 (PAO1-lausanne PKm-lux), and were incubated at 37 °C and agitated to maintain planktonic growth on a shaker at 200 rpm for 16 h.

Assay

The test samples contained: QSSM (PQS, 3OC₁₂-HSL, C₄-HSL and HHQ) in DMSO at the indicated concentrations, (final concentration of DMSO was kept constant (2 μ L for AHLs and 1 μ L for HAQs)); anti-hapten rabbit pIgG sera was diluted with PBS (20 mM, pH 7.2), tested at 1, 10, 100, 200, 300, 400, 500 μ g/mL (the final volume of PBS was kept constant for each test sample and was based on the PBS volume that contained 500 μ g/mL of anti-hapten rabbit pIgG); and 14 μ L of a 1 in 100 (v/v) solution of the appropriate reporter strain in fresh LB broth. All solutions were made up to 200 μ L using fresh LB broth. Pre-bleed pIgG was diluted with PBS (20 mM, pH 7.2) and tested at 200 μ g/mL. 50 μ L of the test solution was removed and transferred to the appropriate 96-well black flat-bottomed microtitre plate (n = 3). A time point zero was taken and the microtitre plate was wrapped in cling-film and incubated in a humid environment at 37 °C. Readings were taken every 60 min until the end-point (decrease in positive control bioluminescence). The readings were corrected by subtracting the values from time point zero.

STATIC BIOFILM ASSAY

WT Nottingham *P. aeruginosa* PAO1 strain was grown in 5 mL sterile LB broth at 37 °C (agitated at 200 rpm) for 16 h. The culture was diluted to a 1 in 100 using sterile M9 minimal media supplemented with glucose (5 mL M9 minimal media: 1 mL M9 salts (48 mM Na₂HPO₄·7H₂O, 22 mM KH₂PO₄, 19 mM NH₄Cl, and 8.6 mM NaCl); 100 μ L filtered (0.2 μ m syringe filter) 20% glucose; 0.5 μ L CaCl₂; 10 μ L MgSO₄ and 3.88 mL dH₂O).

The anti-hapten rabbit pIgG were diluted with PBS and tested at the concentrations indicated. The pre-bleed rabbit pIgG was tested at 200 μ g/mL. The final volume of PBS was kept constant. The test solutions containing sera were inoculated with 3.5 μ L of 1 in 100 culture were prepared (final concentration of culture was 1 in 1000) as 350 μ L solutions with fresh sterile M9 media supplemented with glucose. 100 μ L of the test solution (n = 3) was transferred to a 96-well (rounded) tissue culture microtitre plate and incubated in a humid environment at 37 °C for 24 h.

The supernatant was carefully removed and the microtitre plate was gently washed three times with dH₂O to remove any planktonic cells. The microtitre plate was gently tapped dry, 300 μ L of filtered 1% crystal violet solution was added, and the microtitre plate was incubated for 15 min at rt. Excess crystal violet was removed and the microtitre plate was washed three times with dH₂O or until no excess stain remained. 150 μ L of destain buffer (MeOH/glacial acetic acid/H₂O, 25:0.1:75%) was added to the appropriate wells and gently mixed, 75 μ L of this solution was transferred to a 96-well (flat bottomed) polystyrene microtitre plate and the OD was recorded at 595 nm.

5 RESULT 2 – HAPTENISATION AND CHARACTERISATION

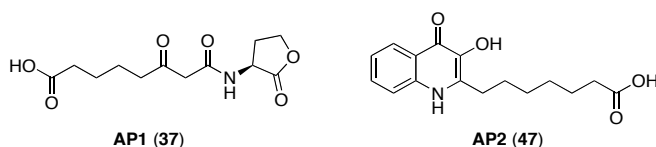
AP1 and **AP2**[^] were produced in sufficient yields to continue with the haptenisation of immunogenic carrier, KLH using the NHS activated method. Hapten-BSA conjugates were also prepared for characterisation purposes as well as use in ELISAs.

5.1 HAPTEN-CARRIER CONJUGATE

5.1.1 HAPTEN AND CARRIER CONJUGATION

Within the immunogenic proteins BSA and KLH ϵ -lysine residues are the most abundant amino acids (BSA – 59 and KLH – 2000) (157). Coupling reagents, such as EDC, are used to form covalent bonds between the carrier and the hapten. The procedure is performed *in situ* and by-products can be removed by ultracentrifugation or dialysis. However, EDC will activate all carboxylic acid groups, increasing the risk of cross-linking between the carrier molecules. This causes aggregation, which can affect the efficiency of the conjugation. An alternative method is to activate the carboxylic acid group of the hapten prior to carrier conjugation. NHS activates carboxylic acid groups by forming an NHS ester, which reacts with the amine residues of the carrier protein to form an amide bond. In this study, the NHS esters were generated using EDC, however to minimise any EDC-mediated cross-linking, the NHS esters of the haptens were isolated prior to protein conjugation. NHS esters have half-lives of a few minutes at alkaline pH even at low temperatures, this hydrolysis reaction competes with the amide bond formation but can be limited by a high protein concentration, and a lower pH, such as pH 7.4 (158).

^



5.1.2 EPITOPE DENSITY

The epitope density refers to the number of hapten groups per carrier molecule, which depends on the number of residues available for modification as well as the hapten; for instance in BSA, only 30–35 ϵ -lysine residues of the 59 are reportedly available for conjugation (158). There are examples of highly substituted haptens, dinitrophenyl (DNP)_{50/60}-BSA, which produced a strong IgM response (220). The optimum epitope density results in antibodies with a strong specificity towards the hapten. An epitope density of 15-30 haptens per BSA molecule equates to high antibody titres but compromised antibody avidity for the hapten (221-223). Conversely, a 13:1 hapten-BSA conjugate produced lower titres of antibodies compared to the 7:1 conjugate (224). Moderate hapten substitution of the carrier ensure that there are sufficient carrier epitopes available for presentation to the carrier dependent T-lymphocytes (225). The immune response largely depends on the nature of the hapten, carrier, and dose, but the optimum epitope density must still be considered to avoid tolerance against the hapten (221-223), a situation in which the immune system has become desensitised to the hapten-carrier conjugate.

5.1.3 CHARACTERISATION METHODS

Hapten-carrier conjugates have been characterised by a variety of methods including UV absorbance spectroscopy, 2,4,6-trinitrobenzenesulfonic acid (TNBS) titration of free lysine residues, mass spectrometry (MS) or sodium dodecyl sulfate polyacrylamide gel electrophoresis (SDS-PAGE) (223, 226, 227). Mass spectrometry (MS), specifically matrix-assisted laser desorption ionization-time of flight (MALDI-TOF), is a relatively more effective and accurate method (226). The matrices used in MALDI-TOF MS absorb the energy from the laser and form reactive species that ionise the sample. MALDI-TOF MS analyses the distribution of the generated ion M_r , and records the M_r of the most abundant ion, the median M_r . Haptenisation resulted in a heterogeneous mixture in regards to M_r , due to the variable number of haptens per protein.

Each hapten-carrier conjugate has a different isoelectric point (pI) relative to unconjugated BSA. The pI corresponds to the pH at which the protein carries no net charge. Unconjugated BSA has a net positive charge, due to the number of lysine residues; modification of the lysine residues will result in an overall negative charge, and a different pI. 2D-SDS PAGE was used to confirm conjugation based on the pI and M_r of the conjugated protein.

The characterisation of hapten-KLH conjugates is limited due to the mass and heterogeneity (227) of KLH, the recorded mass of KLH is between 450 and 13 000 KDa and the protein can dissociate into individual subunits (158). As BSA and KLH were conjugated simultaneously, using the same conditions, the characterisation of the hapten-BSA conjugate and the immune response to the hapten-KLH conjugate was sufficient for the purpose of this study (222, 228).

5.2 RESULTS – HAPTEN-CARRIER CONJUGATE CHARACTERISATION

5.2.1 CONJUGATION

The NHS esters were dissolved in anhydrous DMSO prior to reaction and the solutions were added drop-wise to the carrier protein dissolved in phosphate-buffered solution, pH 7.4. The NHS esters are stable under anhydrous conditions but it was found that conjugation results were better if the NHS esters were used within 24 h. Slight precipitation occurred when the NHS ester was added to the KLH and BSA solutions but no adverse effects on the conjugation reaction were noted. The reaction was left for 24 h after which the conjugates were purified by ultracentrifugation using Vivaspin ultrafiltration cartridges with 10 000 MWCO and 3 000 MWCO membranes, into phosphate buffer solution, pH 7.2. Recovery was variable ranging from 43-91%. The proteins adsorb readily to surfaces and the membranes needed to be washed repeatedly with minimal phosphate buffer solution, pH 7.2 to increase recovery.

5.2.2 MALDI-TOF MS

The matrix, sinapinic acid, was prepared in a 2:1 ratio to sample solution however resolution improved if the matrix was also spotted on the loading plate prior to the matrix/sample solution. Each sample was tested without a BSA standard for detection of unconjugated BSA and then repeated as a spiked sample with unconjugated BSA used as an internal standard.

Haptenisation depended on the conditions used; in slightly alkaline conditions, pH 8 is quite effective as the ϵ -lysine residues are most reactive, however, the stability of the hapten has to be considered. In this study, a pH 7.4 was an acceptable pH to conduct haptenisation, resulting in (median) 13 **AP1** and 18 **AP2** conjugated to the BSA molecule (Figure 5-1, p 87). For the rabbit immunisation, the haptenisation of KLH with **AP1** was repeated in conjunction with haptenisation of BSA with **AP1**. The median of 13 **AP1** per BSA molecule was calculated (spectra not shown). Unfortunately, the spectra indicated that there was some unconjugated BSA in the sample, implying that conjugation was incomplete and by default, unconjugated KLH was present in the **AP1**-KLH conjugate solution used for rabbit immunisation.

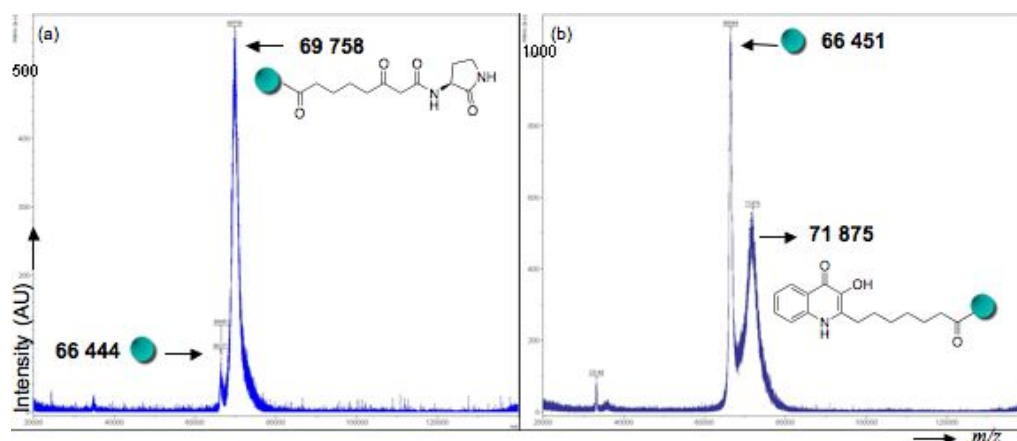


Figure 5-1: MALDI-TOF MS spectra.

(a) **AP1**-BSA MALDI-TOF MS: m/z 69 758 $[M]^+$ with unconjugated BSA MALDI-TOF MS: m/z 66 444 $[M]^+$; (b) **AP2**-BSA MALDI-TOF MS: m/z 71 875 $[M]^+$ with unconjugated BSA MALDI-TOF MS: m/z 66 451 $[M]^+$.

5.2.3 2D-SDS PAGE

In the first dimension, the conjugate moved towards the positive electrode due to the overall net negative charge, and the positively charged BSA standard migrated towards the negative electrode. Migration occurred through the pH gradient, so no further migration occurred once the pI was reached (the protein no longer carried a net charge). The second dimension, which is SDS-PAGE, separated according to the M_r of the protein. The protein acquired a negative charge, from the interaction with the detergent, SDS, and migrated towards the positive electrode. The migration was restricted by the pore size controlled by the percentage of polyacrylamide used in the preparation of the gel. The technique was not sensitive enough to resolve proteins with only small increases in M_r (Figure 5-2, p 88).

Conjugation was confirmed by the different pI relative to the unconjugated BSA standard. Figure 5-2 (c) represents **AP1**-BSA (prepared in conjunction with **AP1**-KLH used for rabbit immunisation) did not show any unconjugated BSA recorded by MALDI-TOF. It was concluded that the amount of unconjugated BSA was insignificant to present problems in the bioassay, and thus by default the amount of unconjugated KLH was also insignificant to present problems in generation of antibodies in naïve rabbits.

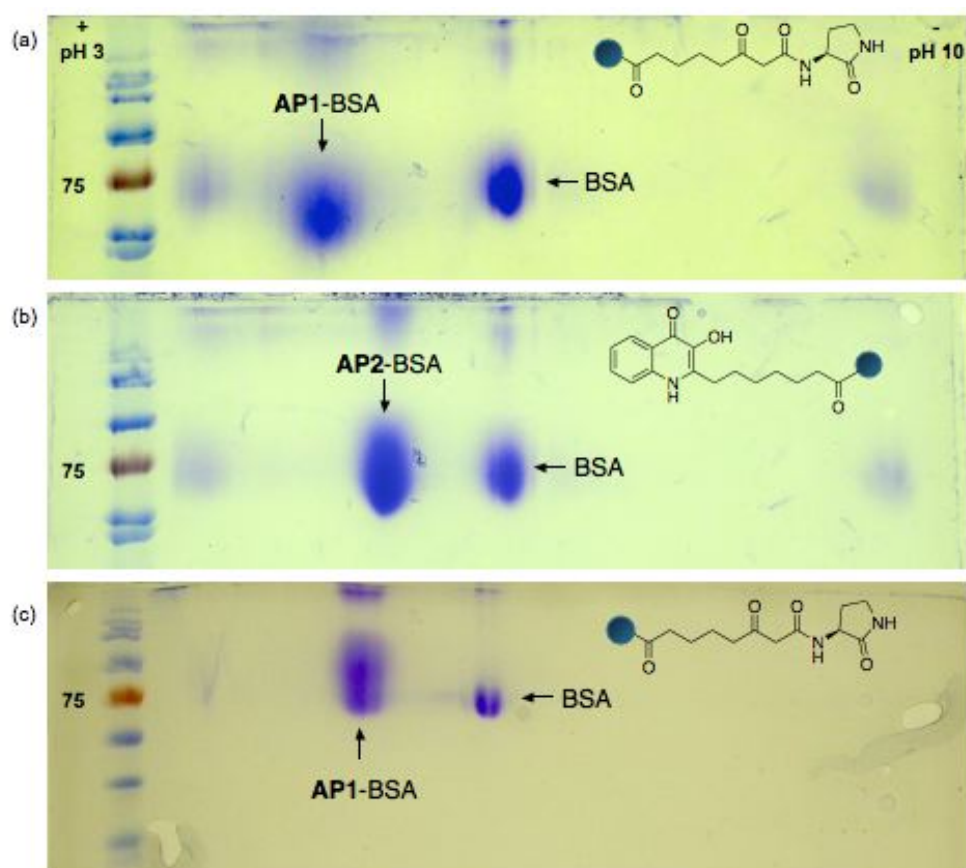


Figure 5-2: 2D-SDS PAGE analysis of hapten-BSA conjugates (pH 3-10, 10%).

For illustration purposes only - the gel of the hapten-BSA conjugate was overlaid on the gel of standard BSA (unconjugated) to show the difference in pI. (a) **AP1**-BSA conjugate; (b) **AP2**-BSA conjugate; (c) **AP1**-BSA conjugate (prepared in conjunction with **AP1**-KLH used for rabbit immunisation).

5.3 RESULTS - ANTIBODY CHARACTERISATION

5.3.1 MOUSE IMMUNISATION

Three out-bred (CD1) mice and in-bred (Balb/c) mice (identified sequentially 1-6) per conjugate were immunised with **AP1-KLH** and **AP2-KLH**. The standard immunisation protocols were followed using FCA for primary immunisation and IFA for the booster immunisations. Unfortunately, due to unforeseen and unrelated circumstances, one Balb/c mouse (mouse 6) died of undetermined but natural causes during the immunisation protocol with the **AP1-KLH** conjugate.

The response of the mice to the hapten-KLH conjugate (Figure 5-4, p 90) and subsequent titres (Figure 5-5, p 91) were determined using an indirect ELISA technique (Materials and methods, p 81), illustrated in Figure 5-3. A secondary Ab conjugated to an enzyme, such as horseradish peroxidase (HRP), is used to detect the quantity of bound primary anti-hapten pAbs to the immobilised hapten-BSA conjugate. The secondary antibody is specific for the antibodies generated by the animal used for immunisation.

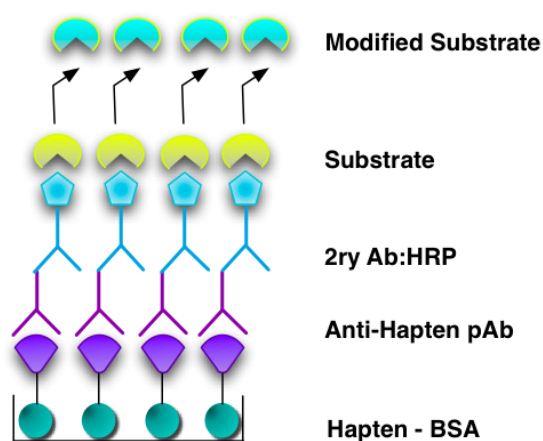


Figure 5-3: Depiction of an indirect ELISA.

The HRP conjugated to secondary Ab:primary anti-hapten Ab:hapten-BSA would metabolise the substrate resulting in a visible modification such as colour, which is proportional to the amount of bound primary Ab to the immobilised hapten-BSA.

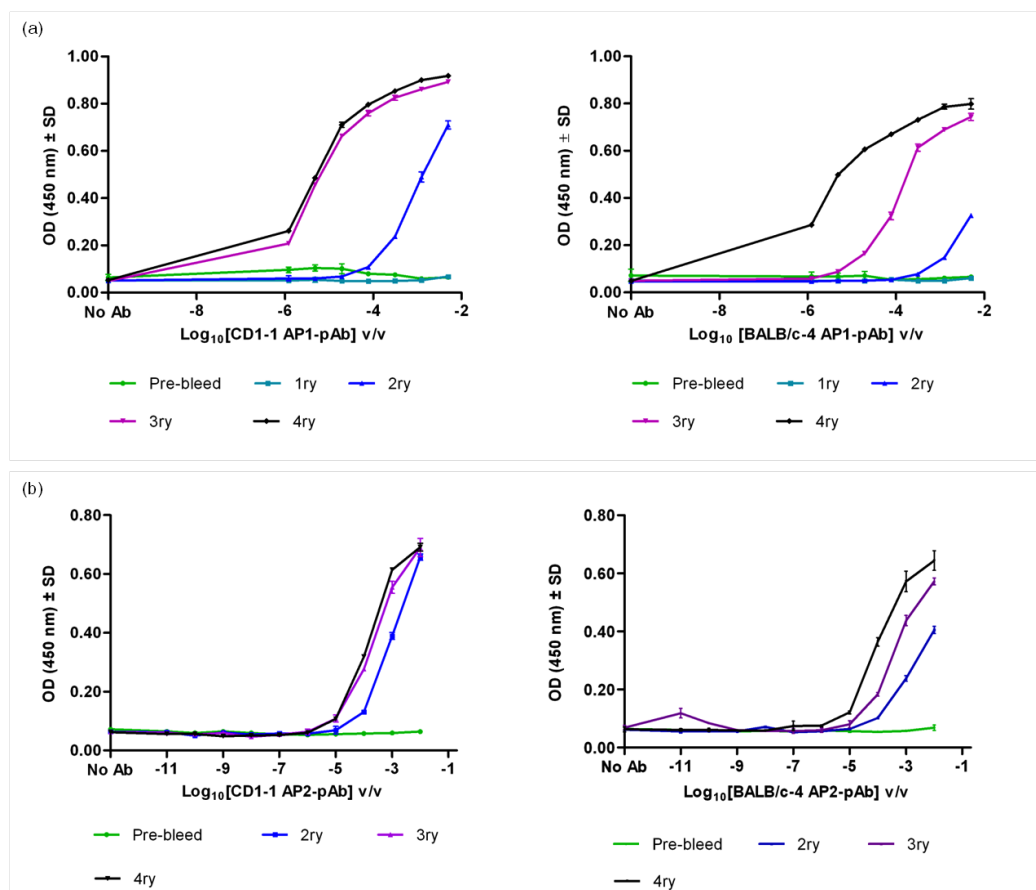
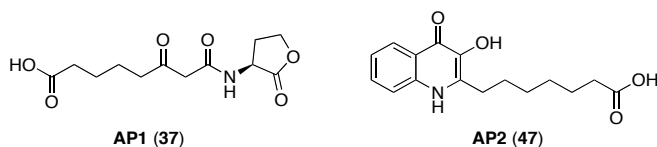


Figure 5-4: The anti-hapten antibody response by CD1-1 and Balb/c-4 mice to each immunisation measured by indirect ELISA.

(a) Anti-**AP1** antibody response by CD-1-1 and Balb/c-4 mice to each immunisation with **AP1-KLH** and (b) Anti-**AP2** antibody response by CD-1-1 and Balb/c-4 mice to each immunisation with **AP2-KLH**. (Data is represented as mean \pm SD, $n = 4$). Pre-bleed has no anti-**AP1** or anti-**AP2** pAbs. The mice responded to the hapten-KLH conjugates in a typical manner, i.e. the antibody titre increased after each booster compared to the primary immunisation. Generally, the out-bred (CD1) mice responded better; **AP1-KLH** conjugate generated higher titres in both sets of mice compared to the more substituted **AP2-KLH**.

^



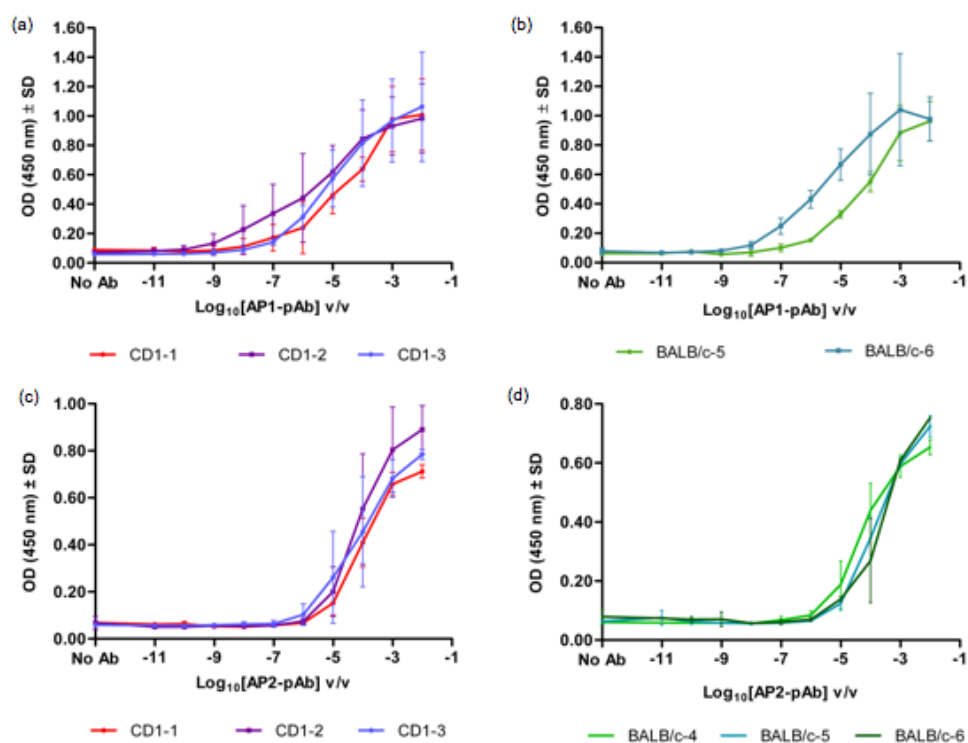


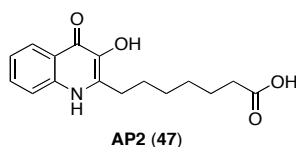
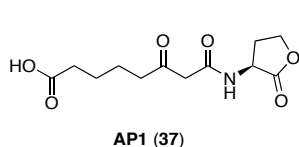
Figure 5-5: Titres of the sera derived from the terminal bleed using indirect ELISA. (a) Anti-AP1-pAb mouse serum from CD1-1-3; (b) Anti-AP1-pAb mouse serum from Balb/c 5-6; (c) Anti-AP2-pAb mouse serum from CD1-1-3 and (d) Anti-AP2-pAb mouse serum from Balb/c 4-6. (Data is represented as mean \pm SD, $n = 4$).

Mouse strain and ID	Anti-AP1-pAb	Anti-AP2-pAb
CD1-1	1:59 078	1:10 680
CD1-2	1:372 759	1:13 895
CD1-3	1:100 000	1:15 849
Balb/c-4	1:484 969	1:26 827
Balb/c-5	1:15 849	1:10 680
Balb/c-6	Deceased	1:4 850

Table 5-1: Mean titres obtained from the terminal bleed for each mouse per conjugate.

The titres were recorded as the dilution of pAb at which the optical density (OD) at 450 nm was 50% of the maximal OD. (Data is represented as mean \pm SD, $n = 4$).

^



5.3.1.1 SPECIFICITY

The mice used for immunisation should be naïve to *P. aeruginosa*, their natural QSSM and the carriers, therefore have no pre-existing memory cells or antibodies with specificity to these antigens. This was confirmed by analysis of the pre-bleed serum, which showed no recognition of the hapten-BSA conjugate (Figure 5-4, p 90 and Figure 5-5, p 91) whereas the generated antibodies against hapten-KLH showed recognition for the hapten-BSA conjugate. The carriers are phylogenetically different, but may share similar epitopes, it was anticipated that the signal indicating the presence of anti-hapten-KLH pAbs was due to pAb avidity to the hapten and not to BSA. This was investigated using unconjugated BSA and KLH as coating antigens in indirect ELISAs (Figure 5-6), in addition to PBS and hapten-BSA.

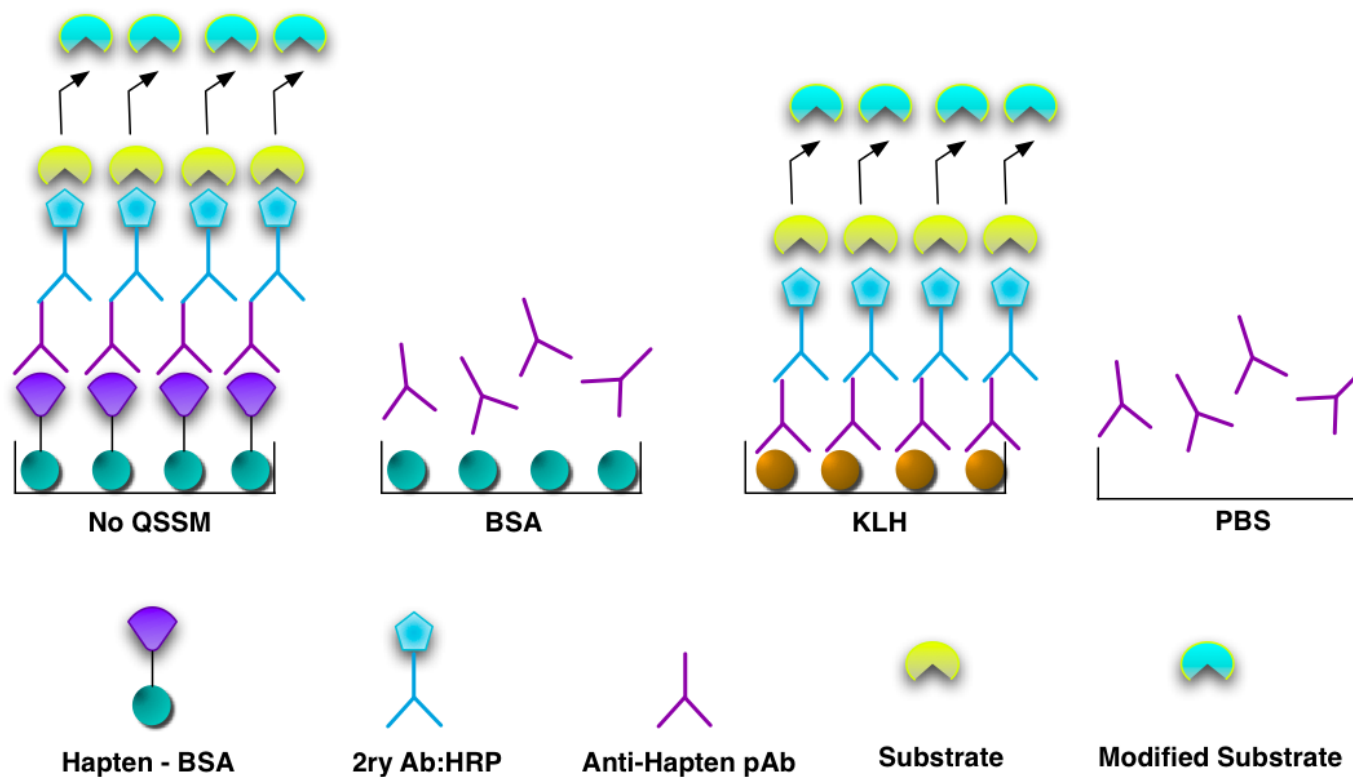


Figure 5-6: Schematic of indirect ELISA for antibody specificity.

The anti-hapten-KLH pAb should not recognise unconjugated BSA. No binding occurs and the unbound anti-hapten pAb are washed away. The secondary anti-mouse IgG:HRP cannot bind and is washed away. The substrate is added but cannot be enzymatically modified, no colorimetric change occurs, implying anti-hapten pAb shows no avidity for unconjugated BSA and does not bind in a non-specific manner (indicated by PBS).

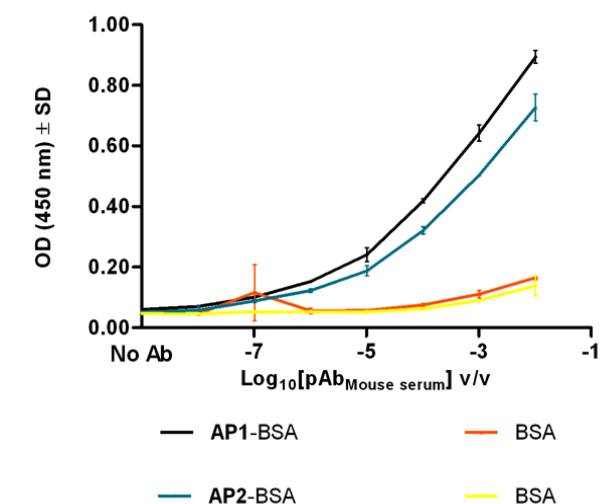


Figure 5-7: Indirect specificity ELISA of pooled serum from CD1 and Balb/c mice.

Serum from CD1-1 and Balb/c-4 mouse for each hapten-carrier conjugate was tested for specificity to BSA. Tests were negative and taken as a representation for the strain. The test was repeated when the serum from each mouse was pooled per conjugate. (Data is represented as mean \pm SD, $n = 4$).

5.3.2 RABBIT IMMUNISATION

Unfortunately, in preliminary studies, pre-bleed mouse serum showed significant negative effect in the anti-QSS assay (8.1.1, p 125). This complicated the characterisation of the potential anti-QSS activity of generated pAb. It was necessary to isolate polyclonal immunoglobulin G (pIgG) from the serum, which was not possible with the small volumes of blood obtained from mice. Immunisation in rabbits, however, provided adequate quantities of serum and confirmed that the conjugates were immunogenic in other species.

Each hapten conjugate was used to immunise one New Zealand white, female rabbit. The pIgG of the serum from the pre- and terminal bleeds were purified by affinity chromatography on protein G-Sepharose column using standard protocols (Materials and methods, p 81). The protein content of the pIgG preparations were estimated using the Bio-rad[®] Bradford assay with BSA as the standard.

5.3.2.1 SPECIFICITY

The pIgG isolated from the pre-bleed of each rabbit showed no avidity to unconjugated BSA, KLH, or the hapten-BSA (data not shown).

5.3.2.1.1 AHL

Unfortunately, the anti-AP1-KLH rabbit serum and subsequent rabbit pIgG were positive for specificity to unconjugated BSA (Figure 5-8, p 95). It was suspected that there may have been

BSA contamination in the **AP1**-carrier conjugate, anti-BSA IgG:HRP was incubated with immobilised **AP1**-KLH conjugate in an indirect ELISA (Figure 5-3, p 89), however, the conjugate tested negative for BSA contamination. This suggested that the pAbs bound non-specifically to BSA.

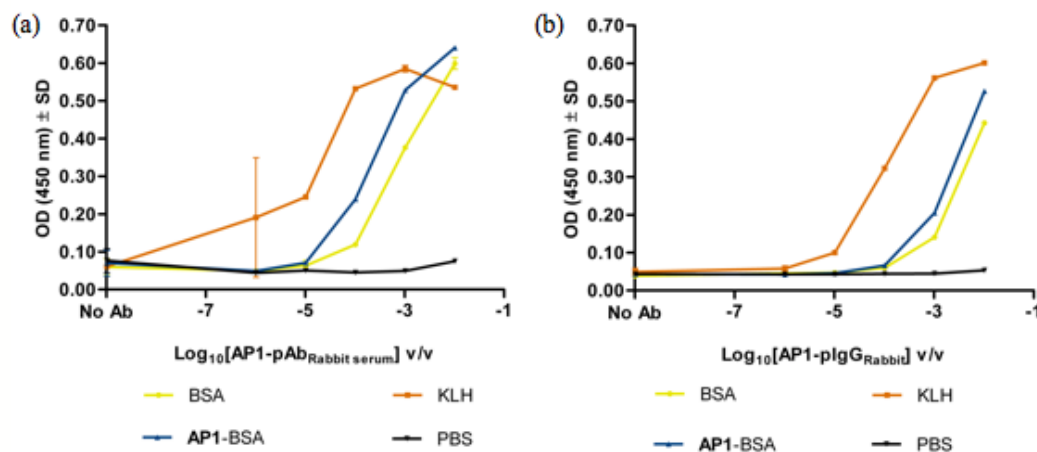


Figure 5-8: Anti-**AP1**-KLH specificity ELISA.

(a) Whole rabbit serum containing anti-**AP1** pAbs (b) Anti-**AP1** pIgG isolated using protein G-Sepharose affinity chromatography. Both assays show significant avidity towards unconjugated BSA, (data is represented as mean ± SD, n = 4).

The pIgG displaying non-specific binding to BSA was adsorbed from the anti-**AP1**-KLH serum using a BSA coated nitrocellulose membrane (Materials and methods, p 82). Adsorption was successful, and the binding to unconjugated BSA was reduced to satisfactory levels indicated by the low OD (450 nm) (Figure 5-9). The non-specific pIgG binding was above the expected levels, but this anomaly was attributed to slight contamination of the PBS, as further assays showed no further non-specific binding.

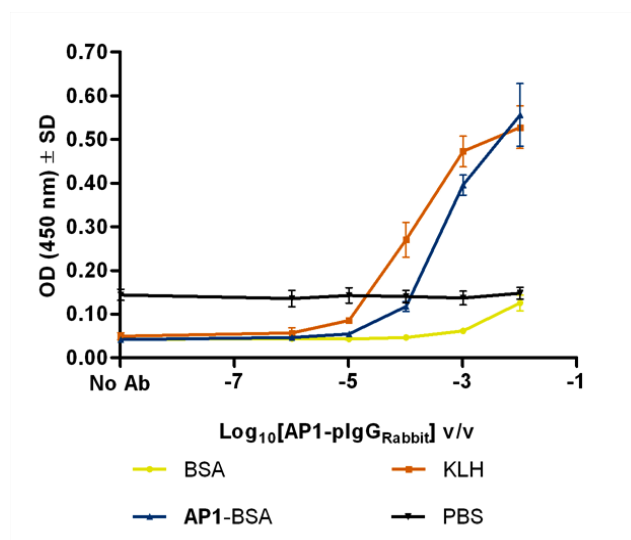


Figure 5-9: Specificity ELISA for rabbit anti-**AP1**-pIgG.

(Data is represented as mean ± SD, n = 4).

5.3.2.1.2 PQS

Non-specific binding was recorded for anti-**AP2**-KLH serum as with anti-**AP2** pIgG sera. **AP2**-KLH was negative for BSA contamination, as confirmed by the specificity assays used to test mouse serum (Figure 5-7, p 94). pIgG was isolated from rabbit serum using protein G-Sepharose affinity chromatography (Materials and methods, p 81). Non-specific binding was reduced as the pIgG concentration became more dilute, therefore, further purification (non-specific pIgG adsorption) was deemed unnecessary.

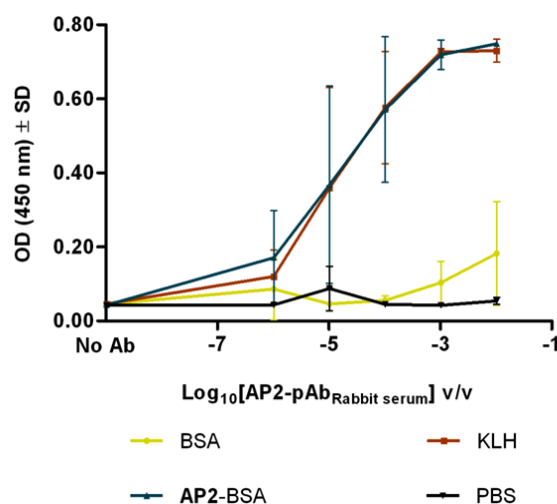
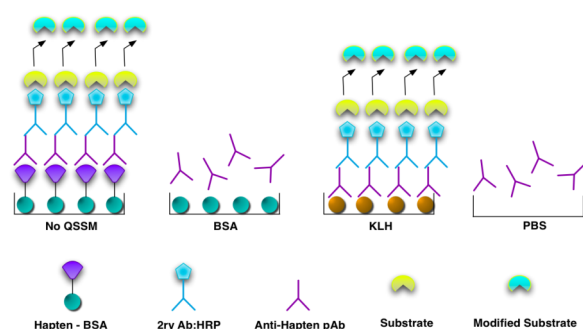


Figure 5-10: Indirect ELISA specificity of rabbit serum against **AP2**-KLH conjugates.

Results showed no significant avidity to BSA, particular at lower concentrations of serum. The titre was calculated as the dilution of antibody at which the OD was 50% of the maximal OD at 450 nm. The titre was calculated as 1:100 000. (Data is represented as mean \pm SD, n = 4).



5.4 DISCUSSION

5.4.1 HAPTEN-CARRIER CONJUGATES AND CHARACTERISATION

AP1- and **AP2**[^]-carrier conjugates were successfully synthesised using the NHS active ester method. Characterisation of the hapten-BSA conjugates by MALDI-TOF MS and 2D-SDS-PAGE confirmed conjugation and epitope density, 13 **AP1** and 18 **AP2** (median) were conjugated to the BSA molecule. The hapten-KLH conjugates could not be characterised, however immunogenicity of these conjugates were shown in mouse and rabbit.

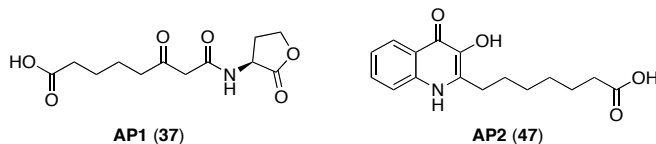
5.4.2 CHARACTERISATION OF ANTI-HAPTEN ANTIBODIES

The mouse anti-hapten serum showed no avidity for unconjugated BSA and titres were reasonable, however, due to the unforeseen non-specific binding seen with rabbit anti-**AP1**-KLH serum, the antibody titre has yet to be established. Time restrictions prevented further purification of the rabbit anti-**AP1**-KLH serum by adsorption method. However, unlike rabbit anti-**AP1**-KLH serum, rabbit anti-**AP2**-KLH serum showed insignificant avidity for BSA and the titre of rabbit anti-**AP2** pAb was determined as 1:100 000.

5.4.3 FUTURE WORK

Labelled haptens will have to be used for characterisation of hapten-KLH conjugates as only the hapten-BSA conjugates could be characterised by MALDI-TOF MS; MALDI-TOF MS can only tolerate certain concentrations of Na⁺ and K⁺, therefore non-NaCl buffers were used for conjugation and ultracentrifugation with the intention of immediate analysis with MALDI-TOF. However, it was found that resolution was better with samples in purified water. Native KLH requires high NaCl content to remain in solution (158), although no adverse effects on solubility of KLH was noted during the small-scale conjugation, on a larger scale, low NaCl buffer may cause solubility issues, therefore future conjugation reactions will be done in PBS, pH 7.4.

^



6 RESULT 3 – CROSS-REACTIVITY

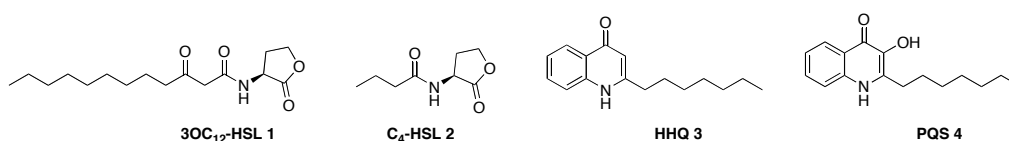
Anti-hapten pAbs have been generated against **AP1** and **AP2**. After appropriate purification, the anti-hapten pAbs showed insignificant binding to unconjugated BSA but significant binding to the appropriate immobilised hapten-BSA conjugate in indirect ELISA demonstrating that the anti-hapten pAbs were specific for the hapten.

P. aeruginosa produces various QSSMs, specifically 3OC₁₂-HSL **1**, C₄-HSL **2** and PQS **4**. The anti-hapten pAbs cross-reactivity to these QSSM had to be established in order to confirm the viability of this approach.

6.1 CROSS-REACTIVITY OF ANTI-HAPTEN ANTIBODIES

The cross-reactivity profile of anti-hapten pAb was established using a series of competitive indirect ELISA. The natural QSSMs were used as the competitive ligands, it was anticipated that the anti-hapten pAb would exhibit avidity for the QSSM, therefore interfere with anti-hapten pAb binding to hapten-BSA (Figure 6-1, p 99).

#



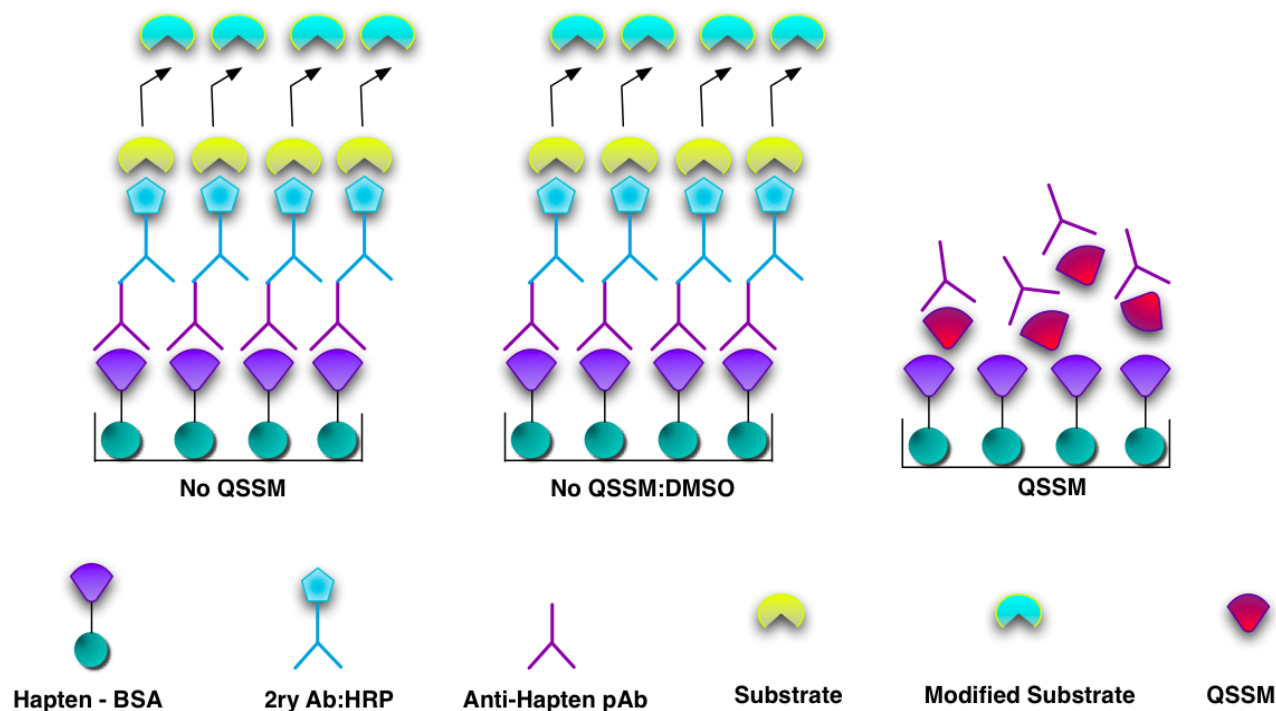


Figure 6-1: Competitive indirect ELISA used to study the cross-reactivity of anti-hapten pAb.

The controls were test pAb with no QSSM/DMSO and test pAb with 2.5% [DMSO] v/v. QSSM used: C₄-HSL, C₆-HSL, C₈-HSL, 3OC₆-HSL, 3OC₈-HSL, 3OC₁₂-HSL and PQS in addition to AP, HSL.HCl, tetramic acid (anti-**AP1** pAbs); PQS, HHQ, 3OC₁₂-HSL anthranilic acid and 3-methyl-quinolin-4(1*H*)-one **74** (anti-**AP2** pAbs). The coating antigen: 0.5 µg/mL [**AP1**-BSA] or [**AP2**-BSA]; 1:20 000 [mouse anti-**AP1** pAb] and 1:25 600 [mouse anti-**AP2** pAb] v/v. Controls (n = 9) were test pAb/no QSSM/no DMSO, test pAb/DMSO, and an anti-BSA secondary pAb:HRP was used to confirm that hapten-BSA (n = 2) had coated the plate as an additional control, (data not shown). The assays were repeated using rabbit anti-**AP2** pAb. CBT were used to optimise the coating hapten-BSA, 0.5 µg/mL [**AP2**-BSA] and 1:125 000 [rabbit anti-**AP2** pAb] v/v.

6.1.1 OPTIMISATION

Using checkerboard titrations (CBT), serial dilutions of the hapten-BSA (coating Ag), were titrated against serial dilutions of test anti-hapten pAb, the optimum concentration of anti-hapten pAb and hapten-BSA that gave an OD between 0.5-0.6 at 450 nm, for anti-hapten pAb:hapten-BSA, were determined.

6.1.2 QSSM AND SOLVENT EFFECT

3OC₁₂-HSL and PQS are moderately hydrophobic and have limited solubility in aqueous solutions; therefore, DMSO was used to increase the QSSM solubility in aqueous solutions. CBT optimisations indicated that DMSO affected hapten-BSA coating in a dose-independent manner. Additionally, DMSO interfered with the binding of anti-hapten pAb with hapten-BSA at dilute concentrations. The minimum concentration of DMSO was 2.5% v/v that caused no significant effects on anti-hapten pAb binding to hapten-BSA however, this restricted the range of QSSM concentrations studied. HHQ, PQS, and 3OC₁₂-HSL precipitated at 1 mM, thus higher concentrations were not tested, for this reason, an IC₅₀ could not be calculated.

6.2 RESULTS

STATISTICAL ANALYSIS

The effect of 2.5% [DMSO] v/v (n = 9) on anti-hapten pAb binding was analysed using one-way analysis of variation (ANOVA) with Dunnett's post-test using the test anti-hapten pAb/no QSSM/no DMSO (n = 9) as the control. Results from test anti-hapten pAb/QSSM (n = 3) were analysed using one-way ANOVA and Dunnett's post-test with anti-hapten pAb:no QSSM/DMSO (n = 3) as the control, (p = < 0.05, *; p = < 0.01, **; and p = < 0.001, ***). All statistical analysis was performed using Graphpad Prism[®] 5, Graphpad Software, La Jolla, CA, USA.

6.2.1 CROSS-REACTIVITY PROFILE OF MOUSE ANTI-AP1 ANTIBODIES

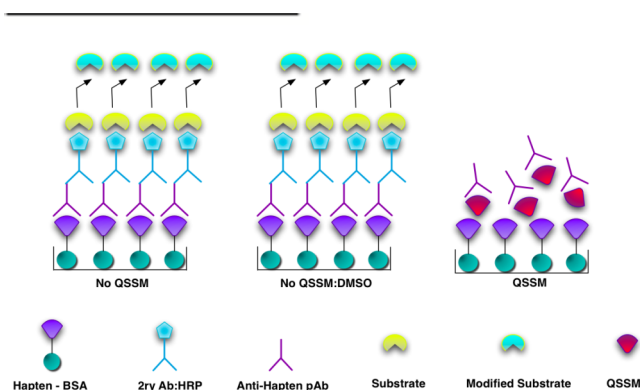
A concentration-dependent inhibition of the binding of anti-AP1 pAb to AP1-BSA was seen with the QSSMs; except for 3OC₁₂-HSL, which significantly (p = < 0.05) inhibited the binding of anti-AP1 pAbs to AP1-BSA at 0.1 µM. This inhibitory effect was lost at 1 µM (Appendix 1, p 149), significant inhibition of the pAb binding was seen at the higher concentrations (≥ 10 µM). This is yet to be explained. Nonetheless, the anti-AP1 pAbs showed a 1000-fold greater response to 3OC₁₂-HSL in comparison to the shorter 3-oxo substituted AHLs (Table 6-1, p 101). The anti-AP1 pAbs demonstrated cross-reactivity for C₄-HSL, but the anti-AP1 pAbs have a 10-fold greater response to the longer unsubstituted AHLs, which is comparable to 3-oxo AHLs counter-parts.

The anti-**AP1** pAbs cross-reacted with the natural QSSM of *P. aeruginosa* (Appendix 1, p 148-151) including the cognate 3OC₈-HSL. No significant cross-reactivity with AP, HSL.HCL, and tetramic acid was seen (data not shown). The pAbs did not distinguish between the 3-oxo and unsubstituted AHLs, suggesting that the key epitope was the lactam ring-external amide moiety.

QSSM	Concentration at which significant ($p = < 0.05$) inhibition occurred (μM)
3OC ₆ -HSL	≥ 100
3OC ₈ -HSL•	≥ 100
3OC ₁₂ -HSL	≥ 0.1
C ₄ -HSL	≥ 1000
C ₆ -HSL	≥ 100
C ₈ -HSL	≥ 100

Table 6-1: Concentration at which significant ($p = < 0.05$) inhibition of the anti-**AP1** pAb binding to **AP1**-BSA occurred (μM).

All data has been graphically represented and shown in Appendix 1 (p 148-151). (Data is represented as mean \pm SD, $n = 3$). • All experiments have been repeated in triplicate except for 3OC₈-HSL, DMSO showed significant effect on the binding of the pAbs to **AP1**-BSA (data not shown), the experiment could not be repeated due to time constraints.



6.2.2 CROSS-REACTIVITY PROFILE OF ANTI-AP2 ANTIBODIES

A concentration-dependent inhibition of the binding of mouse and rabbit anti-**AP2** serum to **AP2**-BSA was demonstrated by PQS, HHQ, and the HMAQ synthon, 3-methyl-quinolin-4(1*H*)-one **74** (Appendix 1, p 153-155). Mouse serum showed a 10-fold greater response to HHQ in comparison to PQS, however rabbit serum binding to **AP2**-BSA was significantly ($p = < 0.05$) inhibited at 0.1 μM [HHQ or PQS] (Table 6-2). However, the rabbit pAb response to 3-methyl-quinolin-4(1*H*)-one **74** was considerably less than that for the HAQs, interestingly, the response of mouse pAbs to PQS and 3-methyl-quinolin-4(1*H*)-one **74** is comparable.

Anti-**AP2** pAbs generated in mice or rabbit show significant cross-reactivity towards the natural QSSM of *P. aeruginosa*, (PQS and HHQ) with PQS being the cognate of **AP2**. 3-Methyl-quinolin-4(1*H*)-one **74** was able to significantly ($p = < 0.05$) inhibit pAb binding to **AP2**-BSA, suggesting that the key epitope of **AP2** is the quinolone ring.

QSSM	Concentration at which significant ($p = < 0.05$) inhibition occurred (μM)	
	Mouse serum	Rabbit serum
PQS 4	≥ 100	≥ 0.1
HHQ 3	≥ 10	≥ 0.1
3-methyl-quinolin-4(1 <i>H</i>)-one 74	≥ 100	≥ 100

Table 6-2: Concentration at which significant ($p = < 0.05$) inhibition of the binding of anti-**AP2** pAb to **AP2**-BSA occurred (μM).

All data has been graphically represented and shown in Appendix 1 (p 153-155). (Data is represented as mean \pm SD, $n = 3$). All experiments have been repeated in triplicate.

6.3 DISCUSSION

6.3.1 CROSS-REACTIVITY

Competitive indirect ELISAs were useful for characterisation of the cross-reactivity of anti-hapten pAbs with the natural QSSMs of *P. aeruginosa*. Mouse anti-**AP1** pAbs demonstrated cross-reactivity with the natural AHL QSSMs, and did not discriminate on structural variations such as acyl chain length, 3-oxo or unsubstituted AHLs. The pAbs showed specificity as no cross-reactivity was detected with AP, HSL.HCl, and tetramic acid (data not shown). In the absence of IC_{50} , the avidity could not be determined, however using the concentration at which the AHL QSSMs were able to significantly ($p = > 0.05$) inhibit the anti-**AP1** pAb:**AP1**-BSA binding, anti-**AP1** pAbs displayed strong cross-reactivity for 3OC₁₂-HSL, but comparatively weaker cross-reactivity for C₄-HSL.

The published haptens (Figure 1-9, **6-9**, p 53), had acyl chain lengths of 9-12 carbons, **AP1** had a chain length of 8 carbons (Figure 3-1, p 60). These data suggest that reduction of one carbon and the lactam ring had no negative impact on the cross-reactivity of the generated anti-**AP1** pAbs with natural QSSM. Therefore, it is possible that the AHL based hapten could tolerate significant changes in acyl chain length (compared to the published haptens), for example, 5-7 carbon length without affecting cross-reactivity with the longer AHLs but improving the cross-reactivity towards C₄-HSL.

Anti-**AP2** pAb demonstrates strong cross-reactivity with PQS and HHQ. The assays were repeated with 3OC₁₂-HSL and anthranilic acid, starting material for the biochemical synthesis of PQS (not shown), but these molecules did not affect anti-**AP2** pAb:**AP2**-BSA binding, unlike 3-methyl-quinolin-4(1*H*)-one **74**, which caused significant inhibition of pAb binding at high concentrations. This confirms that the quinolone structure is the key epitope of **AP2** (Figure 3-2, p 61). Interestingly, 3-methyl-quinolin-4(1*H*)-one **74**, which has no acyl chain and a methyl group at the C3 of the quinolone, is a chemical synthon for the HMAQs of *Burkholderia* spp.

6.3.1.1 LIMITATIONS OF THIS TECHNIQUE

The competitive indirect ELISA (Appendix 1, p 148-151) were also repeated with BSA adsorbed rabbit anti-**AP1** pIgG. CBT optimisation indicated that high concentrations, 1:200-1:800 [rabbit anti-**AP1** pIgG] v/v were needed to obtain an OD (450 nm) of 0.5-0.6. The assay was not considered sensitive using these concentrations. Concentration of rabbit anti-**AP1** pIgG improved the sensitivity to some degree, (1:4 000 [rabbit anti-**AP1** pIgG] v/v against 0.79 µg/mL [**AP1**-BSA]), however, data (not shown) indicated that the concentration of rabbit anti-**AP1** pIgG was too high for any discernable inhibition by the QSSM at the test concentrations.

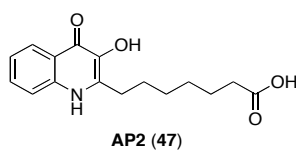
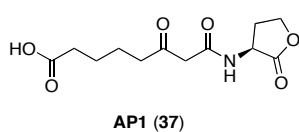
The IC₅₀ should be calculated as the value can provide information on avidity of the anti-hapten-pAb towards the QSSMs. However, the end-point was not reached in any of the experiments due to the limited concentration ranges of QSSM tested, which was due to the poor aqueous solubility of certain QSSM.

6.3.2 FUTURE WORK

The cross-reactivity profile of rabbit anti-**AP1** pIgG will be characterised using the competitive indirect ELISA technique, however, using an alternative antibody detection system, streptavidin-biotin system, which uses a secondary Ab conjugated biotin instead of HRP antibody used in this study. Streptavidin conjugated to HRP is added which has a high affinity for a single biotin molecule, may bind up to four streptavidin molecules subsequently resulting in signal amplification. Lower concentrations of rabbit anti-**AP1** pIgG and QSSM can be used, with concentrations of DMSO lowered accordingly. This revised system will allow

characterisation of the cross-reactivity of rabbit anti-**AP1** pIgG and more importantly, the IC₅₀ can be calculated.

^



7 RESULT 4 - ANTI-QSSM ACTIVITY

Competitive indirect ELISA have shown that anti-hapten pAbs can cross-react with the natural QSSMs, however the assay was not designed to test the anti-QSSM activity of the anti-hapten pAbs. The anti-QSSM activity refers to the pAbs capacity to bind and inhibit the function of QSSMs. *In vivo*, this would imply that the pAbs opsonised the QSSMs.

Reporter plasmids have been constructed and inserted into bacterial strains (Dr Diggle, University of Nottingham), *E. coli* S17.1 and *P. aeruginosa* PAO1, which are then bioluminescent in response to exogenous 3OC₁₂-HSL, C₄-HSL and PQS. It is anticipated that the bioluminescence will be reduced when the strains are grown in the presence of exogenous QSSM and the corresponding anti-hapten pAbs, as the pAbs bind to the QSSM and inhibit the function.

7.1.1 BIOLUMINESCENCE

7.1.1.1 BIOLUMINESCENCE REPORTER

Bioluminescence is a biochemical reaction involving the oxidation of reduced flavin mononucleotide (FMNH₂) and a long chain fatty aldehyde in the presence of oxygen, catalysed by luciferase. Luciferase is encoded by the *Photorhabdus luminescens* genes *luxAB* whilst the fatty aldehyde is encoded by *luxCDE* (229-231). Reporter plasmids have been constructed that feature the *luxCDABE* fused to a specific promoter (Figure 7-1, Figure 7-3, and Figure 7-5).

7.1.2 RESULTS

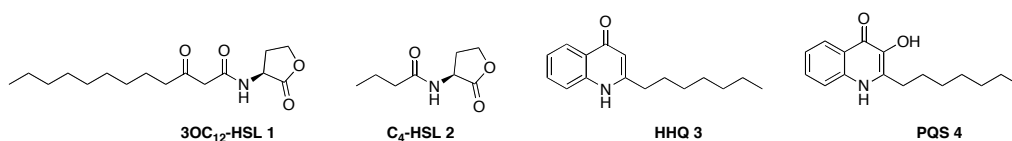
Using the modified protocol (232), the appropriate reporter strain was grown at 37 °C with the appropriate exogenous QSSM at the indicated concentrations, with or without the corresponding anti-hapten rabbit pIgG. Bioluminescence was measured in arbitrary units (AU) at hourly time points. The assay was stopped when bioluminescence of the positive control began to decrease. The time point at which the bioluminescence of the positive control was maximal has been presented in this study (Materials and methods, Bioluminescence, p 82). The variability of this assay was high, and this time point differed for each experiment thus, the data for each experiment have been represented separately for analysis. Due to time constraints, the assays (n = 3) have only been repeated twice.

STATISTICAL ANALYSIS

Positive control is the appropriate reporter strain in PBS/LB media and QSSM (n = 3). Negative control is the reporter strain/PBS/LB media/DMSO (n = 3). Pre-bleed pIgG was a limited resource therefore was tested in one assay for each reporter (n = 3) at 200 µg/mL

against 1 and 10 μ M [QSSM]#. Results from test pAb/QSSM/reporter strain ($n = 3$) were analysed using one-way ANOVA and Dunnett's post-test against the positive control, ($p = < 0.05$, *; $p = < 0.01$, **; and $p = < 0.001$, ***). All statistical analysis was performed using Graphpad Prism[®] software 5, Graphpad Software, CA, USA.

#



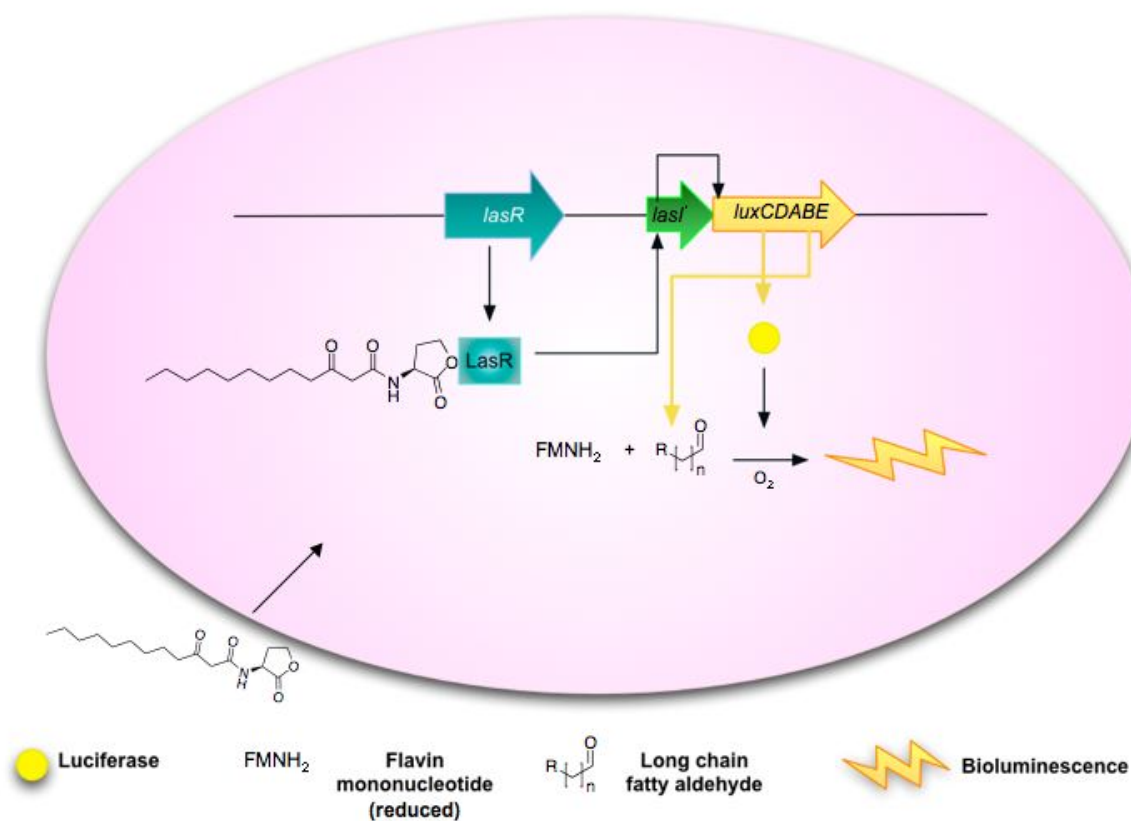
7.1.2.1 3OC₁₂-HSL AND RABBIT ANTI-API pIgG

Figure 7-1: *E. coli* S17.1 reporter strain with the pSB1075 plasmid.

The *E. coli* S17.1 reporter strain has the pSB1075 plasmid and does not produce 3OC₁₂-HSL due to the absence of *lasI*. The biosensor is bioluminescent in response to exogenous 3OC₁₂-HSL. The *lasR* expresses the LasR protein that binds to exogenous 3OC₁₂-HSL, this complex (LasR-3OC₁₂-HSL) binds to the promoter (mutated *lasI'*) fused to the *luxCDABE* construct. This stimulates the expression of luciferase controlled by the *luxAB* and the long chain fatty aldehyde, expressed by *luxCDE*. Luciferase catalyzes the oxidation of reduced FMNH₂ and long chain fatty aldehyde in the presence of oxygen, resulting in bioluminescence. Rabbit anti API-pIgG should bind to exogenous 3OC₁₂-HSL, preventing the LasR-3OC₁₂-HSL complex. No activation of the *luxCDABE* should occur via the promoter and bioluminescence will not result.

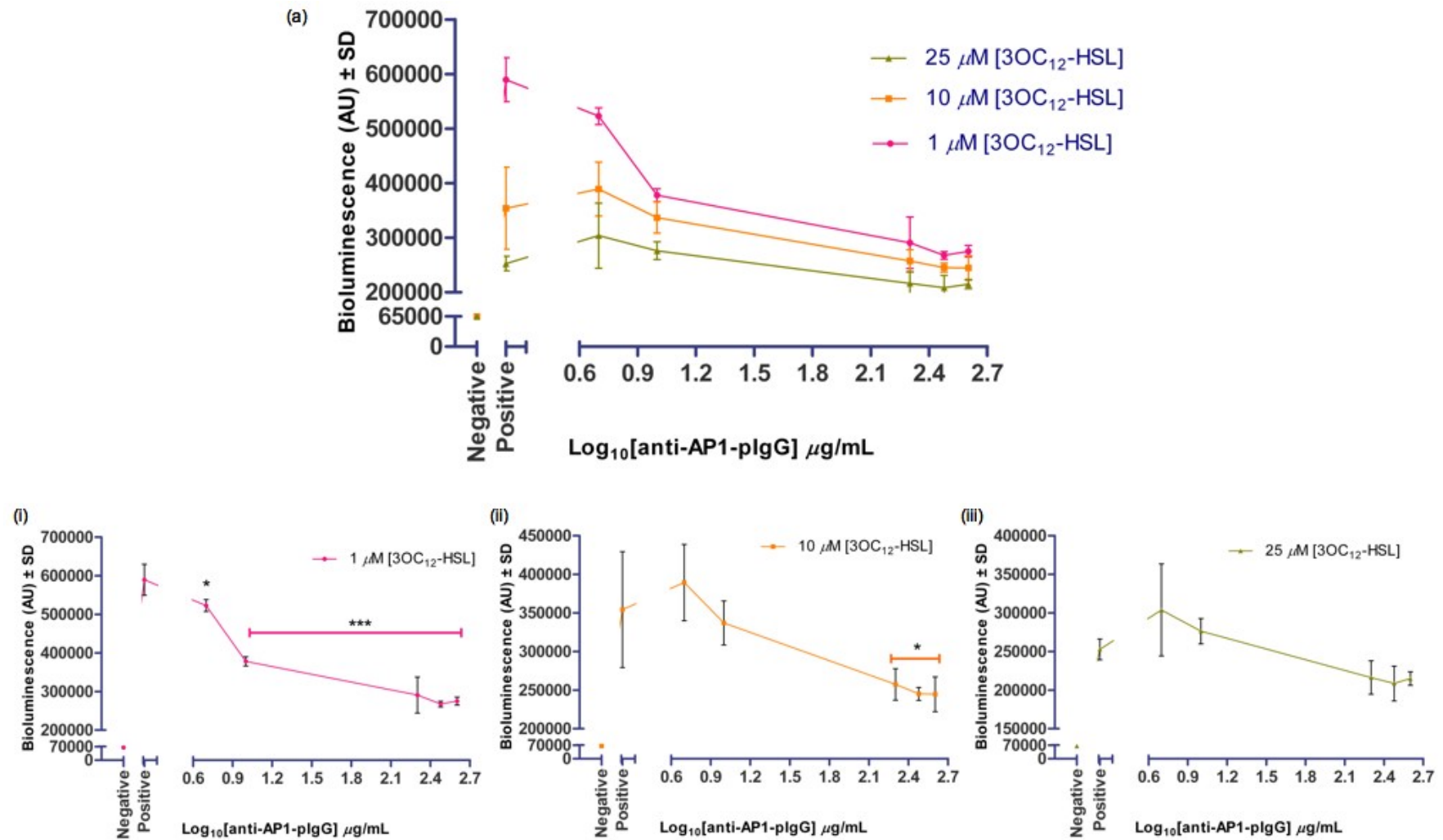
The rabbit pre-bleed pIgG does not significantly affect bioluminescence in response to exogenous 3OC₁₂-HSL at 1 and 10 μ M (Figure 7-2, b) suggesting that it has no effect on the biochemical reaction and confirmed previous ELISA data, which showed that the pre-bleed pIgG has no avidity for 3OC₁₂-HSL.

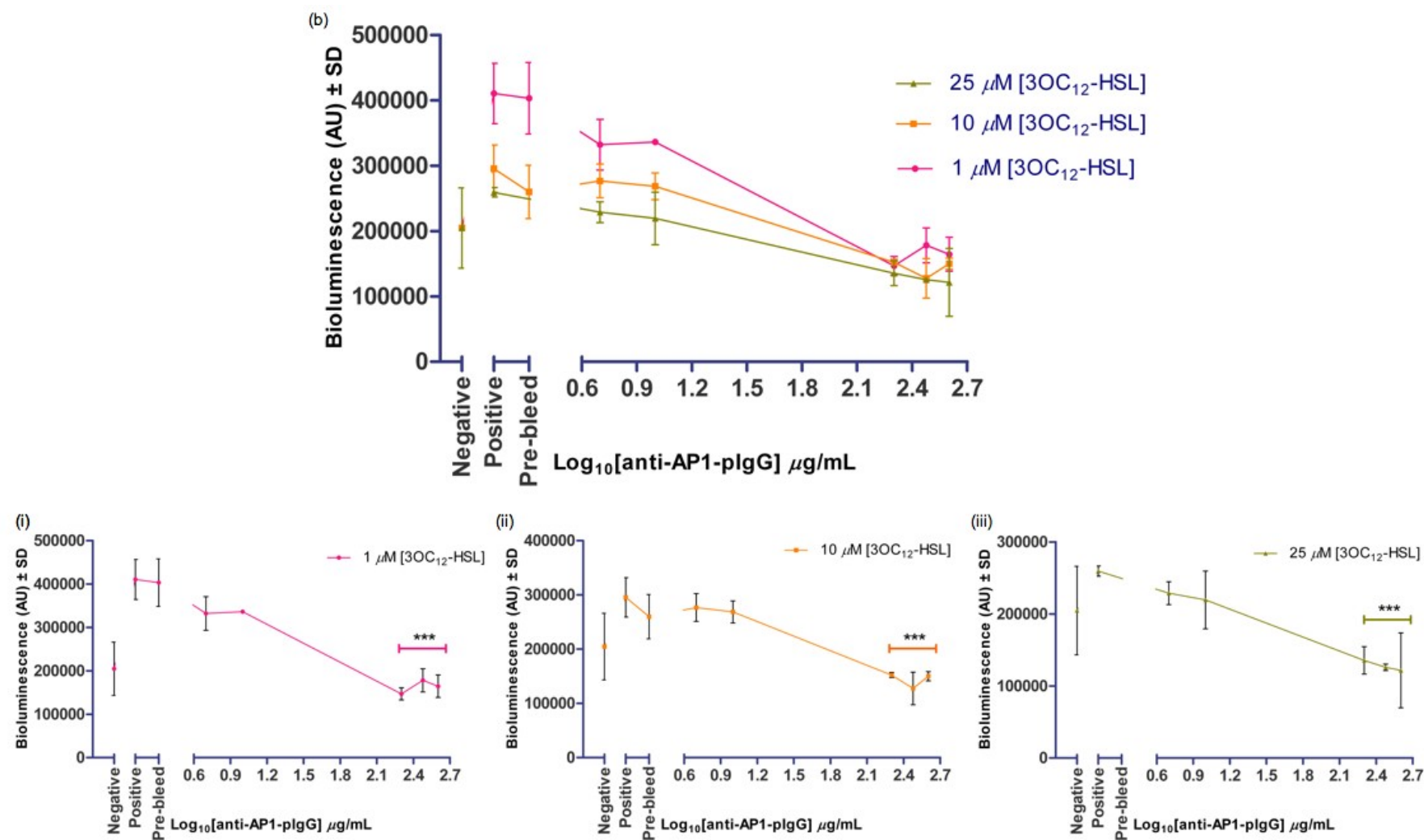
The positive control's bioluminescence was considerably lower in response to 10 and 25 μ M [3OC₁₂-HSL] compared to 1 μ M [3OC₁₂-HSL] (Figure 7-2). This was not expected, as it was anticipated that increasing concentrations of QSSM would increase bioluminescence. However, the data did show that rabbit anti-**API** pIgG reduced bioluminescence in a concentration-dependent manner. Significant reduction ($p = <0.001$, ***) in bioluminescence was seen at 200 – 400 μ g/mL [rabbit anti-**API** pIgG] with 1 and 10 μ M [3OC₁₂-HSL], but only experiment b shows significant reduction in bioluminescence in response to 25 μ M [3OC₁₂-HSL]. Experiment b (Figure 7-2) shows that ≥ 200 μ g/mL [rabbit anti-**API** pIgG] decreases bioluminescence below that of the negative control, however the negative controls have surprisingly high bioluminescence levels in comparison to experiment a (Figure 7-2), in light of this, it was inappropriate to calculate an IC₅₀ without further experimental repetitions.

The results suggest that pre-bleed had no significant effect on bioluminescence, the reductions in bioluminescence by anti-**API** pIgG in response to exogenous 3OC₁₂-HSL was due to a specific anti-3OC₁₂-HSL effect. It is assumed that the pAbs bound to 3OC₁₂-HSL and prevented entry into the cell, therefore no LasR-3OC₁₂-HSL complex was formed and bioluminescence was not stimulated. This is concentration-dependent up to 200 μ g/mL [rabbit anti-**API** pIgG]; greater concentrations did not reduce bioluminescence any further. This may be the anticipated end-point, however, this seems unlikely, as the bioluminescence of negative controls has been recorded to be lower. Nonetheless, anti-**API** pAb has demonstrated specific anti-3OC₁₂-HSL effect.

Figure 7-2: The bioluminescence response of *E.coli* S17.1 reporter strain pSB1075.

The bioluminescence response of *E. coli* S17.1 reporter strain pSB1075 in response to exogenous 3OC₁₂-HSL and rabbit anti-**API** pIgG. (a) and (b) Rabbit anti-**API** pIgG (μ g/mL) (x-axis) was titrated against 1 (i), 10 (ii) and 25 (iii) μ M [3OC₁₂-HSL]. Graphs (i), (ii) and (iii) show significance (ANOVA) of bioluminescence inhibition by the rabbit anti-**API** pIgG compared to the positive control. Negative control was the *E.coli* S17.1 reporter strain pSB1075 in LB broth/PBS and 2 μ L [DMSO]; Positive control was the *E.coli* S17.1 reporter strain pSB1075 with LB broth/PBS and 1 (i), 10 (ii) and 25 (iii) μ M [3OC₁₂-HSL]. (b) Pre-bleed was a limited resource and tested (data is represented as mean \pm SD, $n = 3$) in only one assay, 200 μ g/mL [rabbit pre-bleed pIgG] was titrated against 1 (i) and 10 (ii) μ M [3OC₁₂-HSL]. The data has been represented for the time point at which bioluminescence of the positive control was maximal.





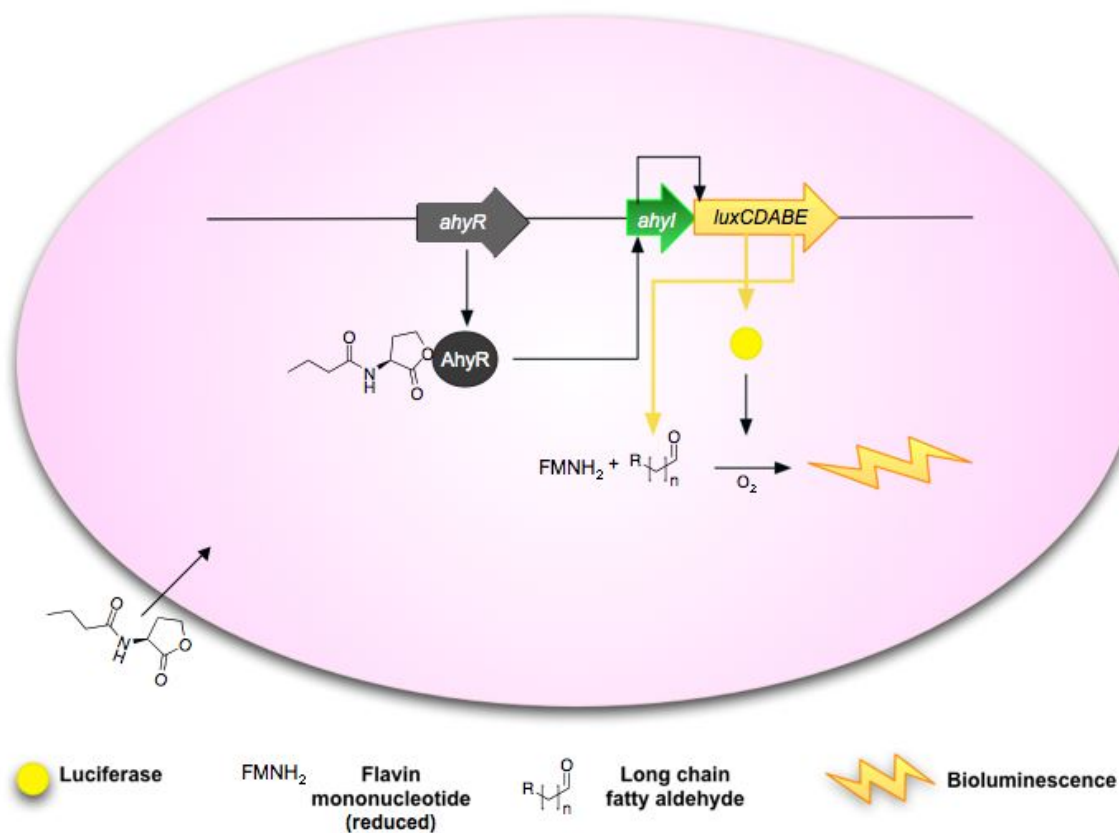
7.1.2.2 *C₄-HSL AND RABBIT ANTI-AP1 pIgG*

Figure 7-3: *E. coli* S17.1 reporter strain contains the pSB536 plasmid.

E. coli S17.1 reporter strain contains the pSB536 construct, which is bioluminescent in response to exogenous C_4 -HSL but contains the *Aeromonas hydrophyla ahyR*, which expresses AhyR and forms a complex with C_4 -HSL. *E. coli* does not produce the QSSM. The AhyR- C_4 -HSL binds to the promoter, *ahyI*, which is fused to the *luxCDABE* construct. The cross-reactivity profile of rabbit anti-AP1 pIgG could not be tested in competitive indirect ELISA, but it is anticipated that it would exhibit a similar profile as the mouse anti-AP1 serum and show cross-reactivity towards C_4 -HSL.

The rabbit pre-bleed pIgG did not significantly affect bioluminescence in response to exogenous C₄-HSL at 1 and 10 μ M (Figure 7-4, p 112), as seen in (Figure 7-2, p 108) suggesting that the pre-bleed pIgG did not exhibit avidity for C₄-HSL.

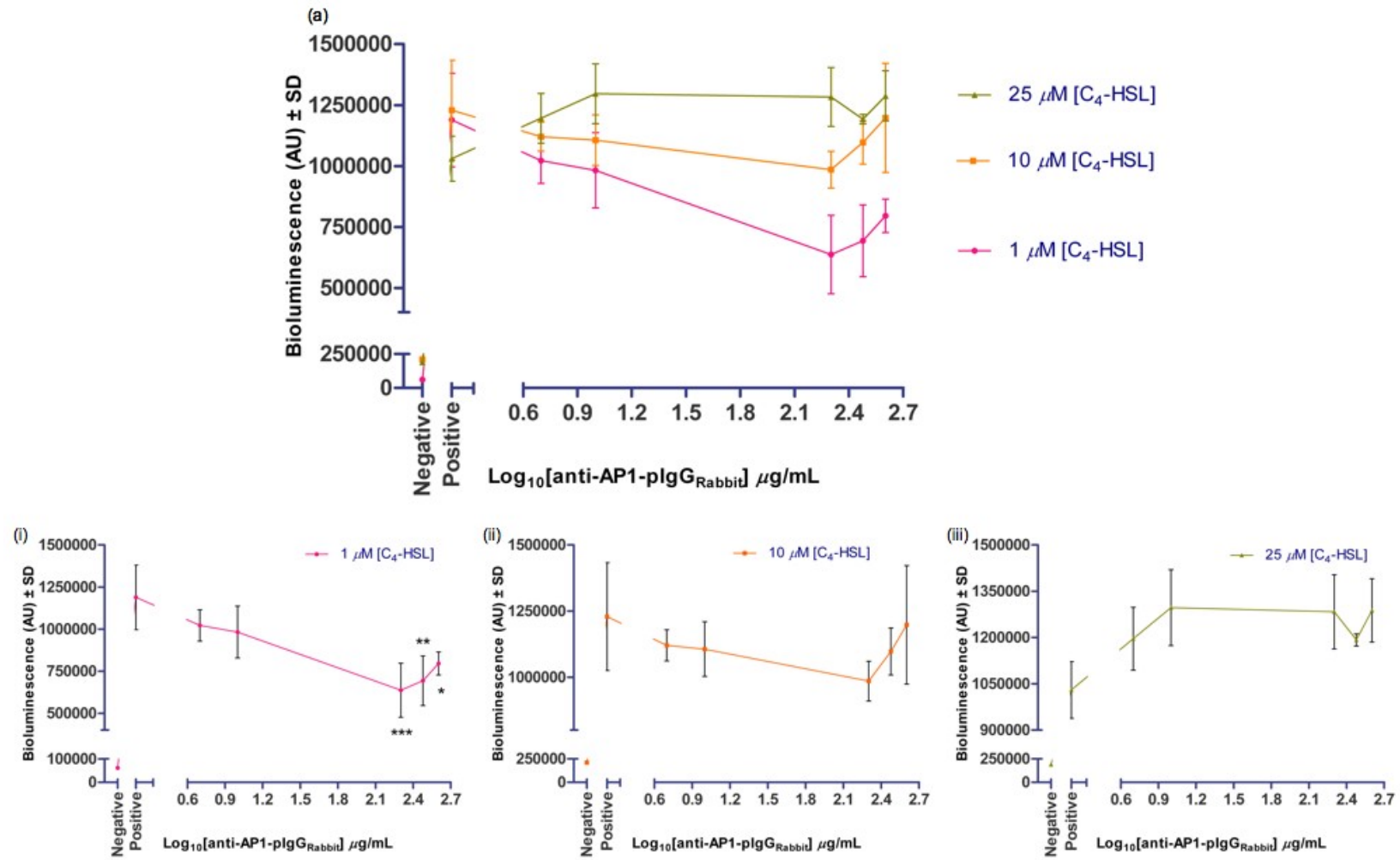
Surprisingly, the bioluminescence (AU) for the positive control in response did not increase in response to increasing exogenous concentrations of C₄-HSL. However, unlike the experiments shown in Figure 7-2 the negative controls were low. There is a tentative indication of a concentration-dependent reduction of bioluminescence in response to 1 μ M [C₄-HSL] by rabbit anti-**API** pIgG up to 200 μ g/mL, however it seems that this inhibitory effect lessens with greater concentrations of anti-**API** pIgG. This trend is reflected to some degree with 10 and 25 μ M [C₄-HSL] in experiment b (Figure 7-4).

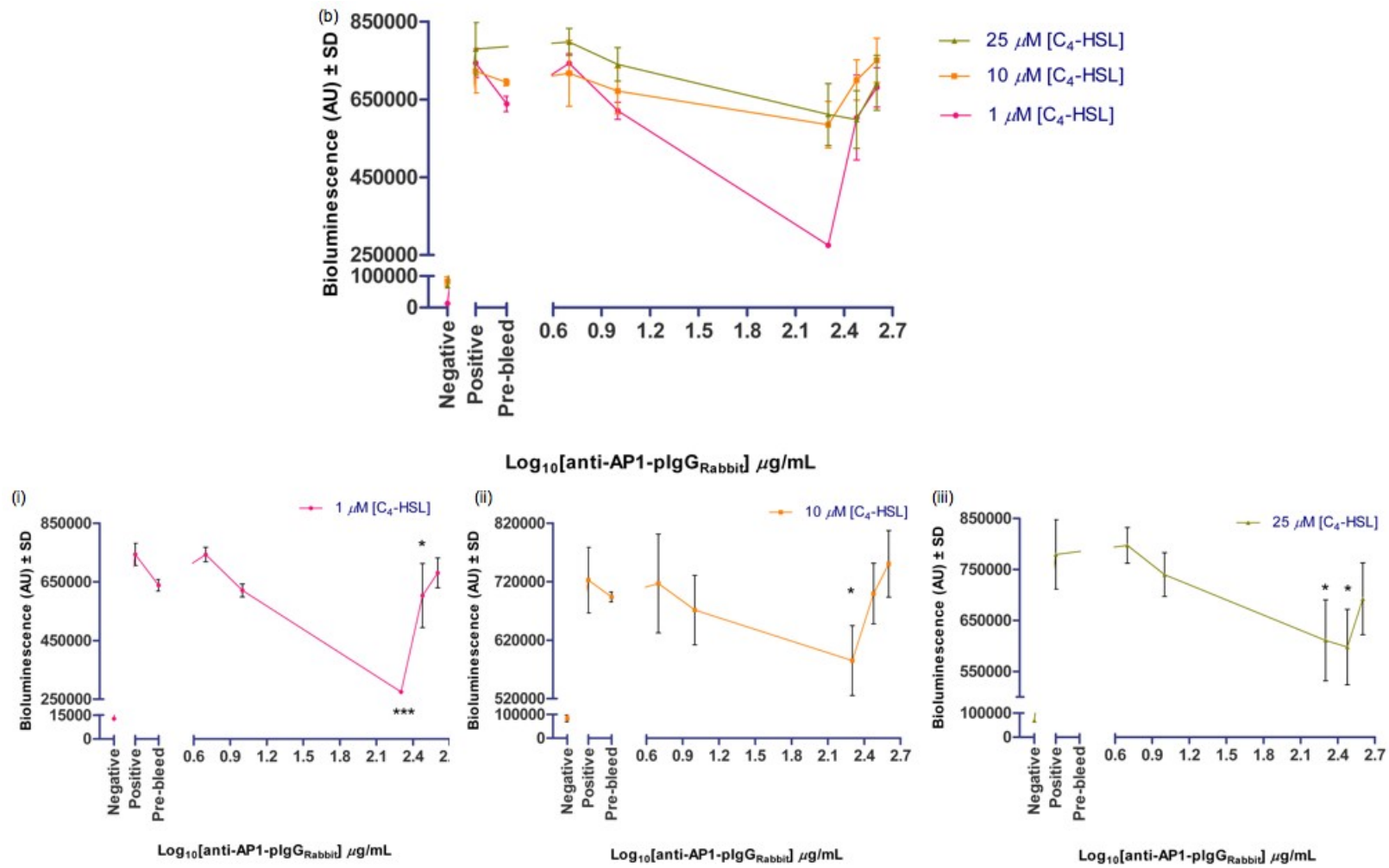
Data from competitive indirect ELISAs suggest that although the pAbs have avidity for C₄-HSL, it is not as strong as seen for 3OC₁₂-HSL. It is suspected that higher concentrations of anti-**API** pIgG will need to be tested in this assay for 10 and 25 μ M. The increase in bioluminescence seen in experiment a (Figure 7-4) for 25 μ M is considered anomalous due to the low bioluminescence recorded for the positive control, as the data collectively shows that rabbit anti-**API** pIgG decreases bioluminescence.

The increase in bioluminescence with greater concentrations (> 200 μ g/mL) of anti-**API** pIgG suggests that the interaction of pAb with C₄-HSL may be weak, in comparison to pAb and 3OC₁₂-HSL, it is possible that the pAb:C₄-HSL complex dissociated easily in excess molar concentration of anti-**API** pIgG. Indeed, data from competitive indirect ELISA suggested that anti-**API** pIgG demonstrated weaker cross-reactivity to C₄-HSL compared to the AHLs tested, implying weaker avidity. Even so, the data has shown that anti-**API** pIgG reduces bioluminescence in response to 1 μ M [C₄-HSL] up to 200 μ g/mL, this effect appears to be specific anti-C₄-HSL effect as pre-bleed pIgG did not significantly affect bioluminescence in response to exogenous C₄-HSL.

Figure 7-4: The bioluminescence response of *E. coli* S17.1 reporter strain pSB536.

The bioluminescence response of *E. coli* S17.1 reporter strain pSB536 in response to exogenous C₄-HSL and rabbit anti-**API** pIgG. (a) and (b) Rabbit anti-**API** pIgG (μ g/mL) (x-axis) was titrated against 1 (i), 10 (ii) and 25 μ M (iii) [C₄-HSL]. Graphs (i), (ii) and (iii) show significance (ANOVA) of bioluminescence inhibition by the rabbit anti-**API** pIgG compared to the positive control. Negative control was the *E. coli* S17.1 pSB536 reporter strain in LB broth/PBS and 2 μ L [DMSO]; positive control was the *E. coli* S17.1 reporter strain pSB536 with LB broth/PBS and 1 (i), 10 (ii) and 25 μ M (iii) [C₄-HSL]. (b) Pre-bleed was a limited resource and tested (data is represented as mean \pm SD, n = 3) in only one assay, 200 μ g/mL [rabbit pre-bleed pIgG] was titrated 1 (i) and 10 μ M (ii) [C₄-HSL]. (Data is represented as mean \pm SD, n = 3). The data has been represented for the time point at which bioluminescence of the positive control was maximal.





7.1.2.3 PQS AND RABBIT ANTI-AP2 pIgG

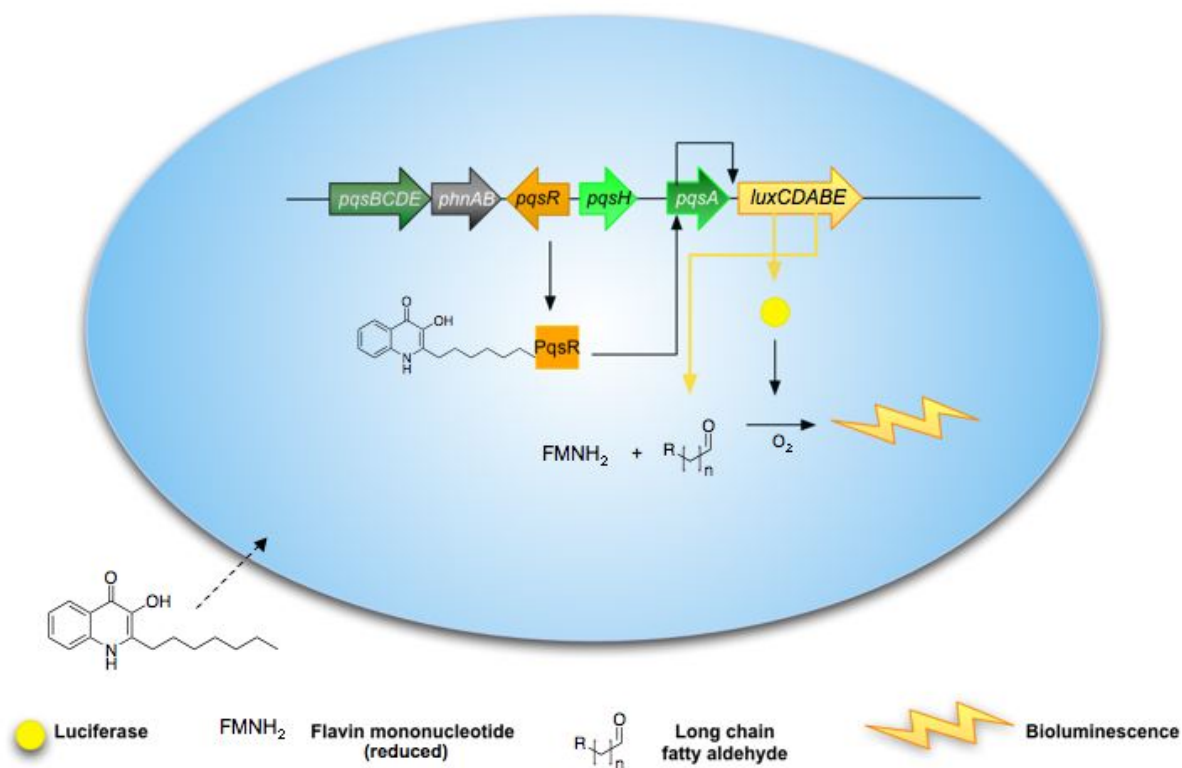


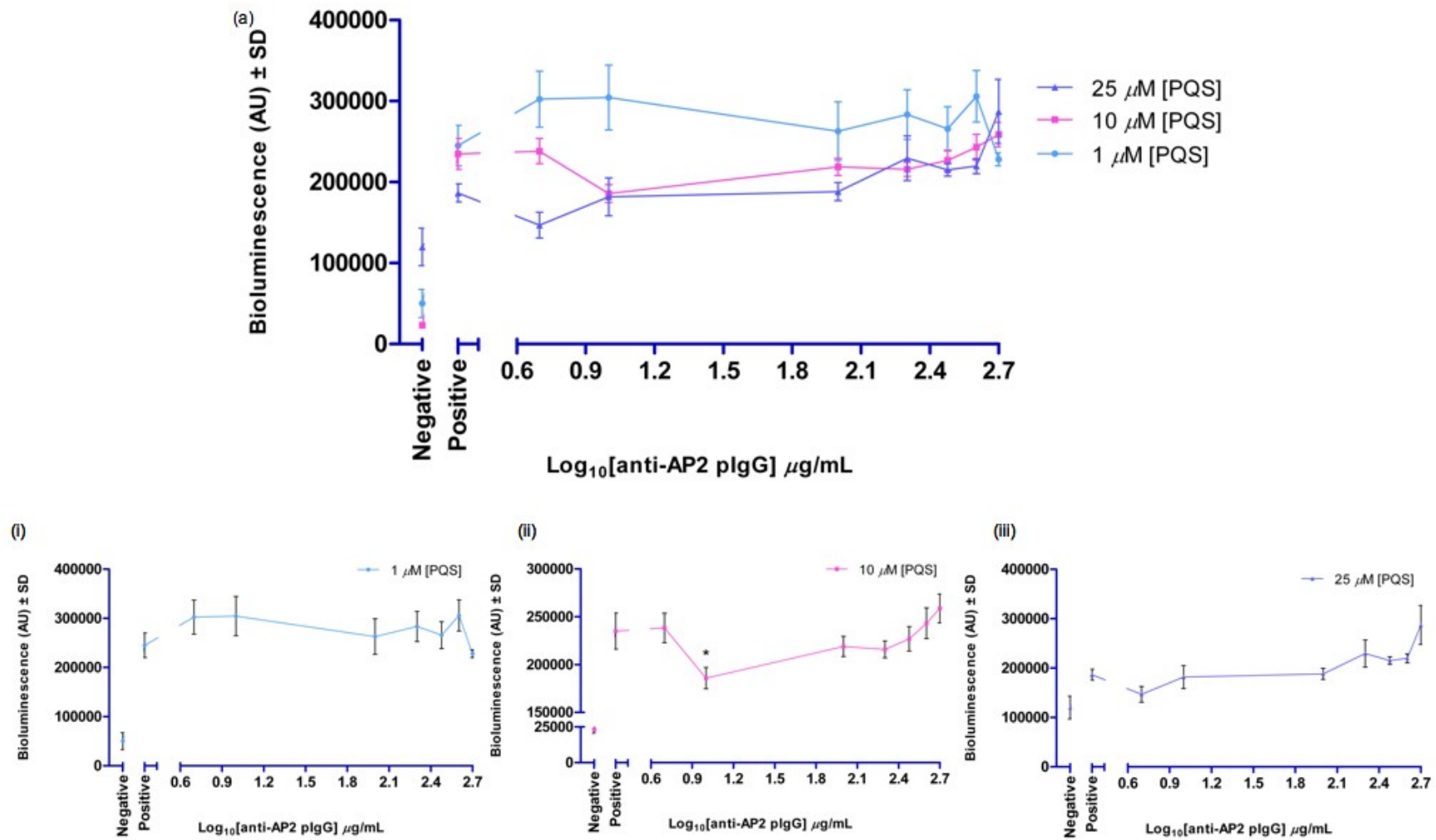
Figure 7-5: *P. aeruginosa* PAO1Δ*pqsA* CTX-*luxCDABE::pqsA* reporter

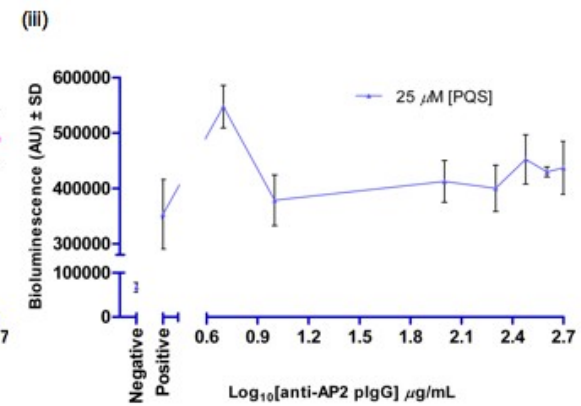
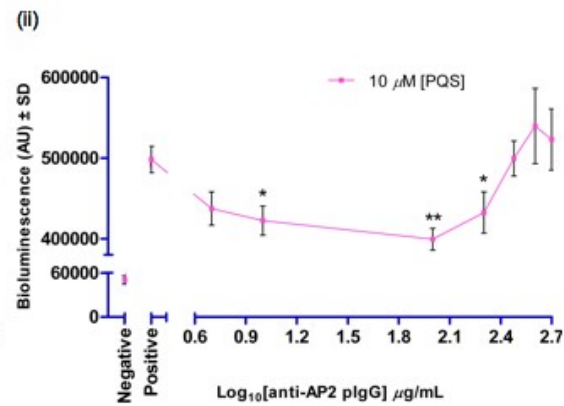
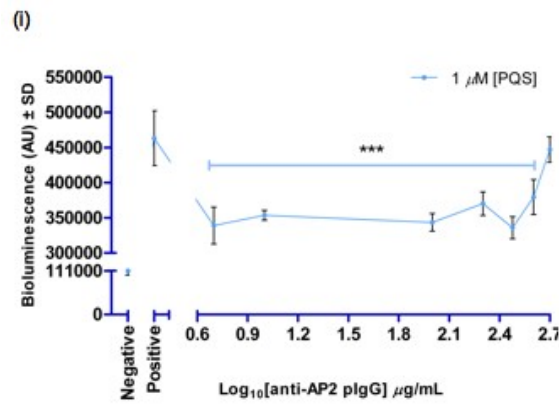
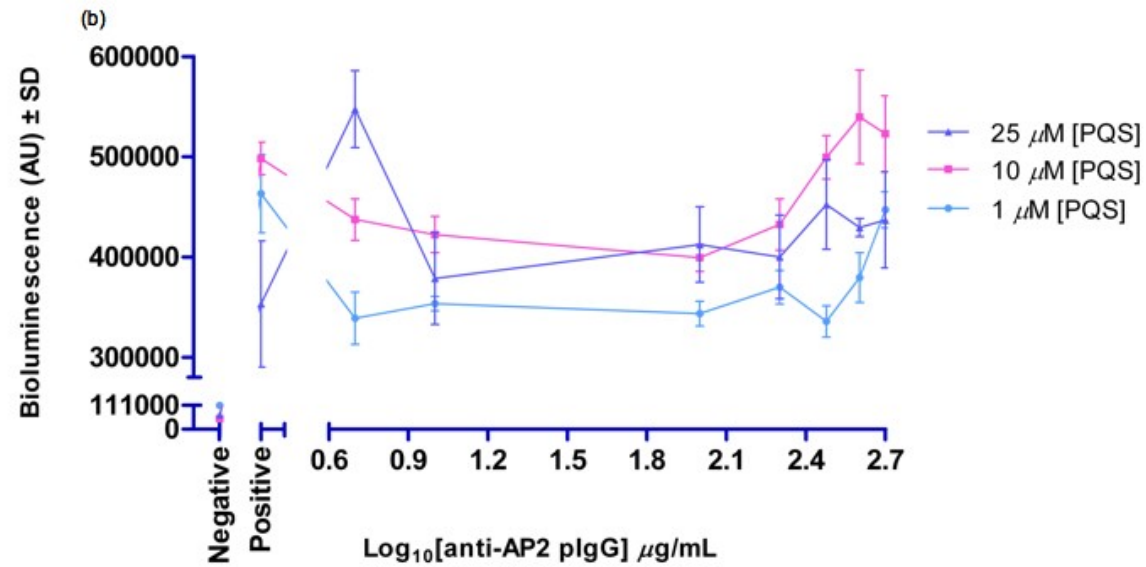
The CTX-*luxCDABE::pqsA* construct has been inserted into the mutated *P. aeruginosa* PAO1Δ*pqsA* strain and is bioluminescent in response to exogenous HAQs. Due to the deletion of *pqsA*, the reporter strain cannot produce HAQs. This reporter will be used with exogenous PQS, which will form the PqsR complex activating the *lux* cassette via the fused promoter *pqsA*.

A clear trend cannot be seen in the data from experiment a and b (Figure 7-6) for 1 and 25 μ M [PQS]. However, both experiments a and b, did show that rabbit anti-**AP2** pIgG significantly reduced bioluminescence in response to 10 μ M [PQS] at 10 μ g/mL, certainly, in experiment b (Figure 7-6) increasing concentration to 200 μ g/mL has significant inhibitory effect on bioluminescence.

Figure 7-6: The bioluminescence response of *P. aeruginosa* PAO1 Δ pqsA CTX-luxCDABE::pqsA reporter strain.

The bioluminescence response of *P. aeruginosa* PAO1 Δ pqsA CTX-luxCDABE::pqsA reporter strain in response to exogenous PQS and rabbit anti-**AP2** pIgG (x-axis). (a) and (b) Rabbit anti-**AP2** pIgG (μ g/mL) was titrated against 1 (i), 10 (ii) and 25 (iii) μ M [PQS]. Graphs (i), (ii) and (iii) show significance (ANOVA) of bioluminescence inhibition by the rabbit anti-**AP2** pIgG compared to the positive control. Negative control was the *P. aeruginosa* PAO1 Δ pqsA CTX-luxCDABE::pqsA reporter strain in LB broth/PBS and 1 μ L [DMSO]; Positive control was the reporter strain with LB broth/PBS and 1 (i), 10 (ii) and 25 (iii) μ M [PQS]. (Data is represented as mean \pm SD, n= 3). The data has been represented for the time point at which bioluminescence of the positive control was maximal.





In contrast, experiment c (Figure 7-7) 200 $\mu\text{g/mL}$ [rabbit anti-**AP2** pIgG] was added to the reporter strain in media and exogenous PQS at the first indication of bioluminescence (3 h). The results indicate that the bioluminescence was significantly reduced in response to 1, 10, and 25 μM [PQS].

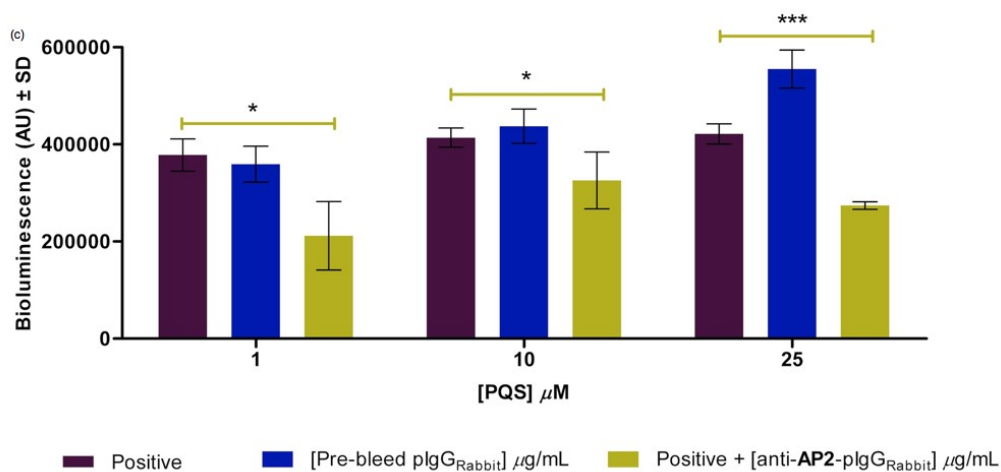


Figure 7-7: The bioluminescence response of *P. aeruginosa* PAO1 $\Delta pqsA$ CTX-*luxCDABE::pqsA* reporter strain.

The bioluminescence response of *P. aeruginosa* PAO1 $\Delta pqsA$ CTX-*luxCDABE::pqsA* reporter strain in response to exogenous PQS and rabbit pre-bleed or anti-**AP2** pIgG. (c) Pre-bleed was a limited resource and tested (data is represented as mean \pm SD, $n = 3$) in only one assay, 200 $\mu\text{g/mL}$ [rabbit pre-bleed pIgG] was titrated against 1, 10 and 25 μM [PQS]. (c) Positive control, reporter strain/PBS/LB media with PQS was incubated until bioluminescence was detected (3 h), 200 $\mu\text{g/mL}$ [rabbit anti-**AP2** pIgG] was added and bioluminescence was recorded at hourly intervals. The data has been represented for the time point at which bioluminescence of the positive control, (pale green) was maximal. Horizontal bars show significance (ANOVA) of bioluminescence inhibition by the rabbit anti-**AP2** pIgG compared to the positive control.

These data did not present a clear trend, however anti-**AP2** pIgG has shown anti-PQS activity by reducing bioluminescence as seen in experiments a and b (Figure 7-6, data for 10 μM [PQS]) and experiment c (Figure 7-7) at 10 – 200 $\mu\text{g/mL}$. This effect appeared to be specific as rabbit pre-bleed IgG showed no inhibitory effect on bioluminescence in response to exogenous PQS (Figure 7-7). Data from competitive indirect ELISAs clearly showed that anti-**AP2** pIgG strongly cross-reacted with PQS, but this was not reflected in this bioluminescence assay, unlike anti-**AP1** pIgG, which demonstrated strong cross-reactivity towards 3OC₁₂-HSL in both competitive indirect ELISA and bioluminescence assays.

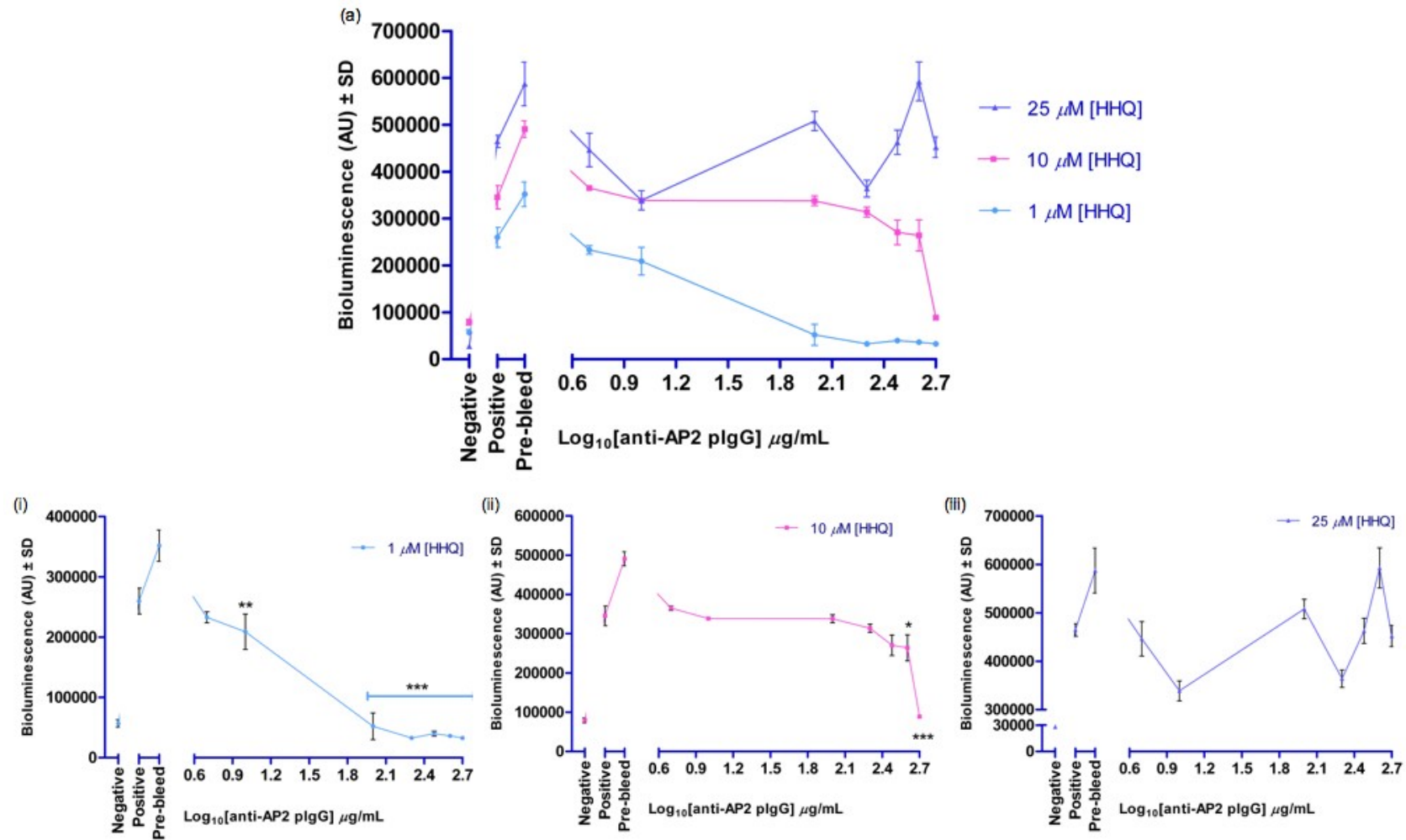
Data from competitive indirect ELISA (Appendix 1, p 153 - 155) showed that rabbit anti-**AP2** pIgG cross-reacted with HHQ. The *P. aeruginosa* PAO1 Δ pqsA CTX-luxCDABE::pqsA reporter strain was bioluminescent in response to exogenous HHQ, therefore, the assay was repeated using exogenous HHQ. This assay was conducted once and could not be repeated due to time constraints.

The bioluminescence (AU) for the positive controls increased with increasing concentrations of exogenous [HHQ]. Rabbit anti-**AP2** pIgG reduced bioluminescence in response to 1 and 10 μ M [HHQ] in a concentration-dependent manner, 100 μ g/mL was sufficient to reduce bioluminescence in response to 1 μ M [HHQ] to below that of the negative control. The IC₅₀ (n = 3) has been calculated to be 14.8-42.8 μ g/mL (3 s.f, $r^2 = 0.979$); 500 μ g/mL [anti-**AP2** pIgG] significantly reduced bioluminescence in response to 10 μ M [HHQ] to near negative control, but the IC₅₀ has been calculated just outside the tested concentration range. No clear trend was seen for 25 μ M [HHQ], it is suspected that greater concentrations of pAbs are needed.

Anti-**AP2** pIgG has demonstrated anti-HHQ effect, which appears to be specific anti-QSSM activity as pre-bleed IgG increased bioluminescence. This correlates with the cross-reactivity seen in competitive indirect ELISA (Appendix 1, p 153 - 155). The concentrations of anti-**AP2** pIgG at which inhibition of bioluminescence in response to 1 and 10 μ M [HHQ] are in a 0.3:1 (pAb:HHQ) molar ratio, it was expected that the pAbs would be in a 1:1 (pAb:QSSM) molar ratio, it is possible that the **AP2** is multi-valent, i.e. the quinolone ring may not be the only epitope.

Figure 7-8: The bioluminescence response of *P. aeruginosa* PAO1 Δ pqsA CTX-luxCDABE::pqsA reporter strain.

The bioluminescence response of *P. aeruginosa* PAO1 Δ pqsA CTX-luxCDABE::pqsA reporter strain in response to exogenous HHQ and rabbit pre-bleed or anti-**AP2** pIgG (x-axis). (a) Rabbit anti-**AP2** pIgG (μ g/mL) was titrated against 1 (i), 10 (ii), and 25 (iii) μ M [HHQ]. Pre-bleed (200 μ g/mL [rabbit pre-bleed pIgG]) was titrated against 1 (i), 10 (ii), and 25 (iii) μ M [HHQ]. The data has been represented for the time point at which bioluminescence of the positive control was maximal. Graphs (i), (ii) and (iii) show significance (ANOVA) of bioluminescence inhibition by the rabbit anti-**AP2** pIgG compared to the positive control. Negative control was the *P. aeruginosa* PAO1 Δ pqsA CTX-luxCDABE::pqsA reporter strain in LB broth/PBS and 1 μ L [DMSO]; positive control was the *P. aeruginosa* PAO1 Δ pqsA CTX-luxCDABE::pqsA reporter strain with LB broth/PBS and 1 (i), 10 (ii), and 25 (iii) μ M [HHQ]. (Data is represented as mean \pm SD, n = 3).



7.2 DISCUSSION

7.2.1 ANTI-QSSM ACTIVITY

The bioluminescence assay was considered appropriate for the determination of anti-QSSM activity by the rabbit anti-hapten pIgG, as reporter strains were bioluminescent in response to exogenous QSSM. Anti-**AP1** pIgG exhibited significant anti-3OC₁₂-HSL activity by reducing bioluminescence in response to 1 μ M [3OC₁₂-HSL] by 53% (200 μ g/mL [rabbit anti-**AP1** pIgG]). This concentration-dependent anti-QSSM activity was more pronounced with 1 μ M but was reflected in data for 10 and 25 μ M [3OC₁₂-HSL]. In contrast, although the pAbs showed anti-C₄-HSL activity, the inhibitory effect was significantly diluted as the concentration of anti-**AP1** pIgG increased. This implied, in conjunction with data from competitive indirect ELISA, that the avidity of anti-**AP1** pIgG for C₄-HSL might be weaker in comparison to 3OC₁₂-HSL.

Rabbit anti-**AP2** pIgG indicated possible anti-PQS activity, as significant inhibition of bioluminescence was only apparent in one assay, when the pIgG were added during the assay. The pAbs demonstrated strong PQS cross-reactivity. The action of the pIgG on the bioluminescence emitting biochemical reaction was tested using a *P. aeruginosa* PACY1 reporter strain (PAO1-lausanne *PKm-lux*), which was constitutively bioluminescent (Pr Cámara, University of Nottingham). Results showed that the pIgG had no effect on bioluminescence therefore the implied anti-PQS activity was a specific effect, even though it was not replicated in assays that had the pAbs at time zero. The anti-**AP2** pIgG showed strong anti-HHQ activity in a concentration dependent manner, confirming the strong cross-reactivity seen in competitive indirect ELISA studies.

PQS is a hydrophobic molecule, 86% of PQS is reportedly transported by membrane vesicles (233). PQS interacts with lipid A of LPS and is incorporated into these vesicles with no loss of biological activity (234). Figure 7-9 illustrates an explanation for the lack of anti-PQS activity seen with bioluminescence assay.

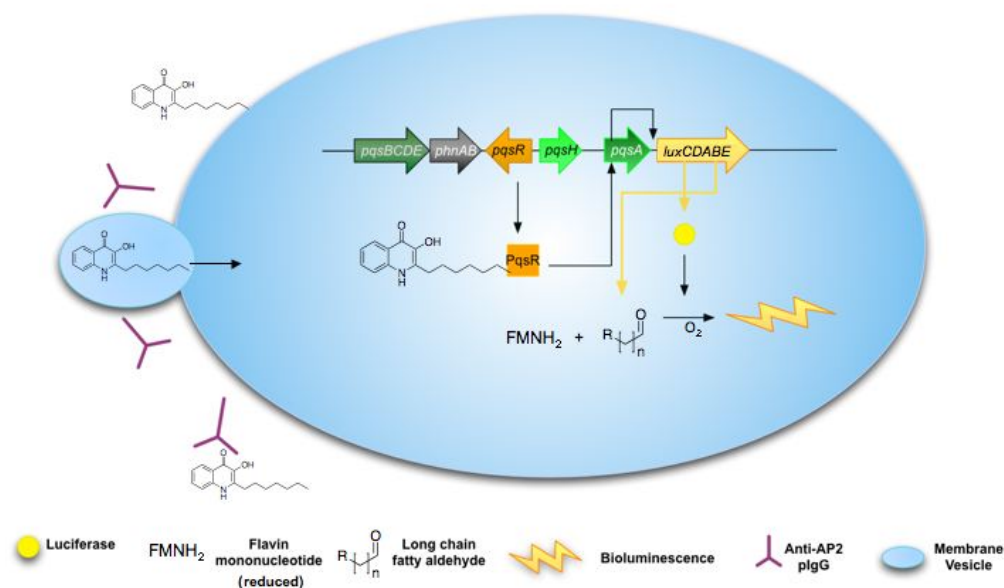


Figure 7-9: PQS bioavailability and anti-AP2 pIgG

Exogenous PQS interacts with LPS of the *P. aeruginosa* PAO1Δ*pqsA*-CTX-*luxCDABE::pqsA* reporter strain forming membrane vesicles. This limits the availability of PQS, thus preventing rabbit anti-AP2 pIgG binding. Competitive indirect ELISA has shown that rabbit anti-AP2 pIgG has avidity for PQS.

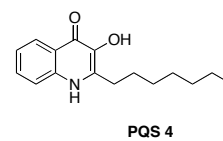
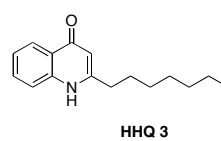
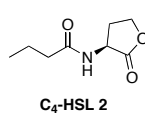
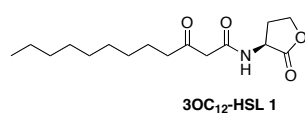
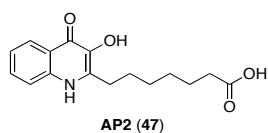
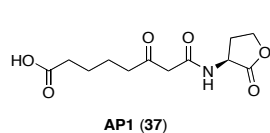
This presents a problem for the anti-AP2⁺ pAbs if PQS is unavailable for binding. Conversely, exogenous PQS could not restore the WT *P. aeruginosa* level of membrane vesicle formation in a PQS negative strain (235), which could mean that PQS may be transported by other means. The anti-AP2 pIgG have demonstrated anti-PQS activity, therefore provided PQS has not entered the cell, the pAbs still have the potential to inhibit the Pqs system.

Masburn *et al.* (234) noted that 2-heptyl and 3-hydroxyl group of PQS were needed for membrane vesicle formation; HHQ is not transported in this manner and diffuses freely in and out of the cell. HHQ is the precursor for PQS and may have QSSM activity in *P. aeruginosa* and *Burkholderia* spp. (68). Anti-AP2 pIgG showed strong anti-HHQ activity by reducing bioluminescence in response to 1 and 10 μ M [HHQ] in a concentration-dependent manner, in a ratio of 0.3:1 pAb:HHQ. Therefore it is possible that anti-AP2 pIgG can inhibit Pqs system by disrupting the conversion of PQS, achieved by inhibiting HHQ, which also serves to reduce the formation of HHQ (Figure 1-6, p 42) and PQS-PqsR formation.

7.2.2 FUTURE WORK

The variability of this assay is high, therefore, further repetitions are needed, in particular for 3OC₁₂-HSL, as the controls were irregular. It is of interest to test greater concentrations of anti-hapten pIgG than those used in this study. The bioluminescence assay (Figure 7-7, p 119) in which anti-AP2 pIgG was added during the assay needs to be repeated as this provided data indicating significant anti-PQS activity. It will be of benefit to investigate if membrane

vesicles are indeed the cause for the lack of anti-PQS activity in experiment a and b (Figure 7-6, p 116).



8 RESULT 5 - ANTI-QSS ACTIVITY

The anti-pAbs cross-react with the QSSMs of *P. aeruginosa* shown by a series of competitive indirect ELISA, as these QSSMs were able to significantly ($p < 0.05$) inhibit the formation of the anti-hapten pAbs:hapten BSA complex.

The anti-hapten pAbs demonstrated anti-QSSM activity by reducing bioluminescence of the reporter strains in response to exogenous QSSMs, the anti-hapten pAbs bind to the QSSM and inhibit the function.

The QSS controls the production of virulence factors, which cause the pathogenicity of *P. aeruginosa*. Anti-QSS activity implies that the QSS is compromised, the bacteria cannot sense the quorum and the environment and are unable to co-ordinate the production of virulence factors. The anti-hapten pAbs have shown significant anti-QSSM activity, however whether this activity translates into anti-QSS activity was yet undefined.

The anti-QSS activity was therefore characterised using assays that measured the production of virulence factors.

8.1.1 DETERMINATION OF ANTI-QSS ACTIVITY OF ANTI-HAPTEN pIgG

QSS appears to be important in biofilm development and maturation (1.5.5, p 46) and is an example of the situation where each division of the QSS is active; an impaired QSS causes abnormal biofilm formation. It was hypothesized that with inhibition of the QSSM activity, the QSS would be disrupted; the bacteria would remain planktonic, unable to communicate and would not convert to the sessile state thus minimising biofilm formation.

Adult human serum acts as a physical barrier preventing the initial attachment and formation of biofilm on plastic surfaces such as catheters (236). Ubiquitous lactoferrin, which has bactericidal properties, prevents biofilm formation by sequestering free iron and stimulating twitching motility (237). Complement proteins are known to inhibit biofilm formation (238). Indeed, in this study, mouse pre-bleed serum had an inhibitory effect in a preliminary static biofilm assay, inhibiting biofilm formation, almost comparable to that seen with the mouse anti-hapten serum. It was concluded that the effect, if any, on QSS of anti-hapten pAbs could only be determined if serum components were removed. The pIgG were used in the static biofilm microtitre assay.

An overnight culture of WT Nottingham *P. aeruginosa* PAO1 strain was grown in M9 media in the presence of pIgG for 24 hours in a 96-well microtitre plate, (Materials and methods, Static biofilm assay, p 83). The formation of biofilm, in the presence of rabbit anti-**AP1** pIgG

or anti-**AP2** pIgG and in combination, was quantified by crystal violet staining. Rabbit pre-bleed pIgG was used as a negative control.

8.1.2 RESULTS

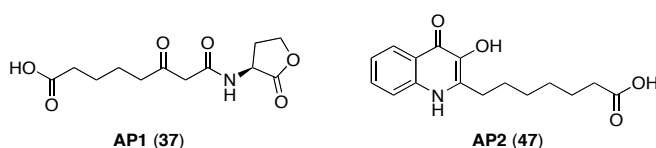
STATISTICAL ANALYSIS

Positive control WT Nottingham *P. aeruginosa* PAO1 in PBS/M9 media (n = 9). Negative control was M9 media and PBS (n = 9). Pre-bleed pIgG was a limited resource therefore could only be used in two assays (n = 3). Results from test pIgG/WT Nottingham *P. aeruginosa* PAO1 (n = 3) were analysed using one-way ANOVA and Dunnett's post-test against the positive control, (p = < 0.05, *; p = < 0.01, **; and p = < 0.001, ***). All statistical analysis was performed using Graphpad Prism[®] software 5, Graphpad Software, CA, USA.

Cell viability tests (data not shown) indicated that pIgG did not affect bacterial growth. Collectively, the data (Figure 8-1, experiment a and b) show that pre-bleed pIgG has no significant inhibitory effect on biofilm formation. The data indicated that rabbit anti-**AP1** pIgG reduced the biofilm formation in a concentration-dependent manner ($\geq 40 \mu\text{g/mL}$), which was significant at 50 – 200 $\mu\text{g/mL}$, in experiment c only. Rabbit anti-**AP2** pIgG also had inhibitory effect on biofilm formation, which was only significant in experiment c at 50 – 200 $\mu\text{g/mL}$, however, the effect was generally less than anti-**AP1** pIgG.

When biofilms were grown with a combination of anti-**AP1** and anti-**AP2**[^] pIgG at the concentrations where an inhibitory effect on biofilm formation was apparent, ($\geq 40 \mu\text{g/mL}$), there was a notable decrease in biofilm formation (experiment a, 80 $\mu\text{g/mL}$ total pIgG, 40:40 $\mu\text{g/mL}$ [anti-**AP1**/anti-**AP2** pIgG]). Experiment b and c showed that a total of 50 $\mu\text{g/mL}$ anti-hapten pIgG (25:25 $\mu\text{g/mL}$ [anti-**AP1**/anti-**AP2** pIgG]) caused significant inhibition of biofilm formation, in a concentration-dependent manner. However, at 400 $\mu\text{g/mL}$ (200:200 $\mu\text{g/mL}$ [anti-**AP1**/anti-**AP2** pIgG]), the reduction in biofilm formation was less than that of the anti-haptens pIgGs used separately at 200 $\mu\text{g/mL}$. This result may be anomalous, this concentration was only tested once and greater concentrations were not tested due to limited time.

^



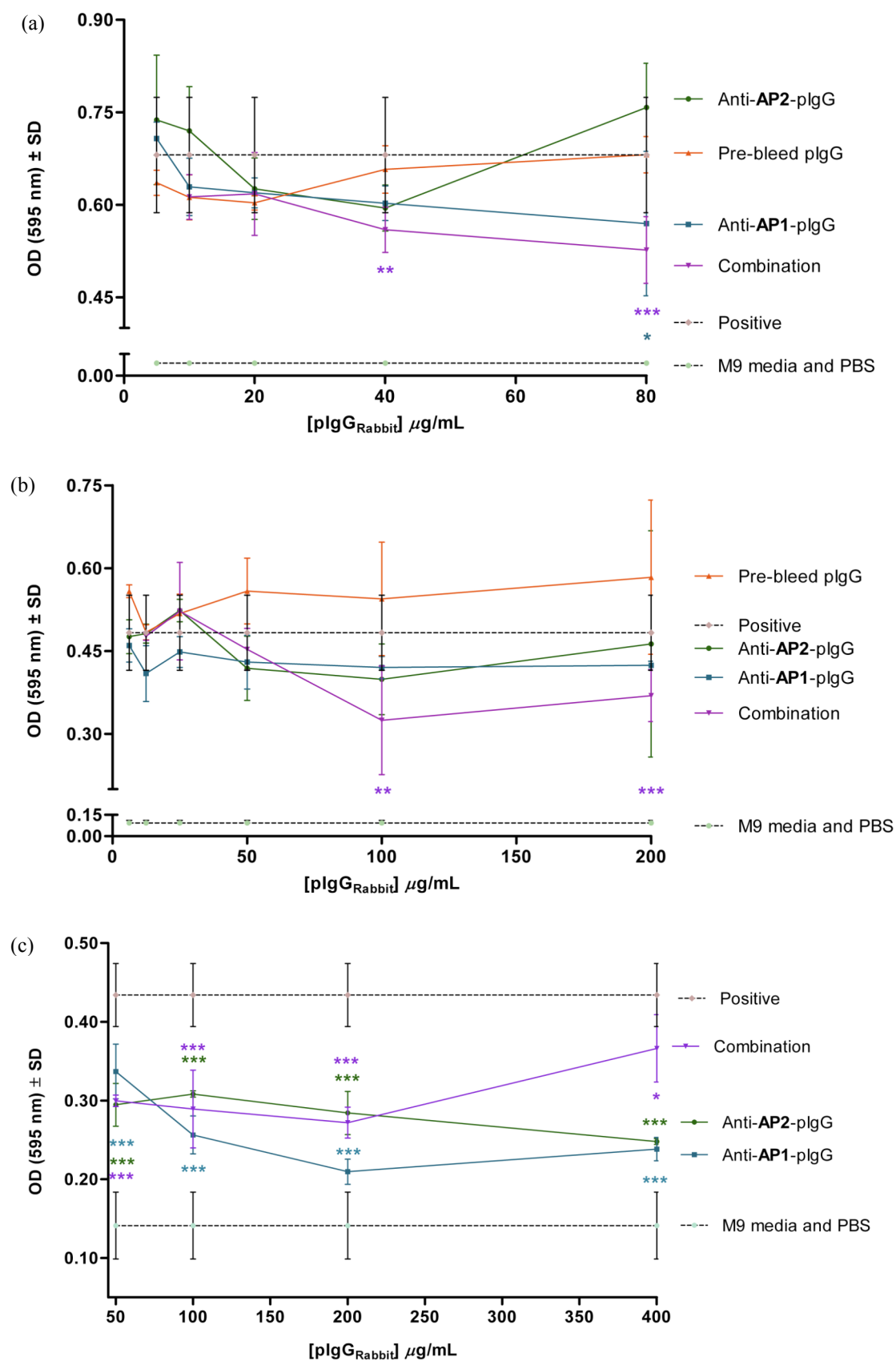


Figure 8-1: Static biofilm formation with and without rabbit anti-hapten pIgG.

(a), (b) and (c) Anti-QSS activity of rabbit anti-hapten pIgG on biofilm formation of WT Nottingham *P.*

aeruginosa PAO1 strain, grown in M9 media at 37 °C for 24 hours (n = 3). 1% [crystal violet] w/v was used to quantify biofilm formation and cell-viability plate assay was conducted during assay (a) and (b), results showed that the anti-hapten pIgG and pre-bleed pIgG did not affect growth (results not shown). Pre-bleed pIgG was a limited resource therefore was used in assay (a) and (b), however no significant inhibition of biofilm formation occurred. Positive control was WT Nottingham *P. aeruginosa* PAO1/M9 media and PBS; negative control is M9 media/PBS; and combination was rabbit anti-**AP1** pIgG:anti-**AP2** pIgG (1:1, $\mu\text{g/mL}$). Significance (ANOVA) is shown in comparison to positive control.

Anti-**AP1** and anti-**AP2** pIgG decreased biofilm formation when used individually, but was significant in only one experiment (Figure 8-1 c), anti-**AP1** had a greater effect than anti-**AP2** pIgG. This appears to be specific anti-QSS activity as pre-bleed generally had no inhibitory action on biofilm formation, but increased biofilm formation in experiment b at higher concentrations. However, when the anti-hapten pIgGs were used in combination, there was a significant concentration-dependent reduction in biofilm formation at $\geq 50 \mu\text{g/mL}$ (25:25 $\mu\text{g/mL}$ [anti-**AP1**/anti-**AP2** pIgG]). The data suggest that the anti-QSS activity, seen when the anti-hapten pIgGs were used in combination, was synergistic. However, it would be beneficial to repeat the assay using greater concentrations $\geq 400 \mu\text{g/mL}$.

8.2 DISCUSSION

QSSi have been tested in static biofilm formation assays and have shown to reduce biofilm formation and tolerance to biocides (132, 150, 239). The anti-hapten pIgG used separately were able to reduce the formation of biofilms but significant inhibition was achieved when the anti-hapten pIgG were used in combination. This effect was attributed to anti-QSS activity, as pre-bleed pIgG had no inhibitory effect on biofilm formation. This is promising, as the data suggests that the anti-hapten pIgG, are not antagonistic, proving that the individual hapten-conjugate of the multi-component anti-QS vaccine would be synergistic.

Published reports suggest that an intact QSS is needed for biofilm development and maturation, due to time limitations the structure of the biofilms formed in presence of the anti-hapten pIgG were not studied nor were the susceptibility to biocides. It is hypothesised that the anti-hapten pIgG will (a) disrupt QS therefore reduce biofilm formation, which has been suggested in this study, and (b) increase the susceptibility of any formed biofilms to biocides, which is yet to be studied.

8.2.1 FUTURE WORK

The static biofilm assay was useful in demonstrating the anti-QSS activity of anti-hapten pAb when used in combination, however, the effect of anti-hapten pIgG on biofilm structure and susceptibility to biocides still needs to be investigated, which unfortunately due to time restrictions was not possible in this study.

The effect of anti-hapten pAbs on other virulence factors needs to be determined, such as elastase, rhamnolipids, and pyocyanin. Attempts have been made (data not shown) to test the effects of anti-hapten pIgG on rhamnolipids using the qualitative rhamnolipid plate assay described by Pinzon and Ju (240) using M9 media however, initial tests were not successful, but with suitable optimisation, this may be a useful assay. These virulence factors are under QSS control therefore will be useful in demonstration of the *in vitro* anti-QSS effect of the anti-hapten pAb.

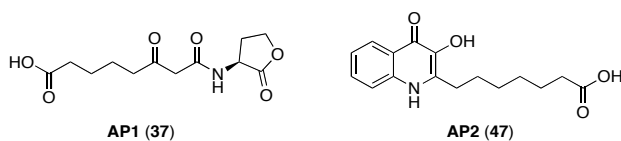
9 SUMMARY OF RESULTS

Synthesis of the haptens, **AP1** and **AP2**[^], was conducted using adapted published methods and sufficient quantities of each hapten were produced to continue with the haptenisation of the immunogenic carrier, KLH. Chemical synthetic routes require further optimisation and should be the focus of future work.

Haptenisation of KLH was successful and the immunogenicity of the **AP1**-KLH and **AP2**-KLH hapten was demonstrated in mice and rabbits. Characterisation of the mouse anti-**AP1**-KLH sera revealed considerable cross-reactivity with 3OC₁₂-HSL confirmed by the anti-QSSM seen in the bioluminescence assay. The cross-reactivity to the long and short AHLs was also shown, however, it was apparent that cross-reactivity with C₄-HSL was weaker in comparison.

Mouse and rabbit anti-**AP2**-KLH sera showed strong cross-reactivity with PQS and HHQ, and showed potential cross-reactivity with HMAQs produced by *Burkholderia* spp., indicated by cross-reactivity with 3-methyl-quinolin-4(1*H*)-one **74**. Rabbit anti-**AP2**-KLH pIgG demonstrated anti-HHQ activity but little anti-PQS activity, however this was attributed to PQS low availability due to transport by membrane vesicles. Anti-hapten pIgG were able to demonstrate an additive inhibition of biofilm formation when used in combination, suggesting that the anti-hapten pIgG have anti-QSS activity.

^



10 FUTURE DIRECTIONS AND CONCLUSION

10.1 FUTURE DIRECTIONS

10.1.1 HAPTEN DESIGN

10.1.1.1 CHAIN LENGTH

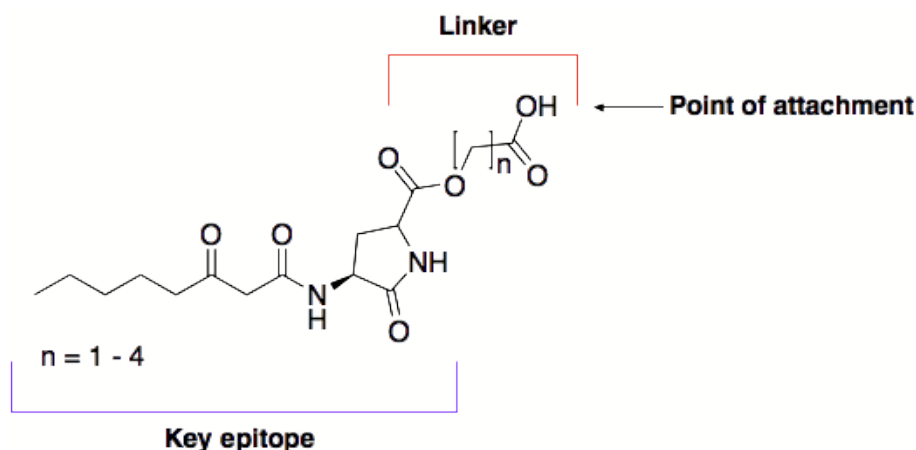
It has been predicted that the acyl chain can be shortened to a 5-7-carbon acyl chain, retaining the 3-oxo moiety, producing a hapten which can generate pAbs that still have significant cross-reactivity with 3OC₁₂-HSL but improved cross-reactivity with C₄-HSL, ultimately improving the anti-QSS activity (6.3, p 102). This will be considered as part of hapten design for the AHL hapten. However, this will not be applicable for **AP2**, as data from the competitive indirect ELISA (Appendix 1, p 153) suggests that the quinolone structure is the key epitope.

10.1.1.2 ORIENTATION

The position of the carrier in relation to the key epitopes is critical for the efficient presentation of the hapten-carrier conjugate to the immune system. It is quite clear that the carrier on attachment should not obscure important structural components and cause any chemical modification. Published reports (224, 241, 242) detail significant impacts on antibody titres and avidity towards the hapten when the position of the carrier was changed - more epitopes were exposed to the immune system.

This study has added to the search for the ideal hapten-conjugate for a multi-component anti-QSS vaccine. However, the AHL hapten still needs further optimisation in order to improve avidity for C₄-HSL. Thus, in preparation, the designed haptens **AP1** and **AP2** have been modified so the carrier will be attached to the ring via a 3-6-carbon linker. It is hypothesised that adjusting the position of the carrier will change the orientation of the hapten and the presentation of this antigen to the immune system. The conserved structural components, such as the ring and external amide moiety (Figure 10-1, a, **AP3**) and the quinolone structure (Figure 10-1, b, **AP4**), which are the key epitopes, will still be exposed, but it is anticipated that the generated antibodies will have a different avidity profile.

(a)



(b)

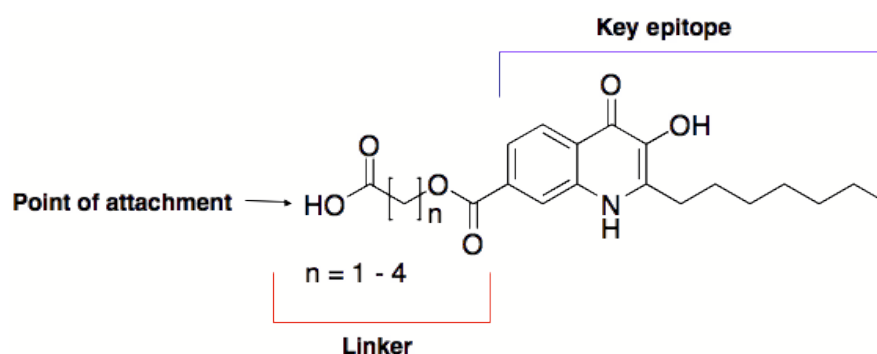
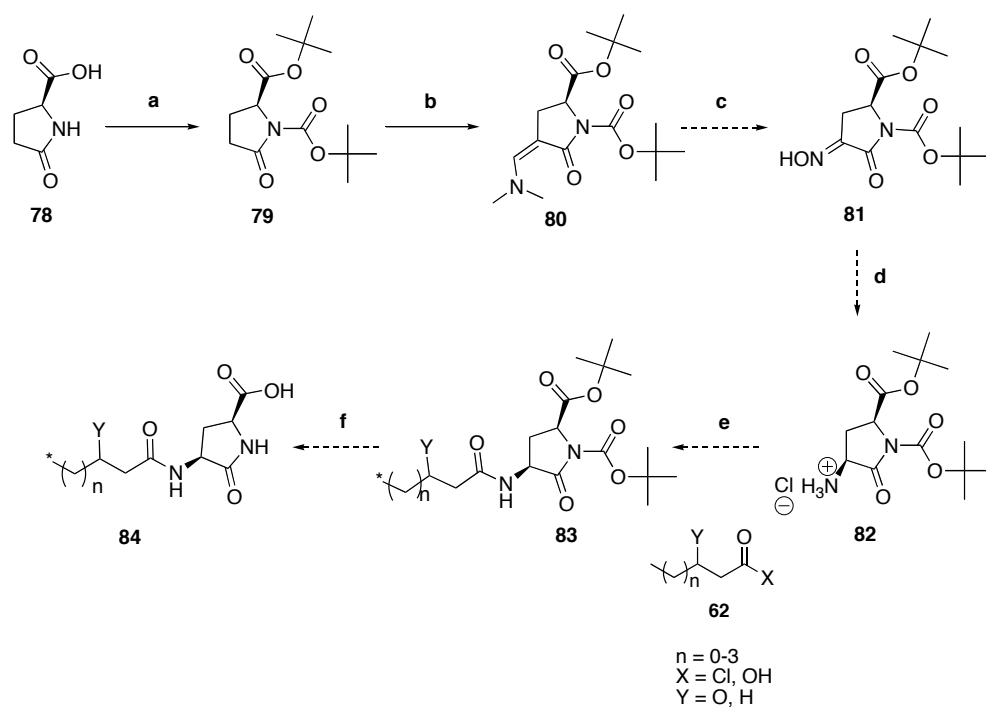


Figure 10-1: Proposed haptens for the investigation of carrier attachment, (a) **AP3**, and (b) **AP4**.

10.1.2 SYNTHETIC STRATEGY FOR AP3 AND AP4

10.1.2.1 (2*S*,4*S*)-4-ACYLAMINO-5-OXOPYRROLIDINE-2-CARBOXYLIC ACIDS, **AP3**

Malavašič *et al.* (243) reported a synthetic strategy, ensuring enantiometric specificity, for (2*S*,4*S*)-4-acylamino-5-oxopyrrolidine-2-carboxylic acids (243). Serendipitously, both the amine and carboxylic acid moiety of L-pyrroglutamic acid **78** could conveniently be protected in a one-pot procedure used for the esterification of carboxylic esters *en*(244). In pilot studies, crude di-protected derivative **79** was treated with *tert*-butoxy-bis(dimethyl-amino)methane to form enamino intermediate **80**. However, nitrosation of **80** in sodium nitrite (NaNO₂) under acidic conditions to furnish the oxime **81** was not successful. The derivatives of **84** are potential haptens and future work should concentrate on the progression of the synthesis.

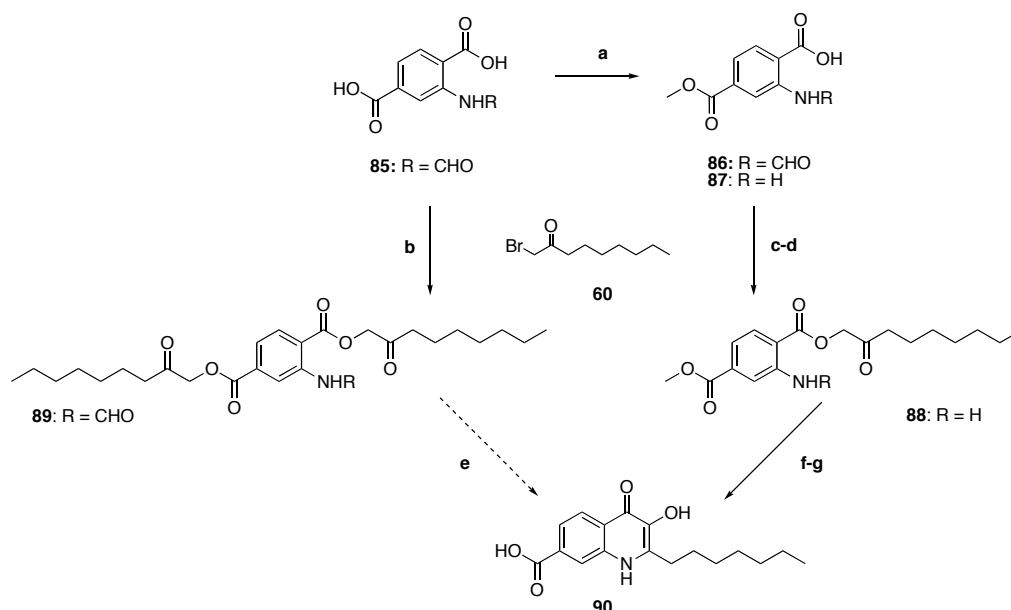


Reagents and conditions: (a) BOC_2O , $t\text{-BuOH}$, cat. DMAP, rt (62%); (b) $\text{tert-butoxy-bis(dimethyl-amino)methane}$, toluene, reflux (41%); (c) NaNO_2 , aq. NaHSO_4 , 0°C ; (d) $\text{H}_2/\text{Pd-C}$ 10%, MeOH , rt; (e) Amidation; (f) TFA: CH_2Cl_2 , (1:1), rt.

Scheme 10-1: Synthesis of (2*S*,4*S*)-4-acylamino-5-oxopyrrolidine-2-carboxylic acids (243).

10.1.2.2 2-HEPTYL-1,4-DIHYDRO-3-HYDROXY-4-OXOQUINOLINE-7-CARBOXYLIC ACID, AP4

Using a combination of two strategies reported by Hradil *et al.* (199) and Soural *et al.* (245) the carboxylic acid moieties of **86** (Scheme 10-2) were di-alkylated to form the intermediate **90**, but cyclisation using NH_4HCO_2 and HCO_2H (199) with microwave irradiation was not successful. The strategy (173) used in method B (Scheme 3-7) was useful, affording 2-heptyl-1,4-dihydro-3-hydroxy-4-oxoquinoline-7-carboxylic acid **91** in modest yields (44%).



Reagents and conditions: (a) **86**, MeOH, H₂SO₄, 60 °C, (49%) (246); (b) **85**, **60**, Et₃N, (CH₃)₂CO, (95%); (c) **86**, **60**, Et₃N, (CH₃)₂CO, (54%); (d) **87**, **60**, Et₃N, (CH₃)₂CO, (54%); (e) NH₄HCO₂, HCO₂H, MW, 120 °C; (f) NH₄HCO₂, HCO₂H, MW, 120 °C; (g) NMP, MW, 250 °C, (44%).

Scheme 10-2: Synthesis of 2-heptyl-1,4-dihydro-3-hydroxy-4-oxoquinoline-7-carboxylic acid, **AP4**, **90**.

10.1.3 OTHER BACTERIAL TARGETS

In this study, mouse anti-**AP1** pAb has exhibited cross-reactivity to the natural AHL QSSM produced by *P. aeruginosa*. It is hypothesised that pAbs generated against the optimised AHL based hapten will cross-react with 3-OH AHLs and longer acyl chains up to 18-carbons. Although **74** is only the synthon for HMAQS, the fact that anti-**AP2** pAb recognised this conserved quinolone structure is promising. Often in disease pathologies, *P. aeruginosa* is a co-infecter, for example in CF, the *B. cenocepacia* complex, which use AHLs and HHQ in QS. It is possible that an anti-QSS vaccine would be effective against many of the Gram-negative bacteria listed in Table 1-5 (p 38). It will be of interest to pursue the development of such a vaccine.

10.1.4 GRAM-POSITIVE AND GRAM-NEGATIVE ANTI-QSS VACCINE

Gram-positive bacteria such as *S. aureus* use QS, Park *et al.* (247) have used their patented hapten (248) to generate a Mab with specificity for the *S. aureus* AI peptide-4 (AIP-4), which inhibits the bacteria QSS and increases survival of a mouse model infected with *S. aureus* by passive immunisation (247). *P. aeruginosa* and *S. aureus* can co-infect hosts, and 3OC₁₂-HSL and C₁₂-tetramic acid has anti-microbial effects on *S. aureus* (96, 97). However, the anti-QSS vaccine targeting Gram-negative bacteria may affect this defence mechanism of *P. aeruginosa*

thereby allowing otherwise suppressed bacterial species to benefit. It would be of interest to combine an anti-QSS vaccine specific for Gram-negative bacteria with an anti-QSS vaccine specific for Gram-positive bacteria as invented by Park and colleagues (248). It is possible, that both vaccines used in conjunction will be antagonistic, however, it is equally possible that this can lead to broad-spectrum anti-QSS vaccine.

10.2 CONCLUSION

The aim of this study was to demonstrate that inhibition of the QSS should include the three systems, Las, Rhl and Pqs QSS, thus improving the efficacy of this approach, and should be done so by a multi-component QSS vaccine. This was only possible by producing an AHL hapten that targeted 3OC₁₂-HSL and C₄-HSL, and a separate PQS hapten, which targeted PQS, a technology that to date has not been reported.

The objectives of this study have been met, and the study has contributed to the development of a multi-component anti-QSS vaccine. These data suggest that the complete inhibition of the QSS is possible and that anti-QSS vaccine is a viable prophylaxis against *P. aeruginosa* in susceptible patients. There is potential for a broad-spectrum anti-QSS vaccine, which could target Gram-negative bacteria and Gram-positive bacteria (10.1.4, p 134).

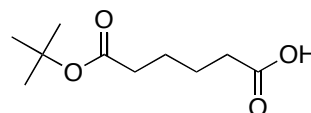
11 EXPERIMENTAL PROCEDURES

GENERAL

All reagents and solvents were purchased from Sigma Aldrich and Alfa Aesar (unless specified) and were used as received from manufacturers. ^1H NMR spectra were recorded as CDCl_3 (unless otherwise stated) sample solutions on Bruker Avance-400 instrument operating at 400 MHz. ^{13}C NMR spectra were recorded as CDCl_3 (unless otherwise stated) sample solutions on Bruker Avance-400 instrument operating at 100 MHz. FT-IR spectra were recorded on Nicolet IR-200 using the range $400 - 4000\text{ cm}^{-1}$ with samples either in the form of KBr discs or as thin film. ES-MS spectra were recorded using Mass (TOF ES \pm) Water 2795 Separation module/Micromass LCT platform. TLC was performed using Merck silica gel 60 GF₂₅₄ pre-coated (0.2 mm).

5-(*tert*-BUTOXYCARBONYL)PENTANOIC ACID (13)

DIC (1.6 mL, 1.27 g, 10 mmol) and catalytic DMAP (126 mg, 1 mmol) were added to a stirred solution of adipic acid (1.47 g, 10 mmol) in anhydrous CH_2Cl_2 (50 mL) at 0°C under an atmosphere of N_2 . After the addition of *tert*-butanol (10 mL),

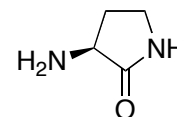


the reaction mixture was left to stir until TLC analysis (EtOAc/PE (40-60 $^\circ\text{C}$), 1:1) indicated no further reaction progression (72 h). The reaction mixture was extracted consecutively with 2 M aq. HCl, and brine, and dried over MgSO_4 . The solvent was rotary evaporated and the residue was further purified by flash column chromatography (eluent EtOAc/PE (40-60 $^\circ\text{C}$), 5:95, then 10:90, then 100:0) or Kugelrohr vacuum distillation to afford the title compound as a yellow viscous oil (1.71 g, 84%). ^1H NMR: δ 1.43 (s, 9H, $\text{C}(\text{CH}_3)_3$), 1.62-1.65 (m, 4H, CH_2CH_2), 2.23 (t, $J = 7.0\text{ Hz}$, 2H, COCH_2), 2.36 (t, $J = 7.1\text{ Hz}$, 2H, COCH_2), 7.39 (br. s, 1H, OH). ^{13}C NMR: δ 23.23 (CH_2), 24.49 (CH_2), 28.04 ($\text{C}(\text{CH}_3)_3$), 33.86 (CH_2), 35.17 (CH_2), 80.32 ($\text{C}(\text{CH}_3)_3$), 173.02 ($\text{COOC}(\text{CH}_3)_3$), 178.26 (COOH). $R_f = 0.24$ (EtOAc:hexane 2:8). HR-ESI-MS: m/z 225.1809 [$\text{M} + \text{Na}$] $^+$. $\text{C}_{10}\text{H}_{18}\text{NaO}_4$ requires 225.1103.

(*S*)-3-AMINO-PYRROLIDIN-2-ONE (35)

METHOD A

L-2,4-diamino butyric acid dihydrochloride (2.1 g, 11.2 mmol) and hexamethyldisilazane (54 mL) were added to MeCN, (100 mL) which had



been dried with molecular sieves (4A). The reaction was heated under reflux for 48 h under N_2 . The pale yellow solution was cooled and added to excess ice-cold MeOH and stirred for 30 min. The solvent was rotary evaporated and the residue was dissolved in CHCl_3 . A precipitate formed, which was removed by filtration and the filtrate was concentrated by rotary evaporation. This procedure was repeated until all solid matter had been removed and the isolated pale yellow solid was dried under vacuum. The title compound

was obtained as an yellow amorphous solid (0.97 g, 88%) and stored in a dessicator. (The title compound discoloured over time. It was stored in a dessicator and as a precaution, the product was dissolved in CHCl_3 and any precipitate was removed before use).

METHOD B

The above protocol was modified by adding 3 drops of chlorotrimethylsilane and the subsequent procedure was followed as described above to afford the title compound as an yellow amorphous solid (1.0 g, 91%). ^1H NMR: δ 1.59 (br. s, 2H, NH_2), 1.80-1.9 (m, 1H, $\text{CH}(\text{H})\text{CH}_2$), 2.46-2.53 (m, 1H, $\text{CH}(\text{H})\text{NH}$), 3.27-3.38 (m, 2H, CH_2), 3.47-3.52 (m, 1H, CHNH_2). ^{13}C NMR: δ 30.87 (CH_2CHNH_2), 43.55 (CH_2NH), 52.21 (CH), 179.69 ($\text{C}(\text{O})\text{NH}$). IR ν (cm^{-1}) 786, 893, 1069, 1292, 1690, 2994, 3185, 3342. HR-ESI-MS: m/z 101.0545 [$\text{M} + \text{H}$], 124.0785 [$\text{M} + \text{Na}$] $^+$, $\text{C}_4\text{H}_8\text{N}_2\text{O}$ requires 100.0636 and $\text{C}_4\text{H}_8\text{N}_2\text{O} \text{Na}^+$ requires 124.0613.

GENERAL PROCEDURES FOR TERT-BUTYL 6-(2,2-DIMETHYL-4,6-DIOXO-1,3-DIOXAN-5-YL)-6-OXOHEXOATE (18)

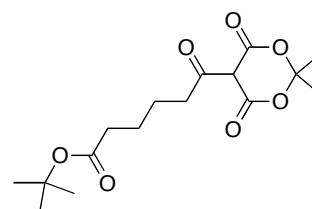
METHOD A

Oxalyl chloride (2 mL) and catalytic amount of anhydrous DMF (1 drop) were added to the stirred 5-(*tert*-butoxycarbonyl)pentanoic acid (**13**, 7.8 mmol) in anhydrous CH_2Cl_2 (8 mL) under N_2 . After completion (TLC, EtOAc), the solvent was rotary evaporated and kept under N_2 to be used without further purification.

Meldrum's acid (**17**, 1.1 g, 7.8 mmol) was added to the stirred acyl chloride in anhydrous CH_2Cl_2 (60 mL) under N_2 followed by the addition of anhydrous pyridine (1.26 mL, 15.6 mmol). The reaction was left to stir at rt for 16 h until complete (TLC, CH_2Cl_2). The crude mixture was extracted consecutively with 2 M aq. HCl and brine.. After drying over MgSO_4 , the solvent was rotary evaporated and dried under vacuum. The product was used without further purification.

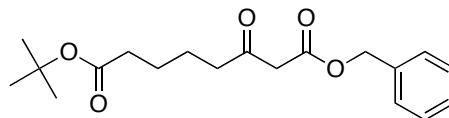
METHOD B

EDC (401.3 mg, 2.1 mmol, Fluorochem Ltd) was added to a stirred mixture of the 5-(*tert*-butoxycarbonyl)pentanoic acid (**13**, 346mg, 1.7 mmol), DMAP (253 mg, 2.1 mmol) in CH_2Cl_2 (10 mL) at 0 °C followed by Meldrum's acid (247 mg, 1.7 mmol) after 5 min. The solution was left to warm to rt and stirred under N_2 for 16 h until complete (TLC, CH_2Cl_2). The crude mixture was extracted consecutively with 2 M aq. HCl and brine, then dried over MgSO_4 . The solvent was rotary evaporated and the residue was triturated with EtOAc/hexane. After the solvent was rotary evaporated, the product was dried under vacuum to afford the tile compound as a yellow oil (0.54 g, 97%) and was used without further purification. (Stored at 2-8°C under N_2 until use). HR-ESI-MS: m/z 327.1492 [$\text{M}-\text{H}$] $^-$, [$\text{C}_{16}\text{H}_{23}\text{O}_7$] $^-$ requires 327.1444.



8-*TERT*-BUTYL-1-BENZYL 3-OXOOCTANEDIOATE (23)

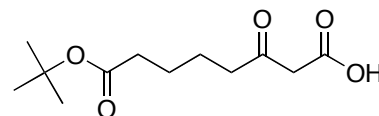
BnOH (615 μ L, 5.9 mmol) was added to a stirred solution of *tert*-butyl-6-hydroxy-6-(2,2-dimethyl-



4,6-dioxo-1,3-dioxan-5-ylidene)hexanoate (**18**, 628 mg, 1.9 mmol) in anhydrous toluene (20 mL) and heated under reflux for 1-2 h until completion (TLC, CH_2Cl_2). The solvent was rotary evaporated and the residue was dissolved in EtOAc. The mixture was extracted consecutively with saturated NaHCO_3 , 2 M aq. HCl, and brine. Once dried over MgSO_4 , the solvent was rotary evaporated. BnOH was removed by Kugelrohr distillation (75 $^\circ\text{C}$) and/or column chromatography (eluent EtOAc/PE (40-60 $^\circ\text{C}$) 5:95, then 10:90, then 100:0) to afford the title compound as a yellow oil (442.6 mg, 67%) after three further washings with PE (40-60 $^\circ\text{C}$). ^1H NMR: δ 1.43 (s, 9H, $\text{C}(\text{CH}_3)_3$), 1.52-1.63 (m, 4H, CH_2CH_2), 2.18 (t, $J = 7.0$ Hz, 2H, CH_2COO), 2.52 (t, $J = 7.0$ Hz, 2H, CH_2COO), 3.47 (s, 2H, $\text{C}(\text{O})\text{CH}_2$), 5.16 (s, 2H, $\text{CH}_2\text{C}_6\text{H}_5$), 7.30-7.36 (m, 6H, C_6H_6). ^{13}C NMR: δ 22.90 (CH_2), 24.52 (CH_2), 28.18 ($\text{C}(\text{CH}_3)_3$), 34.82 (CH_2COO), 42.69 (CH_2CO), 49.30 ($\text{C}(\text{O})\text{CH}_2$), 67.18 (COOCH_2), 80.25 ($\text{C}(\text{CH}_3)_3$), 127.12, 127.80, 128.77 (CH), 135.42 ($\text{CCH}_2(\text{O})$), 167.08 (COOCH_2), 172.76 ($\text{COOC}(\text{CH}_3)_3$), 202.25 ($\text{C}(\text{O})\text{CH}_2$). HR-ESI-MS: m/z 357.1685 $[\text{M} + \text{Na}]^+$, $\text{C}_{19}\text{H}_{26}\text{O}_5\text{Na}^+$ requires 357.1678.

7-(*TERT*-BUTOXYCARBONYL)-3-OXOHEPTANOIC ACID (29)

Pd-C 10% (50 mg) was added to anhydrous THF in an oven-dried RBF under N_2 . The solution was sonicated

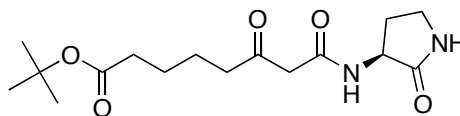


and evacuated three times with N_2 . 8-*tert*-Butyl-1-benzyl 3-oxooctanedioate (**23**, 442.6 mg, 1.3 mmol) was dissolved in minimum anhydrous THF and added via a syringe with rinsings at 0 $^\circ\text{C}$. This was sonicated and evacuated once with N_2 . H_2 was introduced to the system via a three-way tap and the reaction was evacuated three times with H_2 . The solution was stirred under H_2 at 0 $^\circ\text{C}$ until completion (TLC, EtOAc). The solution was passed through a celite pad and the solvent was rotary evaporated to afford the title compound as a pink oil (311.8 mg, 96%). ^1H NMR: δ 1.41 ($\text{C}(\text{CH}_3)_3$), 1.54-1.60 (m, 4H, CH_2CH_2), 2.20 (t, $J = 6.8$ Hz, 2H, CH_2CO), 2.57 (t, $J = 6.8$ Hz, 2H, CH_2CO), 3.47 (s, 2H, $\text{C}(\text{O})\text{CH}_2$), 10.06 (br. s, 1H, OH). ^{13}C NMR: δ 22.75 (CH_2), 24.36 (CH_2), 24.58 (CH_2), 28.13 ($\text{C}(\text{CH}_3)_3$), 35.21 (CH_2CO), 42.77 (CH_2CO), 48.39 ($\text{CH}_2\text{C}(\text{O})$), 80.38 ($\text{C}(\text{CH}_3)_3$), 171.32 (COOH), 173.23 ($\text{COOC}(\text{CH}_3)_3$), 203.38 ($\text{C}(\text{O})\text{CH}_2$). HR-ESI-MS: m/z 242.5499, 243.5589 $[\text{M}-\text{H}]^-$, 264.1600, 267.1235 $[\text{M} + \text{H} + \text{Na}]^+$, $\text{C}_{12}\text{H}_{20}\text{O}_5$ requires 244.1311, $\text{C}_{12}\text{H}_{19}\text{O}_5^-$ requires 243.1232 and $\text{C}_{12}\text{H}_{20}\text{O}_5\text{Na}^+$ requires 267.1201.

***TERT*-BUTYL-7-((*S*)-2-oxopyrrolidin-3-ylcarbamoyl)-6-oxoheptanoate (**36**)**

METHOD A

DIC (206 μ L, 167.9 mg, 1.3 mmol) was added to a stirred solution of 7-(*tert*-butoxycarbonyl)-3-oxoheptanoic acid (**29**, 247.1 mg, 1 mmol) in



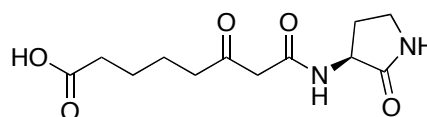
anhydrous CH_2Cl_2 (20 mL) with DMAP (148.7 mg, 1.2 mmol) at 0 °C under N_2 . After 5 min, (*S*)-3-amino-pyrrolidin-2-one (**35**, 101.8 mg, 1 mmol) was added and the mixture was allowed to warm to room temperature and stirred overnight under N_2 . The solvent was rotary evaporated and the residue was dissolved in EtOAc and was extracted consecutively with 1 M aq. KHSO_4 , saturated NaHCO_3 , and brine, then dried over MgSO_4 . The solvent was rotary evaporated and the crude mixture was further purified by column chromatography (eluent DCM/MeOH 9.7:0.3) to afford the title compound as a yellow residue (35.9 mg, 10%).

METHOD B

(*S*)-3-Amino-pyrrolidin-2-one (**35**, 150 mg, 1.5 mmol) was stirred in anhydrous MeCN (10 mL) with *tert*-butyl-6-hydroxy-6-(2,2-dimethyl-4,6-dioxo-1,3-dioxan-5-ylidene)hexanoate (**18**, 544.4 mg, 1.7 mmol) at 40 °C overnight under N_2 . The mixture was warmed to 50–60 °C until completion (TLC, CH_2Cl_2). The solvent was rotary evaporated and the residue was dissolved in EtOAc and was extracted consecutively with 1 M aq. KHSO_4 , saturated NaHCO_3 , and brine, then dried over MgSO_4 . The solvent was rotary evaporated and the crude mixture was further purified by column chromatography (eluent Et_2O /MeOH 9:1) followed by preparative TLC (mobile phase EtOAc:PE (40–60 °C) 0.5:9.5). The title compound was obtained as a yellow residue (91 mg, 19%). ^1H NMR: δ 1.42 (s, 9H, $\text{C}(\text{CH}_3)_3$), 1.58 (m, 4H, CH_2CH_2), 1.91–2.02 (m, 1H), 2.20 (t, $J = 6.6$ Hz, 2H, CH_2COO), 2.56 (t, $J = 6.7$ Hz, 2H, CH_2COO), 2.69 (m, 1H), 3.27–3.46 (m, 4H, (Prominent singlet peak overlap with multiplet, δ 3.44 ($\text{CH}_2\text{C}(\text{O})$ and CH_2 (ring))), 4.40–4.47 (m, 1H), 6.62 (undefined br. s, 1H, NH), 7.61 (s, 1H, NH). ^{13}C NMR: (DMSO- d_6) δ 22.81 (CH_2), 24.43 (CH_2), 28.21 ($\text{C}(\text{CH}_3)_3$), 29.66 (CH_2CHNH_2), 35.29 (CH_2), 39.38 (CH_2NH), 43.26 (CH_2CO), 49.31 ($\text{C}(\text{O})\text{CH}_2$), 50.83 (CH), 80.36 ($\text{C}(\text{CH}_3)_3$), 166.62 ($\text{C}(\text{O})\text{NH}$), 172.87 ($\text{COOC}(\text{CH}_3)_3$), 175.69 ($\text{HNC}(\text{O})\text{NH}$), 205.82 ($\text{C}(\text{O})\text{CH}_2$). HR-ESI-MS: m/z 325.1667 [$\text{M} - \text{H}$] $^-$ and 327.1991 [$\text{M} + \text{H}$]. $\text{C}_{16}\text{H}_{26}\text{N}_2\text{O}_5$ requires 326.1842, [$\text{C}_{16}\text{H}_{25}\text{N}_2\text{O}_5$] $^-$ requires 325.1763 and [$\text{C}_{16}\text{H}_{27}\text{N}_2\text{O}_5$] $^+$ requires 327.1920.

7-((*S*)-2-oxopyrrolidin-3-ylcarbamoyl)-6-oxoheptanoic acid (37**)**

tert-Butyl-7-((*S*)-2-oxopyrrolidin-3-ylcarbamoyl)-6-oxoheptanoate (**36**, 35.9 mg, 0.1 mmol) was stirred in TFA: CH_2Cl_2 (1:1) with 1 drop of dH_2O at rt until

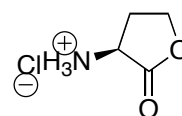


the reaction was complete (TLC, EtOAc). The solvent was rotary evaporated, dissolved in CH_2Cl_2 , and washed with dH_2O twice. After drying over MgSO_4 , the solvent was rotary evaporated and dried under vacuum to furnish the title compound as a pink solid (29.4 mg,

98%). ^1H NMR: (MeOD) δ 1.59-1.62 (m, 4H, CH_2CH_2), 1.96-2.15 (m, 1H, CHH), 2.30 (t, 2H, CH_2), 2.48-2.55 (m, 1H, CHH), 2.62 (t, 2H, $J = 6.4$ Hz, CH_2), 3.32-3.42 (m, 4H, CH_2 and $\text{CH}_2(\text{CO})$), 4.46-4.55 (m, 1H, CH). ^1H NMR: (DMSO- d_6) δ 7.77 (s, 1H, NH), 8.02-8.04 (d, 1H, $J = 8.0$ Hz, NH), 11.98, (br. s, 1H, OH). ^{13}C NMR: (DMSO- d_6) δ 22.38 (CH_2), 23.90 (CH_2), 28.48 (CH_2CHNH_2), 33.44 (CH_2), 38.05 (CH_2NH), 41.58 (CH_2CO), 49.77 ($\text{C}(\text{O})\text{CH}_2$), 50.35 (CH), 166.22 ($\text{C}(\text{O})\text{NH}$), 174.18 (COOH), 174.37 ($\text{HNC}(\text{O})\text{NH}$), 204.61 ($\text{C}(\text{O})\text{CH}_2$). IR ν (cm^{-1}) 1555, 1648, 1715, 2543, 2950, 3077. 3279. HR-ESI-MS: m/z 271.1318 [$\text{M} + \text{H}$] $^+$, 293.1140 [$\text{M} + \text{Na}$] $^+$, $\text{C}_{12}\text{H}_{18}\text{N}_2\text{O}_5$ requires 270.1216 and [$\text{C}_{12}\text{H}_{18}\text{N}_2\text{O}_5\text{Na}$] $^+$ requires 293.1113.

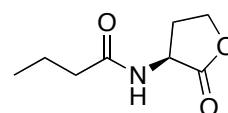
L-HOMOSERINE LACTONE HYDROCHLORIDE

L-homoserine (1 g, 8.4 mmol) was heated under reflux in 3 M HCl (50 mL) overnight. The mixture was concentrated under reduced pressure and then stirred in $(\text{CH}_3)_2\text{CO}$ for 4 h until a white precipitate formed. The precipitate was collected by vacuum filtration, washed with cold $(\text{CH}_3)_2\text{CO}$ and then air-dried to furnish the title compound as white crystals (1.0826 g, 94%). ^1H NMR: δ 2.23-2.34 (m, 1H, CH), 2.52-2.59 (m, 1H, CH), 4.24-4.32 (m, 2H, CH_2), 4.42-4.47 (dt, $J = 1.0$ Hz, 9.0 Hz, 1H, CH), 8.67 (s, 2H, NH_2). ^{13}C NMR: δ 28.43 (CH_2), 59.07 (CH), 67.38 (OCH_2), 174.04 (CO). IR ν (cm^{-1}) 940, 1013, 1073, 1157, 1216, 1505, 1591, 1780, 2524, 2633, 2983. HR-ESI-MS: m/z 85.0824, 126.0976 [$\text{M} + \text{H} + \text{Na}$], $\text{C}_4\text{H}_8\text{ClNO}_2$ requires 137.0244 and $\text{C}_4\text{H}_9\text{NO}_2\text{Na}^+$ requires 126.0531. Mp: 236-238 $^\circ\text{C}$.



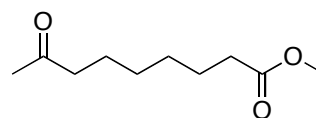
N-((S)-TETRAHYDRO-2-OXOFURAN-3-YL)-BUTANAMIDE

L-Homoserine lactone hydrochloride (138.5 mg, 1 mmol) was added to stirred butyryl chloride (103 μL , 0.9 mmol) in anhydrous CH_2Cl_2 (2 mL) under N_2 . Et_3N (279 μL , 3.7 mmol) was added in one addition and the reaction was left to stir at rt for 16 h until reaction was complete (TLC, EtOAc). The solvent was rotary evaporated. (The product was dissolved in EtOAc and was extracted consecutively with 1 M KHSO_4 , saturated NaHCO_3 , and brine, then dried over MgSO_4 . This resulted in loss of product due to water solubility). The residue was purified by crystallisation in PE (40-60 $^\circ\text{C}$) and EtOAc. The title compound was obtained as white crystals (97.80 mg, 57%) that were dried under vacuum. ^1H NMR: δ 0.94-0.98 (t, $J = 7.4$ Hz, 3H, CH_3), 1.60-1.73 (sextet, $J = 7.4$ Hz, 2H, CH_2), 2.21-2.25 (t d, $J = 1.6, 7.6$ Hz, 2H, CH_2), 2.81-2.88 (m, 1H, CH), 4.25-4.31 (m, 1H, CH), 4.40-4.49 (t d, $J = 1.2, 9.2$ Hz, 1H, CH), 4.53-4.60 (m, 1H, CH), 6.10 (br. s, 1H, NH). ^{13}C NMR: δ 13.81 (CH_3), 19.01 (CH_2), 30.75 (CH_2), 38.17 (CH_2), 49.36 (CH), 66.25 (CH_2), 173.75 (CO), 175.73 (CO). Mp 124.5 - 126 $^\circ\text{C}$. Lit Mp: 120-123 $^\circ\text{C}$ (249).



METHYL 8-OXONONANOATE (41)

Oxalyl chloride (1.1 mL, 13 mmol) was added to a stirred solution of suberic acid *mono* methyl ester (**40**, 1.1 mL, 6.3 mmol) in anhydrous CH₂Cl₂ (10 mL) under N₂ followed by the addition of catalytic anhydrous DMF (1 drop) and left to stir until completion (TLC, CH₂Cl₂). The solvent was rotary evaporated and left under N₂ and used without further purification.



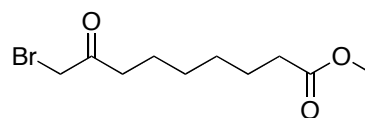
In an oven-dried 2-necked RBF, MeLi (1.6 M in hexane, 7 mL, 246.4 mg, 11.2 mmol) was added to a stirred solution of CuI (1.1 g, 5.6 mmol) in anhydrous Et₂O (40 mL) under N₂ at -78 °C. The solution was stirred until colourless for 30 min. (Yellow residue indicated CuMeLi had formed, which is inert and the reaction did not proceed). The acyl chloride was dissolved in minimum anhydrous THF under N₂ and transferred with washings to the reaction over 5 min via a cannula (final reaction volume 50 mL). The reaction was left to stir for a further 10 min (TLC, CH₂Cl₂) and then quenched with MeOH. After the reaction was allowed to reach 10 °C, saturated NH₄Cl was added and extracted with EtOAc three times. The organic washings were combined, washed twice with brine, and dried over MgSO₄. Once filtered, the filtrate was concentrated by rotary evaporated and the crude product was further purified by Kugelrohr distillation (112.5-125 °C). The title compound was isolated as a clear oil (1.14 g, 75%). (It is recommended to use 2 equivalents of Gilman's reagent). ¹H NMR: δ 1.26-1.34 (m, 4H, CH₂CH₂), 1.54-1.63 (m, 4H, CH₂CO), 2.12 (s, 3H, CH₃), 2.29 (t, *J* = 7.5 Hz, 2H, CH₂), 2.41 (t, *J* = 7.4 Hz, 2H, CH₂), 3.65 (s, 3H, CH₃). ¹³C NMR: δ 23.70 (CH₂), 24.86 (CH₂), 28.89 (CH₂), 29.00 (CH₂), 34.10 (CH₂CO), 43.75 (CH₂COO), 51.59 (COOCH₃), 174.30 (COOCH₃), 209.26 (CO). IR ν (cm⁻¹) 756, 1215, 1729, 2858, 2935, 3019. R_f (EtOAc): 0.81.

GENERAL PROCEDURE FOR α-BROMOKETONE

Bromine (256 μL, 4.6 mmol) was added drop-wise to a stirred solution of the appropriate ketone (851.6 mg, 4.6 mmol) in MeOH (8 mL) at -10 °C. The mixture was warmed to 0 °C and stirred for 1 hr and allowed to warm to rt and stirred for 1 hr. The mixture was cooled to 0 °C and dH₂O (1.4 mL) followed by conc. H₂SO₄ (2.5 mL) were added. The mixture was stirred for 16 h at rt until the reaction was complete (TLC, EtOAc). The solvent was rotary evaporated, dissolved in EtOAc and washed twice with dH₂O, brine and dried over MgSO₄. The solvent was rotary evaporated and dried under vacuum. The product was used without further purification.

Methyl-9-bromo-8-oxononanoate (42)

Methyl-8-oxononanoate (**41**) was used to produce the title compound as a yellow-orange oil (1.20 g, 60%). ¹H NMR: δ 1.28-1.33 (m, 4H, (CH₂)₂), 1.54-1.61 (m, 4H, CH₂), 2.26 (t, *J* = 7.5 Hz, 2H, CH₂), 2.60 (t, *J* = 7.3 Hz, 2H, CH₂), 3.61 (s, 3H, CH₃), 3.84 (s,

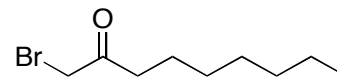


2H, CH₂).

1-bromononan-2-one (60)

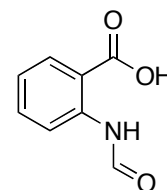
Nonan-2-one (854 μ L, 5 mmol) was used to produce the title

product as a yellow oil (671 mg, 61%). ¹H NMR: δ 0.78-0.81 (m, 3H, CH₃), 1.20-1.26 (m, 8H, (CH₂)₄), 1.49-1.56 (m, 2H, CH₂), 2.56 (t, J = 7.4 Hz, CH₂), 3.83 (s, 2H, CH₂Br). R_f (EtOAc) = 0.97.



N-FORMYL ANTHRANILIC ACID (44)

Anthranilic acid, (**43**, 219.5 mg, 1.6 mmol) was stirred in formic acid 98% (5ml) at rt for 3 days until precipitation formed, which was collected by vacuum filtration. The solid was washed with minimum formic acid 98% and crystallised from EtOAc/PE (40–60 °C) (7:3). The crude product was further



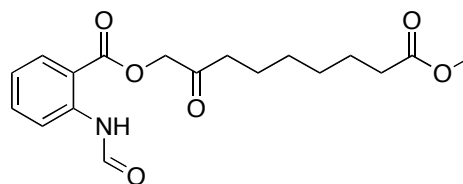
purified by re-crystallisation from EtOAc/PE (40–60 °C) (7:3) to afford the title compound as a white solid (154 mg, 52%). ¹H NMR ((CD₃)₂CO): δ 7.19 (t, J = 7.7 Hz, 1H, CH), 7.59-7.37 (t d, J = 1.6 Hz, 8.7 Hz, 1.6 Hz, 1H, CH), 8.10-8.13 (dd, J = 1.6 Hz, 8.0 Hz, 1H, CH), 8.59 (s, 1H, NHCHO), 8.72 (d, J = 8.4 Hz, 1H, CH), 11.08 (br. s, 1H, OH). ¹³C NMR (MeOD): δ 117.79 (CCOOH), 122.12 (CH), 124.44 (CH), 132.56 (CH), 135.14 (CH), 141.33 (CN), 162.08 (CCOOH), 170.85 (NHCHO). IR ν (cm⁻¹) 751, 1273, 1696, 2557, 2923, 3174. HR-ESI-MS: m/z 164.0271 [M-H], C₈H₇NO₃ requires 165.0426 and C₈H₆NO₃⁻ requires 164.0348. R_f (EtOAc/PE (40-60°C), 7:3) = 0.41 (streak, ninhydrin negative). Mp 167-170 °C (*lit* mp 167 °C).

GENERAL PROCEDURE FOR 2-OXO-ALKYL-2-FORMYL-AMINOBENZOATES

N-formyl anthranilic acid (**44**, 628 mg, 3.8 mmol) was stirred with Et₃N (556 μ L, 4.03 mmol) and the appropriate α -bromoketone (631.4 mg, 2.4 mmol) in (CH₃)₂CO (8 mL) at rt for 16 h until the reaction was complete (TLC, EtOAc). The solvent was rotary evaporated and the crude compound was washed with water. Crystallisation attempts were not successful therefore, the product was used without further purification.

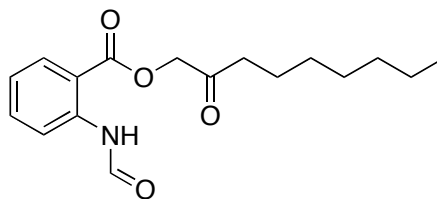
8-(methoxycarbonyl)-2-oxooctyl-2-formyl-aminobenzoate (45)

Methyl 9-bromo-8-oxononanoate (**42**) was used to produce the title compound as a brown oil.



2-oxononyl 2-formyl-aminobenzoate (62)

1-bromononan-2-one (**60**) was used to produce the title compound as a coloured oil.

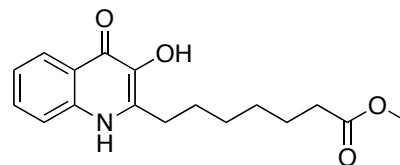
**GENERAL PROCEDURE FOR 2-ALKYL-3-HYDROXY-4(1H)-QUINOLONE**

The appropriate 2-oxo-alkyl-2-formyl-aminobenzoate (553.1 mg), ammonium formate (1 g, 15.9 mmol) was dissolved in excess formic acid 98% (23 mL, 0.61 M) and transferred to microwave vials. In batches, the mixture was subjected to microwave irradiation (300w, 150 psi) at 120 °C for 50 min until the starting material was consumed (TLC, EtOAc). To each vial, dH₂O was added and the mixtures were combined and extracted three times with EtOAc. The organic phase was washed with brine and dried over MgSO₄. The solvent was rotary evaporated and further purified by crystallization in EtOAc. (This reaction produces CO₂ (g) and NH₃ (g) which will produce equivalent pressure. The reaction is conducted in closed vials therefore batch preparation minimises pressure. It was noted that 10 equivalents of ammonium formate and 100 equivalents of formic acid were suitable to furnish the 2-alkyl-3-hydroxy-4(1H)-quinolone).

Methyl-7-(1,4-dihydro-3-hydroxy-4-oxoquinolin-2-yl)heptanoate (46)

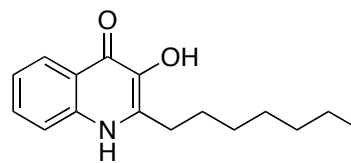
8-(methoxycarbonyl)-2-oxooctyl-2-formyl-aminobenzoate was used to furnish the title compound

and 7-(1,4-dihydro-3-hydroxy-4-oxoquinolin-2-yl)heptanoic acid (**47**) in a mixture (286.4 mg, 60%). HR-ESI-MS: *m/z* 290.1085 [C₁₆H₉NO₄ + H], 304.1353 [M + H], C₁₇H₂₁NO₄ requires 303.1471, and [C₁₇H₂₂NO₄]⁺ requires 304.1549.

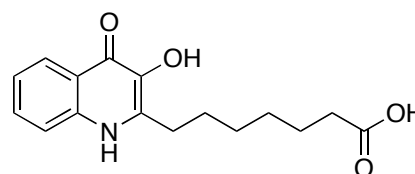
*2-heptyl-3-hydroxy-4(1H)-quinolone (4)*

2-oxononyl 2-formyl-aminobenzoate (**62**) was used to produce the title compound as a brown crystalline solid (85.8 mg, 46%). ¹H NMR: δ 0.85 (t, *J* = 6.5 Hz, 3H, CH₃), 1.04-1.32 (m, 8H, (CH₂)₄), 1.67 (t, 2H, CH₂), 2.73

(t, 2H, CH₂), 7.21 (t, *J* = 6.8 Hz, 1H, CH), 7.54 (s, 2H, (CH)₂), 8.08-8.10 (d, *J* = 8.0 Hz, 1H, CH), 11.45 (br. s, 1H, OH). HR-ESI-MS: *m/z* 260.0898 [M + H], 261.1211; 257.6011 [M - H], 258.6046, C₁₆H₂₁NO₂ requires 259.1572 and [C₁₆H₂₀NO₂]⁻ requires 258.1494.

**7-(1,4-DIHYDRO-3-HYDROXY-4-OXOQUINOLIN-2-YL)HEPTANOIC ACID (47)**

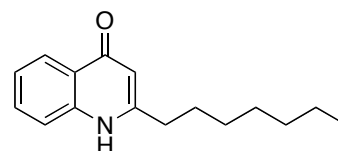
The crude mixture of methyl-7-(1,4-dihydro-3-hydroxy-4-oxoquinolin-2-yl)heptanoate (**46**) was



stirred in 12 M HCl in THF for 18 h and monitored by MS until the reaction was complete. The mixture was further purified by crystallisation from EtOAc to afford the title compound (**47**) as a purple solid film (71.6 mg, 73%). ^1H NMR (500 MHz, DMSO- d_6): δ 1.23-1.34 (m, 4H, CH_2CH_2), 1.47-1.55 (m, 2H, CH_2), 1.66 (m, 2H, CH_2), 2.19 (t, $J = 5.6$ Hz, 2H, CH_2), 2.73 (t, $J = 5.6$ Hz, 2H, CH_2), 7.21-7.23 (m 1H, CH), 7.53 (s 2H, CH), 8.08-8.09 (d, $J = 6.4$ Hz, 1H, CH), 11.44 (br. s, 1H, OH). ^{13}C NMR (500 MHz, DMSO- d_6): δ 28.82 (CH_2), 28.66 (CH_2), 28.76 (CH_2), 28.92 (CH_2), 29.02 (CH_2), 34.09 (CH_2), 118.23 (CH), 121.97 (CH), 122.64 (C:C), 124.94 (CH), 130.42 (CH), 135.95 (C:C), 137.81 (C:C), 173.81 (COOH), 174.95 (CO). HR-ESI-MS: $m/z = 288.1093$ [M - H], $\text{C}_{16}\text{H}_{19}\text{NO}_4$ requires 289.1314 and $[\text{C}_{16}\text{H}_{18}\text{NO}_4]^-$ requires 288.1236.

2-HEPTYL-QUINOLIN-4(1H)-ONE (**3**)

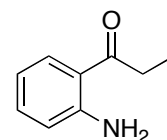
The crude mixture of (*E*)-ethyl 3-(phenylamino)dec-2-enoate (701.8 mg) and Ph_2O (15 mL) were stirred and divided into 5 mL batches. The mixture was microwave irradiated at 250 °C for 10 min. The batches were



combined and the solvent was removed using Genevac instrument. The crude product was washed PE (60-80 °C) and purified by silica column chromatography (eluent: EtOAc 100%). The residue was further purified by crystallization from EtOH to afford the title compound (103.30 mg, 21%) as beige solid. ^1H NMR: δ 0.80 (t, $J = 7.0$ Hz, 3H, CH_3), 1.16-1.26 (m, 8H, CH_2), 1.71 (t, $J = 6.6$ Hz, 2H, CH_2), 2.70 (t, $J = 6.8$ Hz, 2H, CH_2), 6.45 (s, 1H, CH), 7.32 (t, $J = 7.4$ Hz, 1H, CH), 7.58 (t, $J = 7.4$ Hz, 1H, CH), 7.82 (d, $J = 6.8$ Hz, 1H, CH), 8.35, (d, $J = 8.0$ Hz, 1H, CH), 12.71 (br. s, 1H, NH). ^{13}C NMR: δ 14.15 (CH_3), 22.69 (CH_2), 29.10 (CH_2), 29.30 (CH_2), 29.32 (CH_2), 31.77 (CH_2), 34.48 (CH_2), 108.15 (CH), 118.87 (CH), 123.66 (CH), 125.07 (CH), 125.24 (CC), 131.85 (CH), 140.91 (C:C), 155.74 (C:C), 179.02 (CO). HR-ESI-MS: m/z 244.1476[M + H]; 241.8555 [M - H], 242.8600, $\text{C}_{16}\text{H}_{21}\text{NO}$ requires 243.1623, $[\text{C}_{16}\text{H}_{21}\text{NO}]^-$ requires 242.1545 and $[\text{C}_{16}\text{H}_{22}\text{NO}]^+$ requires 244.1701.

1-(2-AMINOPHENYL)-PROPAN-1-ONE (**72**)

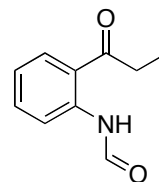
Magnesium turnings (365 mg, 15 mmol) were added under N_2 to an oven-dried RBF with I_2 (solid ball, 10 mg), this was stirred dry for 5 min. Anhydrous Et_2O (25 mL) followed by EtBr (15 mmol) was added and vigorously stirred and heated with a condenser under N_2 at 50 °C for 10 min. The solution was cooled and 2-aminobenzonitrile (**71**, 602.5 mg, 5 mmol) was added under N_2 at -78 °C. This was stirred, warming to rt, for 24 h (TLC, EtOAc). The reaction was quenched by 10% HCl and stirred for 30 min at rt to form a pale yellow solution. This was basified to pH 8 using 2 M NaOH and extracted with EtOAc three times. The combined organic layers were combined and washed with brine and dried over MgSO_4 . The solvent was rotary evaporated to leave the crude residue, which was further purified by silica gel column chromatography (EtOAc: PE,



(40-60°C) 1:9) to afford the title compound as a green solid (108.7 mg, 14%). ¹H NMR: δ 1.22 (t, J = 7.2 Hz, 3H, CH₃), 2.96-3.01 (q, J = 7.2 Hz, 2H, CH₂), 6.29 (br. s, 2H, NH₂), 6.63-6.67 (m, 1H, CH), 7.24-7.28 (m, 1H, CH), 7.45-7.77 (dd, J = 1.4, 8.6 Hz). ¹³C NMR: δ 8.84 (CH₃), 32.40 (CH₂), 115.82 (CH), 117.44 (CH), 117.96 (C:C), 131.15 (CH), 134.18 (CH), 150.37 (CN), 203.46 (CO).

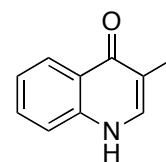
***N*-(2-PROPIONYLPHENYL)-FORMAMIDE (73)**

1-(2-Aminophenyl)-propan-1-one (**72**, 100 mg, 0.7 mmol) was heated in 98% formic acid at 50 °C until reaction was complete (TLC, EtOAc, ninhydrin negative). The mixture was cooled and dH₂O and extracted with EtOAc three times. The organic layers were combined, washed with dH₂O, followed by brine, and dried over MgSO₄. The solvent was rotary evaporated and dried under high vacuum to afford the title compound (98.2 mg, 83%). The compound was used without further purification. ¹H NMR: δ 1.21 (t, J = 7.2 Hz, 3H, CH₃), 3.04-3.09 (q, J = 7.2 Hz, 2H, CH₂), 7.15 (t, J = 7.6 Hz, 1H, CH), 7.54 (t, J = 7.8 Hz, 1H, CH), 7.93-7.95 (d, J = 8.0 Hz, 1H, CH), 8.48 (s, 1H, CH), 8.72-8.74 (d, J = 8.0 Hz, 1H, CH). ¹³C NMR: δ 8.85 (CH₃), 33.28 (CH₂), 121.82 (CH), 121.89 (CH), 123.17 (CCO), 130.74 (CH), 134.95 (CH), 139.85 (CN), 161.76 (NCO), 205.46 (CO).



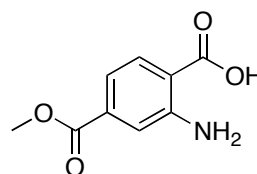
3-METHYLQUINOLIN-4(1H)-ONE (74)

N-(2-propionylphenyl)-formamide (**73**, 98.2 mg, 0.6 mmol) was dissolved in anhydrous 1,4 dioxane (1 mL) followed by NaOH (33 mg, 0.8 mmol). The solution was stirred and subjected to microwave irradiation at 120 °C for 50 min until reaction was complete (MS). Work-up was followed as suggested by the authors, however, the title compound is water soluble. The aq. phase was neutralised and dried by freeze-drying. The product was extracted from the residue with MeOH, the solvent was rotary evaporated and crystallized from EtOAc. The title compound was obtained as dark green solid (31.8 mg, 36%). ¹H NMR: δ 2.70 (s, 3H, CH₃), 7.50 (t, J = 6.8 Hz, 1H, CH), 7.70-7.90 (m, 2H, CH), 8.23 (s, 1H, C(CH₃):CH), 8.31 (d, J = 8.0 Hz, 1H, CH). ¹³C NMR (DMSO-d₆): δ 13.52 (CH₃), 116.47 (CCH₃), 118.01 (CH), 122.50 (CH), 124.10 (C:C), 124.94 (CH), 131.03 (CH), 136.72 (CH), 139.80 (C:C), 176.75 (CO). HR-ESI-MS: m/z 160.0567 [M + H], C₁₀H₉NO requires 159.0684, and [C₁₀H₁₀NO]⁺ requires 160.0762.



4-(METHOXYCARBONYL)-2-AMINO BENZOIC ACID (87)

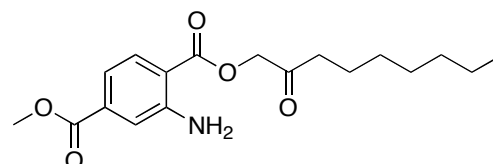
4-Aminobenzene-1,3-dicarboxylic acid (**85**, 1.1 g, 6.1 mmol), anhydrous MeOH (20 mL) and catalytic H₂SO₄ (1.1 mL) were heated under reflux under N₂ for 8 h. The solvent was rotary evaporated to half the volume and diluted with ice and dH₂O. The pH was adjusted to pH 9 by the addition of solid NaHCO₃ and extracted with CHCl₃. The aq. phase was acidified to pH 3-



4 using concentrated HCl and the precipitate was collected by vacuum filtration. Traces of HCl were removed by repeated washing with cold dH₂O to afford the title compound as a yellow solid (592 mg, 49%). ¹H NMR δ 3.88 (s, 3H, CH₃), 7.01-7.03 (dd, J = 1.3, 8.3 Hz, 1H, CH), 7.40 (s, 1H, CH), 7.75-7.80 (d, J = 8.3 Hz, 1H, CH). ¹³C NMR: δ 52.24 (CH₃), 114.31 (CH), 117.39 (CH), 131.66 (CH), 133.89 (C(O)), 151.23 (CN), 166.03 (CCOOCH₃), 169.09 (CCOOH). R_f (EtOAc: MeOH, 8.8:1.2) = 0.35.

4-METHYL-1-(2-OXONONYL)-2-AMINOBENZENE-1,4-DIOATE (88)

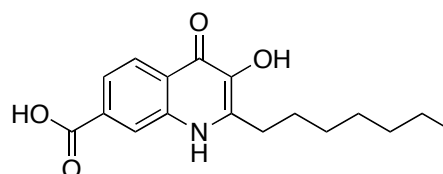
1-Bromononan-2-one (**60**, 544 mg, 2.5 mmol) and 4-(methoxycarbonyl)-2-aminobenzoic



acid (**87**, 483 mg, 2.5 mmol) were stirred with Et₃N (352 μ L, 255.6 mg, 2.5 mmol) in (CH₃)₂CO (30 mL) at rt for 16 h until the reaction was complete (TLC, EtOAc:MeOH, 9.8:0.2). The solvent was rotary evaporated and the crude compound was washed with water. Crystallisation attempts were not successful therefore, the title compound, a yellow solid (447.8 mg, 54%), was used without further purification.

2-HEPTYL-1,4-DIHYDRO-3-HYDROXY-4-OXOQUINOLINE-7-CARBOXYLIC ACID (90)

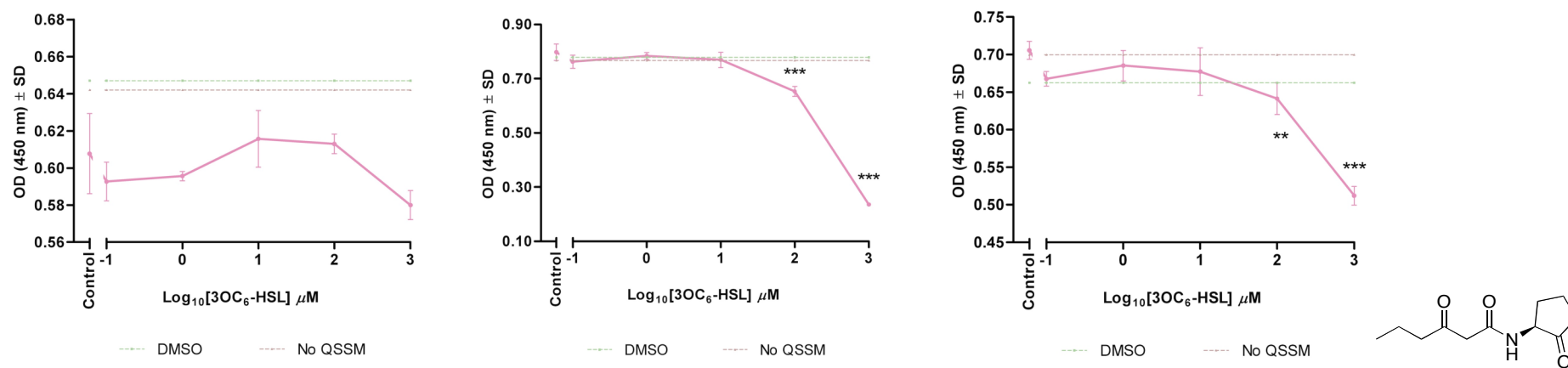
4-Methyl-1-(2-oxononyl)-2-aminobenzene-1,4-dioate (**88**, 31 mg, 0.1 mmol) were dissolved in NMP (1 mL) and subjected to microwave irradiation at 250°C for 10 min (300W, 250 psi).



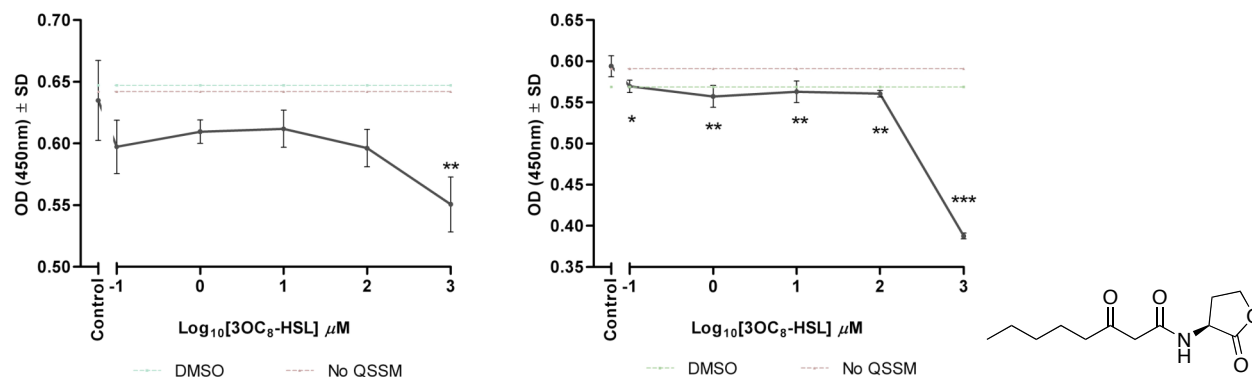
The solvent was removed using the Genevac instrument until dryness. The crude residue was purified crystallisation in EtOAc, the crystals were washed with cold (CH₃)₂CO to afford the title compound as a brown solid (12.4 mg, 44%). ¹H NMR: δ 0.83 (t, J = 6.6 Hz, CH₃), 1.15-1.40 (m, 8H, CH₂), 1.68 (m, 2H, CH₂), 2.76 (m, 2H, CH₂), 7.68-7.71 (d, J = 8.4 Hz, 1H, CH), 8.16-8.18 (d, J = 8.4 Hz, 1H, CH), 8.23 (s, 1H, CH), 11.72 (br. s, 1H, OH). IR ν (cm⁻¹) 1266, 1377, 1493, 1561, 1684, 2854, 2926, 2954, 3129, 3213, 3255, 3398. HR-ESI-MS: m/z 302.0946 [M - H]⁻, 303.0991, C₁₇H₂₁NO₄ requires 303.1471, and C₁₇H₂₀NO₄ requires 302.1392. R_f (EtOAc) = 0.22.

12 APPENDIX 1

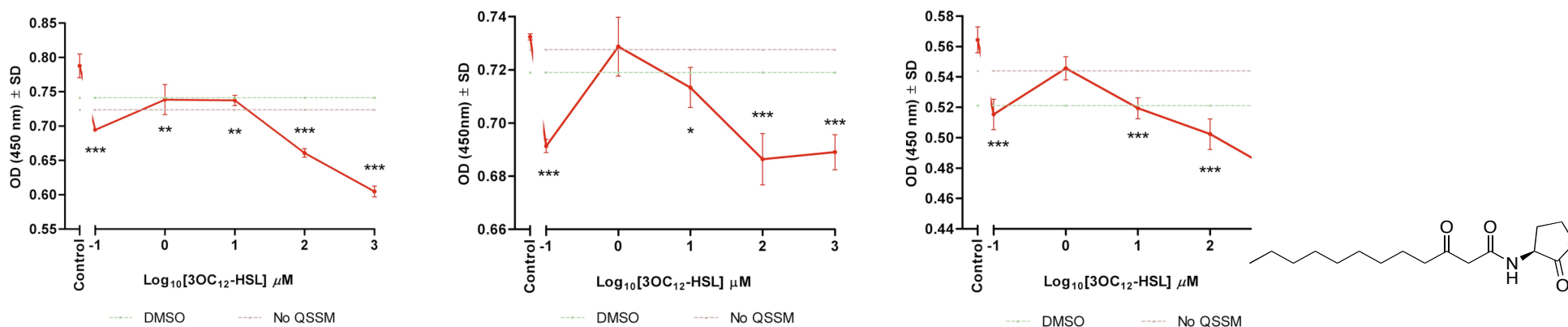
12.1.1 CROSS-REACTIVITY OF ANTI-AP1 ANTIBODIES

Figure 12-1: 3OC₆-HSL and anti-AP1 serum.

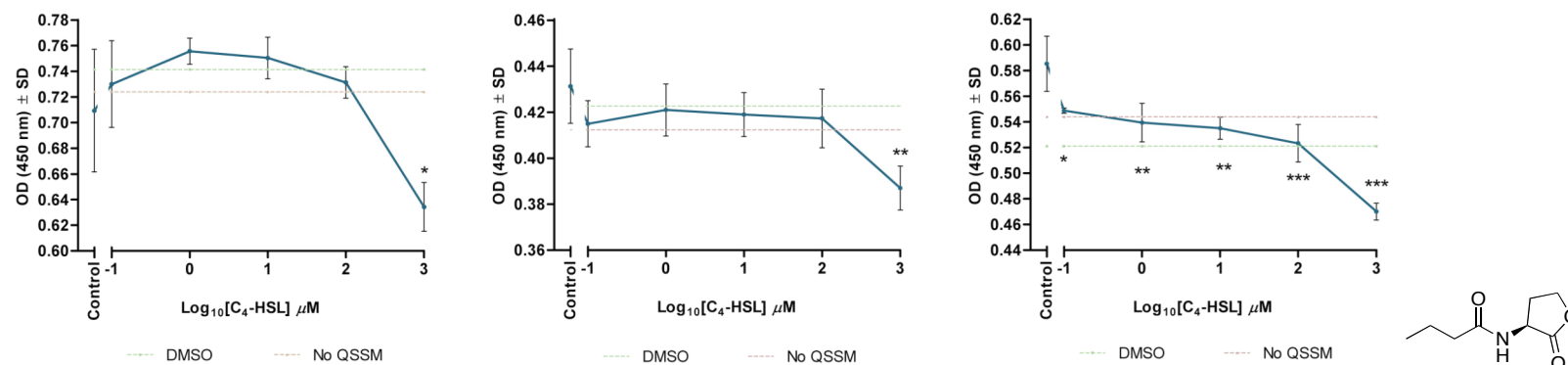
Competitive indirect ELISA using mouse anti-AP1 serum (○) and 3OC₆-HSL as the competitive ligand. (Data is represented as mean ± SD, n = 3).

Figure 12-2: 3OC₈-HSL and anti-API serum.

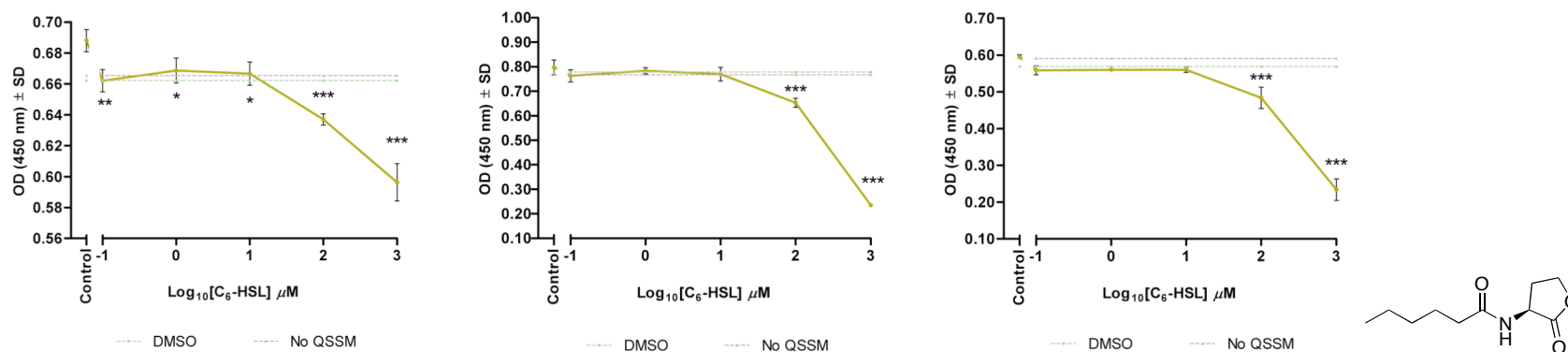
Competitive indirect ELISA using mouse anti-API serum (-) and 3OC₈-HSL used as the competitive ligand. (Data is represented as mean ± SD, n = 3).

Figure 12-3: 3OC₁₂-HSL and anti-API serum.

Competitive indirect ELISA using mouse anti-API serum (-) and 3OC₁₂-HSL as the competitive ligand. (Data is represented as mean ± SD, n = 3).

Figure 12-4: C₄-HSL and anti-API serum.

Competitive indirect ELISA using mouse anti-API serum (-) and C₄-HSL as the competitive ligand. (Data is represented as mean ± SD, n = 3).

Figure 12-5: C₆-HSL and anti-API serum.

Competitive indirect ELISA using mouse anti-API serum (-) and C₆-HSL as the competitive ligand. (Data is represented as mean ± SD, n = 3).

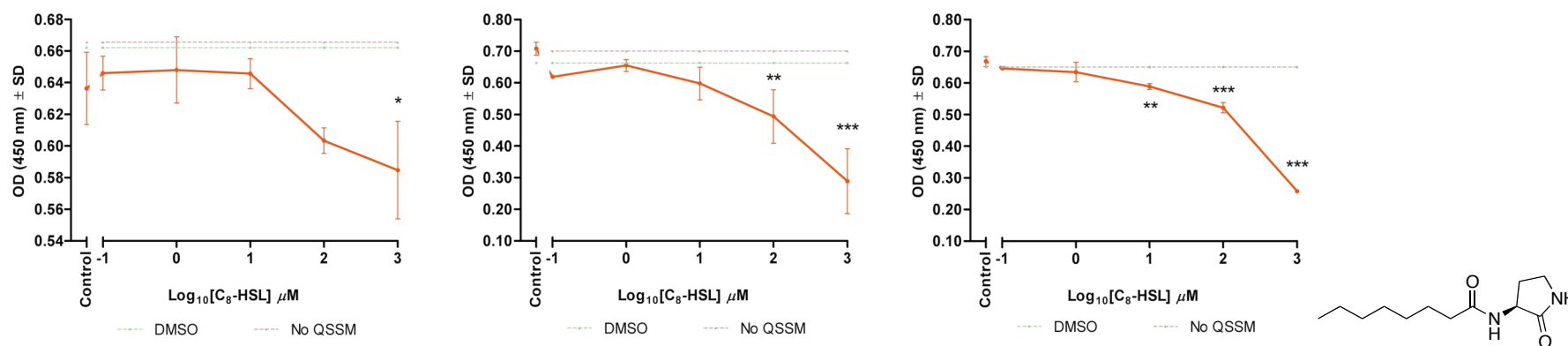


Figure 12-6: C₈-HSL and anti-API serum.

Competitive indirect ELISA using mouse anti-API serum (-) and C₈-HSL as the competitive ligand. (Data is represented as mean ± SD, n = 3).

Figure 12-1 shows significant inhibition of pAb binding to API-BSA at 100 μM and 1 mM [3OC₆-HSL] only. Although the same conditions were used, one assay failed to show a concentration-dependent inhibition. These data tentatively suggest that the anti-API pAbs can cross-react with 3OC₆-HSL. Natural QSSM, 3OC₈-HSL, the cognate of API, at 1 mM, significantly reduced the pAb binding to API-BSA, although there is an indication of a concentration-dependent reduction in pAb binding, it is only significant in one assay. This assay (Figure 12-2) was repeated three times, however, the third assay (not shown) showed significant inhibition of pAb binding to API-BSA by 2.5% [DMSO] v/v. The experiment could not be repeated due to time restrictions. The results tentatively suggest that mouse anti-API serum can cross-react with 3OC₈-HSL but an additional repeat is still required. Results shown in Figure 12-3 indicate that mouse anti-API serum cross-reacts with 3OC₁₂-HSL, with significant reduction in absorbance (450 nm) seen at 100 μM and 1 mM [3OC₁₂-HSL]. Following the significant ($p < 0.001$, ***) inhibition of pAb binding with API-BSA at 0.1 μM [3OC₁₂-HSL] the absorbance increases to near control levels with 1 μM [3OC₁₂-HSL]. The data shows a clear trend but does not show a typical concentration-dependent inhibition. The data in Figure 12-4, suggests that mouse anti-API serum shows some degree of cross-reactivity with C₄-HSL as significant inhibition of pAb binding to API-BSA occurred at

1 mM [C₄-HSL]. Collectively, the data suggests a decrease, although conservative, in mouse anti-**API** serum binding as concentration of [C₄-HSL] increases. In comparison, data shown in Figure 12-5, showed significant inhibition of pAb at 100 μ M and 1 mM [C₆-HSL]. The trend is similar to that seen with 3OC₆-HSL (Figure 12-1). Figure 12-6 shows a concentration-dependent inhibition of pAb by [C₈-HSL], which is significant at concentrations 100 μ M and 1 mM.

12.1.2 CROSS-REACTIVITY OF ANTI-AP2 ANTIBODIES

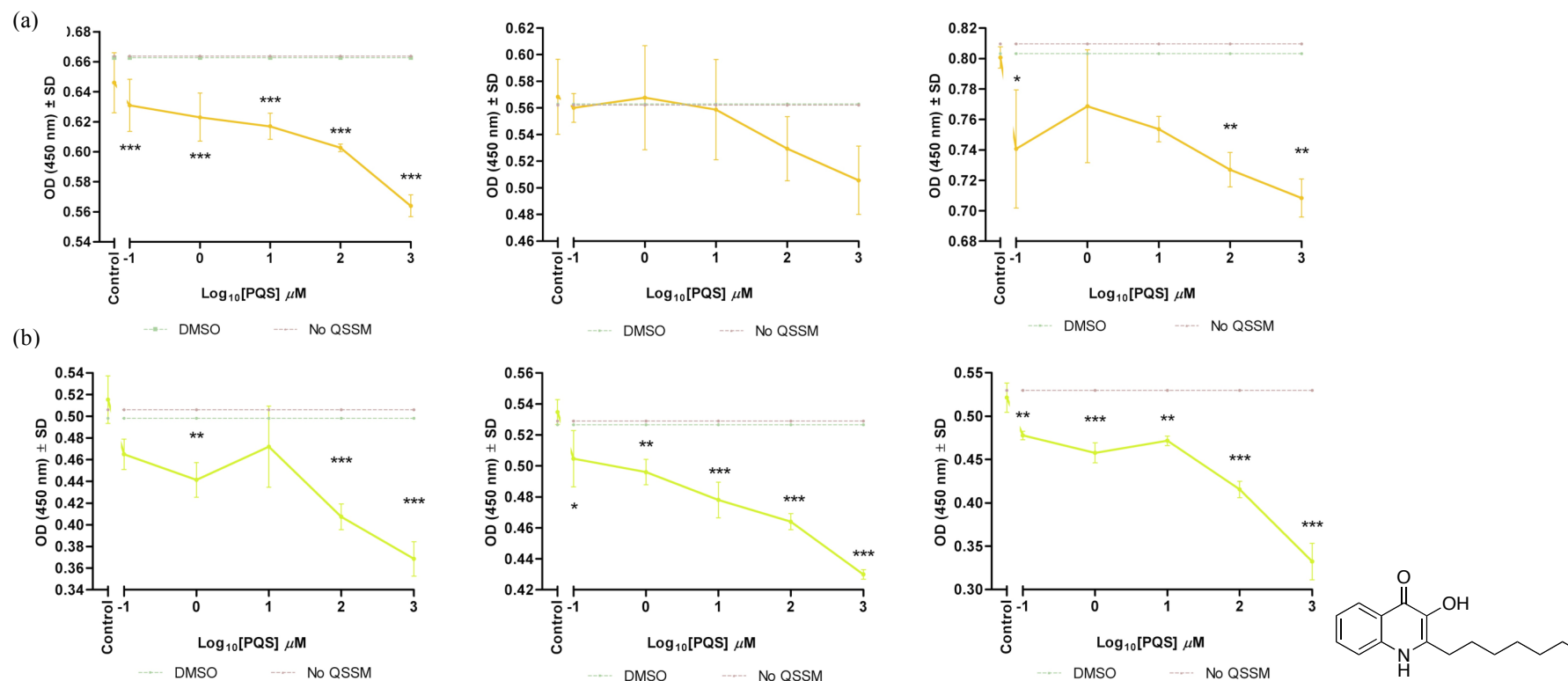


Figure 12-7: PQS and anti-AP2 sera.

(a) Competitive indirect ELISA using mouse anti-AP2 serum (●) and PQS as the competitive ligand. (Data is represented as mean \pm SD, $n = 3$); (b) Competitive indirect ELISA using rabbit anti-AP2 serum (●) and PQS as the competitive ligand. (Data is represented as mean \pm SD, $n = 3$).

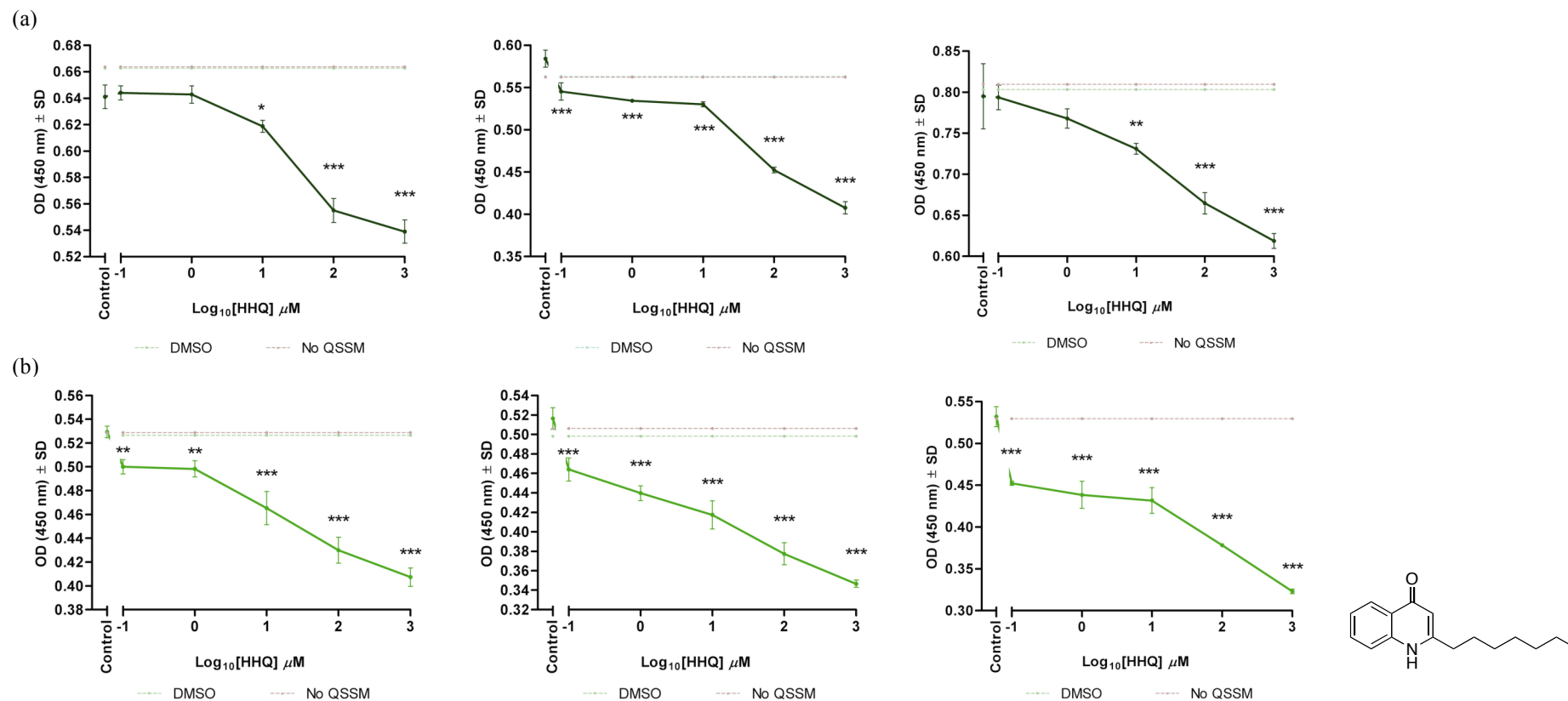


Figure 12-8: HHQ and anti-AP2 sera.

(a) Competitive indirect ELISA using mouse anti-AP2 serum (-) and HHQ as the competitive ligand. (Data is represented as mean \pm SD, n = 3); (b) Competitive indirect ELISA using rabbit anti-AP2 serum (-) HHQ as the competitive ligand. (Data is represented as mean \pm SD, n = 3).

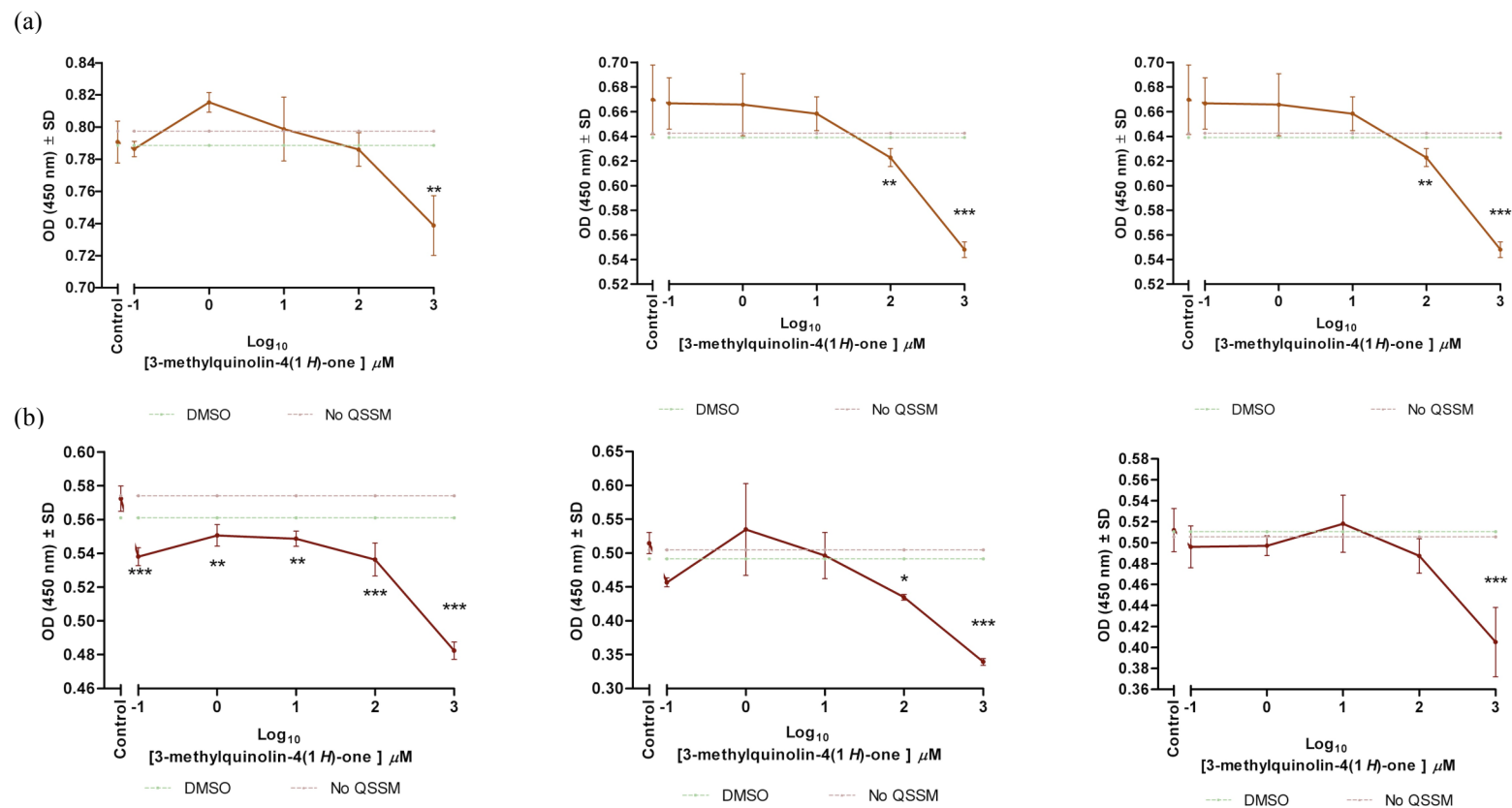


Figure 12-9: 3-Methyl-quinolin-4(1H)-one and anti-AP2 sera.

(a) Competitive indirect ELISA using mouse anti-AP2 serum (-) and 3-methylquinolin-4(1H)-one **74** as the competitive ligand (Data is represented as mean \pm SD, n = 3); (b) Competitive indirect ELISA using rabbit anti-AP2 serum (-) and **74** as the competitive ligand (Data is represented as mean \pm SD, n = 3).

Figure 12-7 shows a general concentration-dependent inhibition of mouse pAb binding by PQS however, only two experiments show significant inhibition at higher concentrations, 100 μ M and 1mM [PQS]. In contrast, data set b has a defined concentration-dependent inhibition of rabbit pAb by PQS with significant inhibition seen even by dilute concentrations of PQS. The anomalous increase in OD (450 nm), suggesting decreased inhibition at 1 μ M (Figure 12-7, (data set a) and 10 μ M (data set b), is reflective of the data seen with 3OC₁₂-HSL (Figure 12-3). PQS is the cognate of **AP2**, the data shows that anti-**AP2** pAb shows avidity for PQS. Figure 12-8 indicates a dependent-dependent inhibition of mouse/rabbit pAb by HHQ. Data strongly suggests that anti-**AP2** pAb cross-reacts with HHQ. Figure 12-6 shows that anti-**AP2** pAb shows cross-reactivity to 3-methyl-quinolin-4(1*H*)-one (**74**); reduction in pAb binding to **AP2**-BSA, albeit only significant at high concentrations, 1 mM [**74**].

13 REFERENCES

1. Bjarnsholt, T., and M. Givskov. 2007. The role of quorum sensing in the pathogenicity of the cunning aggressor *Pseudomonas aeruginosa*. *Analytical and Bioanalytical Chemistry* 387 (2):409-414.
2. Kramer, A., I. Schwebke, and G. Kampf. 2006. How long do nosocomial pathogens persist on inanimate surfaces? A systematic review. *BMC Infectious Diseases* 6 (130).
3. de Kievit, T. R., and B. H. Iglewski. 2000. Bacterial quorum sensing in pathogenic relationships. *Infection and Immunity* 68:4839-4849.
4. Mesaros, N., P. Nordmann, P. Plesiat, M. Roussel-Delvallez, J. Van Eldere, Y. Glupczynski, Y. Van Laethem, F. Jacobs, P. Lebecque, A. Malfroot, P. M. Tulkens, and F. Van Bambeke. 2007. *Pseudomonas aeruginosa*: resistance and therapeutic options at the turn of the new millennium. *Clinical Microbiology and Infection* 13 (6):560-578.
5. van Delden, C. 2004. Virulence factors in *Pseudomonas aeruginosa*. In *Pseudomonas*. J.-L. Ramos, ed. Kluwer Academic/Plenum Publishers, New York. 3-45.
6. Kipnis, E., T. Sawa, and J. Wiener-Kronish. 2006. Targeting mechanisms of *Pseudomonas aeruginosa* pathogenesis. *Medecine et Maladies Infectieuses* 36 (2):78-91.
7. Lyczak, J. B., C. L. Cannon, and G. B. Pier. 2000. Establishment of *Pseudomonas aeruginosa* infection: lessons from a versatile opportunist. *Microbes and Infection* 2 (9):1051-1060.
8. Kindt, T. J., R. A. Goldsby, and B. A. Osborne. 2007. *Kuby Immunology*. W. H. Freeman and Company, New York.
9. Schaber, J. A., W. J. Triffo, S. J. Suh, J. W. Oliver, M. C. Hastert, J. A. Griswold, M. Auer, A. N. Hamood, and K. P. Rumbaugh. 2007. *Pseudomonas aeruginosa* forms biofilms in acute infection independent of cell-to-cell signaling. *Infection and Immunity* 75 (8):3715-3721.
10. Cruvinel, W. d. M., D. Mesquita, Jr., J. A. P. Araujo, T. T. T. Catelan, A. W. S. de Souza, N. P. da Silva, and L. E. C. Andrade. 2010. Immune system - part I: Fundamentals of innate immunity with emphasis on molecular and cellular mechanisms of inflammatory response. *Revista Brasileira de Reumatologia* 50 (4):434-461.

-
11. Gomez, M. I., and A. Prince. 2007. Opportunistic infections in lung disease: *Pseudomonas* infections in cystic fibrosis. *Current Opinion in Pharmacology* 7 (3):244-251.
 12. Boucher, R. C. 2004. New concepts of the pathogenesis of cystic fibrosis lung disease. *European Respiratory Journal* 23:146-158.
 13. Hogardt, M., and J. Heesemann. 2010. Adaptation of *Pseudomonas aeruginosa* during persistence in the cystic fibrosis lung. *International Journal of Medical Microbiology* 300 (8):557-562.
 14. Fothergill, J. L., S. Panagea, C. A. Hart, M. J. Walshaw, T. L. Pitt, and C. Winstanley. 2007. Widespread pyocyanin over-production among isolates of a cystic fibrosis epidemic strain. *BMC Microbiology* 7:45.
 15. Tielen, P., M. Narten, N. Rosin, I. Biegler, I. Haddad, M. Hogardt, R. d. Neubauer, M. Schobert, L. Wiehlmann, and D. Jahn. 2011. Genotypic and phenotypic characterization of *Pseudomonas aeruginosa* isolates from urinary tract infections. *International Journal of Medical Microbiology* 301 (4):282-292.
 16. Rang, H. P., M. M. Dale, and J. M. Ritter. 2000. *Pharmacology*. Churchill Livingstone, Edinburgh.
 17. Döring, G. 2010. Prevention of *Pseudomonas aeruginosa* infection in cystic fibrosis patients. *International Journal of Medical Microbiology* 300 (8):573-577.
 18. Nordmann, P., T. Naas, N. Fortineau, and L. Poirel. 2007. Superbugs in the coming new decade: multidrug resistance and prospects for treatment of *Staphylococcus aureus*, *Enterococcus* spp. and *Pseudomonas aeruginosa* in 2010. *Current Opinion in Microbiology* 10 (5):436-440.
 19. Tenover, F. C. 2006. Mechanisms of antimicrobial resistance in bacteria. *The American Journal of Medicine* 119 (6):S3-S10.
 20. Strateva, T., and D. Yordanov. 2009. *Pseudomonas aeruginosa* - a phenomenon of bacterial resistance. *Journal of Medical Microbiology* 58 (9):1133-1148.
 21. Wroblewska, M. 2006. Novel therapies of multidrug-resistant *Pseudomonas aeruginosa* and *Acinetobacter* spp. infections: the state of the art. *Archivum Immunologiae et Therapiae Experimentalis* 54 (2):113-120.
 22. Gould, I. M. 2008. The epidemiology of antibiotic resistance. *International Journal of Antimicrobial Agents* 32:S2-S9.
-

-
23. Rossolini, G. M., and E. Mantengoli. 2005. Treatment and control of severe infections caused by multiresistant *Pseudomonas aeruginosa*. *Clinical Microbiology and Infection* 11:17-32.
 24. Breidenstein, E. B. M., C. de la Fuente-Nunez, and R. E. W. Hancock. 2011. *Pseudomonas aeruginosa*: all roads lead to resistance. *Trends in Microbiology* 19 (8):419-426.
 25. Stewart, P. S., and J. W. Costerton. 2001. Antibiotic resistance of bacteria in biofilms. *Lancet* 358 (9276):135-138.
 26. Stewart, P. S., and M. J. Franklin. 2008. Physiological heterogeneity in biofilms. *Nature Reviews Microbiology* 6 (3):199-210.
 27. Høiby, N., T. Bjarnsholt, M. Givskov, S. Molin, and O. Ciofu. 2010. Antibiotic resistance of bacterial biofilms. *International Journal of Antimicrobial Agents* 35 (4):322-332.
 28. Hassett, D. J., J. Cuppoletti, B. Trapnell, S. V. Lyman, J. J. Rowe, S. S. Yoon, G. M. Hilliard, K. Parvatiyar, M. C. Kamani, D. J. Wozniak, S. H. Hwang, T. R. McDermott, and U. A. Ochsner. 2002. Anaerobic metabolism and quorum sensing by *Pseudomonas aeruginosa* biofilms in chronically infected cystic fibrosis airways: rethinking antibiotic treatment strategies and drug targets. *Advanced Drug Delivery Reviews* 54:1425-1443.
 29. Anonymous. 2010. Antimicrobial resistance surveillance in Europe 2009. In *Annual Report of the European Antimicrobial Resistance Surveillance Network (EARS-Net)*. European Centre for Disease Prevention and Control, Stockholm.
 30. Anonymous. 2010-2011. Antibiotic Pipeline Surveillance - 2010 to mid 2011. Cardinal Health, Inc.
 31. Butler, M. S., and M. A. Cooper. 2011. Antibiotics in the clinical pipeline in 2011. *Journal of Antibiotics* 64 (6):413-425.
 32. Mesquita Junior, D., J. A. P. Araujo, T. T. T. Catelan, A. W. S. d. Souza, W. d. M. Cruvinel, L. E. C. Andrade, and N. P. d. Silva. 2010. Immune system - part II: Basis of the immunological response mediated by T- and B-lymphocytes. *Revista Brasileira de Reumatologia* 50 (5):552-580.
 33. Medzhitov, R. 2007. Recognition of microorganisms and activation of the immune response. *Nature* 449 (7164):819-826.
 34. Kaufmann, S. H. E. 2007. The contribution of immunology to the rational design of
-

- novel antibacterial vaccines. *Nature Reviews Microbiology* 5 (7):491-504.
35. Holder, I. A. 2004. *Pseudomonas* immunotherapy: a historical overview. *Vaccine* 22 (7):831-839.
36. Döring, G., and G. B. Pier. 2008. Vaccines and immunotherapy against *Pseudomonas aeruginosa*. *Vaccine* 26:1011-1024.
37. Johansen, H. K., and P. C. Gøtzsche. 2008. Vaccines for preventing infection with *Pseudomonas aeruginosa* in cystic fibrosis. *Cochrane Database of Systematic Reviews: Cochrane Cystic Fibrosis and Genetic Disorders Group* (4).
38. Fito-Boncompagni, L., A. Chapalain, E. Bouffartigue, H. Chaker, O. Lesouhaitier, G. Gicquel, A. Bazire, A. Madi, N. Connil, W. Veron, L. Taupin, B. Toussaint, P. Cornelis, Q. Wei, K. Shioya, E. Deziel, M. G. J. Feuilloy, N. Orange, A. Dufour, and S. Chevalier. 2011. Full virulence of *Pseudomonas aeruginosa* requires OprF. *Infection and Immunity* 79 (3):1176-1186.
39. Saha, S., F. Takeshita, S. Sasaki, T. Matsuda, T. Tanaka, M. Tozuka, K. Takase, T. Matsumoto, K. Okuda, N. Ishii, K. Yamaguchi, D. M. Klinman, K.-Q. Xin, and K. Okuda. 2006. Multivalent DNA vaccine protects mice against pulmonary infection caused by *Pseudomonas aeruginosa*. *Vaccine* 24 (37-39):6240-6249.
40. Lu, Q., J.-J. Rouby, P.-F. Laterre, P. Eggimann, A. Dugard, E. J. Giamarellos-Bourboulis, E. Mercier, J. Garbino, C.-E. Luyt, J. Chastre, V. Georgescu-Kyburz, M. P. Rudolf, V. Gafner, H. Lazar, H. Koch, A. Perez, S. D. Kraemer, and M. Tamm. 2011. Pharmacokinetics and safety of panobacumab: Specific adjunctive immunotherapy in critical patients with nosocomial *Pseudomonas aeruginosa* O11 pneumonia. *Journal of Antimicrobial Chemotherapy* 66 (5):1110-1116.
41. Berry, J. D., and R. G. Gaudet. 2010. Antibodies in infectious diseases: Polyclonals, monoclonals and niche biotechnology. *New Biotechnology* 28 (5):489-501.
42. Manafi, A., J. Kohanteb, D. Mehrabani, A. Japoni, M. Amini, M. Naghmachi, A. H. Zaghi, and N. Khalili. 2009. Active immunization using exotoxin A confers protection against *Pseudomonas aeruginosa* infection in a mouse burn model. *BMC Microbiology* 9 (23).
43. Sorichter, S., U. Baumann, A. Baumgart, S. Walterspacher, and B.-U. von Specht. 2009. Immune responses in the airways by nasal vaccination with systemic boosting against *Pseudomonas aeruginosa* in chronic lung diseased. *Vaccine* 27 (21):2755-2759.

-
44. Bumann, D., C. Behre, K. Behre, S. Herz, B. Gewecke, J. E. Gessner, B. U. von Specht, and U. Baumann. 2010. Systemic, nasal and oral live vaccines against *Pseudomonas aeruginosa*: A clinical trial of immunogenicity in lower airways of human volunteers. *Vaccine* 28 (3):707-713.
 45. Hackbarth, C., and R. S. Hodges. 2010. Synthetic peptide vaccine development: Designing dual epitopes into a single pilin peptide immunogen generates antibody cross-reactivity between two strains of *Pseudomonas aeruginosa*. *Chemical Biology & Drug Design* 76 (4):293-304.
 46. Kamei, A., Y. S. Coutinho-Sledge, J. B. Goldberg, G. P. Priebe, and G. B. Pier. 2011. Mucosal vaccination with a multivalent, live-attenuated vaccine induces multifactorial immunity against *Pseudomonas aeruginosa* acute lung infection. *Infection and Immunity* 79 (3):1289-1299.
 47. von Specht, B.-U., B. Knapp, K. D. Hungerer, C. Lucking, A. Schmitt, and H. Domdey. 1996. Outer membrane proteins of *Pseudomonas aeruginosa* as vaccine candidates. *Journal of Biotechnology* 44 (1-3):145-153.
 48. Baumann, U., E. Mansouri, and B.-U. von Specht. 2004. Recombinant OprF-OprI as a vaccine against *Pseudomonas aeruginosa* infections. *Vaccine* 22 (7):840-847.
 49. Weimer, E. T., H. Lu, N. D. Kock, D. J. Wozniak, and S. B. Mizel. 2009. A fusion protein vaccine containing OprF epitope 8, OprI, and type A and B flagellins promotes enhanced clearance of nonmucoid *Pseudomonas aeruginosa*. *Infection and Immunity* 77 (6):2356-2366.
 50. Campodonico, V. L., N. J. Llosa, T. M. Litran, M. Grout, and G. B. Pier. 2009. Comparative evaluation of *Pseudomonas aeruginosa* flagella or flagellin as a vaccine component. *Abstracts of the General Meeting of the American Society for Microbiology* 109.
 51. Holder, I. A., A. N. Neely, and D. W. Frank. 2001. PcrV immunization enhances survival of burned *Pseudomonas aeruginosa* infected mice. *Infection and Immunity* 69 (9):5908-5910.
 52. Pier, G. B. 1982. Safety and immunogenicity of high molecular-weight polysaccharide vaccine from immunotype-1 *Pseudomonas aeruginosa*. *Journal of Clinical Investigation* 69 (2):303-308.
 53. Thomas, L. D., A. W. Cripps, and J. M. Kyd. 2009. Immune response mechanisms against *Pseudomonas aeruginosa* associated with mucosal immunization with protein antigens in a rat model of acute lung infection. *Vaccine* 27 (25-26):3324-3330.
-

-
54. Krause, A., W. Z. Whu, Y. Xu, J. Joh, R. G. Crystal, and S. Worgall. 2011. Protective anti-*Pseudomonas aeruginosa* humoral and cellular mucosal immunity by AdC7-mediated expression of the *Pseudomonas aeruginosa* protein OprF. *Vaccine* 29 (11):2131-2139.
55. Cryz, S. J., E. Furer, and J. U. Que. 1991. Synthesis and characterization of a *Pseudomonas aeruginosa* alginate-toxin-A conjugate vaccine. *Infection and Immunity* 59 (1):45-50.
56. Theilacker, C., F. T. Coleman, S. Mueschenborn, N. Llosa, M. Grout, and G. B. Pier. 2003. Construction and characterization of a *Pseudomonas aeruginosa* mucoid exopolysaccharide-alginate conjugate vaccine. *Infection and Immunity* 71 (7):3875-3884.
57. Campodonico, V. L., N. J. Llosa, L. V. Bentancor, T. Maira-Litran, and G. B. Pier. 2011. Efficacy of a conjugate vaccine containing polymannuronic acid and flagellin against experimental *Pseudomonas aeruginosa* lung infection in mice. *Infection and Immunity* 79:3455-3464.
58. Zaidi, T. S., and G. B. Pier. 2005. Therapeutic efficacy of human monoclonal antibody (Mab) to *Pseudomonas aeruginosa* alginate in prevention and treatment of *Pseudomonas aeruginosa* eye infections. *Abstracts of the General Meeting of the American Society for Microbiology* 105:228.
59. Baer, M., T. Sawa, P. Flynn, K. Luehrsen, D. Martinez, J. P. Wiener-Kronish, G. Yarranton, and C. Bebbington. 2009. An engineered human antibody Fab fragment specific for *Pseudomonas aeruginosa* PcrV antigen has potent antibacterial activity. *Infection and Immunity* 77 (3):1083-1090.
60. Lai, Z. Z., R. Kimmel, S. Petersen, S. Thomas, G. Pier, B. Bezabeh, R. Luo, and J. R. Schreiber. 2005. Multi-valent human monoclonal antibody preparation against *Pseudomonas aeruginosa* derived from transgenic mice containing human immunoglobulin loci is protective against fatal *Pseudomonas* sepsis caused by multiple serotypes. *Vaccine* 23 (25):3264-3271.
61. Felts, A. G., G. Giridhar, D. W. Grainger, and J. B. Slunt. 1999. Efficacy of locally delivered polyclonal immunoglobulin against *Pseudomonas aeruginosa* infection in a murine burn wound model. *Burns* 25 (5):415-423.
62. Rumbaugh, K. P., S. P. Diggle, C. M. Watters, A. Ross-Gillespie, A. S. Griffin, and S. A. West. 2009. Quorum sensing and the social evolution of bacterial virulence. *Current Biology* 19 (4):341-345.
-

-
63. Foweraker, J. 2009. Recent advances in the microbiology of respiratory tract infection in cystic fibrosis. *British Medical Bulletin* 89 (1):93-110.
64. Asad, S., and S. M. Opal. 2008. Bench-to-bedside review: Quorum sensing and the role of cell-to-cell communication during invasive bacterial infection. *Critical Care* 12 (6):236.
65. Ryan, R. P., and J. M. Dow. 2008. Diffusible signals and interspecies communication in bacteria. *Microbiology* 154 (7):1845-1858.
66. Pesci, E. C., J. B. J. Milbank, J. P. Pearson, S. McKnight, A. S. Kende, E. P. Greenberg, and B. H. Iglewski. 1999. Quinolone signaling in the cell-to-cell communication system of *Pseudomonas aeruginosa*. *Proceedings of the National Academy of Sciences of the United States of America* 96 (20):11229-11234.
67. Calfee, M. W., and E. C. Pesci. 2003. Interaction of quorum sensing systems in *Pseudomonas aeruginosa*. *Abstracts of the General Meeting of the American Society for Microbiology* 103:B-153.
68. Diggle, S. P., P. Lumjiaktase, F. Dipilato, K. Winzer, M. Kunakorn, D. A. Barrett, S. R. Chhabra, M. Cámara, and P. Williams. 2006. Functional genetic analysis reveals a 2-alkyl-4-quinolone signaling system in the human pathogen *Burkholderia pseudomallei* and related bacteria. *Chemistry & Biology* 13 (7):701-710.
69. Vial, L., F. Lepine, S. Milot, M.-C. Groleau, V. Dekimpe, D. E. Woods, and E. Deziel. 2008. *Burkholderia pseudomallei*, *B. thailandensis*, and *B. ambifaria* produce 4-hydroxy-2-alkylquinoline analogues with a methyl group at the 3-position that is required for quorum-sensing regulation. *Journal of Bacteriology* 190 (15):5339-5352.
70. Dubern, J.-F., and S. P. Diggle. 2008. Quorum sensing by 2-alkyl-4-quinolones in *Pseudomonas aeruginosa* and other bacterial species. *Molecular Biosystems* 4 (9):882-888.
71. Miller, M. B., and B. L. Bassler. 2001. Quorum sensing in bacteria. *Annual Review of Microbiology* 55:165-199.
72. Williams, P. 2007. Quorum sensing, communication and cross-kingdom signalling in the bacterial world. *Microbiology* 153:3923-3938.
73. Boyer, M., and F. Wisniewski-Dye. 2009. Cell-cell signalling in bacteria: not simply a matter of quorum. *FEMS Microbiology Ecology* 70 (1):1-19.
74. Dekimpe, V., and E. Deziel. 2009. Revisiting the quorum-sensing hierarchy in *Pseudomonas aeruginosa*: the transcriptional regulator RhIR regulates LasR-specific
-

- factors. *Microbiology* 155:712-723.
75. Fletcher, M. P., S. Heeb, S. R. Chhabra, S. P. Diggle, P. Williams, and M. Cámara. 2010. *2-Alkyl-4(1H)-quinolone signalling in Pseudomonas aeruginosa*. Springer Science, Netherlands.
 76. Gooderham, W. J., and R. E. W. Hancock. 2009. Regulation of virulence and antibiotic resistance by two-component regulatory systems in *Pseudomonas aeruginosa*. *FEMS Microbiology Reviews* 33 (2):279-294.
 77. Schuster, M., and E. P. Greenberg. 2006. A network of networks: Quorum-sensing gene regulation in *Pseudomonas aeruginosa*. *International Journal of Medical Microbiology* 296 (2-3):73-81.
 78. Veselova, M. A. 2010. Quorum sensing regulation in *Pseudomonas*. *Russian Journal of Genetics* 46 (2):129-137.
 79. Williams, P., and M. Cámara. 2009. Quorum sensing and environmental adaptation in *Pseudomonas aeruginosa*: a tale of regulatory networks and multifunctional signal molecules. *Current Opinion in Microbiology* 12 (2):182-191.
 80. Farrow, J. M., Z. M. Sund, M. L. Ellison, D. S. Wade, J. P. Coleman, and E. C. Pesci. 2008. PqsE functions independently of PqsR-*Pseudomonas* quinolone signal and enhances the *rhl* quorum sensing system. *Journal of Bacteriology* 190 (21):7043-7051.
 81. Wagner, V. E., D. Bushnell, L. Passador, A. I. Brooks, and B. H. Iglewski. 2003. Microarray analysis of *Pseudomonas aeruginosa* quorum sensing regulons: Effects of growth phase and environment. *Journal of Bacteriology* 185 (7):2080-2095.
 82. Schuster, M., C. P. Lostroh, T. Ogi, and E. P. Greenberg. 2003. Identification, timing, and signal specificity of *Pseudomonas aeruginosa* quorum-controlled genes: a transcriptome analysis. *Journal of Bacteriology* 185 (7):2066-2079.
 83. Rumbaugh, K. P., J. A. Griswold, and A. N. Hamood. 2000. The role of quorum sensing in the *in vivo* virulence of *Pseudomonas aeruginosa*. *Microbes and Infection* 2 (14):1721-1731.
 84. Juhas, M., L. Eberl, and B. Tummler. 2005. Quorum sensing: the power of cooperation in the world of *Pseudomonas*. *Environmental Microbiology* 7 (4):459-471.
 85. Boontham, P., A. Robins, P. Chandran, D. Pritchard, M. Cámara, P. Williams, S. Chuthapisith, A. McKechnie, B. J. Rowlands, and O. Eremin. 2008. Significant

- immunomodulatory effects of *Pseudomonas aeruginosa* quorum sensing signal molecules: possible link in human sepsis. *Clinical Science* 115 343-351.
86. Jacobi, C. A., F. Schiffner, M. Henkel, M. Wailbel, B. Stork, M. Daubrawa, L. Eberl, M. Gregor, and S. Wesselborg. 2009. Effects of bacterial *N*-acyl homoserine lactones on human Jurkat T-lymphocytes-OdDHL induces apoptosis via the mitochondrial pathway. *International Journal of Medical Microbiology* 299 (7):509-519.
 87. Shiner, E. K., D. Terentyev, A. Bryan, S. Sennoune, R. Martinez-Zaguilan, G. Li, S. Gyorke, S. C. Williams, and K. P. Rumbaugh. 2006. *Pseudomonas aeruginosa* autoinducer modulates host cell responses through calcium signalling. *Cellular Microbiology* 8 (10):1601-1610.
 88. Li, H., L. Wang, L. Ye, Y. Mao, X. Xie, C. Xia, J. Chen, Z. Lu, and J. Song. 2009. Influence of *Pseudomonas aeruginosa* quorum sensing signal molecule *N*-(3-oxododecanoyl)-homoserine lactone on mast cells. *Medical Microbiology and Immunology* 198 (2):113-121.
 89. Tateda, K., Y. Ishii, M. Horikawa, M. Ishiguro, and K. Yamaguchi. 2003. The *Pseudomonas* autoinducer *N*-3-oxododecanoyl homoserine lactone accelerates apoptosis in macrophages and neutrophils. *Abstracts of the Interscience Conference on Antimicrobial Agents and Chemotherapy* 43:57.
 90. Kim, K., Y. U. Kim, B. H. Koh, S. S. Hwang, S.-H. Kim, F. Lepine, Y.-H. Cho, and G. R. Lee. 2010. HHQ and PQS, two *Pseudomonas aeruginosa* quorum sensing molecules, down-regulate the innate immune responses through the nuclear factor-kappa B pathway. *Immunology* 129 (4):578-588.
 91. Skindersoe, M. E., L. H. Zeuthen, S. Brix, L. N. Fink, J. Lazenby, C. Whittall, P. Williams, S. P. Diggle, H. Froekiaer, M. Cooley, and M. Givskov. 2009. *Pseudomonas aeruginosa* quorum-sensing signal molecules interfere with dendritic cell-induced T-cell proliferation. *FEMS Immunology and Medical Microbiology* 55 (3):335-345.
 92. Hooi, D. S. W. 2004. Differential immune modulatory activity of *Pseudomonas aeruginosa* quorum sensing signal molecules. *Infection and Immunity* 72 (11):6463-6470.
 93. Telford, G. 1998. The *Pseudomonas aeruginosa* quorum sensing signal molecule *N*-(3-oxododecanoyl)-L-homoserine lactone has immunomodulatory activity. *Infection and Immunity* 66 (1):36-42.
 94. Collier, D. N., L. Anderson, S. L. McKnight, T. L. Noah, M. Knowles, R. Boucher, U.

- Schwab, P. Gilligan, and E. C. Pesci. 2002. A bacterial cell to cell signal in the lungs of cystic fibrosis patients. *FEMS Microbiology Letters* 215 (1):41-46.
95. Wu, H., Z. J. Song, M. Givskov, and N. Høiby. 2004. Effects of quorum-sensing on immunoglobulin G responses in a rat model of chronic lung infection with *Pseudomonas aeruginosa*. *Microbes and Infection* 6 (1):34-37.
96. Qazi, S., B. Middleton, S. H. Muharram, A. Cockayne, P. Hill, P. O'Shea, S. R. Chhabra, M. Cámara, and P. Williams. 2006. *N*-acylhomoserine lactones antagonize virulence gene expression and quorum sensing in *Staphylococcus aureus*. *Infection and Immunity* 74 (2):910-919.
97. Kaufmann, G. F., R. Sartorio, S. H. Lee, C. J. Rogers, M. M. Meijler, J. A. Moss, B. Clapham, A. P. Brogan, T. J. Dickerson, and K. D. Janda. 2005. Revisiting quorum sensing: Discovery of additional chemical and biological functions for 3-oxo-*N*-acylhomoserine lactones. *Proceedings of the National Academy of Sciences of the United States of America* 102 (2):309-314.
98. Smith, R. S., E. R. Fedyk, T. A. Springer, N. Mukaida, B. H. Iglewski, and R. P. Phipps. 2001. IL-8 production in human lung fibroblasts and epithelial cells activated by the *Pseudomonas* autoinducer *N*-3-oxododecanoyl homoserine lactone is transcriptionally regulated by NF-kappa B and activator protein-2. *Journal of Immunology* 167 (1):366-374.
99. Smith, R. S., S. G. Harris, R. Phipps, and B. Iglewski. 2002. The *Pseudomonas aeruginosa* quorum-sensing molecule *N*-(3-oxododecanoyl)homoserine lactone contributes to virulence and induces inflammation *in vivo*. *Journal of Bacteriology* 184 (4):1132-1139.
100. Smith, R. S., R. Kelly, B. H. Iglewski, and R. P. Phipps. 2002. The *Pseudomonas* autoinducer *N*-(3-oxododecanoyl) homoserine lactone induces cyclooxygenase-2 and prostaglandin E-2 production in implications for inflammation. *Journal of Immunology* 169 (5):2636-2642.
101. Wagner, C., S. Zimmermann, G. Brenner-Weiss, F. Hug, B. Prior, U. Obst, and G. M. Hansch. 2007. The quorum-sensing molecule *N*-3-oxododecanoyl homoserine lactone (3OC12-HSL) enhances the host defence by activating human polymorphonuclear neutrophils (PMN). *Analytical and Bioanalytical Chemistry* 387 (2):481-487.
102. Jahoor, A., R. Patel, A. Bryan, C. Do, J. Krier, C. Walters, W. Wahli, G. Li, S. C. Williams, and K. P. Rumbaugh. 2008. Peroxisome proliferator-activated receptors mediate host cell proinflammatory responses to *Pseudomonas aeruginosa* autoinducer. *Journal of Bacteriology* 190 (13):4408-4415.

-
103. Ritchie, A. J., A. O. W. Yam, K. M. Tanabe, S. A. Rice, and M. A. Cooley. 2003. Modification of *in vivo* and *in vitro* T- and B-cell-mediated immune responses by the *Pseudomonas aeruginosa* quorum sensing molecule *N*-(3-oxododecanoyl)-L-homoserine lactone. *Infection and Immunity* 71 (8):4421-4431.
104. Diggle, S. P., S. Matthijs, V. J. Wright, M. P. Fletcher, S. R. Chhabra, I. L. Lamont, X. L. Kong, R. C. Hider, P. Cornelis, M. Cámara, and P. Williams. 2007. The *Pseudomonas aeruginosa* 4-quinolone signal molecules HHQ and PQS play multifunctional roles in quorum sensing and iron entrapment. *Chemistry & Biology* 14 (1):87-96.
105. Häussler, S., and T. Becker. 2008. The *Pseudomonas* quinolone signal (PQS) balances life and death in *Pseudomonas aeruginosa* populations. *PLoS Pathogens* 4 (9).
106. D'Argenio, D. A., M. W. Calfee, P. B. Rainey, and E. C. Pesci. 2002. Autolysis and autoaggregation in *Pseudomonas aeruginosa* colony morphology mutants. *Journal of Bacteriology* 184 (23):6481-6489.
107. Davies, D. G., M. R. Parsek, J. P. Pearson, B. H. Iglewski, J. W. Costerton, and E. P. Greenberg. 1998. The involvement of cell-to-cell signals in the development of a bacterial biofilm. *Science* 280 (5361):295-298.
108. Harmsen, M., L. Yang, S. J. Pamp, and T. Tolker-Nielsen. 2010. An update on *Pseudomonas aeruginosa* biofilm formation, tolerance, and dispersal. *FEMS Immunology and Medical Microbiology* 59:253-268.
109. de Kievit, T. R. 2009. Quorum sensing in *Pseudomonas aeruginosa* biofilms. *Environmental Microbiology* 11 (2):279-288.
110. Allesen-Holm, M., K. B. Barken, L. Yang, M. Klausen, J. S. Webb, S. Kjelleberg, S. Molin, M. Givskov, and T. Tolker-Nielsen. 2006. A characterization of DNA release in *Pseudomonas aeruginosa* cultures and biofilms. *Molecular Microbiology* 59 (4):1114-1128.
111. Diggle, S. P., P. Cornelis, P. Williams, and M. Cámara. 2006. 4-Quinolone signalling in *Pseudomonas aeruginosa*: Old molecules, new perspectives. *International Journal of Medical Microbiology* 296 (2-3):83-91.
112. Boles, B. R., M. Thoendel, and P. K. Singh. 2005. Rhamnolipids mediate detachment of *Pseudomonas aeruginosa* from biofilms. *Molecular Microbiology* 57 (5):1210-1223.
113. Jensen, P. O., T. Bjarnsholt, R. Phipps, T. B. Rasmussen, H. Calum, L. Christoffersen,
-

- C. Moser, P. Williams, T. Pressler, M. Givskov, and N. Høiby. 2007. Rapid necrotic killing of polymorphonuclear leukocytes is caused by quorum sensing-controlled production of rhamnolipid by *Pseudomonas aeruginosa*. *Microbiology* 153:1329-1338.
114. Wagner, V. E., and B. H. Iglewski. 2008. *Pseudomonas aeruginosa* biofilms in cystic fibrosis infection. *Clinical Reviews in Allergy & Immunology* 35 (3):124-134.
 115. Guina, T., S. O. Purvine, E. C. Yi, J. Eng, D. R. Goodlett, R. Aebersold, and S. I. Miller. 2003. Quantitative proteomic analysis indicates increased synthesis of a quinolone by *Pseudomonas aeruginosa* isolates from cystic fibrosis airways. *Proceedings of the National Academy of Sciences of the United States of America* 100 (5):2771-2776.
 116. Singh, P. K., A. L. Schaefer, M. R. Parsek, T. O. Moninger, M. J. Welsh, and E. P. Greenberg. 2000. Quorum sensing signals indicate that cystic fibrosis lungs are infected with bacterial biofilms. *Nature* 407 (6805):762-764.
 117. Bjarnsholt, T., P. O. Jensen, T. H. Jakobsen, R. Phipps, A. K. Nielsen, M. T. Rybtke, T. Tolker-Nielsen, M. Givskov, N. Høiby, and O. Ciofu. 2010. Quorum sensing and virulence of *Pseudomonas aeruginosa* during lung infection of cystic fibrosis patients. *PLoS ONE* 5 (4).
 118. Rumbaugh, K. P., J. A. Griswold, B. H. Iglewski, and A. H. Hamood. 1999. The role of quorum sensing in *Pseudomonas aeruginosa* infections of burn wounds. *Abstracts of the General Meeting of the American Society for Microbiology* 99:218.
 119. Willcox, M. D. P., H. Zhu, T. C. R. Conibear, E. B. H. Hume, M. Givskov, S. Kjelleberg, and S. A. Rice. 2008. Role of quorum sensing by *Pseudomonas aeruginosa* in microbial keratitis and cystic fibrosis. *Microbiology* 154:2184-2194.
 120. Mittal, R., S. Aggarwal, S. Sharma, S. Chhibber, and K. Harjai. 2009. Urinary tract infections caused by *Pseudomonas aeruginosa*: A minireview. *Journal of Infection and Public Health* 2 (3):101-111.
 121. Wu, H., Z. J. Song, M. Givskov, G. Döring, D. Worlitzsch, K. Mathee, J. Rygaard, and N. Høiby. 2001. *Pseudomonas aeruginosa* mutations in *lasI* and *rhII* quorum sensing systems result in milder chronic lung infection. *Microbiology* 147:1105-1113.
 122. Sio, C. F., L. G. Otten, R. H. Cool, S. P. Diggle, P. G. Braun, R. Bos, M. Daykin, M. Cámara, P. Williams, and W. J. Quax. 2006. Quorum quenching by an *N*-acyl-homoserine lactone acylase from *Pseudomonas aeruginosa* PAO1. *Infection and Immunity* 74 (3):1673-1682.

-
123. Papaioannou, E., M. Wahjudi, P. Nadal-Jimenez, G. Koch, R. Setroikromo, and W. J. Quax. 2009. Quorum-quenching acylase reduces the virulence of *Pseudomonas aeruginosa* in a *Caenorhabditis elegans* infection model. *Antimicrobial Agents and Chemotherapy* 53 (11):4891-4897.
124. Teiber, J. F., S. Horke, D. C. Haines, P. K. Chowdhary, J. Xiao, G. L. Kramer, R. W. Haley, and D. I. Draganov. 2008. Dominant role of paraoxonases in inactivation of the *Pseudomonas aeruginosa* quorum sensing signal *N*-(3-oxododecanoyl)-L-homoserine lactone. *Infection and Immunity* 76 (6):2512-2519.
125. Uroz, S., Y. Dessaux, and P. Oger. 2009. Quorum sensing and quorum quenching: The Yin and Yang of bacterial communication. *ChemBioChem* 10 (2):205-216.
126. Pustelny, C., A. Albers, K. Bueldt-Karentzopoulos, K. Parschat, S. R. Chhabra, M. Cámara, P. Williams, and S. Fetzner. 2009. Dioxygenase-mediated quenching of quinolone-dependent quorum sensing in *Pseudomonas aeruginosa*. *Chemistry & Biology* 16 (12):1259-1267.
127. Pan, J., and D. Ren. 2009. Quorum sensing inhibitors: a patent overview. *Expert Opinion on Therapeutic Patents* 19 (11):1581-1601.
128. Hentzer, M., H. Wu, J. B. Andersen, K. Riedel, T. B. Rasmussen, N. Bagge, N. Kumar, M. A. Schembri, Z. J. Song, P. Kristoffersen, M. Manefield, J. W. Costerton, S. Molin, L. Eberl, P. Steinberg, S. Kjelleberg, N. Høiby, and M. Givskov. 2003. Attenuation of *Pseudomonas aeruginosa* virulence by quorum sensing inhibitors. *EMBO Journal* 22 (15):3803-3815.
129. Khan, M. S. A., M. Zahin, S. Hasan, F. M. Husain, and I. Ahmad. 2009. Inhibition of quorum sensing regulated bacterial functions by plant essential oils with special reference to clove oil. *Letters in Applied Microbiology* 49 (3):354-360.
130. Girennavar, B., M. L. Cepeda, K. A. Soni, A. Vikram, P. Jesudhasan, G. K. Jayaprakasha, S. D. Pillai, and B. S. Patil. 2008. Grapefruit juice and its furocoumarins inhibits autoinducer signaling and biofilm formation in bacteria. *International Journal of Food Microbiology* 125 (2):204-208.
131. Truchado, P., F. Lopez-Galvez, M. I. Gil, F. A. Tomas-Barberan, and A. Allende. 2009. Quorum sensing inhibitory and antimicrobial activities of honeys and the relationship with individual phenolics. *Food Chemistry* 115 (4):1337-1344.
132. Bjarnsholt, T., P. O. Jensen, T. B. Rasmussen, L. Christophersen, H. Calum, M. Hentzer, H. P. Hougen, J. Rygaard, C. Moser, L. Eberl, N. Høiby, and K. Givskov. 2005. Garlic blocks quorum sensing and promotes rapid clearing of pulmonary
-

- Pseudomonas aeruginosa* infections. *Microbiology* 151:3873-3880.
133. Galloway, W. R. J. D., J. T. Hodgkinson, S. D. Bowden, M. Welch, and D. R. Spring. 2011. Quorum sensing in Gram-negative bacteria: Small molecule modulation of AHL and AI-2 quorum sensing pathways. *Chemical Reviews* 111 (1):28-67.
 134. Parsek, M. R., D. L. Val, B. L. Hanzelka, J. E. Cronan, and E. P. Greenberg. 1999. Acyl homoserine lactone quorum sensing signal generation. *Proceedings of the National Academy of Sciences of the United States of America* 96(8):4360-4365.
 135. Lesic, B., F. Lepine, E. Deziel, J. Zhang, Q. Zhang, K. Padfield, M.-H. Castonguay, S. Milot, S. Stachel, A. A. Tzika, R. G. Tompkins, and L. G. Rahme. 2007. Inhibitors of pathogen intercellular signals as selective anti-infective compounds. *PLoS Pathogens* 3 (9):1229-1239.
 136. Calfee, M. W., J. P. Coleman, and E. C. Pesci. 2001. Interference with *Pseudomonas* quinolone signal synthesis inhibits virulence factor expression by *Pseudomonas aeruginosa*. *Proceedings of the National Academy of Sciences of the United States of America* 98 (20):11633-11637.
 137. Pesci, E. C., and J. P. Coleman. 2004. Disruption of PQS synthesis using precursor analogs. World Intellectual Property Organization, WO 2004002976 A1.
 138. Farrow, J. M., III, and E. C. Pesci. 2007. Two distinct pathways supply anthranilate as a precursor of the *Pseudomonas* quinolone signal. *Journal of Bacteriology* 189 (9):3425-3433.
 139. Geske, G. D., J. C. O'Neill, and H. E. Blackwell. 2008. Expanding dialogues: from natural autoinducers to non-natural analogues that modulate quorum sensing in Gram-negative bacteria. *Chemical Society Reviews* 37 (7):1432-1447.
 140. Smith, K. M., Y. G. Bu, and H. Suga. 2003. Library screening for synthetic agonists and antagonists of a *Pseudomonas aeruginosa* autoinducer. *Chemistry & Biology* 10 (6):563-571.
 141. McInnis, C. E., and H. E. Blackwell. 2011. Design, synthesis, and biological evaluation of abiotic, non-lactone modulators of LuxR-type quorum sensing. *Bioorganic & Medicinal Chemistry* 19 (16):4812-4819.
 142. Ishida, T., T. Ikeda, N. Takiguchi, A. Kuroda, H. Ohtake, and J. Kato. 2007. Inhibition of quorum sensing in *Pseudomonas aeruginosa* by *N*-acyl cyclopentylamides. *Applied and Environmental Microbiology* 73 (10):3183-3188.
 143. Wang, W., T. Morohoshi, T. Ikeda, and L. Chen. 2008. Inhibition of Lux quorum

- sensing system by synthetic *N*-acyl-L-homoserine lactone analogous. *Acta Biochimica et Biophysica Sinica* 40 (12):1023-1028.
144. Liu, H.-B., J.-H. Lee, J. S. Kim, and S. Park. 2010. Inhibitors of the *Pseudomonas aeruginosa* quorum sensing regulator, QscR. *Biotechnology and Bioengineering* 106 (1):119-126.
145. Yang, L., M. T. Rybtker, T. H. Jakobsen, M. Hentzer, T. Bjarnsholt, M. Givskov, and T. Tolker-Nielsen. 2009. Computer-aided identification of recognized drugs as *Pseudomonas aeruginosa* quorum sensing inhibitors. *Antimicrobial Agents and Chemotherapy* 53 (6):2432-2443.
146. Tateda, K., Y. Ishii, S. Kimura, M. Horikawa, S. Miyairi, and K. Yamaguchi. 2007. Suppression of *Pseudomonas aeruginosa* quorum sensing systems by macrolides: A promising strategy or an oriental mystery? *Journal of Infection and Chemotherapy* 13 (6):357-367.
147. Skindersoe, M. E., M. Alhede, R. Phipps, L. Yang, P. O. Jensen, T. B. Rasmussen, T. Bjarnsholt, T. Tolker-Nielsen, N. Høiby, and M. Givskov. 2008. Effects of antibiotics on quorum sensing in *Pseudomonas aeruginosa*. *Antimicrobial Agents and Chemotherapy* 52 (10):3648-3663.
148. Kende, A. S., B. H. Iglewski, R. Smith, R. P. Phipps, and J. P. Pearson. 2004. Immunogenic conjugates of Gram-negative bacterial auto-inducer molecules and antibodies raised against the same. United States, US 2004/0156856.
149. Charlton, K. A., and A. J. R. Porter. 2004. Methods for the treatment of an infectious bacterial disease with an anti-lactone or lactone derived signal molecules antibody. World Intellectual Property Organization, WO 2004/014423 A1.
150. Charlton, K., A. Porter, L. Thornthwaite, K. A. Charlton, and A. J. R. Porter. 2006. Preventing biofilm formation by population of bacteria, e.g. *Bordetella pertussis* and *Pseudomonas aeruginosa*, involves administering antibody to lactone/lactone-derived signal molecule secreted by bacteria. World Property Intellectual Organization, WO2005111080 A2.
151. Charlton, K. A., A. J. R. Porter, and I. Broadbent. 2005. Autolysis method of Gram-negative bacteria, useful for treating pulmonary infection in e.g. cystic fibrosis, comprises administration of antibody to lactone or lactone-derived signal molecule secreted by Gram-negative bacteria. World Intellectual property Organization, WO 2005/094883 A2.
152. Miyairi, S., K. Tateda, E. Fuse, C. Ueda, H. Saito, T. Takabatake, Y. Ishii, M.

- Horikawa, M. Ishiguro, T. Standiford, and K. Yamaguchi. 2006. Immunization with 3-oxododecanoyl-L-homoserine lactone-protein conjugate protects mice from lethal *Pseudomonas aeruginosa* lung infection. *Journal of Medical Microbiology* 55 (10):1381-1387.
153. Kaufmann, G. F., R. Sartorio, S. H. Lee, J. M. Mee, L. J. Altobelli, D. P. Kujawa, E. Jeffries, B. Clapham, M. M. Meijler, and K. D. Janda. 2006. Antibody interference with *N*-acyl homoserine lactone-mediated bacterial quorum sensing. *Journal of the American Chemical Society* 128 (9):2802-2803.
154. Kaufmann, G. F., J. Park, J. M. Mee, R. J. Ulevitch, and K. D. Janda. 2008. The quorum quenching antibody RS2-1G9 protects macrophages from the cytotoxic effects of the *Pseudomonas aeruginosa* quorum sensing signalling molecule *N*-3-oxo-dodecanoyl-homoserine lactone. *Molecular Immunology* 45 (9):2710-2714.
155. De Lamo Marin, S., Y. Xu, M. M. Meijler, and K. D. Janda. 2007. Antibody catalyzed hydrolysis of a quorum sensing signal found in Gram-negative bacteria. *Bioorganic & Medicinal Chemistry Letters* 17 (6):1549-1552.
156. Kapadnis, P. B., E. Hall, M. Ramstedt, W. R. J. D. Galloway, M. Welch, and D. R. Spring. 2009. Towards quorum-quenching catalytic antibodies. *Chemical Communications* (5):538-540.
157. Lemus, R., and M. H. Karol. 2008. Conjugation of haptens. In *Methods in Molecular Medicine*. M. G. Jones, and P. Lympny, eds. Humana press Inc. 167-182.
158. Hermanson, G. T. 2008. *Bioconjugate Techniques*. Elsevier Academic Print, United Kingdom.
159. Landsteiner, K. 1962. *The specificity of serological reactions*. Dover Publications, Inc., New York.
160. Shreder, K. 2000. Synthetic haptens as probes of antibody response and immunorecognition. *Methods-A Companion to Methods in Enzymology* 20 (3):372-379.
161. Yates, E. A., B. Philipp, C. Buckley, S. Atkinson, S. R. Chhabra, R. E. Sockett, M. Goldner, Y. Dessaux, M. Cámara, H. Smith, and P. Williams. 2002. *N*-acylhomoserine lactones undergo lactonolysis in a pH-, temperature-, and acyl chain length-dependent manner during growth of *Yersinia pseudotuberculosis* and *Pseudomonas aeruginosa*. *Infection and Immunity* 70 (10):5635-5646.
162. Marco, M. P., S. Gee, and B. D. Hammock. 1995. Immunochemical techniques for

- environmental analysis 2: Antibody production and immunoassay development. *TrAC Trends in Analytical Chemistry* 14 (8):415-425.
163. Diggle, S. P., K. Winzer, S. R. Chhabra, K. E. Worrall, M. Cámara, and P. Williams. 2003. The *Pseudomonas aeruginosa* quinolone signal molecule overcomes the cell density-dependency of the quorum sensing hierarchy, regulates *rhl*-dependent genes at the onset of stationary phase and can be produced in the absence of LasR. *Molecular Microbiology* 50 (1):29-43.
164. Duan, K., and M. G. Surette. 2007. Environmental regulation of *Pseudomonas aeruginosa* PAO1 *las* and *rhl* quorum sensing systems. *Journal of Bacteriology* 189 (13):4827-4836.
165. McKnight, S. L., B. H. Iglewski, and E. C. Pesci. 2000. The *Pseudomonas* quinolone signal regulates *rhl* quorum sensing in *Pseudomonas aeruginosa*. *Journal of Bacteriology* 182 (10):2702-2708.
166. Defoirdt, T., N. Boon, and P. Bossier. 2011. Can bacteria evolve resistance to quorum sensing disruption? *PLoS Pathogens* 6 (7).
167. Decho, A. W., R. L. Frey, and J. L. Ferry. 2011. Chemical challenges to bacterial AHL signaling in the environment. *Chemical Reviews* 111 (1):86-99.
168. Winson, M. K., M. Cámara, A. Latifi, M. Foglino, S. R. Chhabra, M. Daykin, M. Bally, V. Chapon, G. P. C. Salmond, B. W. Bycroft, A. Lazdunski, G. Stewart, and P. Williams. 1995. Multiple *N*-acyl-L-homoserine lactone signal molecules regulate production of virulence determinants and secondary metabolites in *Pseudomonas aeruginosa*. *Proceedings of the National Academy of Sciences of the United States of America* 92 (20):9427-9431.
169. Debler, E. W., G. F. Kaufmann, R. N. Kirchdoerfer, J. M. Mee, K. D. Janda, and I. A. Wilson. 2007. Crystal structures of a quorum-quenching antibody. *Journal of Molecular Biology* 368 (5):1392-1402.
170. Eberhard, A., and J. B. Schineller. 2000. Chemical synthesis of bacterial autoinducers and analogs. *Bioluminescence and Chemiluminescence, Part C* 305:301-315.
171. Chhabra, S. R., C. Harty, D. S. W. Hooi, M. Daykin, P. Williams, G. Telford, D. I. Pritchard, and B. W. Bycroft. 2003. Synthetic analogues of the bacterial signal (quorum sensing) molecule *N*-(3-oxododecanoyl)-L-homoserine lactone as immune modulators. *Journal of Medicinal Chemistry* 46 (1):97-104.
172. Pritchard, D. I., B. W. Bycroft, S. R. Chhabra, and D. Hooi. 2001. Substituted-4-

- quinolones. World Intellectual Property Organization, WO 2002/047686.
173. Purcell, I. C. 2007. Bacterial autoinducer derived 4-quinolones as novel immune modulators. In *PhD thesis, School of Pharmacy*. University of Nottingham, Nottingham.
174. Oikawa, Y., S. Kiyoshi, and O. Yonemitsu. 1978. Meldrum's acid in organic synthesis 2: A general and versatile synthesis of beta-keto esters. *Journal of Organic Chemistry* 43 (10):2087-2088.
175. Pellegata, R., M. Pinza, and G. Pifferi. 1978. improved synthesis of gamma-lactams, delta-lactams, and epsilon-lactams. *Synthesis* (8):614-616.
176. Xu, F., J. D. Armstrong, G. X. Zhou, B. Simmons, D. Hughes, Z. H. Ge, and E. J. J. Grabowski. 2004. Mechanistic evidence for an alpha-oxoketene pathway in the formation of beta-ketoamides/esters via Meldrum's acid adducts. *Journal of the American Chemical Society* 126 (40):13002-13009.
177. Prata, C. A. H., Y. Zhao, P. Barthelemy, Y. Li, D. Luo, T. J. McIntosh, S. J. Lee, and M. W. Grinstaff. 2004. Charge reversal amphiphiles for gene development. *Journal of the American Chemical Society* 126 (39):12196-12197.
178. Li, J. J. 2009. *Name Reactions*. Springer-Verlag, Berlin - Heidelberg.
179. Greene, T., and P. Wuts. 2006. *Greene's Protective groups in organic synthesis*. John Wiley & Sons, Inc, Hoboken, New Jersey.
180. Dhaon, M. K., R. K. Olsen, and K. Ramasamy. 1982. Esterification of *N*-protected alpha-amino acids with alcohol/carbodiimide/4-(dimethylamino)pyridine - racemization of aspartic and glutamic acid derivatives. *Journal of Organic Chemistry* 47 (10):1962-1965.
181. Darley, D. J., D. S. Butler, S. J. Prideaux, T. W. Thornton, A. D. Wilson, T. J. Woodman, M. D. Threadgill, and M. D. Lloyd. 2009. Synthesis and use of isotope-labelled substrates for a mechanistic study on human alpha-methylacyl-CoA racemase 1A (AMACR; P504S). *Organic & Biomolecular Chemistry* 7 (3):543-552.
182. Wierenga, W., and H. I. Skulnick. 1979. General, efficient, one-step synthesis of beta-keto esters. *Journal of Organic Chemistry* 44 (2):310-311.
183. Lodyato, V. I., I. L. Yurkova, V. L. Sorokin, O. I. Shadyro, V. I. Dolgopalets, and M. A. Kisel. 2004. Novel (3,5-di-tert-butyl-2-hydroxy-phenylcarbamoyl)-alkanoic acids as potent antioxidants. *Bioorganic & Medicinal Chemistry Letters* 14 (16):4253-4256.

-
184. Niwayama, S., H. J. Cho, and C. L. Lin. 2008. Highly efficient selective monohydrolysis of dialkyl malonates and their derivatives. *Tetrahedron Letters* 49 (28):4434-4436.
185. Hoffman, R. V., H. O. Kim, and J. C. Lee. 1994. 2-[[*p*-Nitrophenyl)sulfonyl]oxy] 3-keto esters as intermediates for the regiospecific preparation of 2-[[*p*-nitrophenyl)sulfonyl]oxy] ketones. *Journal of Organic Chemistry* 59 (7):1933-1936.
186. Caserio, F. F., and J. D. Roberts. 1958. Small-ring compounds 21: 3-Methylenecyclobutanone and related compounds. *Journal of the American Chemical Society* 80 (21):5837-5840.
187. Kudoh, T., C. S. Park, S. T. Lefurgy, M. Sun, T. Michels, T. S. Leyh, and R. B. Silverman. 2010. Mevalonate analogues as substrates of enzymes in the isoprenoid biosynthetic pathway of *Streptococcus pneumoniae*. *Bioorganic & Medicinal Chemistry* 18 (3):1124-1134.
188. Freifeld, I., G. Bose, T. Eckardt, and P. Langer. 2007. Synthesis of gamma-alkylidenebutenolides by formal [3+2] cyclizations of 1,5- and 2,4-bis(trimethylsilyloxy)-1,3,5-hexatrienes with oxalyl chloride. *European Journal of Organic Chemistry* (2):351-355.
189. Smith, M. B., and J. March. 2007. *March's Advanced organic chemistry: Reactions, mechanisms and structure*. John Wiley and Sons, Inc., New Jersey.
190. Frosch, M., A. A. Zardini, S. M. Platt, L. Muller, M. C. Reinig, T. Hoffmann, and M. Bilde. 2010. Thermodynamic properties and cloud droplet activation of a series of oxo-acids. *Atmospheric Chemistry and Physics* 10 (13):5873-5890.
191. Kosicki, G. W., and S. N. Lipovac. 1964. pH and pD dependence of spontaneous and magnesium ion-catalyzed decarboxylation of oxalacetic acid. *Canadian Journal of Chemistry-Revue Canadienne de Chimie* 42 (2):403-415.
192. Kosicki, G. W., R. G. Annett, and S. N. Lipovac. 1964. Lithium chloride catalyzed decarboxylation of oxalacetic acid in ethanol. *Canadian Journal of Chemistry-Revue Canadienne de Chimie* 42 (12):2806-2810.
193. Rompp, A., R. Winterhalter, and G. K. Moortgat. 2006. Oxodicarboxylic acids in atmospheric aerosol particles. *Atmospheric Environment* 40 (35):6846-6862.
194. Montalbetti, C., and V. Falque. 2005. Amide bond formation and peptide coupling. *Tetrahedron* 61 (46):10827-10852.
195. Bruice, P. Y., and T. C. Bruice. 1978. Lack of concertedness in catalysis of
-

- enolization of oxaloacetic acid by general acids and bases - formation of a carbinolamine intermediate in tertiary amine catalyzed enolization reaction. *Journal of the American Chemical Society* 100 (15):4793-4801.
196. Bruice, P. Y. 1989. Catalysis of the enolization of oxaloacetic acid by primary and secondary amines via a carbinolamine intermediate. *Journal of the American Chemical Society* 111 (3):962-970.
197. Spetnagel, W. J., and I. M. Klotz. 1976. Catalysis of decarboxylation of oxalacetic acid by modified poly(ethylenimines). *Journal of the American Chemical Society* 98 (25):8199-8204.
198. Hodgkinson, J. T., W. R. J. Galloway, M. Casoli, H. Keane, X. Su, G. P. C. Salmond, M. Welch, and D. R. Spring. 2011. Robust routes for the synthesis of *N*-acylated-L-homoserine lactone (AHL) quorum sensing molecules with high levels of enantiomeric purity. *Tetrahedron Letters* 52 (26):3291-3294.
199. Hradil, P., M. Grepl, J. Hlavac, and A. Lycka. 2007. The study of cyclization of *N*-acylphenacyl anthranilates with ammonium salts under various conditions. *Heterocycles* 71 (2):269-280.
200. Posner, G. H., C. E. Whitten, and McFarlan, Pe. 1972. Organocopper chemistry: Halo-substituted, cyano-substituted, and carbonyl-substituted ketones from corresponding acyl chlorides and organocopper reagents. *Journal of the American Chemical Society* 94 (14):5106-5108.
201. Clayden, J., N. Greeves, S. Warren, and P. Wothers. 2007. *Organic Chemistry*. Oxford University Press, Oxford.
202. Wong, W.-Y., X.-Z. Wang, Z. He, K.-K. Chan, A. B. Djurisic, K.-Y. Cheung, C.-T. Yip, A. M.-C. Ng, Y. Y. Xi, C. S. K. Mak, and W.-K. Chan. 2007. Tuning the absorption, charge transport properties, and solar cell efficiency with the number of thienyl rings in platinum-containing poly(aryleneethynylene)s. *Journal of the American Chemical Society* 129 (46):14372-14380.
203. Szczepankiewicz, W., and J. Suwinski. 2000. One-pot synthesis of 3-(2-cyanophenyl)-quinazolin-4(3*H*)-one. *Chemistry of Heterocyclic Compounds* 36 (7):922-924.
204. Somanathan, R., and K. M. Smith. 1981. Synthesis of some 2-alkyl-4-quinolone and 2-alkyl-4-methoxyquinoline alkaloids. *Journal of Heterocyclic Chemistry* 18 (6):1077-1079.

-
205. Behrman, E. J., R. L. Kiser, W. F. Garas, E. C. Behrman, and B. M. Pitt. 1995. Conversion of 4-quinolones into 3-hydroxy-4-quinolones via the corresponding sulfates. *Journal of Chemical Research-S* (5):164-165.
206. Soung, M. G., M. Matsui, and T. Kitahara. 2000. Regioselective synthesis of beta- and gamma-thujaplicins. *Tetrahedron* 56 (39):7741-7745.
207. Hradil, P., and J. Jirman. 1995. Synthesis of 2-aryl-3-hydroxyquinolin-4(1*H*)-ones. *Collection of Czechoslovak Chemical Communications* 60 (8):1357-1366.
208. Hodgkinson, J. T., W. Galloway, S. Saraf, I. R. Baxendale, S. V. Ley, M. Ladlow, M. Welch, and D. R. Spring. 2011. Microwave and flow syntheses of *Pseudomonas* quinolone signal (PQS) and analogues. *Organic & Biomolecular Chemistry* 9 (1):57-61.
209. Zewge, D., C. Y. Chen, C. Deer, P. G. Dormer, and D. L. Hughes. 2007. A mild and efficient synthesis of 4-quinolones and quinolone heterocycles. *Journal of Organic Chemistry* 72 (11):4276-4279.
210. Eaton, P. E., G. R. Carlson, and J. T. Lee. 1973. Phosphorus pentoxide-methanesulfonic acid - convenient alternative to polyphosphoric acid. *Journal of Organic Chemistry* 38 (23):4071-4073.
211. Bangdiwala, B. P., and C. M. Desai. 1953. Studies in the synthesis of 4-hydroxyquinoline using acetic anhydride and sulphuric acid - 1. *Journal of the Indian Chemical Society* 30 (9):655-656.
212. Hradil, P., J. Hlavac, and K. Lemr. 1999. Preparation of 1,2-disubstituted-3-hydroxy-4(1*H*)-quinolinones and the influence of substitution on the course of cyclization. *Journal of Heterocyclic Chemistry* 36 (1):141-144.
213. Jones, C. P., K. W. Anderson, and S. L. Buchwald. 2007. Sequential Cu-catalyzed amidation-base-mediated camps cyclization: A two-step synthesis of 2-aryl-4-quinolones from *o*-halophenones. *Journal of Organic Chemistry* 72:7968-7973.
214. Huang, J., Y. Chen, A. O. King, M. Dilmeghani, R. D. Larsen, and M. M. Faul. 2008. A mild, one-pot synthesis of 4-quinolones via sequential Pd-catalyzed amidation and base-promoted cyclization. *Organic Letters* 10 (12):2609-2612.
215. Ding, D. R., X. Li, X. Wang, Y. L. Du, and J. K. Shen. 2006. Microwave-assisted rapid and straightforward synthesis of 2-aryl-4-quinolones from acylated 2'-aminoacetophenones. *Tetrahedron Letters* 47 (39):6997-6999.
216. Beifuss, U., and S. Ledderhose. 1997. A new two-step synthesis of quinolone
-

- alkaloids based on the regioselective addition of organometallic reagents to 4-silyloxyquinolinium triflates. *Synlett* (3):313-315.
217. Moon, S. S., P. M. Kang, K. S. Yoon, S. J. Yun, and B. Binpark. 1995. Synthesis of plant growth promoting and fungicidal 4-quinolinone metabolites of *Pseudomonas cepacia*. *Bulletin of the Korean Chemical Society* 16 (11):1128-1130.
218. Chakrabarty, M., S. Khasnobis, Y. Harigaya, and Y. Konda. 2000. Neat formic acid: An excellent *N*-formylating agent for carbazoles, 3-alkylindoles, diphenylamine and moderately weak nucleophilic anilines. *Synthetic Communications* 30 (2):187-200.
219. Shintani, R., T. Yamagami, T. Kimura, and T. Hayashi. 2005. Asymmetric synthesis of 2-aryl-2,3-dihydro-4-quinolones by rhodium-catalyzed 1,4-addition of arylzinc reagents in the presence of chlorotrimethylsilane. *Organic Letters* 7 (23):5317-5319.
220. Klaus, G. G. B., and A. M. Cross. 1974. Influence of epitope density on immunological properties of hapten-protein conjugates 1: Characteristics of immune-response to hapten-coupled albumin with varying epitope density. *Cellular Immunology* 14 (2):226-241.
221. Singh, K. V., J. Kaur, G. C. Varshney, M. Raje, and C. R. Suri. 2004. Synthesis and characterization of hapten-protein conjugates for antibody production against small molecules. *Bioconjugate Chemistry* 15 (1):168-173.
222. Fodey, T. L., N. M. Greer, and S. R. H. Crooks. 2009. Antibody production: Low dose immunogen vs. low incorporation hapten using salmeterol as a model. *Analytica Chimica Acta* 637 (1-2):328-332.
223. Adamczyk, M., J. C. Gebler, and P. G. Mattingly. 1996. Characterization of protein-hapten conjugates 2: Electrospray mass spectrometry of bovine serum albumin-hapten conjugates. *Bioconjugate Chemistry* 7 (4):475-481.
224. Pedersen, M. K., N. S. Sorensen, P. M. H. Heegaard, N. H. Beyer, and L. Bruun. 2006. Effect of different hapten-carrier conjugation ratios and molecular orientations on antibody affinity against a peptide antigen. *Journal of Immunological Methods* 311 (1-2):198-206.
225. Feldmann, M. 1972. Induction of immunity and tolerance *in vitro* by hapten protein conjugates 3: Hapten inhibition studies of antigen binding to B-cells in immunity and tolerance. *Journal of Experimental Medicine* 136 (3):532-545.
226. Adamczyk, M., A. Buko, Y. Y. Chen, J. R. Fishpugh, J. C. Gebler, and D. D. Johnson. 1994. Characterization of protein hapten conjugates 1: Matrix-assisted laser-

- desorption ionization mass spectrometry of immune BSA hapten conjugates and comparison with other characterization methods. *Bioconjugate Chemistry* 5 (6):631-635.
227. Marco, M. P., S. Gee, and B. D. Hammock. 1995. Immunochemical techniques for environmental analysis 1: Immunosensors. *TrAC Trends in Analytical Chemistry* 14 (7):341-350.
228. Kaufmann, G. F., J. Park, A. V. Mayorov, D. M. Kubitz, and K. D. Janda. 2011. Generation of quorum quenching antibodies. In *Quorum Sensing: Methods and Protocols*. K. P. Rumbaugh, ed. Humana Press. 299-311.
229. Winson, M. K., S. Swift, L. Fish, J. P. Throup, F. Jorgensen, S. R. Chhabra, B. W. Bycroft, P. Williams, and G. Stewart. 1998. Construction and analysis of *luxCDABE*-based plasmid sensors for investigating *N*-acyl homoserine lactone-mediated quorum sensing. *FEMS Microbiology Letters* 163 (2):185-192.
230. Diggle, S. P., M. P. Fletcher, M. Cámara, and P. Williams. 2011. Detection of 2-alkyl-4-quinolones using biosensors. In *Quorum Sensing: Methods and Protocols*, 2011 ed. K. P. Rumbaugh, ed. Humana Press. 21-30.
231. Stewart, G. S. A. B., and P. Williams. 1992. Lux genes and the applications of bacterial bioluminescence. *Journal of General Microbiology* 138:1289-1300.
232. Fletcher, M. P., S. P. Diggle, S. A. Crusz, S. R. Chhabra, M. Cámara, and P. Williams. 2007. A dual biosensor for 2-alkyl-4-quinolone quorum-sensing signal molecules. *Environmental Microbiology* 9:2683-2693.
233. Mashburn, L. M., and M. Whiteley. 2005. Membrane vesicles traffic signals and facilitate group activities in a prokaryote. *Nature* 437 (7057):422-425.
234. Mashburn-Warren, L., J. Howe, K. Brandenburg, and M. Whiteley. 2009. Structural requirements of the *Pseudomonas* quinolone signal for membrane vesicle stimulation. *Journal of Bacteriology* 191 (10):3411-3414.
235. Hodgkinson, J., S. D. Bowden, W. R. J. D. Galloway, D. R. Spring, and M. Welch. 2010. Structure activity analysis of the *Pseudomonas* quinolone signal molecule. *Journal of Bacteriology* 192 (14):3833-3837.
236. Hammond, A., J. Dertien, J. A. Colmer-Hamood, J. A. Griswold, and A. N. Hamood. 2010. Serum inhibits *Pseudomonas aeruginosa* biofilm formation on plastic surfaces and intravenous catheters. *Journal of Surgical Research* 159 (2):735-746.
237. Singh, P. K., M. R. Parsek, E. P. Greenberg, and M. J. Welsh. 2002. A component of

- innate immunity prevents bacterial biofilm development. *Nature* 417 (6888):552-555.
238. Sun, D. Q., M. A. Accavitti, and J. D. Bryers. 2005. Inhibition of biofilm formation by monoclonal antibodies against *Staphylococcus epidermidis* RP62A accumulation-associated protein. *Clinical and Diagnostic Laboratory Immunology* 12 (1):93-100.
239. Hentzer, M., K. Riedel, T. B. Rasmussen, A. Heydorn, J. B. Andersen, M. R. Parsek, S. A. Rice, L. Eberl, S. Molin, N. Høiby, S. Kjelleberg, and M. Givskov. 2002. Inhibition of quorum sensing in *Pseudomonas aeruginosa* biofilm bacteria by a halogenated furanone compound. *Microbiology* 148:87-102.
240. Pinzon, N. M., and L.-K. Ju. 2009. Improved detection of rhamnolipid production using agar plates containing methylene blue and cetyl trimethylammonium bromide. *Biotechnology Letters* 31 (10):1583-1588.
241. Ino, A., T. J. Dickerson, and K. D. Janda. 2007. Positional linker effects in haptens for cocaine immunopharmacotherapy. *Bioorganic & Medicinal Chemistry Letters* 17 (15):4280-4283.
242. Crabbe, P., C. Van Peteghem, M. Salden, and F. Kohen. 2000. Influence of the hapten conjugation site on the characteristics of antibodies generated against metabolites of clostebol acetate. *Journal of Agricultural and Food Chemistry* 48 (8):3633-3638.
243. Malavašič, Č., B. Brulc, P. Čebašek, G. Dahmann, N. Heine, D. Bevk, U. Grošelj, A. Meden, B. Stanovnik, and J. Svete. 2007. Combinatorial solution-phase synthesis of (2S,4S)-4-acylamino-5-oxopyrrolidine-2-carboxamides. *Journal of Combinatorial Chemistry* 9 (2):219-229.
244. Takeda, K., A. Akiyama, H. Nakamura, S. Takizawa, Y. Mizuno, H. Takayanagi, and Y. Harigaya. 1994. Dicarbonates - convenient 4-dimethylaminopyridine catalyzed esterification reagents. *Synthesis* (10):1063-1066.
245. Soural, M., J. Hlavac, P. Hradil, I. Frysova, M. Hajduch, V. Bertolasi, and M. Malon. 2006. Synthesis and cytotoxic activity of substituted 2-phenyl-3-hydroxy-4(1H)-quinolinones-7-carboxylic acids and their phenacyl esters. *European Journal of Medicinal Chemistry* 41 (4):467-474.
246. Doria, G., C. Passarotti, R. Magrini, R. Sala, P. Sberze, M. Tibolla, G. Arcari, R. Ceserani, and R. Castello. 1984. New derivatives of pyrrolo and pyrido[2,1-b]quinazoline as antiulcer agents. *Farmaco-Edizione Scientifica* 39 (11):968-978.
247. Park, J., R. Jagasia, G. F. Kaufmann, J. C. Mathison, D. I. Ruiz, J. A. Moss, M. M. Meijler, R. J. Ulevitch, and K. D. Janda. 2007. Infection control by antibody

- disruption of bacterial quorum sensing signaling. *Chemistry & Biology* 14:1119-1127.
248. Janda, K. D., G. F. Kaufmann, and J. Park. 2009. Antibody-mediated disruption of quorum sensing in bacteria. World Intellectual Property Organization, WO 2009/055054 A2.
249. Xu, F., T. Byun, H.-J. Dussen, and K. R. Duke. 2003. Degradation of *N*-acylhomoserine lactones, the bacterial quorum-sensing molecules, by acylase. *Journal of Biotechnology* 101:89-96.